AMERICAN MATHEMATICAL SOCIETY

Lecture Notes Prepared in Connection With the

Summer Seminar on Space Mathematics

held at

Cornell University, Ithaca, New York

July 1, 1963 - August 9, 1963

Part III

UNPUBLISHED PRELIMINARY DATA

Supported by the

National Aeronautics and Space Administration under Research Grant NsG 358

Air Force Office of Scientific Research under Grant AF-AFOSR 258-63

Army Research Office (Durham) under Contract DA-31-124-ARO(D)-82

Atomic Energy Commission under Contract AT(30-1)-3164

Office of Naval Research under Contract Nonr(G)00025-63

National Science Foundation under NSF Grant GE-2234

25103

Decay of Orbits

by

P.J. Message

Expression for the Drag Force

Idealised Case

A body of mass m moves with speed V through a medium, of density ρ, at rest. In an interval of length δt, it captures the particles originally within a cylinder of length $V \delta t$, and cross section essentially equal to the cross section of the body (A, say). Thus the accreted mass is $AV \delta t \rho$, and if the increase in velocity is δV, we must have

$$mV = (m + AV \delta t \rho)(V + \delta V),$$

whence

$$m\frac{dV}{dt} = - AV^2 \rho . \qquad (1)$$

Practical Assumption

This derivation takes no account of the thermal motion of the medium. However the force (P) is found to be very nearly proportional to V^2 except for very small velocities, and we can put with close accuracy

$$P = - \tfrac{1}{2} C_D A V^2 \rho , \qquad (2)$$

where C_D, which is called the "drag coefficient," is close to 2 if the mean free path in the medium is large compared to the dimensions of the body, becoming nearer to unity if the reverse is the case.

If the satellite is rotating steadily, the components of the force which are perpendicular to the relative velocity will cancel out almost entirely. If the rotation is about the axes of greatest moment of inertia, the mean value of A will remain constant. Ionisation of the atmosphere is not likely to be important, since it is less than 5% at

evaluated at perigee, where the density is much greater than elsewhere on the orbit. Thus we may effectively regard F as constant.

Then the drag force is

$$\underline{P} = -\tfrac{1}{2} C_D A \rho V \underline{V} = -\tfrac{1}{2} C_D A \rho F v^2 \left(\frac{\underline{V}}{V}\right) \quad . \tag{5}$$

The component of $\underline{V}$ in the direction of the radius vector is

$$\frac{\underline{V} \cdot \underline{r}}{r} = \frac{\underline{v} \cdot \underline{r}}{r} \qquad \text{(using (3))}$$

$$= v \sin X,$$

where $\frac{\pi}{2} - X$ is the angle between the velocity and the radius vector. The component of $\underline{V}$ in the transverse direction in the orbit plane is

$$\frac{\underline{V} \cdot (\underline{h} \times \underline{r})}{hr} = \left\{ v^2 r^2 - (\underline{v} \cdot \underline{r})^2 - (\underline{\Omega} \times \underline{r}) - \underline{v} r^2 \right\} / (hr)$$

(using (3))

$$= \left\{ v^2 r^2 \cos^2 X - \Omega h r^2 \cos i \right\} / (hr)$$

$$= v \cos X - \Omega r \cos i. \quad \text{(since } h = rv \cos X\text{)}$$

The component of $\underline{V}$ in the direction of $\underline{h}$ is

$$\frac{\underline{V} \cdot \underline{h}}{h} = -\frac{\underline{\Omega} \cdot (\underline{r} \times \underline{h})}{h} \qquad \text{(using (3))}$$

$$= \left\{ (\underline{\Omega} \cdot \underline{v}) r^2 - (\underline{\Omega} \cdot \underline{r}) (\underline{r} \cdot \underline{v}) \right\} / h.$$

Now $\underline{\Omega} \cdot \underline{r} = \Omega r \sin \delta$

$$= \Omega r \sin i \sin(\omega + f),$$

heights of less than 400 kilometers. In any case a change of C_D with time will not affect many of the results.

Effect of Rotation of the Atmosphere

This effect is small, so a simple assumption is justified. Let us suppose that the atmosphere rotates with the same angular velocity as the Earth, $\underline{\Omega}$, say. Then its velocity at the point $\underline{r}$, where the origin is at the Earth's centre, is $\underline{\Omega} \times \underline{r}$. If the satellite is at $\underline{r}$ with velocity $\underline{v}$, its velocity relative to the atmosphere is $\underline{V}$, where

$$\underline{V} = \underline{v} - \underline{\Omega} \times \underline{r}. \tag{3}$$

Thus (writing $V = |\underline{V}|$, $v = |\underline{v}|$, etc.)

$$V^2 = v^2 - 2\underline{v} \cdot (\underline{\Omega} \times \underline{r}) + (\underline{\Omega} \times \underline{r})^2$$

$$= v^2 - 2\underline{\Omega} \cdot \underline{h} + (\underline{\Omega} \times \underline{r})^2$$

$$= v^2 - 2\Omega h \cos i + \Omega^2 r^2 \cos^2 \delta ,$$

where $\underline{h} = \underline{r} \times \underline{v}$, is the angular momentum per unit mass of the satellite about the Earth's centre, δ is its declination, and i the inclination of its orbit to the equator. We put

$$V^2 = v^2 F, \tag{4}$$

$$\text{so that } F = 1 - \frac{2\Omega h \cos i}{v^2} + \frac{\Omega^2 r^2 \cos^2 \delta}{v^2} \tag{4a}$$

The third term in F may usually be neglected, being less than about 1/250, and the second term, which is of the order of 1/15, may be

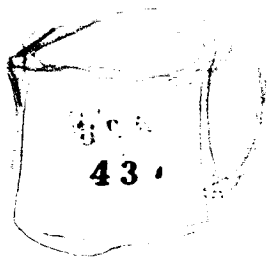

where ω is the argument of perigee, and f the time anomaly. Also

$$\underline{\Omega} \cdot \underline{v} = \Omega v \sin i \cos (\omega + f - X) ,$$

so

$$\frac{\underline{V} \cdot \underline{h}}{h} = \Omega r \sin i \cos (\omega + f).$$

Therefore if $\hat{\underline{r}}$, $\hat{\underline{s}}$ and $\hat{\underline{h}}$ are unit vectors in the radial, transverse, and normal to orbit directions respectively, the drag force may be written

$$\underline{P} = - \tfrac{1}{2} C_D A \rho \sqrt{F} v^2 \left\{ \sin X \hat{\underline{r}} + \left(\cos X - \frac{\Omega r \cos i}{v}\right) \hat{\underline{s}} + \frac{\Omega r \sin i}{v} \cos (\omega + f) \hat{\underline{h}} \right\}$$

Since $\underline{v} = v(\sin X \hat{\underline{r}} + \cos X \hat{\underline{s}})$, this may be written

$$\underline{P} = - \frac{m}{2} k \rho v \left\{ \underline{v} - \Omega r \cos i \hat{\underline{s}} + \Omega r \sin i \cos (\omega + f) \hat{\underline{h}} \right\}, \quad (6)$$

where $k = \dfrac{C_D A \sqrt{F}}{m}$, (7)

m being the mass of the satellite.

The Effect of the Tangential Component

The Equation of Motion

The component of $\underline{P}$ parallel to the velocity $\underline{v}$ is the largest part. The equation of motion, considering only this part, is

$$\ddot{\underline{r}} = - \text{grad } V - \tfrac{1}{2} k \rho v \underline{v} , \quad (7a)$$

where $V(\underline{r})$ is the gravitational potential.

The Energy

If $E = \frac{1}{2} v^2 + V$, then

$$\frac{dE}{dt} = \dot{\underline{v}} \cdot \underline{v} + \underline{v} \cdot \text{grad } V = - \tfrac{1}{2} k \rho v^3. \qquad (8)$$

Now $V = - \frac{\mu}{r} - R$, where R is the disturbing function for the oblateness, and so

$$E = \tfrac{1}{2} v^2 - \frac{\mu}{r} - R.$$

$$= - \frac{\mu}{2a} - R.$$

$$\therefore \frac{\mu}{2a^2} \dot{a} - R = - \tfrac{1}{2} k \rho v^3.$$

The change of the major semi axis $\underline{a}$ due to the drag is therefore

$$\dot{a} = - \frac{k \rho a^2 v^3}{\mu} . \qquad (9)$$

The Angular Momentum

If $\underline{h} = \underline{r} \times \underline{v}$,

$$\frac{d\underline{h}}{dt} = \underline{r} \times \ddot{\underline{r}} = \underline{r} \times \text{grad } R - \tfrac{1}{2} k \rho v \underline{h} .$$

The change due to the drag is therefore

$$\frac{d\underline{h}}{dt} = -\tfrac{1}{2} k\rho\, v\underline{h} \ . \qquad (10)$$

Therefore the direction of $\underline{h}$ is unaltered, and so the position of the orbit plane is unchanged by the tangential component.

Since $h = \int \left\{\mu a(1 - e^2)\right\}$, with (9),

$$\dot{e} = -\frac{1}{2e} k\rho(1 - e^2)\, v\, (\frac{av^2}{\mu} - 1)$$

$$= -\frac{1}{e} k\rho(1 - e^2)\, v\, (\frac{a}{r} - 1). \qquad (11)$$

In terms of the eccentric anomaly E,

$$\dot{a} = -k\rho\, na^2 \left(\frac{1 + e\cos E}{1 - e\cos E}\right)^{3/2} , \qquad (9a)$$

$$\text{and} \quad \dot{e} = -k\rho\, na(1 - e^2)\cos E\, \frac{(1 + e\cos E)^{1/2}}{(1 - e\cos E)^{3/2}} . \qquad (11a)$$

Hence the secular rates of change are

$$\overline{\dot{a}} = -\frac{1}{2\pi} kna^2 \int_0^{2\pi} \rho\, \frac{(1 + e\cos E)^{3/2}}{(1 - e\cos E)^{1/2}}\, dE , \qquad (12)$$

$$\text{and} \quad \overline{\dot{e}} = -\frac{1}{2\pi} kna(1 - e^2) \int_0^{2\pi} \rho\cos E \left(\frac{1 + e\cos E}{1 - e\cos E}\right)^{\frac{1}{2}} dE . \qquad (13)$$

King - Hele uses the quantity $x = ae$, whose secular rate of change is therefore

$$\overline{\dot{x}} = -\frac{1}{2\pi} kna^2 \int_0^{2\pi} \rho(e + \cos E) \left(\frac{1 + e\cos E}{1 - e\cos E}\right)^{\frac{1}{2}} dE . \qquad (14)$$

King - Hele's First Order Theory of the Orbit

In polar coordinates (r, θ) in the fixed plane of the motion the equations are

$$\ddot{r} - r\dot{\theta}^2 = -\frac{\mu}{r^2} - \tfrac{1}{2} k \rho v^2 \sin X,$$

$$\frac{1}{r}\frac{d}{dt}(r^2\dot{\theta}) = -\tfrac{1}{2} k \rho v^2 \cos X . \qquad (15)$$

Putting $u = \frac{1}{r}$, and $h = r^2\dot{\theta}$, and eliminating the time as independent variable, we obtain

$$\frac{d^2u}{d\theta^2} + u = \frac{\mu}{h^2} \qquad (16)$$

and $$\frac{dh}{d\theta} = -\frac{k\rho v}{2u^3} . \qquad (17)$$

We use the Poisson method of succesive approximation, putting

$$u = u_0 + \delta_1 u + \delta_2 u + \ldots .$$

and $$h = h_0 + \delta_1 h + \ldots . \qquad (18)$$

Unperturbed Solution

$$\frac{d^2u_0}{d\theta^2} + u_0 = \frac{\mu}{h_0^2} = \frac{1}{p_0} , \text{ say}$$

$$\frac{dh_0}{d\theta} = 0. \qquad (19)$$

whence h_0, and therefore P_0, is constant, and we obtain the equation of the ellipse

$$u_0 = \frac{1}{P_0}\left\{1 + e_0 \cos(\theta - \omega_0)\right\}, \tag{20}$$

where e_0 and ω_0 are disposable constants.

First Order Solution

The equations are

$$\frac{d^2 \delta_1 u}{d\theta^2} + \delta_1 u = -\frac{2\mu}{h_0^3}\,\delta_1 h \tag{21}$$

and $$\frac{d\,\delta_1 h}{d\theta} = -\frac{k\rho v_0}{2u_0^3}\,, \tag{22}$$

where v_0 is v computed for the unperturbed orbit (20). From these we obtain

$$\frac{d^3 \delta_1 u}{d\theta^3} + \frac{d\,\delta_1 u}{d\theta} = \frac{\mu k \rho V_0}{h_0^3 u_0^3} = g(\theta - \omega_0)\,, \text{ say.} \tag{23}$$

A particular solution is

$$\frac{d}{d\theta}(\delta_1 u) = \int_{\theta_0}^{\theta} g(\theta' - \omega_0)\sin(\theta - \theta')\,d\theta',$$

whence

$$\delta_1 u(\theta) = \int_{\theta_0}^{\theta} d\theta'' \int_{\theta_0}^{\theta''} d\theta' \; g(\theta' - \omega_0) \sin(\theta'' - \theta')$$

$$= \int_{\theta_0}^{\theta} d\theta' \int_{\theta'}^{\theta} d\theta'' \; g(\theta' - \omega_0) \sin(\theta'' - \theta')$$

$$= \int_{\theta_0}^{\theta} d\theta' \; g(\theta' - \omega_0) \left\{ 1 - \cos(\theta - \theta') \right\} . \qquad (24)$$

The equations (12) and (14) may also be derived from this by considering the change in u from perigee to perigee, which leads to the expression

$$\Delta q = - q^2 \int_0^{2\pi} df \; g(f) \; (1 - \cos f) \qquad (25)$$

for the change in one period of the perigee distance q and also the change in u from apogee to apogee, which leads to

$$\Delta q' = - q'^2 \int_0^{2\pi} df \; g(f) \; (1 + \cos f) \qquad (26)$$

for the change in the apogee distance q'. Then transforming from the true anomaly f to the eccentric anomaly E, and use of $a = \frac{1}{2}(q + q')$, and $x = \frac{1}{2}(q' - q)$, leads to the previously found forms of equations (12) and (14).

The Form of the Atmosphere

We assume the surfaces of constant density to be ellipsoids of revolution, with the Earth's rotational axis as axis of symmetry. If

we assume the ellipticity of each ellipsoid to be the same as that of the geoid (King-Hele gives the value 0.003353), then at a height of 300 kilometers our ellipsoids remain within 1 kilometer distance of the ellipsoids in which the ellipticity varies to maintain hydrostatic equilibrium. Thus the polar equation of each surface may be written

$$r = r_0 \left\{ 1 - \epsilon \sin^2 \delta + O(\epsilon^2) \right\} , \qquad (27)$$

where δ is the declination. Along a given radius vector, the density is nearly proportional to exp (-r/H), where H is the "scale height." If the perigee distance changes by more than about 100 kilometers, we must take account of the variation of H with altitude, but in fact this distance usually changes by less than 60 kilometers in the first 95% of the satellite's lifetime.

We will not consider the variations of density with time. Such changes do occur, with the period of the Sun's axial rotation, with that of the Earth's rotation (due to differences of day and night), and the sunspot cycle. These changes do not however affect the relative changes of a and x.

Thus we will take the density as

$$\rho = \rho_0 \exp \left\{ - \beta r (1 + \epsilon \sin^2 \delta) \right\} , \qquad (28)$$

where $\beta = 1/H$.

King - Hele's Treatment of the Secular Changes

Confining ourselves to small orbital eccentricities, we use the expansions

$$\frac{(1 + e \cos E)^{3/2}}{(1 - e \cos E)^{1/2}} = 1 + 2e \cos E + 3/4\ e^2 (1 + \cos 2E) + O(e^3)$$

and $(\cos E + e) \left(\frac{1 + e \cos E}{1 - e \cos E}\right)^{\frac{1}{2}} = \cos E + 3/2\ e + 1/2\ e \cos 2E$

$$+ 11/8\ e^2 \cos E + 1/8\ e^2 \cos 3E + O(e^3).$$

Also $\sin^2 \delta = \frac{1}{2} \sin^2 i \left\{ 1 - \cos 2(\omega + f) \right\}$

$$= \tfrac{1}{2} \sin^2 i \left\{ 1 - \cos 2(\omega + E) + e \cos (2\omega + E) \right.$$

$$\left. - e \cos (2\omega + 3E) + O(e^2) \right\}$$

Hence the equations (12) and (14) yield, using also $r = a(1 - e \cos E)$,

$$\dot{\bar{a}} = - \frac{1}{2\pi} na^2 k \rho_0 \exp(-\beta a) \int_0^{2\pi} dE \exp(\beta ae \cos E) \left[1 + 2e \cos E + \right.$$

$$3/4\ e^2(1 + \cos 2E) - c \left\{ 1 + e \cos E - \cos 2(\omega + E) - 3/2\ e \cos(2\omega + E) + \right.$$

$$\left. \left. 1/2\ e \cos (2\omega + 3E) \right\} + O(e^3, ce^2) \right] , \qquad (2a)$$

and $\dot{\bar{x}} = - \frac{1}{2\pi} na^2 k \rho_0 \exp(-\beta a) \int_0^{2\pi} dE \exp(\beta ae \cos E) \left[\cos E + \right.$

$$3/2\ e + 1/2\ e \cos 2E + 11/8\ e^2 \cos E + 1/8\ e^2 \cos 3E -$$

$$c \left\{ \cos E - 1/2 \cos (2\omega + E) - 1/2 \cos (2\omega + 3E) + e - \right.$$

$$\left. 1/2\ e \cos 2\omega - e \cos 2(\omega + E) + 1/2\ e \cos (2\omega + 4E) \right\} +$$

$$\left. O(e^3, ce^2) \right] , \qquad (30)$$

where $c = \frac{1}{2}\beta a \epsilon \sin^2 i$, which is usually less that 0.2.

Bessel Functions of Imaginary Argument

The functions $I_n(Z) = i^{-n} J_n(iZ)$ may be shown to satisfy the generating relation

$$\sum_{n=-\infty}^{\infty} I_n(Z)\, t^n = \exp\left\{\tfrac{1}{2} Z\left(t + \frac{1}{t}\right)\right\}, \qquad (31)$$

from which, putting $t = e^{(i\varphi)}$, we see that I_n must be

$$I_n(Z) = \frac{1}{2\pi}\int_{-\pi}^{\pi} \exp(-in\varphi)\exp(Z\cos\varphi)\, d\varphi$$

$$= \frac{1}{2\pi}\int_{0}^{2\pi} \cos n\varphi \cdot \exp(Z\cos\varphi)\, d\varphi, \qquad (32)$$

after a little rearrangement.

Also we see that

$$\int_0^{2\pi} \exp(Z\cos\varphi)\sin n\varphi\, d\varphi = 0 \qquad (33)$$

So, putting $\beta ae = Z = ax$, equations (29) and (30) yield

$$\bar{\dot{a}} = -na^2 k \rho_0 \exp(\beta a)\left[I_0 + 2I_1 e - I_0 c + 3/4\,(I_0 + I_2)\, e^2 + \left\{I_2 + (3/2\, I_1 - 1/2\, I_3)\, e\right\} c\cos 2\omega + O(e^3, ce^2)\right], \qquad (34)$$

$$\text{and } \overline{\dot{x}} = -na^2 k \rho_0 \exp(\beta a)\left[I_1 + 1/2\,(3I_0 + I_2)\,e - I_1 c + \right.$$

$$1/8\,(11I_1 + I_3)\,e^2 + (I_2 - I_0)\,ce + 1/2\left\{(I_1 + I_3) + (I_0 - I_4)\,e\right\}\cos 2\omega +$$

$$\left. O(e^3, ce^2)\right] . \qquad (35)$$

Dinsion gives

$$\overline{\frac{da}{dx}} = \frac{I_0}{I_1} + 2e - \tfrac{1}{2}\left(3\frac{I_0}{I_1} + \frac{I_2}{I_1}\right) e + \left(\frac{I_2}{I_1} - \tfrac{1}{2} - \tfrac{1}{2}\frac{I_3}{I_1}\right) c \cos 2\omega +$$

$$O(e^2, ce). \qquad (36)$$

Phase I

We have the asymptotic formula

$$I_n(Z) \sim \frac{\exp Z}{\sqrt{2\pi Z}}\left\{1 - \frac{4n^2 - 1^2}{1!\ 8Z} + \frac{(4n^2 - 1^2)(4n^2 - 2^2)}{2!\ (8Z)^2} - \ldots\right\}$$

$$\text{as } Z \longrightarrow \infty , \qquad (37)$$

which is found to be useful if $Z > 3$, that is if $\frac{ae}{H} > 3$. Now since H is about 50 kilometers within about 50%, and a is about 7000 kilometers, this means that this formula is useful if the eccentricity is greater than about 0.02. The part of the motion for which this is true is called "Phase I" by King - Hele. Use of this formula in (36) gives

$$\frac{da}{dx} = \frac{I_0}{I_1} - \frac{1}{\beta a} - \frac{3}{2\beta^2 ax} + \frac{e^2}{\beta x} - \frac{2c}{\beta^2 x^2}\cos 2\omega + \theta(e^2, ce) \quad (38)$$

Differentation of (31) with respect to Z, and equating coefficients gives

$$\frac{dI_n}{dZ} = \tfrac{1}{2}\,(I_{n-1} + I_{n+1}) \ , \tag{39}$$

and differentation with respect to t similarly gives

$$nI_n = \tfrac{1}{2}\,Z(I_{n-1} - I_{n+1}) \ , \tag{40}$$

and hence, on eliminating I_{n+1},

$$\frac{dI_n}{dZ} + \frac{n}{Z}\,I_n = I_{n-1} \ . \tag{41}$$

With n = 1, this gives

$$\frac{I_0}{I_1} = \frac{1}{Z} + \frac{1}{I_1}\frac{dI_1}{dZ} \ . \tag{42}$$

This enables equation (38) to be integrated to give (omitting the term in cos 2ω for the moment)

$$a - a_0 = \frac{1}{\beta}\,\ln\left(\frac{x}{x_0}\right) + \frac{1}{\beta}\,\ln\left\{\frac{I_1(\beta x)}{I_1(\beta x_0)}\right\} - \frac{x - x_0}{\beta a} + \frac{3}{2\beta^2 a_0}\,\ln\left(\frac{x}{x_0}\right) + O\left(\frac{x}{\beta},\ ae^5,\ \frac{ae^2}{\beta^3 x^3}\right) \ , \tag{43}$$

suffix zero indicating initial values. Using the expansion for I_1, this gives, noting that the perigee distance q is given by q = a - x,

$$q - q_0 = -\tfrac{1}{2}\,H\left[\left(1 - \frac{5H}{2a_0}\right)\ln\left(\frac{e_0}{e}\right) + (e_0 - e)\left\{\frac{3H(1 + e_0)}{4a_0 e e_0} - 1 + \frac{e + e_0}{2}\right\}\right] + O\left(ae^5,\ \frac{H^3}{a^2 e}\right) \ . \tag{44}$$

Returning to the term in cos 2ω , we note first that if we substitute (43) into (35) we obtain, for the dominant term,

$$\dot{x} = -\frac{K}{x} + \ldots ,$$

where K is a constant. Thus

$$x^2 = x_0^2 - 2Kt + \ldots .$$

We know that, from the oblateness effect, the most important change of ω with time is a linear increase or decrease, according to whether the inclination is greater or less than the critical value. In either case, we may write to a first approximation,

$$\omega = A + B_{DC}^{\ 2} ,$$

where A and B are constants.

We may now include the cos 2ω term in our result. Integration of this term leads to the addition to the right hand side of equation (44) of the terms

$$-\frac{2cH^2}{x_0}\left(\cos 2\omega_0 - \frac{x_0}{x}\cos 2\omega\right)$$

$$-4c\pi H^2\sqrt{|B|/\pi}\left\{\cos A\int_{2x_0\sqrt{|B|/\pi}}^{2x\sqrt{|B|/\pi}}\cos\left(\tfrac{1}{2}\pi\phi^2\right)d\phi\right.$$

$$\left.+\frac{B}{|B|}\sin A\int_{2x_0\sqrt{|B|/\pi}}^{2x\sqrt{|B|/\pi}}\sin\left(\tfrac{1}{2}\pi\phi^2\right)d\phi\right\} . \qquad (44a)$$

Since the orbital period is given by $T/T_0 = (a/a_0)^{3/2}$, a relation similar to (44) may easily be derived between T, e, T_0, e_0 and H.

This relation, and the complete expression (44), have been used by King - Hele with success to derive H from the known values of q, T and e of a satellite's orbit at two stages in its lifetime, and from such determinations he has studied the variation in H with altitude and discovered its large changes as the sunspot cycle progresses.

Phase 2

For $e < 0.02$, we use the relations (39) through (42) to put equations (36) into the form

$$\beta \frac{da}{dZ} = \frac{1}{\beta Z} + \frac{1}{I_1}\frac{dI_1}{dZ} + \frac{1}{2\beta a}\frac{d}{dZ}\left\{4Z\frac{I_0}{I_1} - 6\ln(ZI_1)\right\}$$

$$- \frac{0.88}{Z} c \cos(A + BH^2Z^2) + O(e^2, ec),$$

and from this is derived, by integrating and putting $q = a - x$,

$$q - q_1 = -H\left[(1 - \frac{3H}{a_1})\ln\left\{\frac{Z_1 I_1(Z_1)}{ZI_1(Z)}\right\} + \frac{2H}{a_1}\left\{\frac{Z_1 I_0(Z_1)}{I_1(Z_1)} - \frac{ZI_0(Z)}{I_1(Z)}\right\}\right.$$

$$- Z_1 + Z + 0.44c\left\{\cos A \int_{|B|H^2Z_1^2}^{|B|H^2Z^2} \cdot \frac{\cos\phi}{\phi}\, d\phi\right.$$

$$\left.\left. - \sin A \frac{B}{|B|} \int_{|B|H^2Z_1^2}^{|B|H^2Z^2} \cdot \frac{\sin\phi}{\phi}\, d\phi\right\} + O(e^2, 0.06c)\right] , \quad (45)$$

where the suffix "1" indicates initial values in phase 2.

For a treatment of orbits of high eccentricity, see King - Hele's paper III.

The Effect on the Apse, Node, and Inclination Including the Non - Tangential Components

We will now take account of all of the components of the drag force. If we write R, S, and W for its components per unit mass in the radial, transverse and normal to orbit plane directions respectively, then from (6) we have

$$R = -\tfrac{1}{2} k \rho v^2 \sin X,$$

$$S = -\tfrac{1}{2} k \rho (v^2 \cos X - v \Omega r \cos i), \qquad (46)$$

and $$W = -\tfrac{1}{2} k \rho v \Omega r \sin i \cos (\omega + f).$$

The equation for the apse longitude is (see e.g. Brouwer and Clemence, p. 306),

$$\frac{d\omega}{dt} = -\frac{b \cos f}{na^2 e} R + \frac{r(2 + e \cos f) \sin f}{nabe} S + 2 \sin^2 (\tfrac{1}{2} i) \frac{d\Omega}{dt}$$

$$= -\frac{k \rho v \sin f}{e} \left\{ 1 - \tfrac{1}{2} \frac{r^2 \Omega \cos i}{h} (2 + e \cos f) \right\}$$

$$+ 2 \sin^2 (\tfrac{1}{2} i) \frac{d\Omega}{dt}, \qquad (47)$$

after some reductions, in which we make use of the relations $rv \cos X = h = nab$, and $v \sin X = \frac{na^2}{b} e \sin f$. The first term is an odd function of f, and so its mean value over an orbit is zero. The equation for the node longitude is

$$\frac{d\delta b}{dt} = \frac{r \sin(\omega + f)}{nab \sin t} W = -\frac{1}{4} \frac{k \rho v}{nab} \Omega r \sin 2(\omega + f). \quad (48)$$

This is also an odd function of f, and we conclude that the contributions of the drag to the secular motions of both the apse and the node are zero.

The equation for the orbital inclination is

$$\frac{di}{dt} = \frac{r \cos(\omega + f)}{nab} W = -\frac{1}{2} \frac{k \rho v}{nab} \Omega r^2 \sin i \cos^2(\omega + f), \quad (49)$$

which clearly has a strictly negative secular part, whose leading term in expansion in powers of e is

$$-\frac{1}{4} k \rho_0 a \Omega \sin i \exp(-\beta a) I_0. \quad (50)$$

References

G.E. Cook, D.G. King - Hele and Doreen M.C. Walker
I. Spherically symmetrical atmosphere. Proceedings of the Royal Society, Volume A257, pp. 224 - 49, 1960.
II. With oblate atmosphere. Loc. cit., Volume A264, pp. 88-121, 1961.

D.G. King - Hele
III. High eccentricity orbits. Loc. cit., Volume A267, pp. 541 - 57, 1962.

D.G. King - Hele and Janice Rees

Scale height in the upper atmosphere, derived from changes in satellite orbits. Loc. cit., Volume A270, pp. 562 - 87, 1962.

25104

The Dominant Features of the Long Period Librations of the Trojan Minor Planets

by

P.J. Message

The Dominant Features of the Long Period Librations of the Trojan Minor Planets

The problem of three bodies possesses a class of solutions in which the bodies move so that the triangle they define is always equilateral, as was shown by Lagrange. This type of solution found application in the study of the solar system with the discovery of minor planets moving so as to appoximate to such a configuration with the Sun and Jupiter. These planets are known as the "Trojan Planets," and are named after heroes of the Trojan War. The present treatment seeks to present the long period features of motion in the vicinity of the equiangular triangle configurations, making use of the elements of an osculating orbit, and methods taken from the work on the motion of these planets of W.M. Smart (Memoirs of the Royal Astron. Soc., Volume 62, Part 3, 1918), and H.G. Hertz (A.J., Volume 50, p. 121, 1943), taking into account only the gravitational attractions of the Sun and Jupiter, which of course dominate the motion.

The Equations of Motion

Consider the system comprising the bodies S and J, of masses m_S and m_J, and position vectors ρ_S and ρ_J in an inertial frame, and a third body P with position vector ρ_P, which has no attraction on the other two. The equations of motion are

$$\ddot{\rho}_S = \zeta m_J \frac{(\rho_J - \rho_S)}{(r')^3}$$

$$\ddot{\rho}_J = \zeta m_S \frac{(\rho_S - \rho_J)}{(r')^3} \qquad (1)$$

$$\ddot{\rho}_P = \zeta m_S \frac{(\rho_S - \rho_P)}{r^3} + \zeta m_J \frac{(\rho_J - \rho_P)}{\Delta^3}$$

where $r' = |\rho_J - \rho_S|$, $r = |\rho_S - \rho_P|$, $\Delta = |\rho_J - \rho_P|$.

We use the relative position vectors

$$\underline{r} = \underline{\rho}_P - \underline{\rho}_S, \text{ and } \underline{r}' = \underline{\rho}_J - \underline{\rho}_S, \tag{2}$$

and the first two of (1) give

$$\ddot{\underline{r}}' = -\frac{\mu \underline{r}'}{(r')^3} , \tag{3}$$

where $\mu = \zeta(m_S + m_J)$. (4)

This is the equation of the Keplerian two-body problem, and we suppose that its solution is an ellipse of major semi-axis $\underline{a}'$, and eccentricity e', which is the orbit of J relative to S. The first and third equations give the equation for the relative motion of P and S as

$$\ddot{\underline{r}} = -\frac{\zeta m_S \underline{r}}{r^3} + \frac{\zeta m_J(\underline{r}' - \underline{r})}{\Delta^3} - \frac{\zeta m_J \underline{r}'}{(r')^3} . \tag{5}$$

Now in the equiangular triangle configuration, the orbit of P relative to S is identical in size, shape and period to that of J relative to S, and therefore is a solution of the equation

$$\ddot{\underline{r}} = -\frac{\mu \underline{r}}{r^3} \tag{6}$$

So we rewrite (5) in the form

$$\ddot{\underline{r}} = -\frac{\mu \underline{r}}{r^3} + \text{grad } R, \tag{7}$$

where $R = \mu m' \left\{ \frac{1}{\Delta} - \frac{\underline{r} \cdot \underline{r}'}{(r')^3} - \frac{1}{r} \right\}$, (8)

with $m' = \frac{m_J}{m_S + m_J}$. (9)

The solution of (6) will be regarded as the osculating orbit of P, and R is therefore the distrubing function for the action of J on P.

Now if σ is the angle subtended by P and J at S, we have

$\underline{r} \cdot \underline{r}' = rr' \cos\sigma$, and $\Delta^2 = r^2 + (r')^2 - 2rr' \cos\sigma$. From these we find that

$$\frac{\partial R}{\partial r} = \mu m' \left\{ - \frac{1}{\Delta^3} (r - r' \cos\sigma) + \frac{1}{r^2} - \frac{\cos\sigma}{(r')^2} \right\} ,$$

and $$\frac{\partial R}{\partial (\cos\sigma)} = \mu m' \left\{ \frac{rr'}{\Delta^3} - \frac{r}{(r')^2} \right\} .$$

Both of these vanish if S, J and P form an equiangular triangle, since then $r = r' = \Delta$, and $\sigma = \pi/3$. Therefore, since R only depends on the position of P through its dependence on r and $\cos\sigma$, grad R vanishes while such a configuration holds, and the motion of P is governed by equation (6). But one solution of this is the elliptical orbit identical with that of J, but oriented at $\pi/3$ to it in such a way that the equilateral configuration of SJP is always preserved, and this is therefore a solution of the original equations, confirming Lagrange's result for the case of the three body problem here considered.

We suppose the motion of P to take place entirely in the plane of the orbit of J, in which the time longitudes of P and J are Ψ

and Ψ', respectively, and their mean longitudes are λ and λ', respectively. Then if the elements of the osculating orbit of P are a, e, ω, ϵ, we use variables

$$\begin{aligned} \delta a &= a - a', \\ \phi &= \lambda - \lambda', \\ k &= e \cos \omega \end{aligned} \tag{10}$$

and $h = e \sin \omega$,

which satisfy the equations, derived easily from the Lagrange equations for the elements,

$$\begin{aligned} \frac{d}{dt}(\delta a) &= \frac{2}{na} \frac{\partial R}{\partial \phi}, \\ \frac{d\phi}{dt} &= n - n' - \frac{2}{na} \frac{\partial R}{\partial(\delta a)} + \frac{B}{2na^2}\left(k\frac{\partial R}{\partial k} + h\frac{\partial R}{\partial h}\right), \\ \frac{dk}{dt} &= -\frac{A}{na^2}\frac{\partial R}{\partial h} - \frac{B}{2na^2} k \frac{\partial R}{\partial \phi}, \end{aligned} \tag{11}$$

and $$\frac{dh}{dt} = \frac{A}{na^2}\frac{\partial R}{\partial k} - \frac{B}{2na^2} h \frac{\partial R}{\partial \phi},$$

where $A = \sqrt{1 - e^2} = 1 - \frac{1}{2}(k^2 + h^2) + O(k^4, h^4, k^2h^2)$ (12)

and $B = \frac{2}{e^2}\left\{\sqrt{1 - e^2} - 1 + e^2\right\} = 1 - \frac{1}{4}(k^2 + h^2) + O(k^4, h^4, k^2h^2)$ (13)

The disturbing function takes the form

$$R = \mu m' \left\{ \frac{1}{\Delta} - \frac{r}{(r')^2} \cos (\psi - \psi') - \frac{1}{r} \right\} . \qquad (14)$$

We expand it, making use of the expressions in which $\ell = \lambda - \omega$ is the mean anomaly,

$$\begin{aligned} r &= a \left\{ 1 + \tfrac{1}{2} e^2 - e \cos \ell - \tfrac{1}{2} e^2 \cos 2\ell + O(e^3) \right\} , \\ r \cos (\psi - \omega) &= a \left\{ - 3/2\, e + (1 - 3/8\, e^2) \cos \ell + \tfrac{1}{2} e \cos 2\ell \right. \\ &\qquad \left. + 3/8\, e^2 \cos 3\ell + O(e^3) \right\} , \qquad (15) \\ r \sin (\psi - \omega) &= a \left\{ (1 - 5/8\, e^2) \sin \ell + \tfrac{1}{2} e \sin 2\ell + \right. \\ &\qquad \left. 3/8\, e^2 \sin 3\ell + O(e^3) \right\} , \end{aligned}$$

and their counterparts for J. Making use of these expansions, we find for the secular and long - period part of R, that is, the part which does not involve λ or λ', and the part which involves them only in the slowly varying combination $\psi = \lambda - \lambda'$, respectively,

$$\bar{R} = \frac{\mu m'}{a'} \left\{ \frac{1}{\sqrt{2(1 - \cos \phi)}} - \cos \phi + X \right\} , \qquad (16)$$

where $X = \left(\frac{\delta a}{a'} \right) \left\{ 1 - \cos \phi - \frac{1}{2\sqrt{2(1 - \cos \phi)}} \right\} +$

$$\left(\frac{\delta a}{a'} \right)^2 \left\{ - 1 + \frac{3}{8\sqrt{2(1 - \cos \phi)}} - \frac{1}{4\sqrt{2}(1 - \cos \phi)^{3/2}} \right\}$$

$$+ g_1(\phi) (k^2 + h^2) + g_2(\phi) (kk' + hh') + g_3(\phi) (hk' - kh') , \qquad (17)$$

where $g_1(\phi) = \frac{7}{8\sqrt{2}(1 - \cos \phi)^{3/2}} - \frac{5}{16\sqrt{2}\sqrt{1 - \cos \phi}} + \frac{1}{2} \cos \phi ,$

$$g_2(\phi) = -\frac{7}{4\sqrt{2}(1-\cos\phi)^{3/2}} + \frac{11}{8\sqrt{2}\sqrt{1-\cos\phi}} - \frac{\sqrt{1-\cos\phi}}{8\sqrt{2}} - \cos 2\phi,$$

$$\text{and} \quad g_3(\phi) = \left\{ -\frac{5}{4\sqrt{2}(1-\cos\phi)^{3/2}} + \frac{1}{8\sqrt{2}(1-\cos\phi)^{1/2}} - 2\cos\phi \right\} \sin\phi \tag{18}$$

Terms of the third and higher degrees in $\frac{\delta a}{a'}$, k, h, k' and h' have been neglected.

The Relative Equilibrium Solutions

We suppose that the long period part of the problem has been separated from the short period part by Von Zeipel's transformation or an equivalent procedure, and proceed to solve the equations for the mean and long period parts of the elements. The transformations will add to the disturbing function terms proportional to $(m')^2$ and higher powers of m', but we will work now only to the first order in m'. The equations then take the form

$$\frac{d}{dt}(\delta a) = \frac{m'na^2}{a'}\left[\sin\phi\left\{2 - \frac{1}{\sqrt{2}(1-\cos\phi)^{3/2}}\right\} + 2\frac{\partial X}{\partial a}\right]$$

$$= m'na'\sin\phi\left[2 - \frac{1}{\sqrt{2}(1-\cos\phi)^{3/2}} + 3\left(\frac{\delta a}{a'}\right)\left\{2 - \frac{1}{2\sqrt{2}(1-\cos\phi)^{3/2}}\right\}\right], \tag{19}$$

$$\frac{d\phi}{dt} = n - n' - \frac{2m'na^2}{a'}\frac{\partial X}{\partial \delta a} + \frac{m'na}{2a'}\left(k\frac{\partial X}{\partial k} + h\frac{\partial X}{\partial h}\right)$$

$$= n - n' + m'n\left[\frac{1}{\sqrt{2(1-\cos\phi)}} - 2 + 2\cos\phi + \left(\frac{\delta a}{a'}\right)\left\{-1 + \frac{1}{2\sqrt{2(1-\cos\phi)}} + \frac{1}{\{2(1-\cos\phi)\}^{3/2}} + 2\cos\phi\right\}\right], \tag{20}$$

$$\frac{dk}{dt} = -\frac{m'na}{a'}\frac{\partial X}{\partial h} - \frac{m'na}{2a'}k\left[\sin\phi\left\{2 - \frac{1}{\sqrt{2}(1-\cos\phi)^{3/2}}\right\} + \frac{\partial X}{\partial \varphi}\right]$$

$$= -m'n\left\{2hg_1(\phi) + h'g_2(\phi) + k'g_3(\phi)\right\}$$

$$-\tfrac{1}{2}m'nk\sin\phi\left\{2 - \frac{1}{\sqrt{2}(1-\cos\phi)^{3/2}}\right\}, \qquad (21)$$

and $$\frac{dh}{dt} = \frac{m'na}{a'}\frac{\partial X}{\partial k} - \frac{m'na}{2a'}h\left[\sin\phi\left\{2 - \frac{1}{\sqrt{2}(1-\cos\phi)^{3/2}}\right\} + \frac{\partial X}{\partial \varphi}\right]$$

$$= m'n\left\{2kg_1(\phi) + k'g_2(\phi) - h'g_3(\phi)\right\}$$

$$-\tfrac{1}{2}m'nh\sin\phi\left\{2 - \frac{1}{\sqrt{2}(1-\cos\phi)^{3/2}}\right\}, \qquad (22)$$

The equation (19) shows that δa is constant only if $\phi = \pi$, which is the collinear relative equilibrium configuration with P and J on opposite side of S, or if $\delta a = 0$ and $2 - \frac{1}{\sqrt{2}(1-\cos\phi)^{3/2}} = g$ the latter requiring $\cos\phi = \frac{1}{2}$, that is, $\phi = \pm \pi/3$. This is the equiangular triangle configuration. Substituting in (20) shows that ϕ is constant, since $n = n'$, and, putting $\phi = \pm \pi/3$ in (18), (21) and (22) give

$$\frac{dk}{dt} = -m'n\left\{27/8\ h - 27/16\ h' \mp 27/16\sqrt{3}\ k'\right\}, \qquad (23)$$

and $$\frac{dh}{dt} = m'n\left\{27/8\ k - 27/16\ k' \pm 27/16\sqrt{3}\ h'\right\}. \qquad (24)$$

We can have k and h constant provided

$$h = 1/2\ h' \pm \sqrt{3}/2\ k' = e'\sin(\omega' \pm \pi/3), \qquad (25)$$

and $$k = 1/2\ k' \mp \sqrt{3}/2\ h' = e'\cos(\omega' \pm \pi/3). \qquad (26)$$

Thus $e = e'$, and $\omega = \omega' \pm \pi/3$, confirming that the orbit of P is congruent to that of J, but inclined to it at an angle $\pi/3$.

Librations About the Relative Equilibrium Positions

Put $\phi = \pi/3 + \delta\phi$. Then, to first order in m', $\delta\phi$, and δa, equations (19) and (20) lead to

$$\frac{d}{dt}(\delta a) = m'na' \left\{ 9/2\ \delta\phi \pm 3\sqrt{3}/2 \left(\frac{\delta a}{a'} \right) \right\} + O\left\{ (m')^2 \right\} \qquad (27)$$

and $$\frac{d}{dt}(\delta\phi) = -\frac{3n}{2a'}\ \delta a + O(m'n) ,$$

from which

$$\frac{d^2}{dt^2}(\delta\phi) \mp 3\sqrt{3}/2\ m'n \frac{d}{dt}(\delta\phi) + 27/4\ m'n^2\ \delta\phi = O(m'n^2) \qquad (28)$$

A trial solution $\delta\phi \propto \exp(\alpha t)$ leads to

$$\alpha^2 \mp 3\sqrt{3}/2\ m'n\ \alpha + 27/4\ m'n^2 = 0 ,$$

so that

$$\alpha = \pm \frac{3\sqrt{3m'}}{2} n\, i_e + O(m'n) . \qquad (29)$$

Thus the second term in (28) is of order $(m')^{3/2}n^2$, and so is of an order to which this equation has not been completely derived. Thus the expression (29) cannot be extended to higher powers in m' without computing some of the neglected powers of m' in (27), which would require knowledge of terms of order $(m')^2$ in $\bar{R}$.

To our accuracy, then, the solution for a and ϕ is

$$\begin{aligned} \delta\phi &= A \sin (\nu t + \epsilon) \\ \delta a^f &= - \sqrt{3m'}\, A \cos (\nu t + \epsilon) \end{aligned} \qquad (30)$$

where A and ϵ are disposable constants, and $\nu = \frac{3\sqrt{3m'}}{2} n$. Now for Jupiter, $m' = 1/1047$, and hence $\nu = 0.08028\ n$. The orbital period of Jupiter is 11.862 years, and so the period of the libration in a and ϕ is $\frac{11.862}{0.08028} = 147.8$ years. The amplitudes of the oscillations in $a' \delta \phi$ and δa are in the ratio $1 : \sqrt{3m'}$, that is 1· 8·6 : 1, and these correspond approximately to oscillations in the transverse and radial directions, so that this libration, when its amplitude A is small, is approximately an ellipse, with its centre at the equiangular triangle point, whose axes are in the ratio of 18·6 : 1, the minor axis being in the direction towards S.

For the eccentricity and apse, put

$$k = e' \cos (\omega' \pm \pi/3) + \delta k, \qquad (31)$$

and $h = e' \sin (\omega' \pm \pi/3) + \delta h.$

The equations (23) and (24) now give

$$\frac{d}{dt} (\delta k) = - 27/8\ m'n\ \delta h, \qquad (32)$$

and $\frac{d}{dt} (\delta h) = 27/8\ m'n\ \delta k.$

The solution of these is

$$\begin{aligned} \delta k &= C \cos (\gamma t + \delta) \\ \delta h &= C \sin (\gamma t + \delta) \end{aligned} \qquad (33)$$

where C and δ are disposable constants, and $\gamma = 27/8\ m'n =$ (34)
0.003222 n, substituting the value for Jupiter. The period of this motion is $2\pi/\gamma$ = 3682 years. Thus the eccentricity and apse longitude are given by

$$e \cos \omega = e' \cos (\omega' \pm \pi/3) + C \cos (\gamma t + \delta)$$
$$\text{and } e \sin \omega = e' \sin (\omega \pm \pi/3) + C \sin (\gamma t + \delta) . \qquad (35)$$

If $C < e'$, ω librates about $\omega' \pm \pi/3$, if $C > e'$, ω increases monotonially through all values.

The treatment of these librations in rotating rectangular coordinates in the restricted problem does not exhibit this very long period oscillation directly, but shows a short period oscillation corresponding to a small eccentricity, but with period differing from that of Jupiter by an amount corresponding to the motion of the apse given by (35) when $e' = 0$.

The relative equilibrium positions may be considered as a special case of periodic solutions associated with a commensurability of period, but differ from other such cases in that there are here two independent free librations about the solution, in place of only one, as in the other cases, and also in that the mean orbital period in librating solutions in the present case is always exactly equal to that of Jupiter, while the librating and periodic solutions associated with other commensurabilities in general have periods not exactly commensurable with that of Jupiter, since the exact linear relation that exists involves the apse motion as well as the mean motions in longitude.

25105

MODELS OF GAS FLOWS WITH CHEMICAL AND RADIATIVE EFFECTS

By

F. K. Moore

LECTURE NOTES

MODELS OF GAS FLOWS WITH CHEMICAL AND RADIATIVE EFFECTS

F. K. Moore

I DIFFERENTIAL EQUATIONS AND BASIC MODELS

In the course of these lectures we will consider flows with chemical activity and in which radiative effects are of significance, and in particular, those dealing with problems pertaining to re-entry and propulsion. We will be concerned mainly with chemical effects, and will not go into detail in connection with electrical (ionization) effects.

Entry Phenomena

Briefly, the hypersonic entry of a vehicle into an atmosphere may be described as follows: Initially, as the vehicle begins to penetrate the very rarefied outer atmosphere, it is subjected to a bombardment by the gas particles in its path. In the region where the mean free path of the molecules is very large compared with the dimensions of the body, the rebounding molecules do not interfere with other approaching molecules, and the vehicle suffers only the retarding effect due to direct collisions with the particles in its path. Further penetration into the denser regions of the atmosphere results in the establishment of a "Flow field", characterized by a mean free path somewhat less than the characteristic dimension of the vehicle. Thus, rebounding molecules encounter other molecules in the region surrounding the vehicle, so that the particles in the path of the vehicle are, to some extent, warned of its approach. As still lower altitudes are reached, these warning signals coalesce into a strong shock wave standing ahead of the vehicle.

Atmospheric entry, then, involves a progression from free molecular flow to continuum flow. In the region of the shock, collisions promote excitation of higher levels of internal energy of the molecules (vibration and rotation) resulting in first, dissociation, and if the velocity is sufficiently high, ionization of the gas. The flow field is shown schematically in Fig. 1.

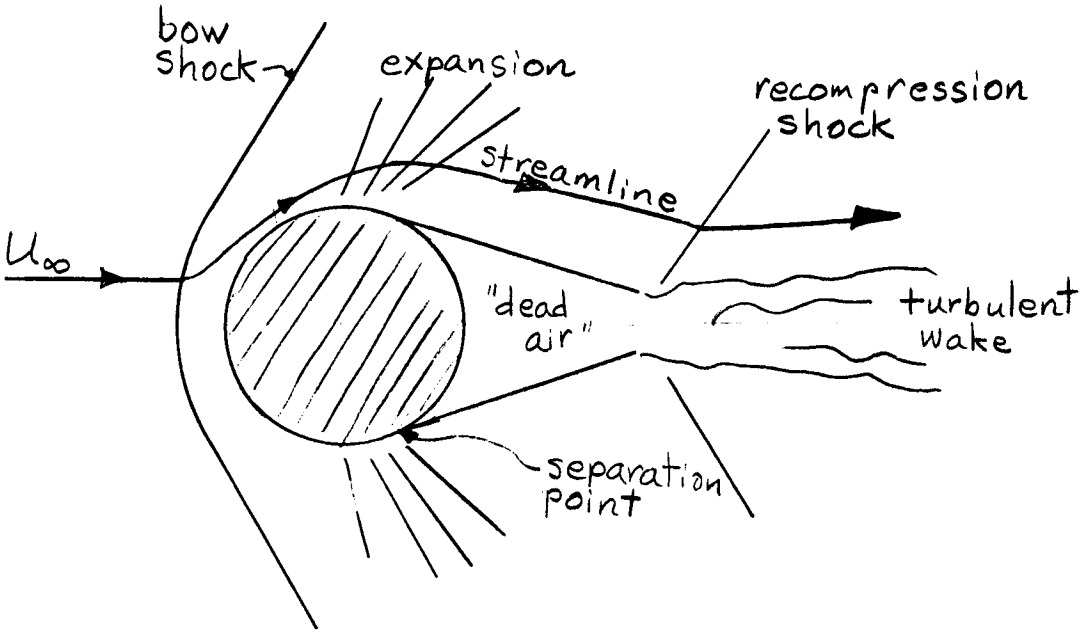

Fig. 1

Such flow fields of highly excited air are studied to determine rates of heat transfer at the surface of the vehicle. In their study, one must consider the behavior of the "real" gas at elevated temperatures. Furthermore, the nature of the flow field governs the mechanics of the motion of

the vehicle, the drag being of particular interest. One also finds that ionization of the flowfield affects communications with the vehicle. Thus, the study of high-temperature gas is of great importance.

As the temperature of a gas is increased on passing through a shock, compositional changes will take place. Considering air, we have the following dissociation processes:

$$O_2 \rightleftharpoons O + O$$

$$N_2 \rightleftharpoons N + N$$

as well as those involving NO formation, ionization, and others. Fig. 2 shows the concentrations of air versus temperature, at equilibrium. We note from the figure that oxygen shows a marked increase in dissociation at about 4000° K, whereas nitrogen does not dissociate appreciably until temperatures in excess of 8000° K are reached. 8000° K corresponds to velocities greater than those encountered in earth orbits, such high speeds being characteristic of entry from a lunar trajectory.

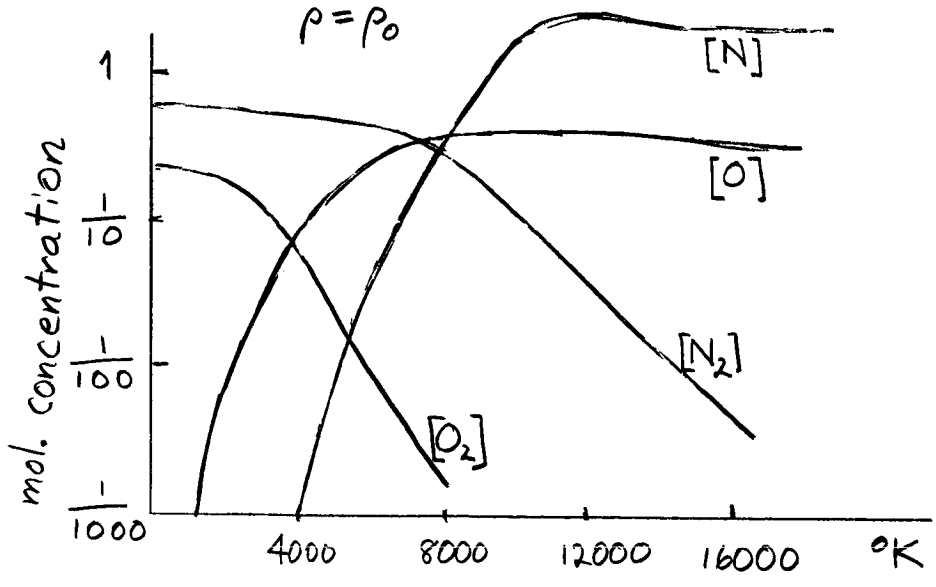

Fig. 2

In atmospheric entry problems, radiant heat transfer may be important. At orbital velocities, radiant heat transfer is relatively insignificant. However, at escape (capture) velocity typical of a lunar flight, radiation represents a major portion of the heat transfer. The following relations indicate the relative importance of convective and radiative transfer, and the dependence upon velocity: Let q be the heat load to the vehicle:[1]

then

$$q_{conv.} \propto \sqrt{\rho/L}\, U_\infty^3$$

$$q_{rad.} \propto \rho^{3/2} L\, U_\infty^{10}$$

where ρ is the density, L is a characteristic body dimension, and U_∞ is the vehicle velocity. The very strong dependence of radiative transfer on velocity is to be expected, because $q_{rad.} \propto T^4$ and $T \propto U_\infty^2$. Thus, one finds that at 25,000 ft/sec. q_{rad} is approximately 10% of the heat load, while at 35,000 ft/sec. q_{rad} is the dominant heat load factor.

Nonequilibrium

The composition of the gas at any point in the flow field is, of course, dependent upon the chemical kinetics of the gas. If the gas chemistry does not have time to equilibrate, that is to say, if the composition is not the same as the equilibrium composition for the local temperature, one has a nonequilibrium flow. At very high speeds and very high altitudes, flows may be dominated by nonequilibrium effects.

Of course, in a general sense, all flows are "nonequilibrium" situations. In basic fluid dynamics, the Reynolds number

$$Re = \rho U_\infty L/\mu$$

is a governing parameter, where U_∞ is a characteristic velocity, L is a characteristic length, ρ is the density and μ the viscosity. Now, the Reynolds number is in fact a comparison of relaxation time with the time of passage of the flow. Consider the time required for a diffusive process to occur, i.e., the relaxation time:

$$\tau_{relax.} = \rho L^2/\mu$$

For very large distances, a very long relaxation time is required, similarly, diffusive effects are slow for very small viscosity. Now, compare $\tau_{relax.}$ with the time of passage of the flow over a body of characteristic dimension L:

$$\tau_L = L/U_\infty$$

The ratio of these two characteristic times is

$$\frac{\tau_{relax.}}{\tau_L} = \frac{\rho L U_\infty}{\mu} \equiv Re \qquad (1)$$

This ratio is just the Reynolds number of the flow, and compares the time for a mixing process to occur with the time of flow passage over the body.

Similar parameters appear in other flows, and by way of comparison, we note that using the time of diffusion of a magnetic field yields

$$\frac{L^2 \mu_m \sigma}{L/U_\infty} = L U_\infty \mu_m \sigma \equiv Rm$$

where Rm is the so-called magnetic Reynolds number. The ratio of chemical relaxation time to the time of passage yields the following:

$$\frac{\tau_{chem.}}{\tau_L} = \frac{\tau_{chem.}}{L/U_\infty} \qquad (2)$$

This may be of unit order in high-speed flows at high altitudes.

For ordinary, viscous hydrodynamic flows, Re >> 1, i.e., the diffusive relaxation time is much greater than the time of passage. In this case the flow may be said to be dynamically "frozen" - there is insufficient time for the decay process to reach equilibrium. If the chemical parameter $\tau_{chem.}/\tau_L \gg 1$, we may speak of chemical freezing. Now, if the ratio $\tau_{chem.}/\tau_L = \mathcal{O}(1)$ one encounters serious difficulties in analysis, just as in ordinary hydrodynamic flows one encounters analytical problems when the Reynolds number is of order unity. On the other hand, if the ratio is much less than one, (equilibrium flow) great simplifications result.

The study of chemically reacting flows is, as one would expect, considerably more complicated than nonreacting flows. In the latter, one finds similarities from dimensional analysis, and these can be used to great advantage. In chemical kinetics, however, such similarities do not generally occur, and therefore one must attempt to solve particular problems and hope to find simplifications which will render the analysis tractable.[2]

Equations of Motion

From basic fluid dynamics we have:

continuity: $$\frac{\partial \rho}{\partial t} + \nabla \cdot (\rho \underline{v}) = 0 \qquad (3)$$

Since the gas consists of several constituents we require a continuity equation for the separate constituents:

$$\rho \frac{Dc_i}{Dt} - W_i = -\frac{\partial}{\partial n}(\rho c_i u_{n_i}) \qquad (4)$$

where $$\frac{D}{Dt} \equiv \frac{\partial}{\partial t} + \underline{v} \cdot \nabla$$

and the other symbols are:

c_i the mass fraction of the i'th constituent

ρ the density

W_i a production term to be discussed shortly

$\partial/\partial n$ the gradient normal to the surface

u_{n_i} the diffusion velocity of the i'th constituent

Eq. (4) states that the rate of increase of the particular species is equal to the rate of production (by chemical reaction) of that species, minus the diffusion of that species across some control surface. We note that:

$$\sum_i c_i = 1$$

The bracketed quantity on the right hand side of Eq. (4) deserves attention. We can write:

$$\rho c_i u_{n_i} = \rho m_i \left(\sum_i \frac{c_i}{m_i}\right)^2 \sum_j m_i D_{ij} \left\{ \frac{\partial}{\partial n}\left(\frac{c_i}{\sum_i \frac{m_j}{m_i} c_i}\right) + \left[\frac{\sum_i c_i \left(1 - \frac{m_j}{m_i}\right)}{\sum_i \frac{m_j}{m_i} c_i}\right] \frac{\partial \ln p}{\partial n} \right\} + D_i^T \frac{\partial \ln T}{\partial n}$$

The terms here are:

D_{ij} diffusion coefficient for inter-diffusion of constituents.

$\frac{\partial \ln p}{\partial n}$ the "pressure diffusion", i.e., due to grad p. (In most flowfields $\partial p/\partial n$ may be neglected here.)

$D_i^T \frac{\partial \ln T}{\partial n}$ thermal diffusion term - diffusion due to temperature gradient only, and is usually neglected, since the coefficient is small.

Thus, u_{n_i} is seen to depend largely upon the concentration gradient.

Equation of state: $$p = \rho \left(\sum_i \frac{c_i}{m_i}\right) \mathcal{R} T \qquad (5)$$

where $\mathcal{R}$ is the universal gas constant.

Momentum equation: $$\rho \frac{Dv}{Dt} + \nabla p = \frac{\partial}{\partial n}\left(\mu \frac{\partial v}{\partial n}\right) \qquad (6)$$

Energy equation:

$$\rho \frac{DH}{Dt} - \frac{\partial p}{\partial t} - \underline{v} \cdot \nabla p - q_R = \mu \left(\frac{\partial u}{\partial n}\right)^2 + \frac{\partial}{\partial n}\left[\lambda \frac{\partial T}{\partial n} - \rho \sum_i u_{n_i} H_i\right] \qquad (7)$$

and we identify the following quantities:

H is specific enthalpy, and $H = \sum_i H_i = \sum_i c_i (h_i + h_i^{(0)})$ where h_i is specific internal enthalpy and $h_i^{(0)}$ is the (potential) chemical energy of dissociation

q_R is a heat source term, for example, radiation heating

$\mu \left(\frac{\partial u}{\partial n}\right)^2$ the viscous dissipation term

$\lambda \frac{\partial T}{\partial n}$ the heat conduction term

$\sum_i u_{n_i} H_i$ the diffusion of enthalpy

Lumped Constituents

A useful approximation, or gas model, frequently employed is that of "lumped constituents". In effect, we normally use the lumped constituents idea in aerodynamic problems, letting air take on an average molecular weight, etc., neglecting interdiffusion of constituents as well as chemical reaction. For low-temperature problems, it is not necessary that the constituents be similar.

In cases where chemistry is involved, we can use the same approach to simplify the analysis. Briefly, for air, we have a mixture of O_2 and N_2, and in dissociating flows we have, in addition, O and N. Let us combine these four constituents, considering O and N as a monatomic gas which we denote by A, and O_2 and N_2 as a diatomic gas, denoting it A_2. We then have a two-constituent gas, and the i's of Eqs. (4) to (7) may have the values 1, 2. Now, this "lumping" requires that the molecular weights of the two gases be nearly the same, as well as that there is no net diffusion

or reaction between gases lumped in the same group. That is, we assume that the interdiffusion of O and N is small, and that the reactions between O and N are negligible, and similarly for the "A_2" portion of the gas. It is also necessary that the heats of dissociation be nearly the same for both reacting pairs. Thus, we shall consider reactions of the form:

$$A_2 \rightleftharpoons A + A$$

and the right hand side of Eq. (4) becomes:

$$\rho c_i u_{ni} = \rho \mathcal{D} \frac{\partial c_i}{\partial n}$$

Binary Mixture

We will now use the subscript 1 to denote A atoms, and 2 to denote A_2 molecules. The equation for specific enthalpy may then be written[5]:

$$H = \frac{RT}{m_2}\left\{5c_1 + 4c_2\left[\frac{7}{8} + \frac{1}{4}\left(\frac{T_v/T}{e^{T_v/T}-1}\right)\right]\right\} + c_1 h_1^{(0)} \qquad (8a)$$

where $\frac{5Rc_1}{m_2}$ is the specific heat at constant pressure of a monatomic gas, $\frac{7}{2}\frac{Rc_2}{m_2}$ is that of a rotationally-excited diatomic gas, and the term $\left(\frac{T_v/T}{e^{T_v/T}-1}\right)c_2$ accounts for energy of vibration, and finally, $c_1 h_1^{(0)}$ is the energy of dissociation. T_v is the characteristic temperature for vibration. Since T_v is about 3000° K for air, the quantity $\frac{1}{4}\left(\frac{T_v/T}{e^{T_v/T}-1}\right) \approx 0$ for air at room temperature. Also, we note that

$$0 < \left(\frac{T_v/T}{e^{T_v/T}-1}\right) < 1$$

Lighthill Ideal Dissociating Gas

The foregoing gas model is not calorically perfect, for Eq. (8a) indicates that the specific heat depends upon temperature. Lighthill[5] observed that the bracketed quantity above was very nearly constant for a large range of temperature and he assumed that $\frac{T_v/T}{e^{T_v/T}-1} = \frac{1}{2}$ (midway between the extremes 0 and 1, thus rendering the model calorically perfect. This is the first Lighthill gas approximation, and with it we have:

$$H = \frac{RT}{m_2}(4+c_1) + c_1 h_1^{(0)} \tag{8b}$$

which is the relationship for the enthalpy of an ideal, calorically perfect, dissociating gas. A further approximation due to Lighthill is as follows: Consider the equilibrium concentrations of the atoms and molecules, according to the law of mass action,

$$\left(\frac{c^2}{1-c}\right)_{eq.} = \frac{\rho_D}{\rho} e^{-\frac{2h^{(0)}}{RT/m_2}} \tag{9}$$

where c is the atom concentration. From this equation it is seen that at high altitudes, i.e., low densities, one could expect to find higher concentrations of atoms. The characteristic density is actually dependent upon temperature:

$$\rho_D \propto \sqrt{T}\left(1-e^{T_v/T}\right)$$

For temperatures of interest, ρ_D exhibits a relative maximum, and is fairly constant, and is therefore assumed constant, without introducing serious error. In fact, we may add to Lighthill's argument the observation that ρ_D reaches a maximum at precisely the temperature

$$T = \frac{2T_v}{e^{T_v/T}-1}$$

This is the temperature at which eq. (8b) is exact; i.e., the square bracket

of Eq. $(\overset{a}{\hat{8}})$ for specific enthalpy is just equal to unity. Thus, Eqs. (8b) and (9) are consistent descriptions of a dissociating gas which is just 50% excited vibrationally.

The foregoing "Lighthill model" is not particularly powerful analytically, though T_v is eliminated as a parameter. It does not result in any appreciable simplification in machine calculations. The main value of the model has been that it provides a standard dissociating gas in terms of which various computations and theories may be compared.

Dissociation Kinetics

Consider the reaction

$$M + A_2 \underset{k_D}{\overset{k_R}{\rightleftharpoons}} A + A + M$$

where M may be A_2 or A. M is the third party to the process and is the particle which, in collision, shares the energy of either dissociation or recombination. We can write

$$\frac{W_1}{\rho} = \text{const.}\, \frac{T^{-(s+1)}\rho}{1+c}\left[1-c+2\frac{k_D^{(1)}}{k_D^{(2)}}c\right]\left[(1-c)e^{-T_D/T} - \frac{\rho}{\rho_D}c^2\right] \qquad (10)$$

where W_1 is the production rate for atoms (zero for equilibrium), and T^{-s} is a temperature dependence factor. This equation embodies the relation between k_D and k_R at equilibrium $(W_1 = 0)$ obtained from the mass action law. The first square bracket accounts for the different third body in the collision, i.e., whether M is A or A_2. The term $(1-c)e^{-T_D/T}$ in the second bracket deals with the forward reaction (dissociation), while the term $\left(-\frac{\rho}{\rho_D}c^2\right)$ deals with the reverse reaction (recombination). Substituting for $\frac{\rho}{\rho_D}$ from Eq. (9) renders the second square bracket zero, which is the result desired for equilibrium. It is important to note that the

dissociation in Eq. (10) is second order in density, while the recombination term is third order in density.

In addition,

$$\frac{k_D^{(1)}}{k_D^{(2)}} \approx 35 \frac{T}{T_D} \text{ , from experiment}^{3,4}.$$

Freeman, in a paper emphasizing the Lighthill model, has, in effect, taken the first square bracket to be equal to a constant. This simplification of Eq. (10) is therefore often taken as one of the specifications of Lighthill's ideal gas.

II SOUND WAVES

Perturbation Equations for Chemical Nonequilibrium

For sound waves (acoustics) with chemical relaxation and radiative effects, we first write the perturbation equations for a binary mixture of gases. The primed quantities denote the perturbations, e.g.,

$$\rho = \rho_0 + \rho' \quad , \quad p = p_0 + p' \quad , \quad \underline{v} = \underline{v}'$$

The linearized equations are then:

Continuity: $$\frac{\partial \rho'}{\partial t} + \rho_0 \nabla \cdot \underline{v}' = 0$$

Momentum: $$\rho_0 \frac{\partial \underline{v}'}{\partial t} + \nabla p' = 0$$

Energy: $$\rho_0 \frac{\partial H'}{\partial t} - \frac{\partial p'}{\partial t} = 0$$

State: $$\frac{p'}{p_0} = \frac{c'}{1+c_0} + \frac{\rho'}{\rho_0} + \frac{T'}{T_0}$$

Production Equation: $$\frac{W_1}{\rho_0} \propto \left[(1-c) e^{-T_D/T} - \frac{\rho}{\rho_D} c^2\right]$$

From Eq. (9), $\left(\frac{c^2}{1-c}\right)_{eq} = \frac{\rho_D}{\rho} e^{-T_D/T}$, we substitute in Eq. (10) for ρ/ρ_D and obtain $\frac{W_1}{\rho} \propto \left[(1-c)e^{-T_D/T} - \frac{c^2(1-c_{eq})}{c_{eq}^2} e^{-T_D/T}\right]$ which, after factoring, including $\left[\frac{(1-c_{eq})(1-c)}{c_{eq}^2} e^{-T_D/T}\right]^{-1}$ in a proportionality factor, and changing sign, gives

$$-\frac{W_1}{\rho} \propto \left[\frac{c^2}{1-c} - \frac{c_{eq}^2}{1-c_{eq}}\right] \tag{12}$$

All the quantities lumped into the proportionality factor are functions of state. Now, if equilibrium prevails, $c = c_{eq}$ and we have $W_1 = 0$. If $c \neq c_{eq}$, the expression indicates that the production rate will vary, to cause the mixture to tend toward equilibrium. In this derivation we ~~have~~ express the mass fraction as $c = c_0 + c'$ and assumed that c' is a small quantity. We also note that $c_{eq} = c_0 + c_{eq}'$, where c_0 is the free-stream equilibrium concentration, to account for the dependence of c_{eq} upon local temperature and density. From the proportionality, Eq. (12), we can linearize the term,

$$\frac{c^2}{1-c} - \frac{c_{eq}^2}{1-c_{eq}}$$

to obtain $c_0 \frac{2-c_0}{1-c_0}(c' - c_{eq}')$ and finally write

$$-\frac{W_1}{\rho_0} = \frac{1}{\tau}(c' - c_{eq}') = -\frac{\partial c'}{\partial t} \tag{13}$$

Here all the proportionality terms are lumped into τ, which is a relaxation time.

We now generate a sound wave within the gas and examine its effects. If c_{eq}' were constant, one would simply solve Eq. (13) to find:

$$c' = c_{eq}'\left(1 - e^{-t/\tau}\right)$$

This is a relaxation equation, where the concentration goes from an initial to a final level following a simple exponential curve. However, since c_{eq} is a function of temperature and density, such a solution is rarely of value.

We now specify, as in ordinary acoustics, that the wave be curl-free, so that:

$$\underline{v}' = \nabla\phi$$

where ϕ is the potential. The acoustic equation obtained from Eqs. (11) and (13) is now[6, 7, 11, 12, 13, 14]

$$\tau^* \frac{\partial}{\partial t}\left(\frac{\partial^2\phi}{\partial t^2} - a_f^2 \nabla^2\phi\right) + \frac{\partial^2\phi}{\partial t^2} - a_e^2 \nabla^2\phi = 0 \qquad (14)$$

The second bracket is the usual acoustic wave equation, with a_e, the equilibrium sound speed (isentropic) given by:

$$a_e = \sqrt{\gamma R T}$$

(R is the universal gas constant divided by the molecular weight)

τ^* is a reference relaxation time, and if τ^* is large, we have frozen flow, since the first bracket predominates. The first bracket is the frozen wave operator, wherein the velocity of propagation is a_f, the frozen sound speed. a_f is found to be somewhat greater than a_e, and one may think of the gas as being stiffer in the frozen flow case. If the relaxation time is short, i.e., τ^* small, we may neglect the first bracket, and we have ordinary equilibrium flow, with acoustic propagation of small disturbances at the speed a_e.

If τ^* is of the order of the period of the disturbance, the equation can be solved exactly, but the solution is not particularly edifying. It is of more interest to begin by considering a wave with a discontinuity, i.e., a jump wave as produced by a piston. A general solution of the classical wave equation is $\phi = \phi(x - at)$, which includes the step function

$\phi = 1(x-at)$. We represent the piston and wave motions on a t-x plot, as in Fig. 3.

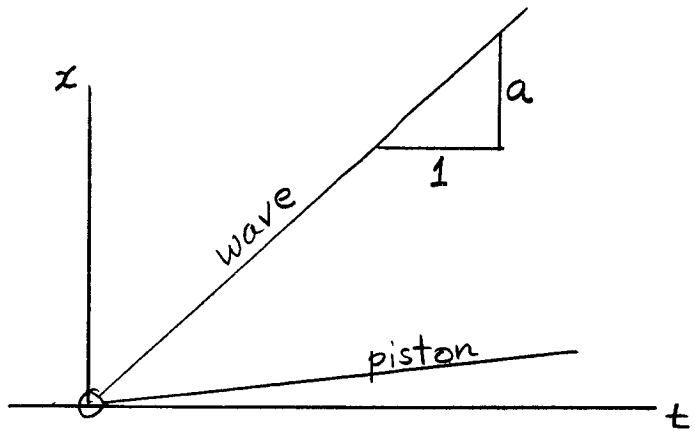

Fig. 3

In the case of combined waves subject to Eq. (14), one expects a solution closely related to that for the classical wave equation. Accordingly, we transform to coordinates ξ and η, where

$$\left.\begin{aligned} \xi &\equiv \frac{1}{a_f \tau^*}(x-at) \\ \text{and} \quad \eta &\equiv \frac{1}{a_f \tau^*}\, x \end{aligned}\right\} \tag{15}$$

Thus, ξ is the distance measured from $\overset{a}{\wedge}$ characteristic as yet undefined, and η is the distance the piston has traveled. Eq. (14) becomes

$$-\frac{a}{a_f}\left[\frac{a^2}{a_f^2}\phi_{\xi\xi\xi} - (\phi_{\xi\xi\xi} + 2\phi_{\xi\xi\eta} + \phi_{\xi\eta\eta})\right]$$

$$+\left[\frac{a^2}{a_f^2}\phi_{\xi\xi} - \frac{a_e^2}{a_f^2}(\phi_{\xi\xi} + 2\phi_{\xi\eta} + \phi_{\eta\eta})\right] = 0 \tag{16}$$

where the subscripts denote partial differentiation. The highest order derivatives must vanish

$$\frac{a^2}{a_f^2}\,\phi_{\xi\xi\xi} - \phi_{\xi\xi\xi} = 0$$

and hence we must have $a = a_f$, and we conclude that jump-waves must propagate at the frozen sound speed.

Now, the terms involving $\phi_{\xi\xi}$ must also combine to equal zero, thus:

$$-\frac{a}{a_f}\left(-2\phi_{\xi\xi\eta}\right) + \frac{a^2}{a_f^2}\,\phi_{\xi\xi} - \frac{a_e^2}{a_f^2}\,\phi_{\xi\xi} = 0$$

and because $a = a_f$,

$$2\phi_{\xi\xi\eta} + \left(1 - \frac{a_e^2}{a_f^2}\right)\phi_{\xi\xi} = 0$$

Upon integrating once, along the wave front, we find

$$\left(\phi_{\xi\xi}\right)_{\xi=0} = e^{-\epsilon\eta} \tag{17}$$

where

$$\frac{1}{2}\left(1 - \frac{a_e^2}{a_f^2}\right) \equiv \epsilon$$

is a rather small quantity. This equation shows that the jump amplitude decreases with distance, (i.e., $\eta \propto x$) and we have a decay of amplitude of the wave head, as illustrated in Fig. 4:

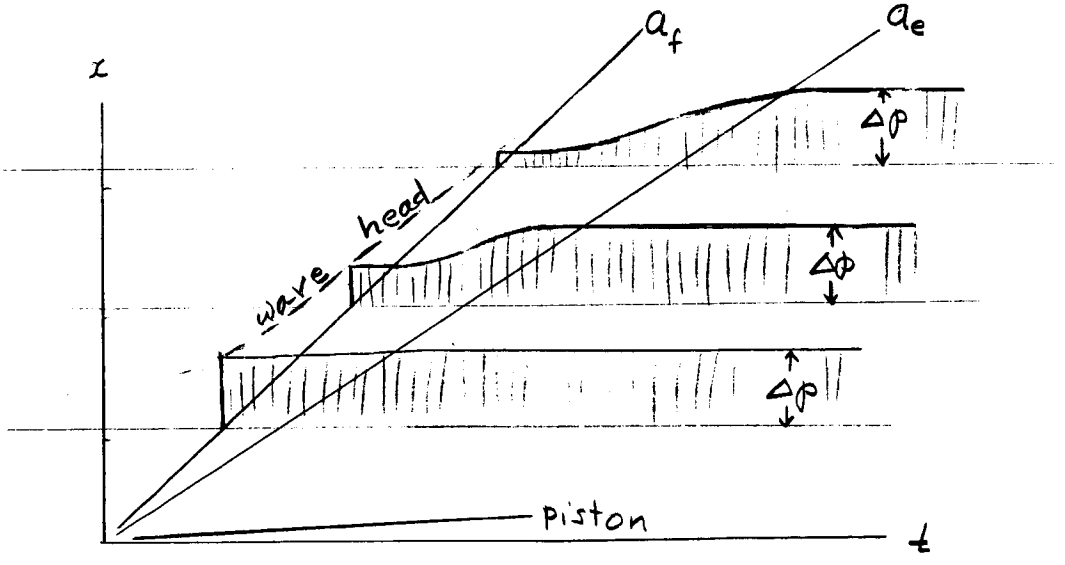

Fig. 4[7]

The Telegraph Equation

Allowing ϵ to approach zero, and redefining the piston-travel coordinate by $\epsilon\eta \equiv \zeta$, we get a new equation, after integrating Eq. (16) once with respect to ζ:

$$\phi_{\xi\zeta} + \phi_{\xi} - \phi_{\zeta} = 0 \tag{18}$$

for small ϵ. This Eq.)18) is related to the telegraph equation, and provides a model for the relaxing sound wave. Eq. (18) can be solved exactly:

$$v' = e^{-(\xi+\zeta)} \frac{\partial}{\partial \xi} \int_0^{\xi} I_0\left[2\sqrt{\zeta(\xi-\omega)}\right] e^{\omega} f(\omega)\, d\omega$$

where I_0 is a zero-order Bessel function of an imaginary argument, and $f(\omega)$ is a source function for the piston motion. The nature of the solution indicates how the frozen wave decays and changes to an ordinary wave. The decay is due to energy absorption in dispersing the wave. Thus, when chemical activity is present, and we have nonequilibrium conditions, there results an interplay between the chemical kinetics and the dynamic processes. This results in the dispersion of the wave. The relaxation time plays a rôle somewhat analogous to that of viscosity.

Waves Affected by Heat Sources

Turning now to the acoustic problem involving heat sources which might be thought of as due to radiative heat transfer, we write the equations of motion for one dimension:

$$\left.\begin{aligned} &\text{Continuity} && \frac{\partial \rho'}{\partial t} + \rho_0 \frac{\partial u'}{\partial x} = 0 \\ &\text{Momentum} && \rho_0 \frac{\partial u'}{\partial t} + \frac{\partial p'}{\partial x} = 0 \\ &\text{Energy} && \rho_0 \frac{\partial H'}{\partial t} - \frac{\partial p'}{\partial t} = q'(T') \\ &\text{State} && \frac{p'}{p_0} = \frac{\rho'}{\rho_0} + \frac{T'}{T_0} \end{aligned}\right\} \qquad (19)$$

and we note that the right hand side of the energy equation is a heat source term and plays somewhat the same rôle as does the chemical production term in Eqs. (11). We also have $u' = \phi_x$, $p' = -\rho \phi_t$ as before. Manipulation of these equations yields

$$\phi_{tt} - a^2 \phi_{xx} = -\frac{\gamma - 1}{\rho_0} q'(T') \qquad (20)$$

where a is the ordinary isentropic sound speed. A second equation also results, which is

$$\phi_{tt} - \frac{a^2}{\gamma} \phi_{xx} = -R \frac{\partial T'}{\partial x} \qquad (21)$$

where a^2/γ is the "isothermal" sound speed: For an isothermal wave, $a_T^2 = \left(\frac{\partial p}{\partial \rho}\right)_T = RT$, and thus $a^2/\gamma = a_T^2$.

The problem now is to combine Eqs. (20) and (21). If $q' = q'(T')$, then, in principle, T' may be eliminated between Eqs. (20) and (21). In order to illustrate the effects of radiative transfer, whereby the hot region loses heat to the cold region, we will be more specific, and write the simple proportionality

$$q' = -\left[\frac{1}{k} \quad \frac{\rho_0 R}{\gamma - 1}\right] T'$$

Then, elimination of T' yields Eq. (14) again, except that τ^* is replaced by k ! Thus,

$$k\frac{\partial}{\partial t}\Box_s^2\phi + \Box_T^2\phi = 0 \qquad (22)$$

where $\Box^2$ is the wave operator, $\frac{\partial^2}{\partial t} - a^2\frac{\partial^2}{\partial x^2}$, the subscripts s and T being for the isentropic and the isothermal sound speeds respectively. If k is very large, we get the isentropic wave. If k is very small we get the isothermal wave. For cases where radiation is intense, the effect of the radiative heat transfer will generally be to redistribute the energy and reduce temperature gradients. We note at this point that a^2 is only slightly greater than a^2/γ since γ is near unity, and one could also derive a form of the telegraph equation Eq. (18)) for this heat addition case.

Relation to Radiation Transport [8, 9]

The foregoing assumption, that $\partial q'/\partial T' = \text{const.}$ is not actually valid for radiative transport, and we must examine more fully the transport of energy by radiation to determine the proper general expression for q_R.

Radiative energy emitted by an element of the hot gas may be absorbed by another element, at some distance, or "penetration depth" from the first. This distance is expressed as a reciprocal absorption coefficient, $1/\alpha_\nu$ for a given frequency ν. For a gas, $1/\alpha_\nu$ could be as long as one kilometer. If the gas is in a uniform state over distances much larger than this, full "radiative equilibrium" prevails, and there is no heat flux, because the heat emitted and absorbed by each element is the same. However, in problems of interest in hypersonic flows, one must consider the hot gases at the nose to be confined to a small region, only centimeters thick. We cannot therefore, assume full radiative equilibrium (see Fig. 5).

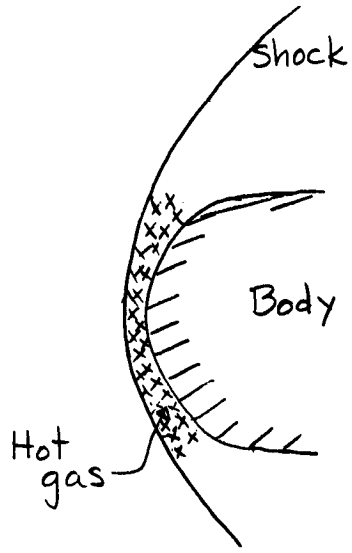

Fig. 5

In flow about such bodies, the path length of radiation is large compared to a characteristic dimension for temperature change in the flow. It is necessary then, to evaluate the integral,

$$q_R = \int_0^\infty (A_\nu - E_\nu)\, d\nu \tag{23}$$

where A_ν is radiant energy absorbed, and E_ν is energy emitted, in the frequency range ν to $\nu + d\nu$. The theory to be outlined is in "Radiative Transfer" by S. Chandrasekhar (Dover Press)[8], and is reviewed also by Lighthill[9], Goulard[10], and Vincenti and Baldwin[11].

Quasi-equilibrium Assumption

In dealing with Eq. (23), it is commonly assumed that atoms and molecules are in local thermal equilibrium, so that the gas element emits as a black body. This requires that particle collisions be much more frequent than photon emissions. Then, one may write

$$E_\nu = 4\pi \alpha_\nu B_\nu$$

where B_ν is the black-body energy flux obtained from the statistical mechanics of a "photon gas", and $\int_0^\infty B_\nu d\nu = \frac{1}{\pi}\sigma T^4$, σ being the Stefan-Boltzmann constant. Now, by the "quasi-equilibrium" assumption the absorption coefficient α_ν is also taken to have its black-body value, not only for emission, but for absorption as well:

$$A_\nu = \alpha_\nu \int_0^{4\pi} I_\nu(\Omega)\, d\Omega \tag{23a}$$

For full radiative equilibrium, $I_\nu = B_\nu/4\pi$, but here we must imagine that the "spectral intensity", I_ν, results from emission somewhere else at some other temperature. Ω is the solid angle defining the direction of the incoming radiation (see Fig. 6). I_ν may be found from the "equation of radiative transfer" (Chandrasekhar, page 9).

$$-\frac{\partial I_\nu}{\partial s} = \alpha_\nu (I_\nu - B_\nu) \tag{24}$$

which says that along its path, s, the intensity diminishes by absorption $(\alpha_\nu I_\nu)$ and is augmented by black-body emission $(\alpha_\nu B_\nu)$, scattering into or out of the beam being neglected.

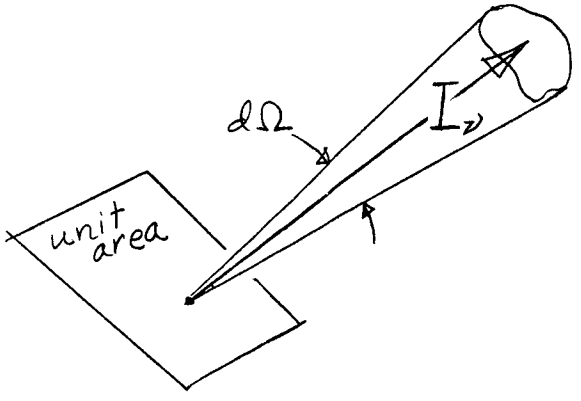

Fig. 6

Eq. (24) may be solved for I_ν, subject to boundary conditions about bounding surfaces, and the result, via Eq. (23a), may be used to evaluate q_R from Eq. (23). In carrying out this process, a constant value of α_ν is commonly assumed. This disregard of the frequency dependence of α is called the "gray-gas" assumption. (This has been recently described in Ref. 11.)

The Rosseland Limit

We have mentioned that $1/\alpha$ may be as large as 10^5 cm. A characteristic length, say L, is likely to be much larger than this (radiative equilibrium) only in astrophysical problems. If $1/\alpha$ is small (but not negligibly so) compared with L, then it may be regarded as a photon free path length, and in this "Rosseland limit", radiative transfer depends upon grad T, just as heat transfer by conduction does. In fact, Rosseland found,

$$q_R = \frac{16}{3} \frac{\sigma T^3}{\alpha} \text{grad } T$$

The foregoing Rosseland formula cannot be used for shock layers because $L << 1/\alpha$, in general. However, the quasi-equilibrium assumption is usually quite good. Ordinarily, there are, say, 10^{10} collisions per sec. for particles, and $c\alpha$ is $3 \times 10^{10}/10^5$ or only about 10^5 photon interactions per second, and thus, the requirement is met. At very high altitude, the collision frequency would be too low to maintain quasi-equilibrium, and radiation transfer would be "collision limited".

Radiation pressure and the contribution of radiation to the internal energy of the gas is usually neglected. The following example will serve to indicate the magnitude of these effects and show why it is reasonable to omit them. Consider the intensity of black-body radiation from a source at 8000° K. The energy flux E_R is given by

$$E_R = \frac{1}{\pi}\sigma T^4 \approx \frac{5.67\cdot10^{-8}\cdot 4.1\cdot10^{15}}{3.14} \approx 8\cdot10^3 \frac{\text{joule}}{\text{cm}^2\,\text{sec}}$$

To find the corresponding specific density E_D, i.e., the internal energy of radiation, we divide by the velocity of light, C,

$$E_D \approx \frac{8\cdot10^3}{3\cdot10^{10}} \approx 3\cdot10^{-7} \frac{\text{joule}}{\text{cm}^3} = 3\frac{\text{erg}}{\text{cm}^3}$$

and the radiation pressure is

$$P_R = \frac{1}{3}E_D \approx 1 \frac{\text{dyne}}{\text{cm}^2}$$

Thus, while the energy transfer by radiation is considerable, the internal energy due to radiation, and radiation pressure, are both negligible when compared to the enthalpy of the order of 10^8 erg/cm^3, and the static pressure of the order of 10^5 dyne/cm^2, which are typical of hypersonic flows.

Application of Radiative Transfer Theory to Waves[11, 12, 13]

The problem of the effect of thermal radiation on acoustic waves has been investigated quite thoroughly in Refs. 11 and 13. In Ref. 11, two dimensionless parameters of the problem are discussed; i.e., the "Bueger number",

$$N_{Bu} \equiv \alpha L$$

and the "Boltzmann Number".

$$N_{Bo} \equiv \frac{c_p \rho V}{\sigma T^3}$$

These two parameters govern the combination of fluid convection and radiative transfer. Physically, these parameters have the following meaning:

$N_{Bo} \to \infty$	implies a completely cold gas (i.e., $T \to 0$)
$N_{Bo} \to 0$	implies a very hot gas
$N_{Bu} \to \infty$	implies a completely opaque gas ($\frac{1}{\alpha}$ small)
$N_{Bu} \to 0$	implies a completely transparent gas

These upper and lower limits of the two parameters lead to limiting cases of sound wave propagation with radiative effects. If $N_{Bo} \to \infty$ (completely cold gas) or $N_{Bu} \to 0$, (completely transparent gas) the solution to the problem is the classical isentropic acoustic wave, because no radiative transfer takes place under these circumstances. If $N_{Bu} \to \infty$ (completely opaque gas), the classical isentropic wave is again the solution, because in this case, although radiation may be intense, it is immediately reabsorbed near its point of emission, and once again no net radiative transfer takes place. If the gas is quite hot, and quite transparent, radiation tends to smooth out temperature gradients, and an acoustic wave travels at the isothermal sound speed rather than the isentropic sound speed. Thus waves vary in their speeds of propagation, changing from the isentropic sound speed at small N_{Bu} to the isothermal sound speed in a range near $1.5\, N_{Bu} = \frac{N_{Bo}}{\gamma \cdot 8,33}$. Also, within this range of "velocity dispersion" the damping of the wave due to radiation reaches a maximum. For large values of N_{Bu}, the wave speed returns to the isentropic sound speed, and there may appear another sharp local peak in the damping.

In the analysis of harmonic waves[11], it appears that in addition to the classical acoustic wave traveling at either the isentropic or the isothermal sound

speed, there is a second, radiation induced, harmonic wave[11], which has no counterpart in classical acoustic theory. The speed and damping of this wave are strongly dependent upon N_{B_0} and N_{Bu}. Its speed varies from infinite at $N_{Bu} = 0$, to zero at $N_{Bu} \to \infty$ for all values of N_{B_0}. The damping varies from zero at $N_{Bu} = 0$ to infinite at $N_{Bu} \to \infty$. For a fixed finite value of N_{Bu}, the damping goes from a finite value at $N_{B_0} \to \infty$ to zero at $N_{B_0} = 0$, at the same time the wave speed goes from a very high value to a low value, then back again to a very high value. In general, this second wave has greater damping and higher speed than the classical wave, but at very high temperatures the damping may be comparable for both waves, and for a sufficiently opaque gas, the speeds may be essentially the same.

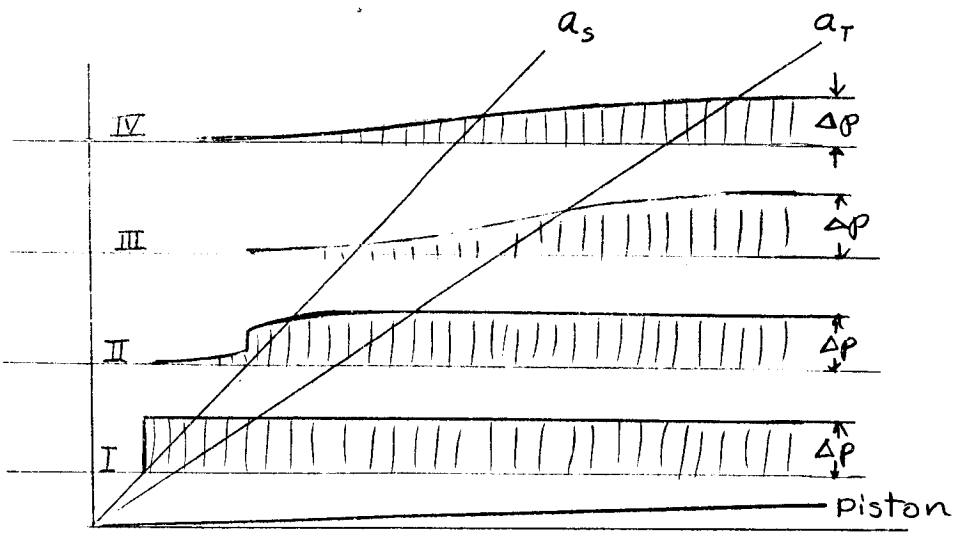

Fig. 7[13]

In some ways, study of the progress of a single jump wave (rather than a harmonic wave) in a dispersive medium yields a plainer picture of the trend of events. Fig. 7 sketches Baldwin's result[13] for

the pressure of a jump wave produced by an impulsively-moved piston. Close to the piston (location I), the wave is only slightly dispersed, and $N_{Bu} \ll 1$, because the wave thickness (L) is small. Thermal energy will, however, begin to leak across the wave front, as indicated at location II, and a decay of the jump amplitude becomes evident. At III, where $L \propto$ is no longer small, the front is very much flattened, and the wave progresses at the isothermal sound speed. At IV, the profile continues to spread out as we approach radiative equilibrium, but the wave center now travels at the isentropic sound speed again, and we have $q_R \to 0$, in the limit as $N_{Bu} \to 0$. A complete discussion of the foregoing problem is given in Ref. 13.

Waves of Finite Strength

Behind a strong shock wave there is a large, sudden temperature rise. The very hot gases behind the shock will radiate and tend to smooth out the wave (See Fig. 8).

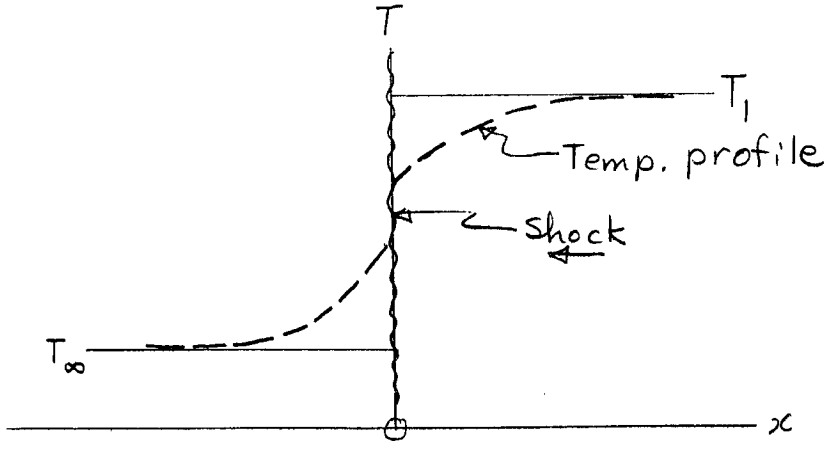

Fig. 8

The temperature profile will tend to be that shown by the dotted line. Radiation effects may then furnish the resistance, like that of viscosity, necessary for shock formation, but acting at longer range.

Clarke[12] has investigated the effects of radiative transfer on such waves of finite strength. This investigation was carried out under the grey gas and quasi-equilibrium assumptions already mentioned. It is found that waves can be maintained entirely by radiation. The situation is quite analogous to heat addition in a constant area channel, wherein heat added always tends to drive the flow toward sonic speed. In this case, as in Ref. 6, both classical and radiation-induced waves are included, the entire spectrum of both being considered to make up the shock.

It is important to realize that radiative effects in flows can be large, especially for superorbital speeds, and may play an important role. The analysis of these effects is very complicated, but possibly one may hope that some simplifying assumption will appear (similar to the Telegraph Equation assumption) in order to make these problems more tractable analytically.

III SHOCK WAVES

We now turn to the problem of blunt body flows with shock waves and examine the effects of chemical nonequilibrium. We will also introduce models for the analysis of such flows.

Description of Strong Shock

First, we will briefly review shock waves and the Rankine-Hugoniot relations for very strong shocks. We distinguish between the two shock configurations shown in Fig. 9(a) and (b). Fig. 9(a) shows a plane, freely propagating shock, such as in a shock tube. Fig. 9(b) shows a bow shock

about a blunt body traveling at hypersonic speed. In this case one has the additional complications of the turning of the flow around the body, which causes the shock to curve, and the existence of a stagnation point. We shall deal with inviscid flows unless otherwise stated.

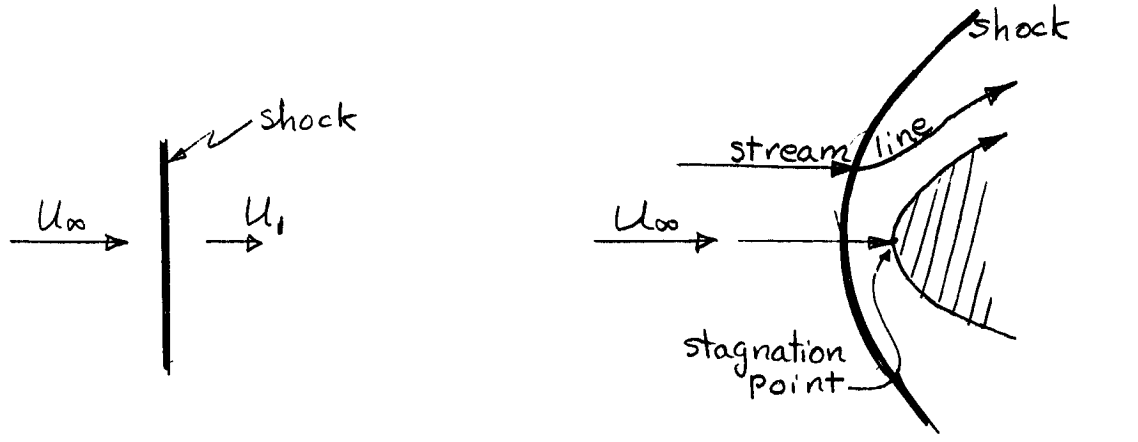

(a) Plane Shock (b) Shock at Blunt Body

Fig. 9

We shall consider only the very strong shocks in which dissociative and radiative effects are important.

Normal Shock Relations (plane, one-dimensional)

The differential equations (3), (6), and (7), neglecting transport effects, are

$$\left.\begin{aligned} &\text{Energy} && \rho u \frac{\partial H}{\partial x} = u \frac{\partial p}{\partial x} \\ &\text{Momentum} && \frac{\partial p}{\partial x} + \rho u \frac{\partial u}{\partial x} = 0 \\ &\text{Continuity} && \frac{\partial (\rho u)}{\partial x} = 0 \end{aligned}\right\} \qquad (25)$$

The integrated forms of these equations apply across shock waves (we do not prove this, here). Now, from continuity $u^2 \frac{\partial \rho}{\partial x} + \rho u \frac{\partial u}{\partial x} = 0$. Combining this with the momentum equation, we find

$$\rho \frac{\partial H}{\partial x} = -\rho u \frac{\partial u}{\partial x}$$

Integrating, we find $H_\infty + \frac{1}{2} u_\infty^2 = H_1 + \frac{1}{2} u_1^2$,

where ∞ signifies evaluation far ahead, and 1 far behind, the shock. Now, in the free stream, $H_\infty << u_\infty^2$. therefore, we may disregard H_∞. Similarly, $\frac{1}{2} u_1^2$ is small compared to H_1.

Therefore, for very strong shocks we may write

$$H_1 \cong \frac{1}{2} u_\infty^2 \tag{26}$$

which says that the enthalpy behind the shock is just the kinetic energy ahead of the shock.

Turning to pressure, we have $\frac{\partial p}{\partial x} = -\rho u \frac{\partial u}{\partial x}$ which may be integrated since ρu = const., to give

$$p_\infty + \rho_\infty u_\infty^2 = p_1 + \rho_1 u_1^2$$

Now, $p_\infty << \rho_\infty u_\infty^2$ (since $\rho_\infty u_\infty^2$ is just twice the free stream dynamic pressure,) and $p_1 >> \rho_1 u_1^2$

Thus:

$$p_1 \cong \rho_\infty u_\infty^2 \tag{27}$$

The pressure behind the strong shock comes from the conversion of essentially all the free stream momentum into a force, through deceleration of the flow.

We now assume an ideal gas for the purposes of an order-of-magnitude analysis, and note that $R/c_p = 1 - 1/\gamma$.

For the Temperature Ratio, $H_1 = c_p T_1 = \frac{1}{2} u_\infty^2$, so

$$\frac{T_1}{T_\infty} \cong \frac{\frac{1}{2} u_\infty^2}{c_p T_\infty} = \frac{\gamma - 1}{2} M_\infty^2 \tag{28}$$

Pressure ratio: $$\frac{p_1}{p_\infty} \simeq \frac{\rho_\infty u_\infty^2}{p_\infty} = \gamma M_\infty^2 \tag{29}$$

Density Ratio: $$\frac{\rho_1}{\rho_\infty} = \frac{p_1}{p_\infty} \cdot \frac{T_\infty}{T_1} \cong \frac{2\gamma}{\gamma - 1} \tag{30}$$

and we note that $2\gamma/(\gamma-1)$ is approximately 10. It is important to note that the density ratio is finite, while the pressure and temperature ratios are unbounded, increasing as the square of the Mach number.

Now let $\frac{1}{2}(\gamma - 1) \equiv \epsilon$, a small quantity. We now investigate the order of magnitudes of changes in the variables behind the shock, since we are interested in the concentration of atoms, rates of pressure change, etc.

$$\frac{\partial}{\partial x}\left(\frac{p}{\rho_\infty u_\infty^2}\right) = \frac{u^2}{u_\infty^2} \frac{\partial}{\partial x}\left(\frac{\rho}{\rho_\infty}\right) \sim \epsilon^2 \cdot \frac{1}{\epsilon} = \epsilon$$

Also, since $\rho_\infty u_\infty = \rho_1 u_1$, we have $u_1/u_\infty \sim \epsilon$. Thus, if ϵ is small, pressure varies more slowly than density. Also,

$$\frac{\rho}{\rho_\infty} \frac{\partial}{\partial x}\left(\frac{H}{u_\infty^2}\right) = \frac{\partial}{\partial x}\left(\frac{p}{\rho_\infty u_\infty^2}\right) \sim \epsilon$$

so

$$\frac{\partial}{\partial x}\left(\frac{H}{u_\infty^2}\right) \sim \epsilon \frac{1}{1/\epsilon} = \epsilon^2$$

$p/(\rho_\infty u_\infty^2)$ is of order 1 behind the shock and the derivative with respect to the nondimensional distance x is of order ϵ. (Note that x is a distance characteristic of the relaxation thickness of the flow.) We have then, the following order of magnitude relations behind the shock:

$$\frac{p}{\rho_\infty u_\infty^2} \sim 1 \quad ; \quad \frac{\partial}{\partial x}\left(\frac{p}{\rho_\infty u_\infty^2}\right) \sim \epsilon$$

$$\frac{H}{u_\infty^2} \sim 1 \quad ; \quad \frac{\partial}{\partial x}\left(\frac{H}{u_\infty^2}\right) \sim \epsilon^2$$

These relations indicate that concentration and temperature "trade off" behind the shock, since ρ, c and T are the only quantities which vary appreciably. Enthalpy is very nearly constant, and pressure varies only slightly downstream of the shock.

We now examine the processes behind the shock, and inquire into the behavior of the concentration of atoms. We assume $T_D = 60,000°$ K for air. Now by Eq. (10) for steady flow of a Lighthill gas[20]

$$u\frac{\partial c}{\partial x} = \frac{w_1}{\rho} = \text{const.}\ \rho\, \frac{T^{-(s+1)}}{1+c}\left[(1-c)e^{-T_D/T} - \frac{\rho}{\rho_D}c^2\right] \qquad (10a)$$

and we note that the square bracket goes to zero for equilibrium. This is the "production law" for atoms. Now when the gas is subjected to a step increase in temperature, by passing through a strong shock, the first chemical process will be dissociation, resulting from two-body (binary) collisions. Initially, recombination (a ternary process) will have little or no effect; however, as time passes recombination must become increasingly strong, and finally balance dissociation at equilibrium.

Binary Scaling[15, 21]

For the present, we will confine our attention to that part of the flow immediately behind the shock where we can neglect recombination. Now, setting $w_1/\rho \equiv \frac{1}{\tau}$, neglecting the second term in brackets, and noting that $p \propto \rho_\infty$, then we may write that $\tau_{relax.} \propto 1/\rho_\infty$. Because $\tau_{passage} = L/u_\infty$,

we have $\frac{\tau_{relax}}{\tau_{passage}} \propto \frac{U_\infty}{\rho_\infty L}$.

This ratio is a parameter of the flow. $\rho_\infty L$ occurs in a group and constitutes a similarity parameter for Eq. (10a), recombination neglected. If we recall the simple case

$$c = c_{eq}\left(1 - e^{-t/\tau}\right)$$

and replace t by x/U_∞ and $\tau \sim 1/\rho_\infty$, then we have

$$c = c_{eq}\left(1 - e^{-\frac{x}{L}\cdot\frac{\rho_\infty L}{U_\infty}\cdot const.}\right)$$

If U_∞ is constant, then $\rho_\infty L$ becomes a scaling parameter for this relaxing flow. The same holds true for the more complicated production law given earlier, provided initial composition is fixed. We have what amounts to a restricted Reynolds similarity. This is not surprising, of course, because viscosity is a binary effect.

Calculations for a Lighthill Gas

Following Gibson[15], we consider the case where the pressure and enthalpy are nearly constant. Now $u\frac{\partial c}{\partial x} = f(T)\,\rho\,\frac{1-c}{1+c}\,e^{-T_D/T}$ represents Eq. (10)$_a$ for steady flow and no recombination, and

$$T = \frac{H - h^{(0)}c}{\frac{R}{m_2}(4+c)}$$

for a Lighthill gas. If H is constant (and it is, for all practical purposes, behind the shock) this means that $T = T(c)$, and

$$f(T) = F(c)$$

We now define a new variable χ such that

$$\chi = \int_0^x \rho\frac{dx}{u} \quad , \quad \text{so that} \quad \frac{\partial}{\partial x} = \frac{\rho}{u}\frac{\partial}{\partial \chi}$$

Substituting into the rate equation,

$$\frac{\partial c}{\partial \chi} = f(T)\,\frac{1-c}{1+c}\,e^{-T_D/T} \tag{33}$$

so that the right hand side is a function of c only, and

$$\chi = I(c) \quad , \text{or} \quad c = I^{-1}(\chi).$$

In this situation, if we plot the concentration c versus χ, we get the universal curve drawn by Gibson[15, 21], as shown in Fig. 10

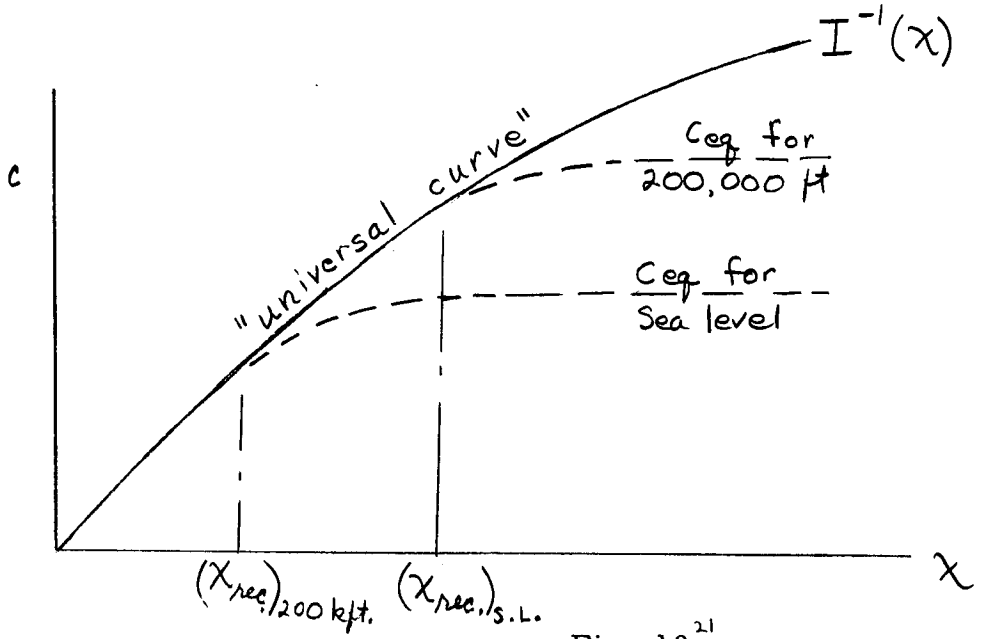

Fig. 10[21]

Thus, a binary scaling scheme is found for strong shock waves. Note that the variable χ contains $\rho_\infty L$ as a parameter, and depends additionally on U_∞ and x/L.

Gibson[21] was able to show that even the departures from the universal curve of Fig. 10 can be predicted when binary scaling is not quite applicable. In the complete equation

$$\frac{dc}{d\chi} = \frac{dc}{dI}\left(1 - \frac{\rho}{\rho_D}\,\frac{c^2}{1-c}\,e^{T_D/T}\right) \tag{33a}$$

The second term is replaced by I/I_∞ (I_∞ is the final equilibrium value of $I(c)$.) Justification of this step is described in Ref. 21, for cases of high equilibrium dissociation level. The solution of Eq. (33a) is, then,

$$I = I_\infty \left(1 - e^{-\chi/I_\infty}\right) \tag{33b}$$

This remarkable formula recalls the simple relaxation law previously discussed, where $I(c)$ now plays the role of c. The effects due to recombination are shown as dotted lines in Fig. 10, and appear only as departures from the universal plot near the end of the curve in question. Physically, we expect that the lower the density, the higher will be the proportion of binary collisions, i.e., those promoting dissociation. Recombination results from three body collisions, and is proportional to ρ^3, and thus appears as a small effect near the ends of the curves. The scaling law renders the initial (dissociation) portion of the curves similar, regardless of initial density (altitude). For the scaling law to be useful, there are two required conditions:

1. Shock wave must be very strong.
2. Altitude must be very high (i.e., ρ small).

Scaling Limit

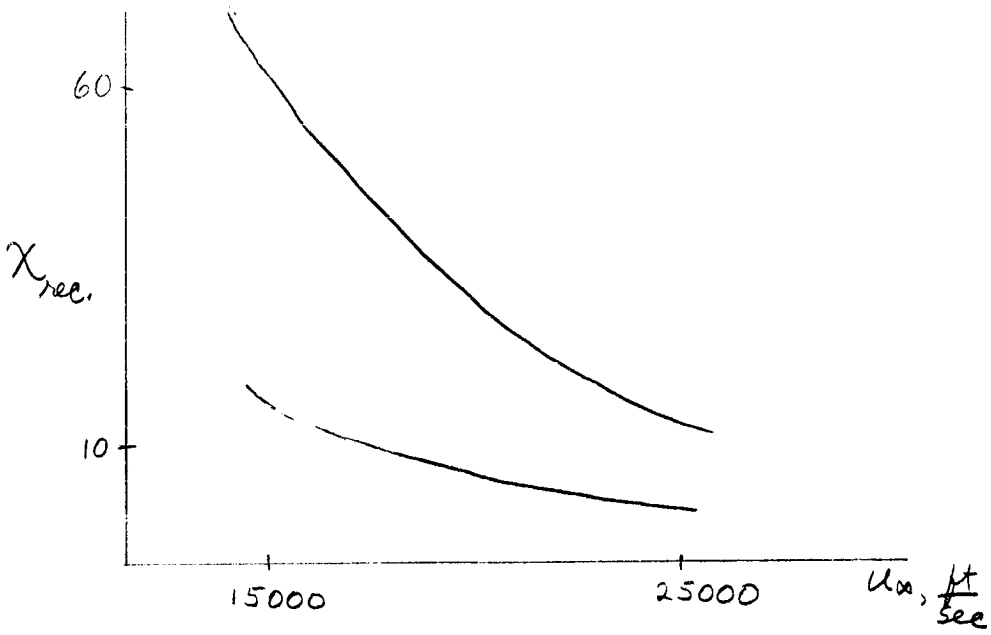

Fig. 11[21]

Clearly, as χ increases, the recombination effects become more important, and Fig. 11 (from 21) indicates qualitatively the limits of $\chi_{rec.}$, the value of χ beyond which the recombination term can no longer be neglected. The criterion chosen for Fig. 11 is that the recombination rate is approximately 3/10 of the dissociation rate .

Referring to Eq. (33a), we see that when ρ is small (high altitude) a larger value of c , and hence χ , can be reached before the second term is comparable to 1. Also, when the speed is lowered, the density is not greatly affected, but c_∞ is much less, so the effect of c^2 in Eq. (33a) holds down the value of that term as χ increases, and again a higher value of χ is permitted.

Calculations for Real Air

The calculations just described for a Lighthill gas certainly emphasize the value of binary scaling for strong shock waves at low density. There have been many calculations of chemistry behind strong shocks in real air[16, 17]. These may be presented in terms of the scaling variable χ. The set of reactions that have been studied are

$$\left.\begin{array}{ll} O_2 \rightleftharpoons 2O \\ N_2 \rightleftharpoons 2N \end{array}\right\} \text{ Dissociative}$$

$$\left.\begin{array}{ll} N + O_2 \rightleftharpoons NO + O \\ NO + N \rightleftharpoons N_2 + O \end{array}\right\} \text{ Exchange of "Shuffle" reactions}$$

$$N + O \rightleftharpoons NO^+ + e^- \quad \text{Ionization} \qquad (34)$$

In general the "shuffle reactions" are predominantly to the right, which promotes the formation of oxygen atoms, and encourages the depletion of N by recombination into N_2 or NO. In other words, the mechanism for the recombination of nitrogen is more powerful than the recombination mechanism for oxygen. The shuffle reactions are binary in nature, and thus have particular importance at high altitude.

Fig. 12 shows various concentrations plotted versus χ, as is done in Ref. 21. These are simply sketches, and details should be sought in Ref. 21.

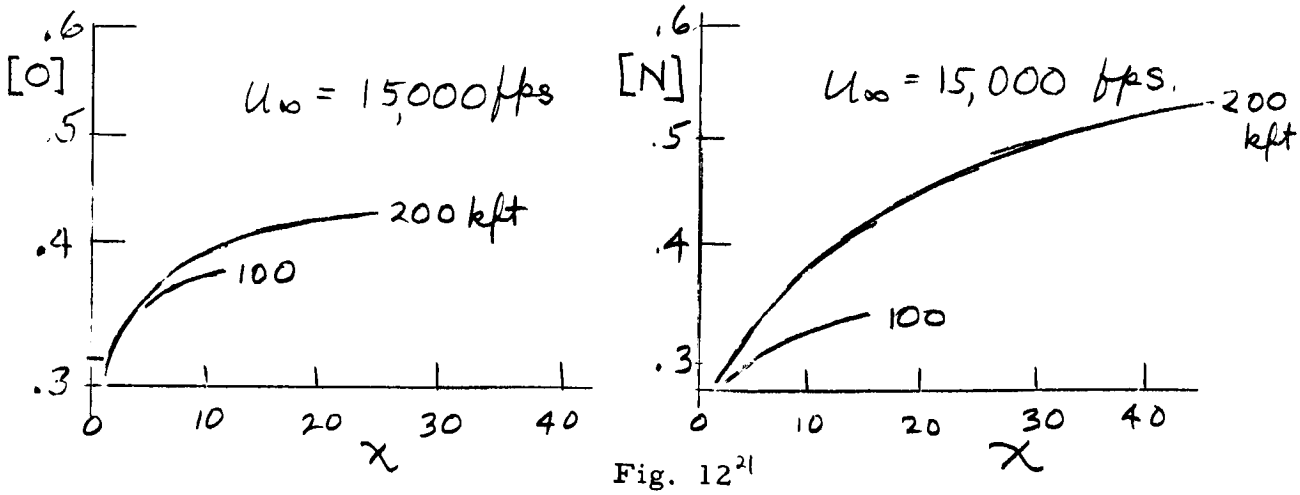

Fig. 12[21]

The sketches indicate that binary scaling works for real air about as well as for the Lighthill gas.

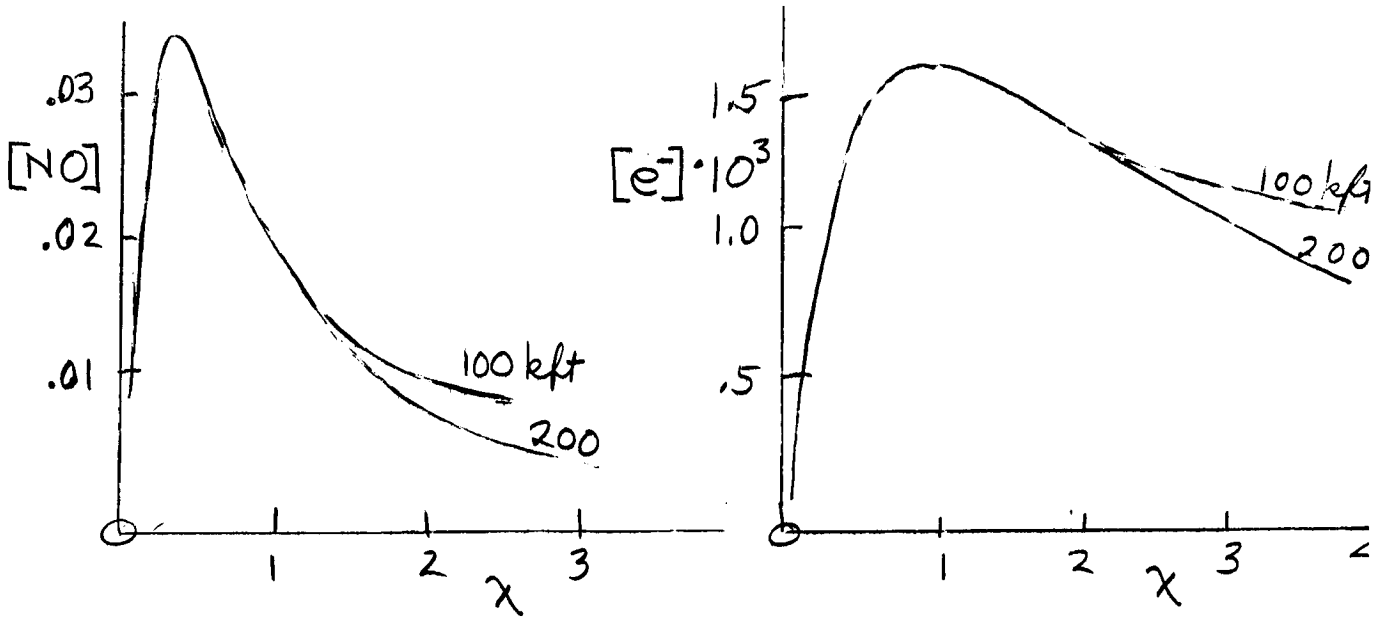

Fig. 13[21]

Also illustrated in Fig. 13, is the phenomenon of overshoot of NO and e^-, typical of high-energy flows (here, the shock speed was 23, 000 fps).

The overshoot of electron concentration may be understood as a consequence of the abnormally high translational temperature just behind the shock. Since translation equilibrates first, the ideal-gas temperature is reached - about 25, 000° K for 23, 000 fps. at 200, 000 ft. altitude. In about 5 mm behind the shock, O dissociation manages to take up its equilibrium share of energy, and, by then, the translational temperature has dropped to 8000° K. Of course, while the temperature is at the higher level, radiation and ionization are intense.

Vibrational Coupling

Actually, the overall process of equilibration is strongly affected by vibration. Fig. 14 sketches the sequence: First vibrational

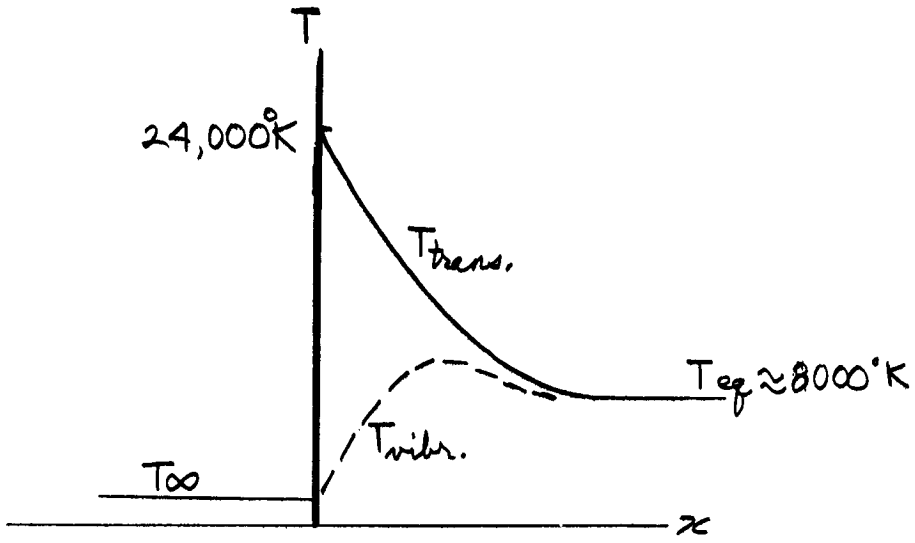

Fig. 14

excitation begins to rise (Rotation is nearly as fast as translation), and dissociation follows. But, since dissociation occurs chiefly from excited vibrational states, vibration and dissociation are kinetically coupled[18]. Also, when dissociation does occur, it depletes the higher vibrational states[19]. Thus, at high energy and low density, the kinetic model for air must include vibration. We note, however, that vibrational excitation is a binary process, and the previous scaling considerations apply.

IV BLUNT BODY FLOWS

We turn now to problems of the inviscid flow about blunt bodies moving at hypersonic velocity, and consider the effect of chemical reactions. We shall be concerned with very strong shocks, as before, but now the shock is curved about the body, as sketched in Fig. 15.

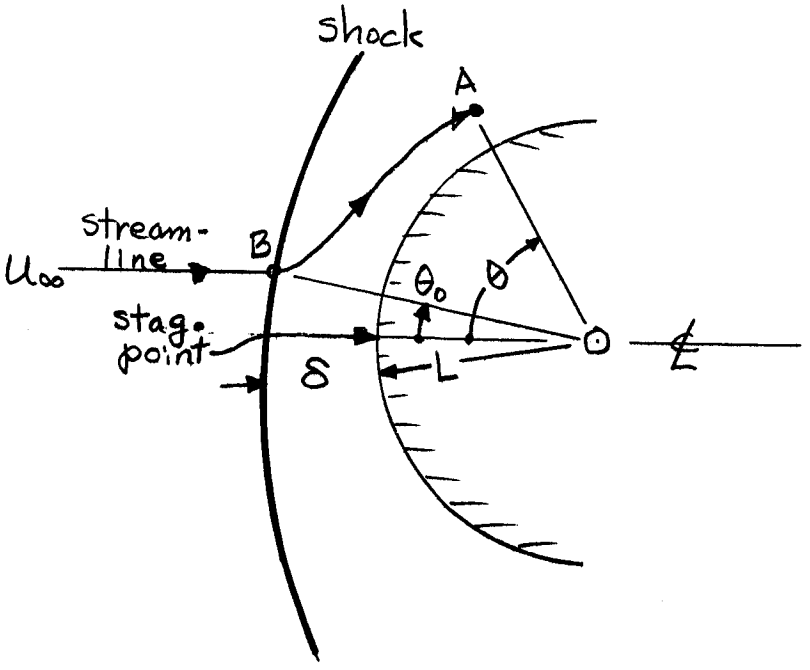

Fig. 15

The Newtonian Approximation

The radius of curvature of the nose is denoted by L with O as the center of curvature. The standoff distance of the shock is δ, and we introduce the independent variable θ to measure position. For example, if we wish to investigate the streamline which passes through A, B, we designate the position of penetration of the shock by the angle θ_0

and later position by θ. The free stream velocity is U_∞ and at A its component tangential to the body is $U_\infty \sin\theta$. With the assumption of a strong shock wave, the order of magnitude of the shock layer thickness may be determined as follows: From Eq. (30), $\rho/\rho_\infty \sim 1/\epsilon$, and ϵ is rather small. Now, consider a cylinder in the free stream (with axis parallel to the free stream velocity), subtended by an angle θ. The mass flow through a cross section of this cylinder is $\sim$

$$\rho_\infty U_\infty (L \sin\theta)^2 \pi$$

The tangential flow in the region between the shock and the body, at a location θ, is $\sim$

$$\rho U_\infty \sin\theta \, (\pi L \sin\theta)\delta$$

These flows must be equal, and after cancellation, we have

$$\frac{\delta}{L} = \frac{\rho_\infty}{\rho} \sim \epsilon$$

and the "shock layer" is quite thin compared with the body dimension. This result leads to the "Newtonian" model for the analysis of blunt body flows, wherein the colliding particles are assumed to give up their normal component of momentum on impact with the body (or the shock, which is the same thing, by assumption) and subsequently move tangent to the surface. This is a particular kind of reflection, neither specular nor diffuse.

For a plane, freely propagating shock, we found that the pressure changes slowly behind the shock. With a body immersed in the flow, however, the shock is curved and the pressure variations are large. We have, by direct application of "Newtonian" theory, $p/(\rho_\infty U_\infty^2) \propto \cos^2\theta$, and hence $\frac{\partial}{\partial x}\left(\frac{p}{\rho_\infty U_\infty^2}\right) \sim 1$, where x is the ratio of distance

measured along a streamline to the nose radius L. Previously, for a plane shock, we had that pressure gradient was of order ϵ (x being measured relative to a relaxation distance.) Correspondingly, we now have $\frac{\partial}{\partial x}\left(\frac{H}{u_\infty^2}\right) \sim \epsilon$ ($\sim \epsilon^2$ for the plane shock), and, from the momentum equation, $\frac{u}{u_\infty} \sim \sqrt{\epsilon}$ ($\sim \epsilon$ for the plane shock).

The Newtonian theory requires modification to account for centrifugal forces and effects of shock-layer thickness. Centrifugal force corrections for a sphere[20] modify the result $p \propto \cos^2\theta$ so that $p = 0$ (a sort of centrifugal separation) is predicted to occur at $\theta = \pi/3$.

Binary Scaling

If we re-examine Eq. (33), we see that the crucial thing for binary scaling is that H remain nearly constant. This is so for blunt body flows, because $\gamma - 1$ is small. The pressure is not constant, but its variation can be absorbed in χ Thus, Gibson and Marrone[21] show that we can carry over the binary scaling analysis to blunt-body cases, ζ being given by the same function of χ :

$$\zeta = I^{-1}(\chi)$$

where

$$\chi \equiv \int \frac{\rho\, ds}{u} \qquad (34a)$$

s being measured along a streamline. ρ and u may be found from Newtonian theory, and we observe the binary scaling rule that results:

$$\chi = \int \frac{\rho\, ds}{u} = \rho_\infty L\, fn(u_\infty, \theta)$$

Scaling Limits

From Eq. (34a), we see that as we approach the stagnation point of the body, $u \to 0$ and thus $\chi \to \infty$, so we cannot expect binary scaling to apply right there. On the other hand, as we travel along a streamline like B-A in Fig. 15, we know that $\rho \to 0$ at 60° (for a sphere), and thus χ reaches some limiting value, which might be less than χ_{rec}! Fig. 16, which sketches information in Ref. 21,

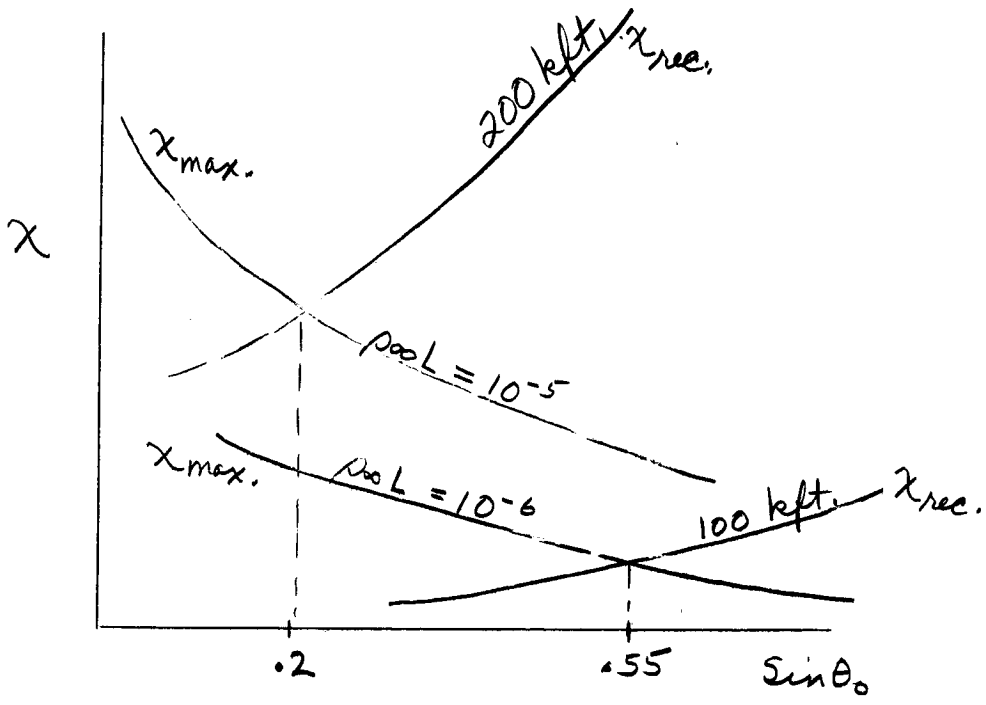

Fig. 16[21]

compares χ_{max} and χ_{rec} under a number of conditions. For L = 30 cm and altitude 200 kft, the limiting value of χ along the streamline $\theta_0 = \arcsin(1/5)$ just equals $\chi_{rec.}$, the scaling limit for that altitude. Thus, for streamlines beginning farther from the axis, the universal curve of Fig. 10 applies all the way to 60°, while along streamlines closer to the axis the function $c(\chi)$ will break away from the universal curve.

Of course, even right at the axis ($\theta_0 = 0$), the actual departures from binary scaling occur near the surface, so one may speak of a recombination thickness δ_{rec} which is perhaps a small fraction of the shock-layer thickness, or "stand-off distance" δ. Fig. 17 shows how δ_{rec}/δ varies with $\rho_\infty L$ [21],

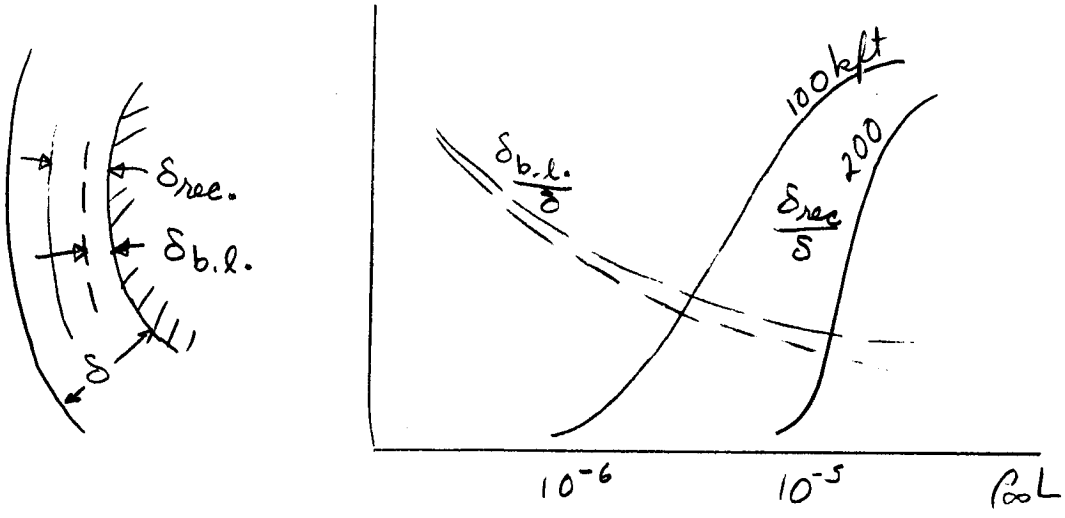

Fig. 17[21]

It appears that recombination plays a negligible role at 200 kft, if L is less than that for which $\rho_\infty L \approx 10^{-5}$. Viscous effects at the nose should be included. They scale completely with $\rho_\infty L$, as indicated by the boundary layer thickness $\delta_{b.l.}$ on Fig. 17.

In summary, we can use binary scaling for the nose region, at high altitude ($\rho_\infty L$ small) for flow suddenly heated by a strong (hypersonic) bow shock[21], concluding that dimensionless variables depend on $\rho_\infty L$ for the same u_∞ and same initial composition. Under these conditions nonequilibrium chemistry and ionization may be analyzed quite simply.

Example: Stand-off Distance[21]

Fig. 18[21] shows Newtonian calculations of δ/L showing the expected scaling for small values of $\rho_\infty L$. Also shown are two points gotten from computed solutions with full air chemistry. Their agreement

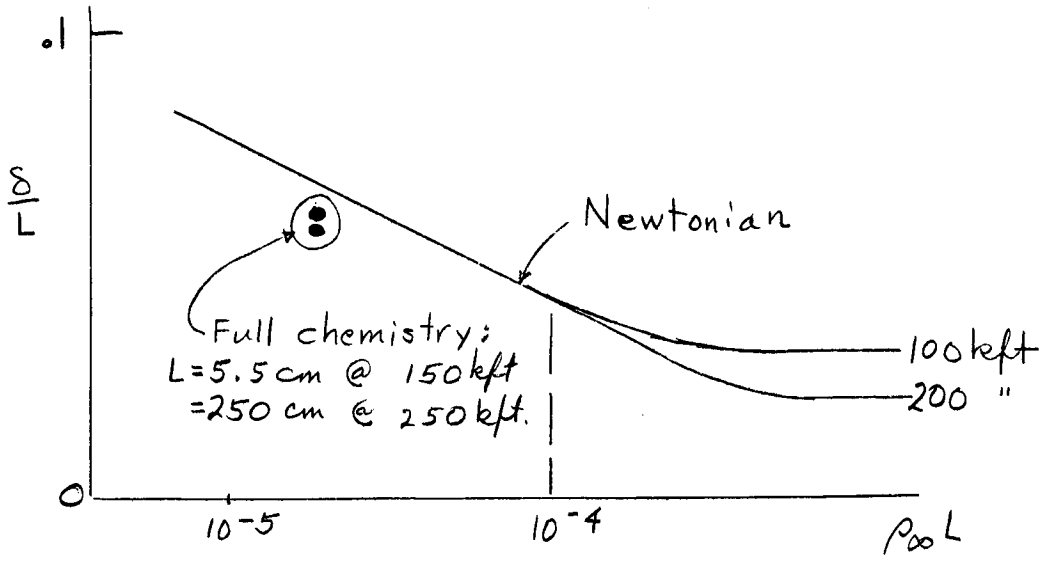

Fig. 18[21]

with the scaling rule, even for scales differing by 100, is an excellent indication of general applicability of the binary model.

Exact Solutions for Blunt Bodies

The "exact" calculations just mentioned were done by a method due to Lick[22], whereby a shock shape is assumed, and the full equations, with chemistry are numerically integrated inward to "find the body". Hall, Eschenroeder, and Marrone [17] made calculations by this method, using the 5 reactions cited previously. Here, we encounter a feature not present in the plane shock problem: Now, as the flow proceeds, it cools, and the recombination may quench before equilibrium is reached.

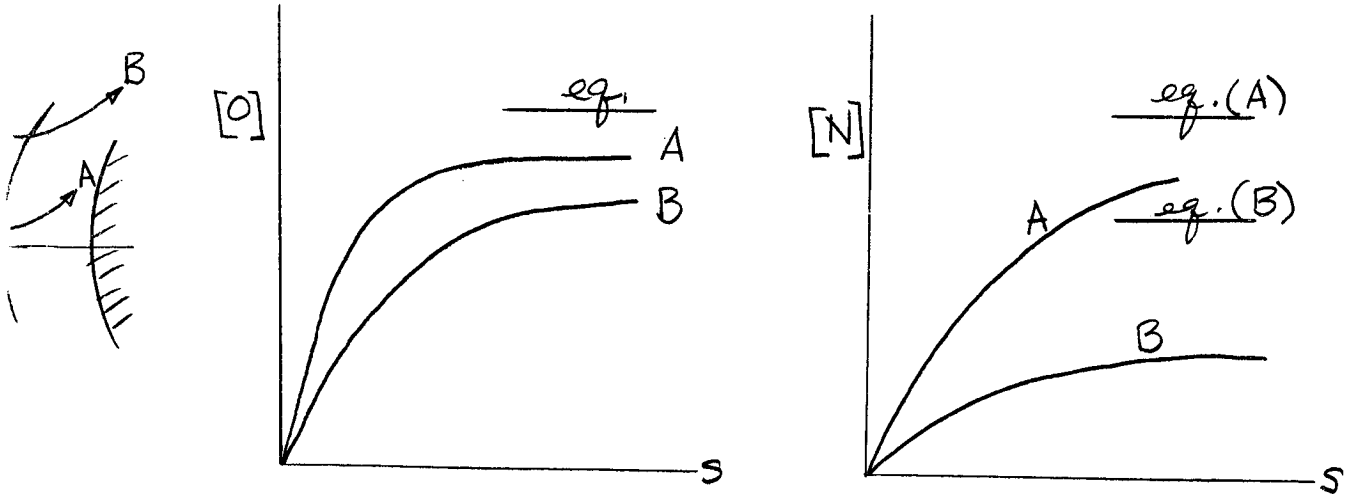

Fig. 19[17]

Fig. 19 shows this effect[17] for two streamlines, at U_∞ = 23,000 fps. The "faster" streamline, B, shows more freezing effect than A, as we

would expect. The freezing of N is more pronounced because the exchange reactions tend to deplete N, and keep O high. Thus reactions are binary, and are the favored recombination reactions at low density.

The freezing effect just described is important to assess in preparation for analyzing afterbody and wake flows.

V NONEQUILIBRIUM IN NOZZLE EXPANSIONS

We have, so far, briefly discussed chemical effects in high velocity, blunt body flows, with particular reference to the nose region. We now consider the flow over the remainder of the body, and examine the effects of chemical activity upon this "downstream" portion of the flow field. Referring to Fig. 20a we consider a pair of stream surfaces extending downstream from the nose region. Following these streamlines, we find that in the afterbody flow the gas undergoes an expansion, with cooling and chemical recombination. We can think of this flow as being like the expansion of a very hot gas through a nozzle[23, 24]. The nose region corresponding to a reservoir of hot dissociated gas. We, then, learn much about the flow over afterbodies by considering channel flows, as illustrated in Fig. 20b. Of course, such channel flow studies are of interest not only for hypersonic applications, but also for rocket nozzles and shock tunnels.

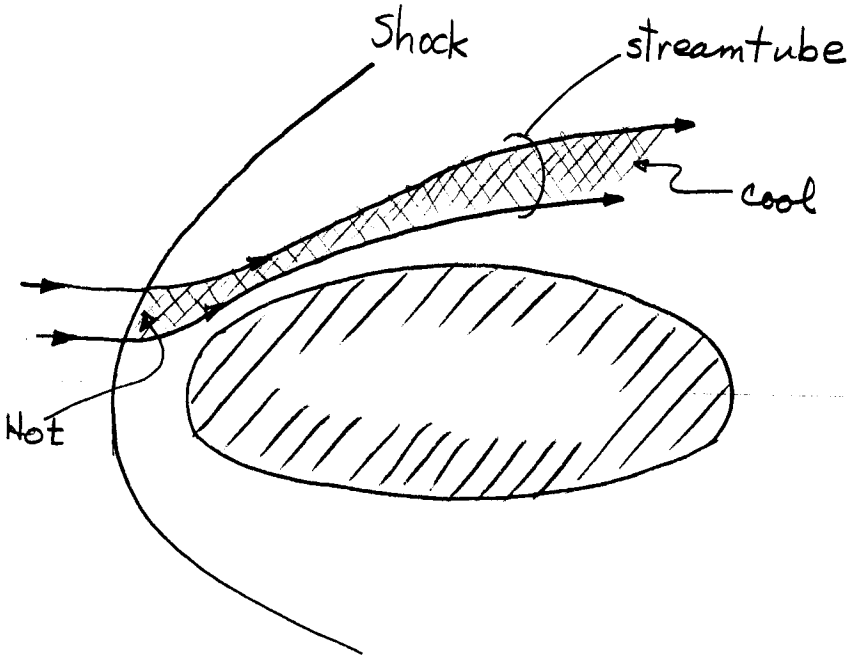

Fig. 20a

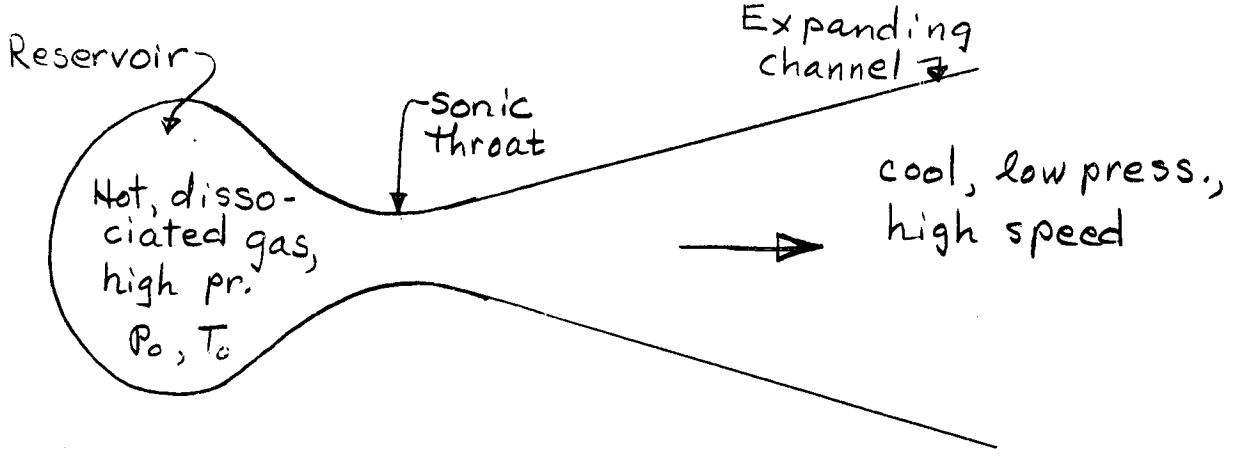

Fig. 20b

Expansion and cooling experienced by the gas in passing through a nozzle of course results in chemical recombination and reduction of the high levels of other modes of excitation. Thus, processes occur which are the reverse of those discussed previously for the nose region of the blunt body.

Equation for Nozzle Flows with Nonequilibrium Chemistry

We write the equations for channel flow, neglecting transverse velocity components compared to the axial components. Then, measuring x down the channel, and assuming a single mode of dissociation, the equations reduce to

$$\left.\begin{aligned} &\text{Continuity of Species}: && u\frac{\partial c}{\partial x} = \frac{W_1}{\rho} \\ &\text{Continuity}: && \rho u A = \text{const.} \\ &\text{Momentum}: && \frac{dp}{\rho} + u\,du = 0 \\ &\text{Energy}: && H + \tfrac{1}{2}u^2 = \text{const.} \\ &\text{State}: && p = (1+c)\rho RT \end{aligned}\right\} \qquad (35)$$

We consider, as usual, that the enthalpy H consists of the internal degrees of freedom plus the energy of dissociation. (We do not use the Lighthill model at this point.) In the solution of these equations, the production term is the major problem, since rates of production and recombination are involved, in a complicated manner, in channel flows.

For the nonreacting nozzle flows, there is a critical mass flow determined by the mass flow at the throat of the nozzle when M = 1. Mass flow at the throat is thus a parameter of the problem, with a^* (sound speed at M = 1) being known. With chemical activity, however, a^* is no longer known in advance, and the consequent lack of a definite mass-

flow parameter makes real numerical (machine) solutions for the problem, via forward integration from equilibrium, very difficult. Another difficulty concerns initial departures from equilibrium, where $\partial^n c/\partial x^n = 0$ Computationally, one has something similar to an essential singularity; thus, integration away from equilibrium tends to require very fine-grained calculations.

Early work in the field of nonequilibrium channel flows was done by Bray[23], and by Hall and Russo[24]. Hall and Russo used, first, a Taylor series expansion of about 10 terms in $1/\sqrt{A}$ (A is area ÷ throat area) to carry the calculations to the throat. By iteration of these results, a mass flow was established. Then, downstream of the throat, a modified Runge-Kutta scheme was used. For a hyperbolic channel shape,

$$A = 1 + \frac{x^2}{L^2}$$

where L is a suitable length parameter, the results[24] appear as follows, for atom concentration versus area ratio

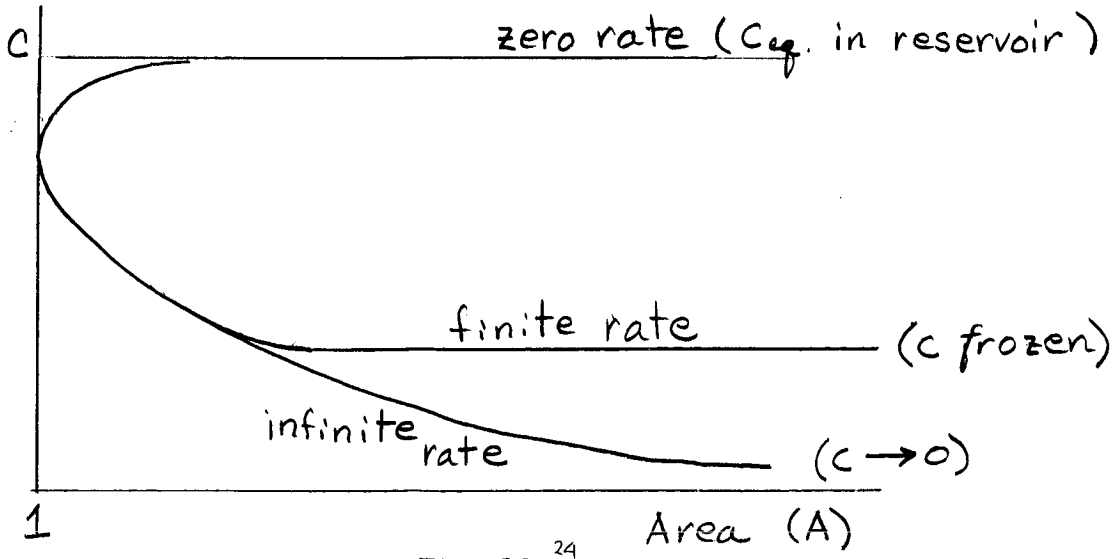

Fig. 20 c[24]

If equilibrium is maintained throughout the flow, which implies a recombination rate approaching infinity, we get the "equilibrium" curve shown above. As a result of cooling and expansion, density decreases; we recall that

$$\frac{w_1}{\rho} \propto \left[(1-c)\, e^{-T_D/T} - \rho_D c^2\right]$$

Since density decreases, the rate of recombination decreases, therefore there is a point where the process of recombination cannot keep up. (That is, the three body collisions necessary for recombination become too infrequent to maintain equilibrium.) The result is that freezing occurs, rather suddenly, as shown in the upper branch of the curve in Fig. 20c. Concentration is constant downstream of the freezing point. Such freezing of the flow is of great importance in two cases:

1. Propulsion systems.
   In a rocket nozzle, the freezing results in the loss of kinetic energy, because some of the energy is frozen in the form of dissociation and vibration energy, and is thus not available for propulsion.
2. Hypersonic wind tunnels.
   In such test tunnels, we do not wish to have a dissociated flow at the test section, therefore we must take care to avoid too-early freezing.

In Fig. 21, a plot of temperature versus area ratio is shown for infinite, finite, and zero rates of recombination.

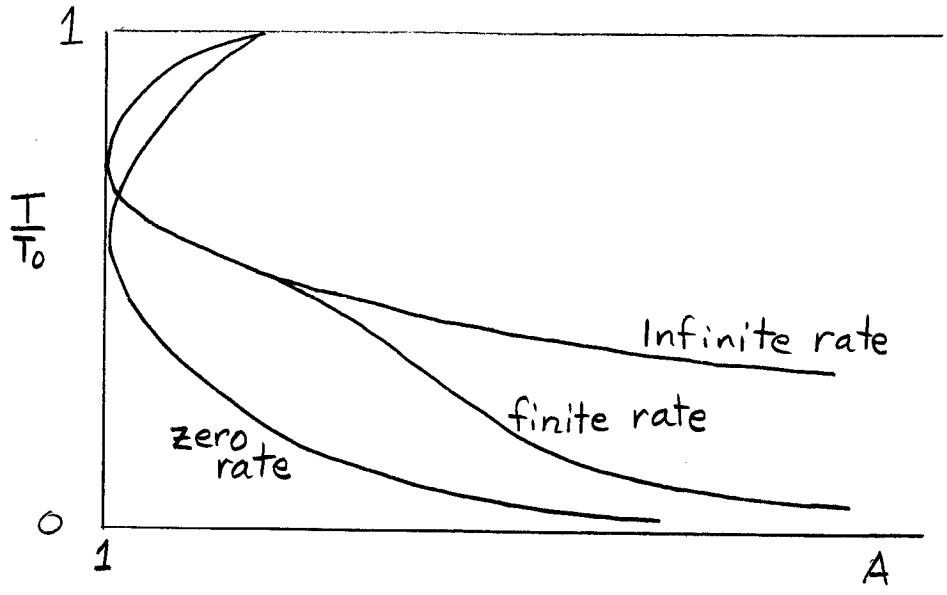

Fig. 21[24]

From Fig. 21 we can see the effect of the recombination rate upon the temperature of the flow. (T_0 is the reservoir temperature.) Comparison with Fig. 20c shows how temperature and concentration "trade off".

A plot of pressure versus area ratio exhibits the following general form:

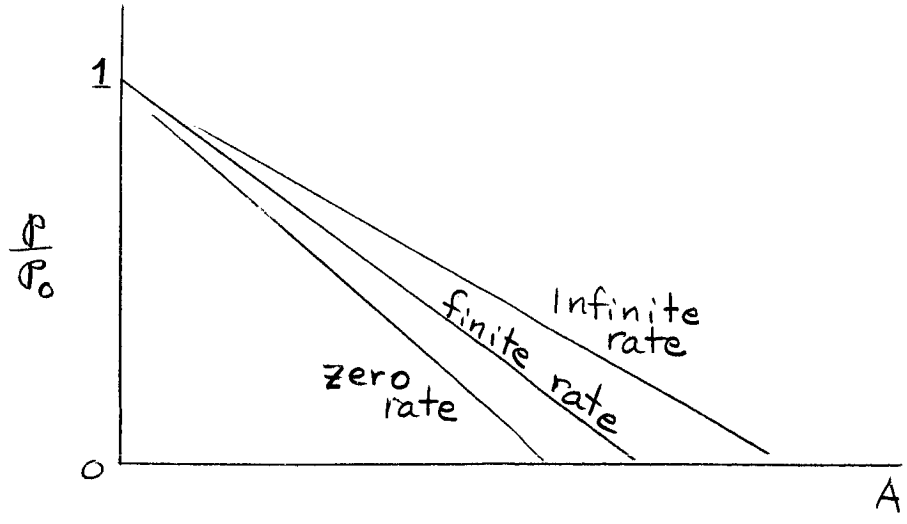

Fig. 22[24]

We note that the difference between infinite and zero rates is not as great as for temperature. Thus, velocity is not coupled to concentration as closely as is temperature. The foregoing figures are based on a temperature of 6000° K and a pressure of 100 atmospheres in the reservoir.

The final frozen level of concentration is lower for longer channels of the same shape, since the longer the channel, the greater the time during which the recombination process can proceed. Plotting length versus frozen concentration, we have a relationship as shown in Fig. 23

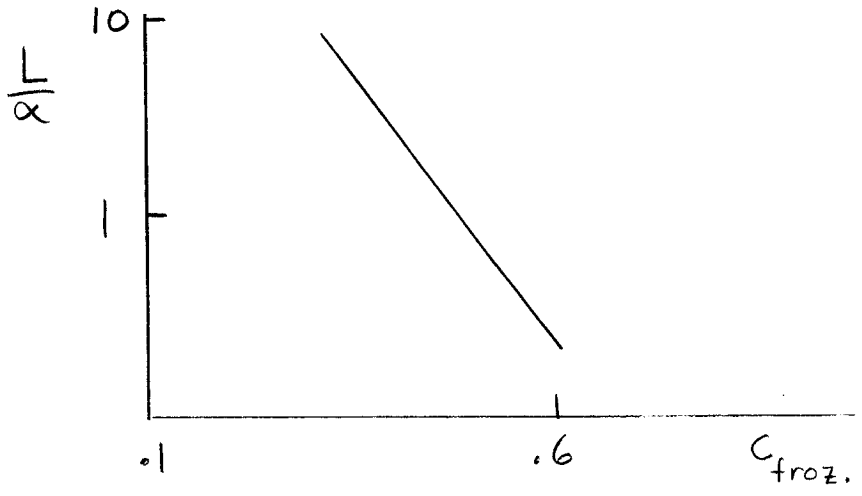

Fig. 23[24]

Approximate Freezing Criteria

It is of interest to predict the occurrence of freezing in the channel, but since channel flows are characterized by recombination processes, there is no possibility of applying a binary scaling law.

The change of concentration along an equilibrium path is fixed by the geometry of the channel. We must now inquire whether the recombination rate will be sufficient to maintain equilibrium, and if not, where

along the channel freezing will occur. This problem has been studied by Bray[25], and Hall and Russo[24]. Bray assumed that the rate for equilibrium flow is given in terms of channel geometry, etc., so that $(Dc/Dt)_{eq.}$ is known. One then asks when this is greater than the recombination rate:

$$\left|\frac{Dc}{Dt}\right|_{eq.} > \text{const.}\,(\rho^2 T^{-S} c^2)_{eq.}$$

where $\rho^2 T^{-S} c^2$ is the recombination rate term. The left hand side is an aerodynamic requirement, and we ask when it is greater than a quantity proportional to $\rho^2 T^{-S} c^2$. Bray employed the equilibrium mass action law for a Lighthill gas to eliminate the density, so that

$$(\rho^2 T^{-S} c^2)_{eq.} \sim \left(\frac{1-c}{c}\right)^2_{eq.} e^{-2T_D/T}\, T^{-S}$$

Then Bray's freezing criterion is

$$\left(\frac{1-c}{c}\right)^2 \frac{e^{-2T_D/T}}{(1+c)T} = \text{const.} \tag{36}$$

Hall and Russo assumed that

$$\frac{\partial c}{\partial x} = -\frac{c - c_{eq\text{-}finite}}{r}$$

where r (a function) represents a reaction length or typical path for relaxation increasing down the channel. C_{eq}, finite is the (fictitious) C_{eq} for the temperature and density calculated on a finite-rate basis. One may easily show that

$$\left|\frac{\partial c}{\partial x}\right| \lll \frac{c_{eq,\,finite}}{r} \tag{37}$$

where the upper inequality holds for equilibrium flow, and the lower inequality holds for frozen flow. The freezing criterion is defined, ~~concentration~~ arbitrarily, by the equal sign. Reference to Fig. 24 indicates these three cases.

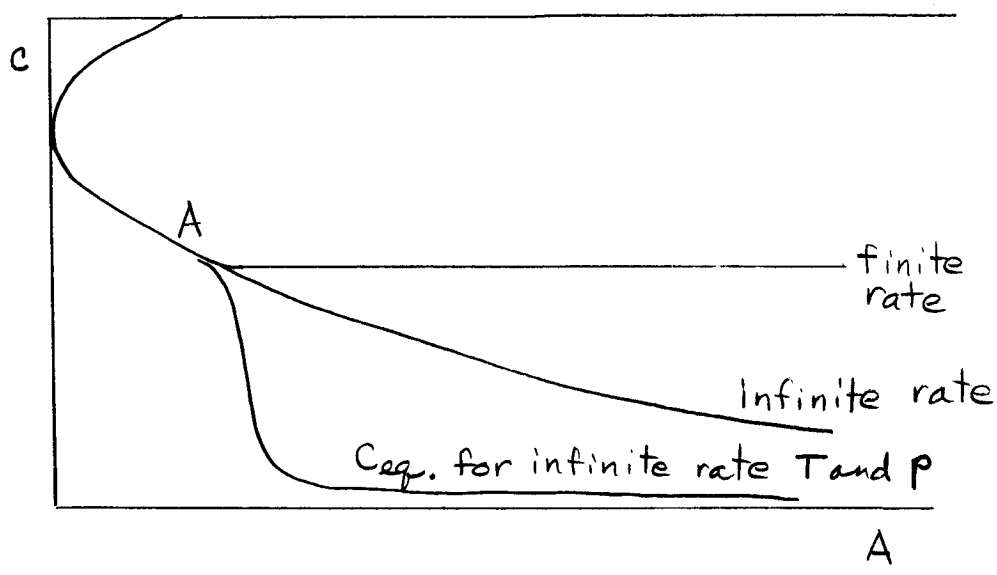

Fig. 24[14]

At point A, (Fig. 24) where the curve splits into three possible paths, we can predict $\partial c/\partial x$. The average rate during the abrupt freezing process is $\frac{1}{2}(\partial c/\partial x)_{inf.}$ Also, since $c_{eq,finite}$ drops so quickly to zero, its average value is $\frac{1}{2} c_{inf.}$ The freezing criterion is then

$$\left(\frac{\partial c}{\partial x}\right)_{inf.} = \left(\frac{c}{r}\right)_{inf.}$$

Machine calculations show the freezing process to be rather sudden, and at point A the freezing line breaks sharply away from the infinite or finite rate equilibrium lines.

Entropy and the Sudden-Freezing Model

The question of the entropy of the flow, while one of great interest, is also one of considerable difficulty. Entropy is defined only for a state which can be reached by an equilibrium process. For the early, equilibrium flow the entropy is well defined, and the expansion is isentropic. The change from equilibrium to frozen flow is one which is nonisentropic, unless the freezing is mathematically sudden. However, completely frozen flow is again isentropic, because chemistry no longer participates.

The formula for entropy of a gas in equilibrium is

$$dS = \frac{dE + p\,dV}{T} \tag{38}$$

Using Lighthill's gas and the state equation,

$$\frac{dS}{R} = 3\frac{dT}{T} + T_D\frac{dc}{T} - (1+c)\frac{d\rho}{\rho} \tag{38a}$$

This form, as it stands, cannot be integrated to give a variable of state, except for frozen concentration, that is, for c constant. Then,

$$\frac{S_{fr.}}{R} = 3\ln T - (1+c)\ln\rho + \text{const.} \tag{39}$$

For equilibrium, we have another relation,

$$\frac{c^2}{1-c} = \frac{\rho_D}{\rho}e^{-T_D/T}$$

by which one of the original three variables may be eliminated. Thus,

$$\frac{S_{eq.}}{R} = 3\ln T + (1+c)\frac{T_D}{T} + c + 2\ln\frac{c}{1-c} + \text{const.} \tag{40}$$

applies for equilibrium. The constant in Eq. (39) may be chosen so that Seq. goes over to $S_{fr.}$ continuously at a sudden freezing point.

The Mollier Diagram

Bray noted[25] that his freezing criterion, (Eq. 36) gives another relation between C or T, which, substituted into Eq. (40), gives the freezing state in terms of S only:

$$c_{fr.} = c(S_o) \; ; \; T_{fr.} = T(S_o) \tag{41}$$

Thus, one may construct a Mollier-type diagram[25], as shown schematically in Fig. 25.

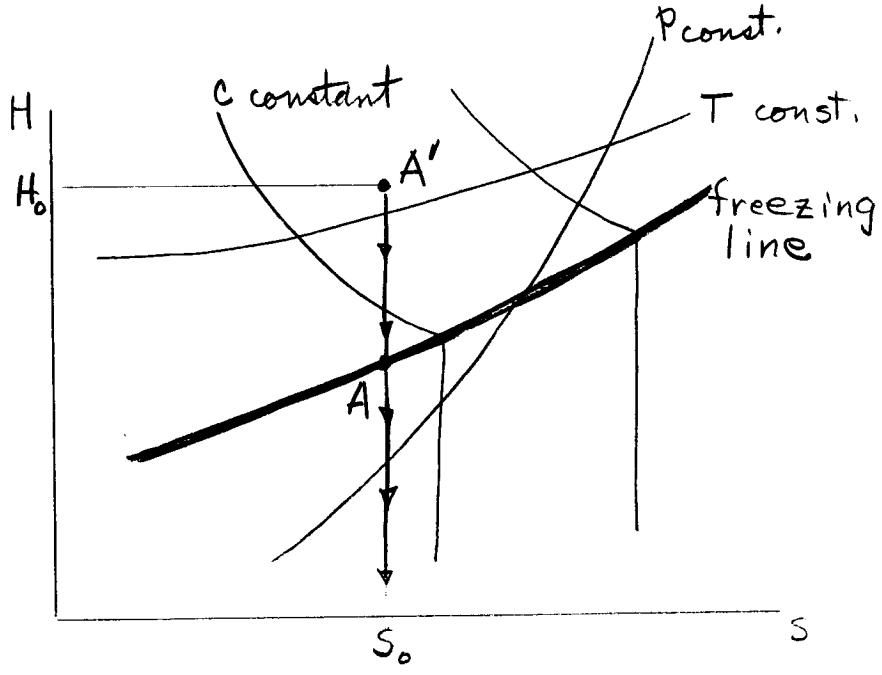

Fig. 25[25]

According to this diagram, if we start a flow from a point of known enthalpy, A', the process proceeds along the vertical isentrope through the "freezing line". Actually, of course there may be a narrow freezing zone rather than a freezing line. In any case, this kind of diagram represents a very useful condensation of results, when freezing is sudden.

An approach to the problem of more gradual freezing has been made by considering two subsystems[26] which flow out of equilibrium with each other. Then one can define entropy for these subsystems, each of which is internally, in equilibrium. However, this is a dubious approach.

Calculations for Real Air

More complete machine calculations have been made[34], including the five reactions (Eq. (34)) important at high temperature. As usual, the exchange or shuffle reactions favor recombination of N. Results of calculations for the concentrations of the various species are shown in Fig. 26[34].

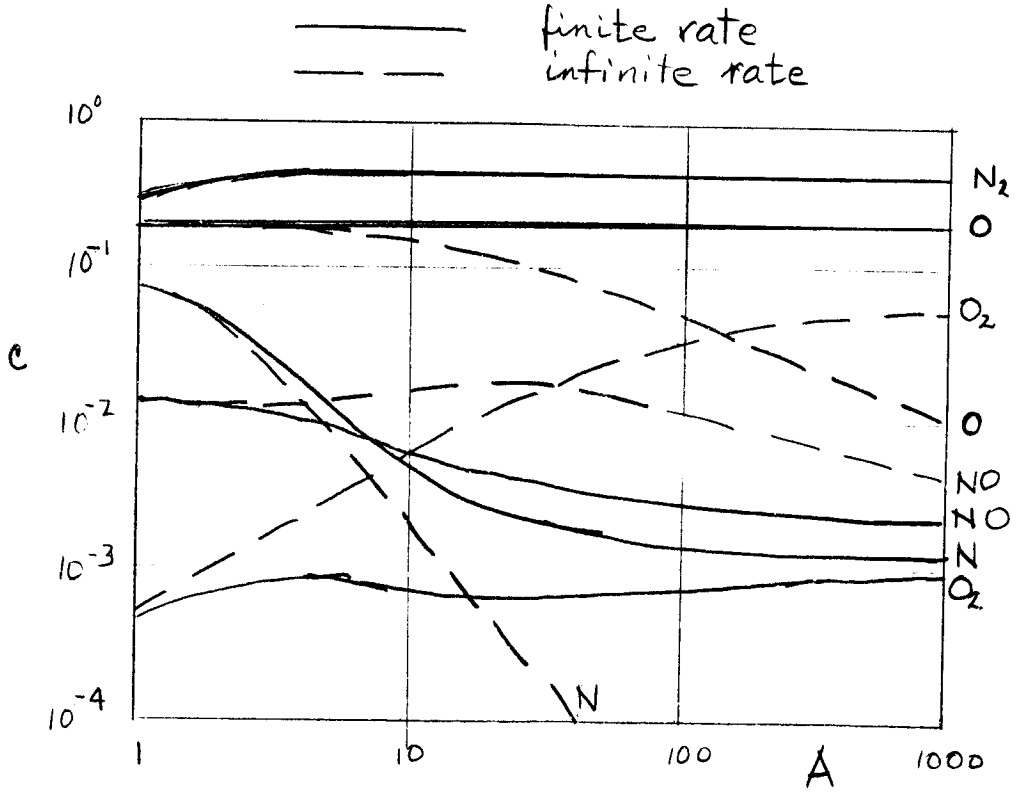

Fig. 26[34]

An important feature of such a flow is that the recombination of nitrogen is vigorous, via the NO reactions, and O concentration, as a result, stays high, freezing almost immediately.

We must now attempt to apply these results to flows about bodies.

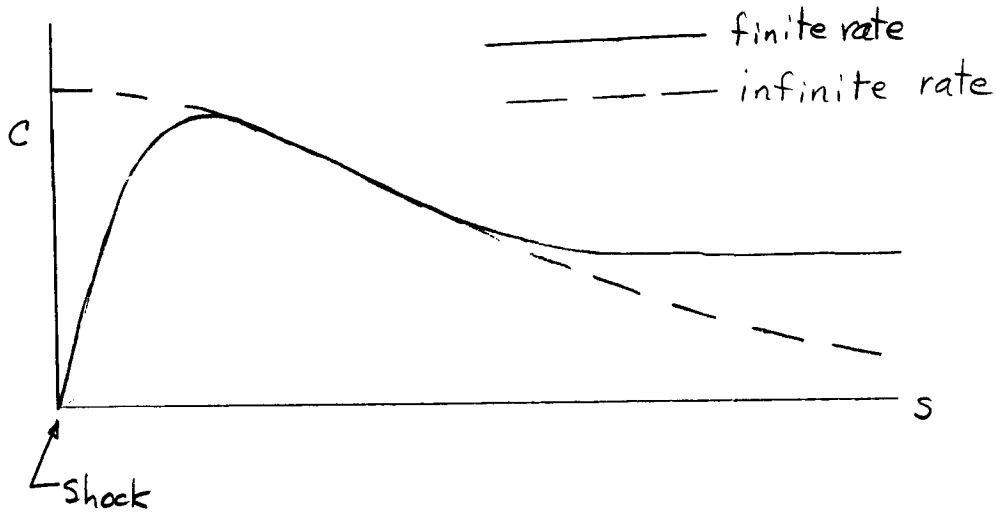

Fig. 27

Stream Tube Applications

Referring to Fig. 20a we return to the idea that the flow through a stream tube about the body is essentially described by a nozzle flow model such as we have just been discussing. The region of hot dissociated gas near the stagnation point serves as a high pressure, high energy reservoir. In general, the nozzle flow analysis cannot be applied without some reservations, due to the transverse gradients existing in the flow field. If, however, we know the nature of the flow (i.e., the streamlines) we can apply the nozzle flow analysis, with the most serious error being due to the pressure mismatch at the boundaries between stream tubes. Recalling Fig. 22, we note that the pressure is not seriously affected by the chemistry, however, and we can accept the nozzle flow analysis as a

reasonable approximation. A large uncertainty exists in connection with conditions at the nose of the body, however; in general, we cannot be sure that we have an equilibrium reservoir.

To illustrate the uncertainties involved we compare the sketches, Figs. 27 and 28.

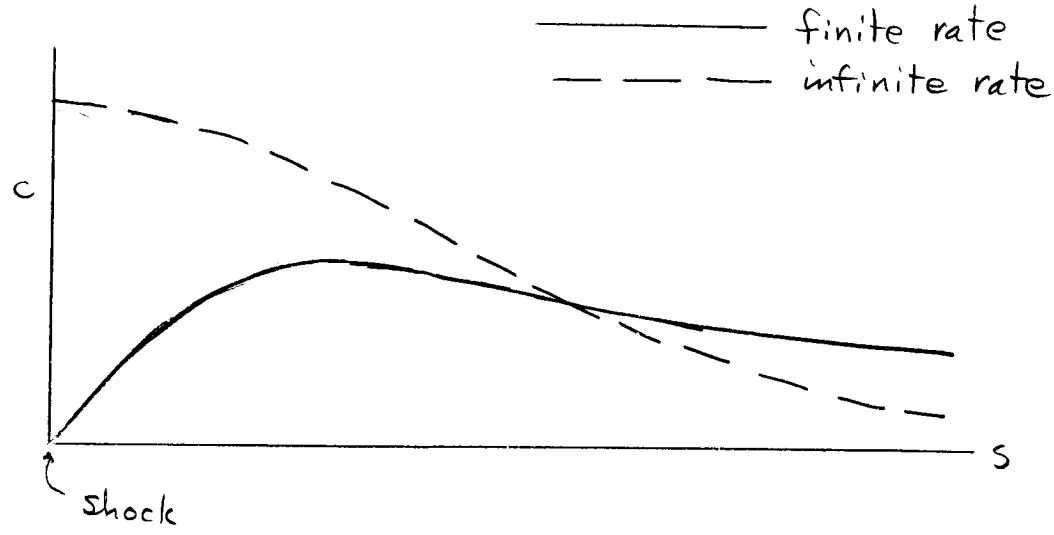

Fig. 28

In both, we plot concentration against distance along the body. In Fig. 27 dissociation rate is rapid, and equilibrium is reached before cooling begins. Freezing then occurs downstream. In Fig. 28 we note the

possibility that the concentration in the nose cap region fails to reach equilibrium. Clearly, the dynamics of subsequent freezing will be different than in the case of the equilibrium reservoir.

VI TRANSPORT PROPERTIES

The final topic of this series will deal with the effects of viscosity on nonequilibrium flows. We first consider transport properties, and in Part VII will deal with viscous flows. We will attempt to find flow models for nonequilibrium flows including viscous terms. We have already noted that chemical activity and radiative transfer result in phenomena not unlike viscous effects, i.e., damping and dispersion in acoustic waves and shocks. The time lags encountered in chemical kinetics relate to the time lags in viscous effects.

Equations of a Binary Mixture

We shall consider a multicomponent high temperature gas (in particular, air). The transport quantities appear as terms on the right-hand side of the conservation equations of Part I, and now these are rewritten as

$$\left.\begin{aligned} -\frac{\partial}{\partial n}(\rho c u_n) &= \frac{\partial}{\partial n}\left(\rho \mathcal{D} \frac{\partial c}{\partial n}\right) \\ \frac{\partial}{\partial n}\left(\mu \frac{\partial u}{\partial n}\right) & \\ \mu\left(\frac{\partial u}{\partial n}\right)^2 + \frac{\partial}{\partial n}\left[\lambda \frac{\partial T}{\partial n} + \rho \mathcal{D}\left(\frac{\partial c}{\partial n}\frac{H_1}{c_1} - \frac{\partial c}{\partial n}\frac{H_2}{1-c_1}\right)\right] & \end{aligned}\right\} \quad (42)$$

We indicate the physical meaning of these terms:

$\frac{\partial}{\partial n}\left(\rho \mathcal{D} \frac{\partial c}{\partial n}\right)$ is a concentration gradient effect;

$\frac{\partial}{\partial n}\left(\mu \frac{\partial u}{\partial n}\right)$ is the viscous shear stress term;

and $\mu \frac{\partial u}{\partial n} + \frac{\partial}{\partial n}\left[\lambda \frac{\partial T}{\partial n} + \rho \mathcal{D}\left(\frac{\partial c}{\partial n}\frac{H_1}{c_1} - \frac{\partial c}{\partial n}\frac{H_2}{1-c_1}\right)\right]$

consists of a term to account for enthalpy increase due to dissipation, a heat conduction term, and a term to account for diffusion of enthalpy.

Enthalpy flux arises from the unequal transport of atoms and molecules. If more atoms than molecules are transported across a surface, then, since the atoms carry the dissociation energy, $h^{(0)}$, there is a net flux of enthalpy across the surface. Thus the final term consists of the diffusion velocity quantity, $\rho \mathcal{D} \frac{\partial c}{\partial n}$, and $h^{(0)}$ is the property transported. We assume that $h^{(0)}$ is much greater than the internal energy of molecules, i.e., $H_{int.} << c h^{(0)}$.

From the Eqs. (42) we see that we must specify three mixing parameters, $\mathcal{D}$, λ, and μ. We now define two important dimensionless parameters:

Prandtl number:

$$Pr \equiv \frac{\mu c_p}{\lambda} \tag{43}$$

which compares viscous effects to heat transfer effects; and

Lewis number

$$Le \equiv \frac{\rho c_p \mathcal{D}}{\lambda} \tag{44}$$

which compares diffusion effects to heat conduction. The Prandtl number and Lewis number are both of unit order, and Pr $\approx$ 3/4. Lewis number is frequently approximated by unity; however; this may not be very accurate, since Lewis number depends upon temperature approximately as shown in Fig. 29.

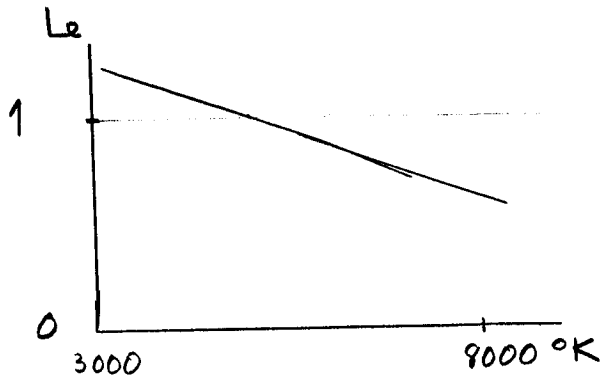

Fig. 29

Using the nondimensional parameters, we note that

$$\frac{\partial}{\partial n}\left(\rho \mathcal{D} \frac{\partial c}{\partial n}\right) = \frac{\partial}{\partial n}\left(\frac{Le}{Pr} \mu \frac{\partial c}{\partial n}\right)$$

and $$\mu\left(\frac{\partial u}{\partial n}\right)^2 + \ldots = \mu\left(\frac{\partial u}{\partial n}\right)^2 + \frac{\partial}{\partial n}\left\{\frac{\mu}{Pr}\left[\frac{\partial H}{\partial n} + (Le-1)\, h^{(0)} \frac{\partial c}{\partial n}\right]\right\} \quad (45)$$

noting that $c_p T = H - h^{(0)} c$.

If we assume $Le = 1$[27], the last term on the right hand side vanishes, and the energy equation is much simplified, since the heat flux and energy equation do not explicitly involve chemistry. We assume, then that diffusion and viscosity effects are so related that $Le = 1$.

We note at this point that gas viscosity increases with an increase in temperature, as opposed to the decrease in viscosity with temperature in liquids. One may explain this behavior by considering the interpenetration of particles, which is greater for more energetic (higher temperature) gas particles. Thus a hot, or rarefied gas has a high viscosity. In dissociating flows, one finds that atoms have a greater penetrating depth than molecules, and therefore the dissociated gas is more viscous than undissociated gas. This is shown qualitatively in Fig. 30.

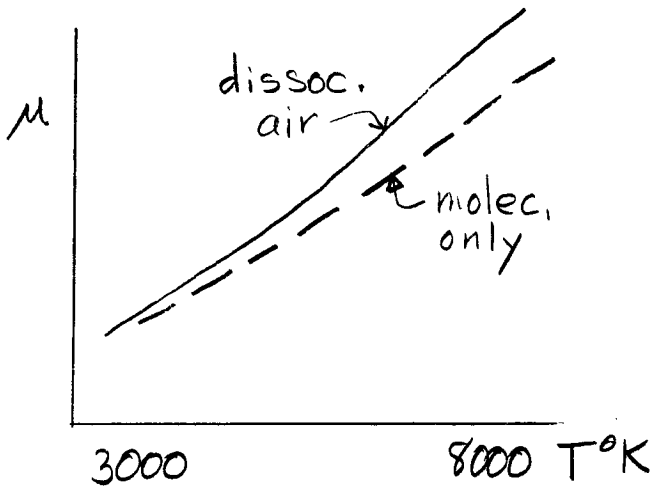

Fig. 30[38]

The collisional models used to calculate the viscosity of multi-component, high-temperature gases are various; the matter is reviewed in Ref. 37.. Actually, it is usually more important to have the right model for high-temperature molecular collisions than it is to account for the presence of atoms[38]. For flow problems, viscosity enters through the product $\rho\mu$, and ρ is a stronger function of c (through the state equation) than is μ. In any case, a simple perturbation formula[38] accounts quite well for the dependence of μ on c:

$$\mu = \mu_{\substack{\text{molec.}\\ \text{only}}} \left[1 + 0.3\,c + \mathcal{O}(c^2)\right]$$

An important question at this point is: Where do we measure viscosity in flows with large temperature variations? We wish to use a constant value for viscosity (or, rather density times viscosity), but what value is most representative? In general, the answer is to evaluate

viscosity in the hottest part of the flow. This is because the hottest part is also (usually) the region of lowest density, and hence forms a very thick layer compared with cooler parts. Properties of the thick layer dominate transport, and the viscosity of this layer rather well represents the effective viscosity of the whole flow.

Surface Catalysis

Consider a semi-infinite region bounded by a solid surface, and denote the surface conditions by the subscript zero. If an atom strikes and adheres to the surface, a second atom may strike it and recombine, the two then leaving the surface as a molecule. In such a recombination, a three body collision is not required, since the wall acts as the third body. The recombination is essentially a one body process. A wall may, then, act as a catalyst for recombination, and surface catalysis is of great importance in nonequilibrium flows. We can write a surface catalysis rate equation as follows:

$$\left(\rho \mathcal{D} \frac{\partial c}{\partial n}\right)_{wall} = \Gamma \sqrt{\frac{RT}{\pi m_1}} \left(c - c_{eq.}\right)_{wall} \qquad (46)$$

Where the left hand side is the rate of arrival of atoms at the surface, by diffusion, Γ is the catalytic efficiency of the surface, the radical is a molecular velocity term, and the last bracket is the departure from equilibrium concentration at the surface. The rate of arrival is then seen to depend upon the degree of nonequilibrium at the surface. If $c = c_{eq}$ there is no net arrival of atoms, i.e., $\partial c/\partial n = 0$. The

quantity Γ is usually not well known since the physical chemistry of catalytic reactions is not fully understood.

VII VISCOUS FLOWS

We have seen how chemical relaxation leads to the dispersion of waves, and other effects analogous to those due to viscosity. Often, relaxation and viscous processes must be considered together.

Couette Flow

Among problems of viscous, heating conducting flows with dissociation, the case of Couette flow is the simplest. Consider two infinite parallel plates, separated by a distance δ, the lower plate being fixed and the upper plate moving at some velocity u_δ (which might be very high). In such a flow the shear force is constant, and the velocity and temperature profiles might be sketched in Fig. 31. Many flows of interest can be represented, at least qualitatively, by suitably defined

Couette flow situations. A variation of this problem is to hold both plates fixed and then impose a temperature difference between the plates.

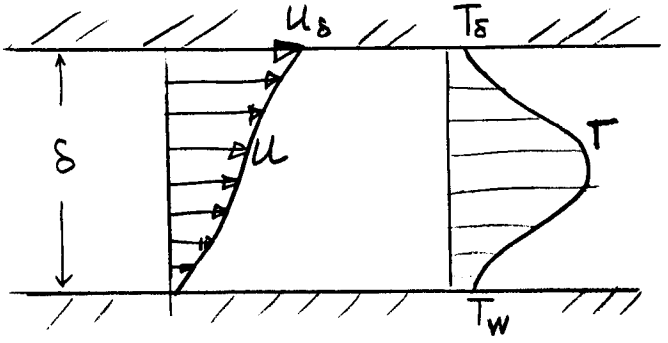

Fig. 31

The differential equations are:

Momentum: $\mu \frac{du}{dy} = \text{const.}$ (47a)

Energy: $\mu \left[Pr\, u \frac{du}{dy} + \frac{dH}{dy} + (Le-1) Pr\, h_1^{(0)} \frac{dc}{dy} \right] = \text{const.}$ (47b)

Atom Production: $\frac{d}{dy}\left(Le\, \mu \frac{dc}{dy} \right) = W_1$ (47c)

Boundary conditions would specify velocity and temperature at the two surfaces, as well as the catalytic condition

$$\left(Le\, \mu \frac{dc}{dy} \right)_w = Pr\, \Gamma \sqrt{\frac{RT_w}{\pi m_2}} \left(c - c_{eq} \right)_w \tag{47d}$$

at the wall.

Now, one can eliminate μ between Eqs. (47a) and (47b) and integrate the resulting equation[35]. Thus, if $Le \approx 1$, and both walls are cold (Fig. 31), one gets

$$\frac{H}{H_w} \approx 1 + \frac{1}{5} Pr\, M_\delta^2 \left(\frac{u}{u_\delta} - \frac{u^2}{u_\delta^2} \right) \tag{48a}$$

Maximum enthalpy occurs when the above bracket is 1/4, i.e., at $\frac{u}{u_\delta} = 1/2$. Then,

$$\left(\frac{H}{H_w}\right)_{max} = 1 + \frac{Pr M_\delta^2}{20} \qquad (48b)$$

and if

$$M_\delta = 25, \quad \left(\frac{H}{H_w}\right)_{max} \approx 30 \quad \text{at } y = \tfrac{1}{2}\delta$$

That is, the enthalpy at the center line is 30 times that at the plates. The foregoing indicates the large amount of heat which is introduced by viscous dissipation, most of which is absorbed in dissociation.

Consider now that the plates are both stationary, so that there is no dissipation. However, the upper one is at a very high temperature (See Fig. 32a. Eqs. (47) give relatively simple solutions for this problem, which is quite a good model for the conditions found at the stagnation region in hypersonic flow.

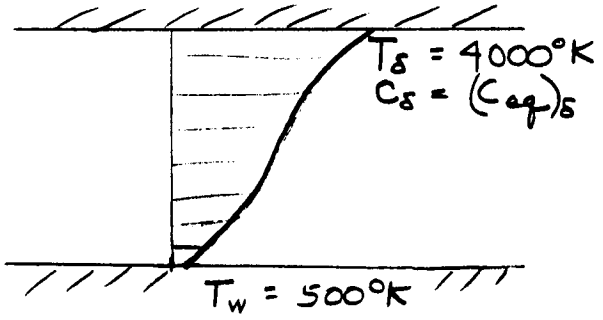

Fig. 32a

Now, for $Le = 1$, $\mu \frac{\partial H}{\partial y} = \text{const.}$, and for the equilibrium case we may express a measure of heat transfer as $Q \approx .65$ (this unit will remain an undefined "Nusselt number", serving only as a comparison for various cases of heat conduction). From Fig. 32a, we note that the temperature gradient is smallest between the plates because a greater

proportion of the heat flux is due to diffusion of atoms in that region, while at the extreme surface temperatures heat is transferred chiefly by conduction.

Let us now examine the "frozen" case, where in this context, frozen means that the atom concentration is not changed by chemical reaction. That is, $W=0$, and for this frozen case, $L_{eu}\frac{\partial c}{\partial y}$ = const. This relation requires that the flux of atoms be constant at every layer. We consider that equilibrium exists at the upper plate, but not necessarily at the lower plate.

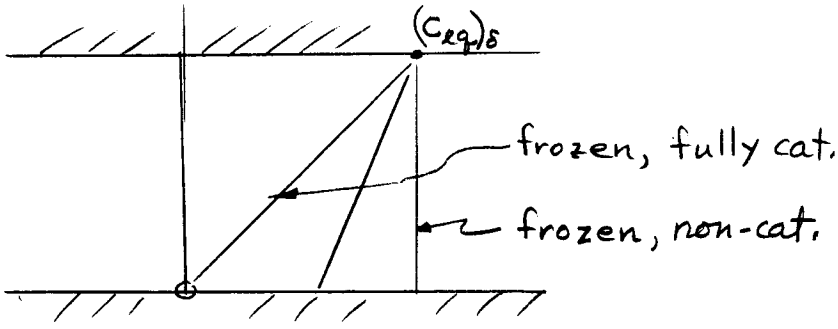

Fig. 32b

Any of the straight lines in the above Fig. 32b satisfy the condition $\frac{\partial c}{\partial y}$ = const. (Assume $L_e\mu$ = const., for convenience.) Suppose the lower surface is cold, so that $(c_{eq})_w=0$; then if the wall is completely noncatalytic, i.e., $\Gamma=0$, then $\frac{\partial c}{\partial y}$ must vanish, according to Eq. (46). If, on the other hand, the wall is fully catalytic, i.e., $\Gamma\to\infty$, then $c-c_{eq}\to 0$ for finite $\frac{\partial c}{\partial n}$. In the frozen, noncatalytic case, the heat

transfer (purely by conduction) is expected to be small, and using the unit introduced earlier, we find $Q \approx .3$. However, if the chemistry is frozen and the wall fully catalytic, there is a chemical reaction at the surface, that is, the energy of dissociation is deposited at the surface upon recombination, but there is no chemical activity in the gas. In this case, heat transfer is high and we get roughly $Q \approx 0.60$. Thus, a fully catalytic wall will experience about the same heat transfer whether or not there is gas-phase chemistry.

This kind of simple "Couette" calculation provides a sort of qualitative model[28] for the more complete calculations of the hypersonic stagnation-point flow[31].

Couette Flow with Radiation

Here, we consider that layers of the gas may exchange heat by radiation:

$$\frac{\mu}{Pr}\frac{dH}{dy} + q_R = \text{const.}$$

Such a problem has been studied by Goulard and Goulard[29] for Couette flow, with a very large temperature difference between the two plates. The gas is assumed to be quite transparent, $\delta << \frac{1}{\alpha_\nu}$ so that we do not have radiative equilibrium. However, we assume "quasi-equilibrium" and also assume a "gray gas". In this case the result from reference 29 is:

$$\frac{\mu}{Pr}\frac{\partial H}{\partial y} + 2\int_{\tau}^{\tau_\delta} B(\tau')d\tau' - 2\int_{0}^{\tau} B(\tau')d\tau' = \text{const.}$$

where $d\tau = \alpha\, dy$ and $B = \sigma T^4$; that is, B is B_ν integrated over all ν. The terms have the following meaning: $\partial H/\partial y$ represents heat conduction downward (Fig. 33) from any point toward the low temperature wall. The term $2\int_{\tau}^{\tau_\delta} B(\tau')d\tau'$ represents downward

radiative transfer of heat for layers above $\hat{\tau}$, and the last term is upward radiation for the layers below $\hat{\tau}$. The net effect of radiative transfer is a smoothing out of the temperature profile. Temperature profiles and energy flux are shown in Fig. 33.

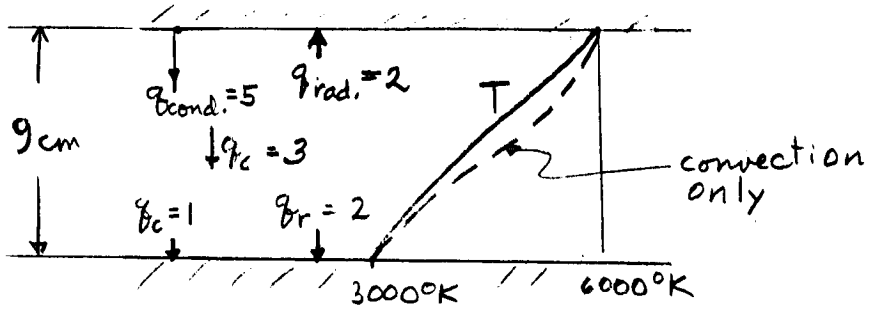

Fig. 33[29]

The presence of radiation revises the balance of heat flux. If the overall heat flux level is, say, a value of 3 watts/cm^2/sec., then at the upper plate, analysis[29] shows that 5 w/cm^2/sec. are due to downward convection, diminished by 2 w/cm^2/sec. due to upward radiation. At y = 1/2 there is a heat flux of 3 w/cm^2/sec. downward due to convection and the upward radiation contribution tend to cancel. At the lower wall, there is then only 1 w/cm^2/sec. downward due to convection and 2 w/cm^2/sec. downward due to radiation. Chung[36] has analyzed Couette flow with ionization, including effects of the plasma sheath.

Viscous Waves

A somewhat different kind of problem which provides a "model" for boundary layer flow is that of a single plate in a semi-infinite expanse of gas, the plate being suddenly moved or heated[30]. Here, we consider an

unsteady problem in independent variables t and x to correspond to a two-dimensional steady problem. Since the plane surface is doubly infinite, all $\partial/\partial x = 0$, and the problem is linear: We may put all $D/Dt = \partial u/\partial t$.

If a step change of temperature or velocity occurs at the plate, a viscous, dissipative, conductive, or diffusive wave spreads into the gas above. In the absence of chemistry, the heat flux to the plate goes inversely with the wave thickness: $Q \propto 1/\sqrt{t}$. Thus, we will speak of heat transfer in terms of a Nusselt number $Q\sqrt{t}$ which would ordinarily be constant.

First suppose temperature of the plate drops slightly, the gas above being dissociated. At first, there hasn't been time enough for any change in c (whatever the value of Γ) and the Nu is small, compared with the value later on, when c also falls and the chemical energy is given up to the surface, or near the surface in the gas. Ultimately, equilibrium must be achieved, for any Γ, though the value of Γ affects the speed of equilibration.

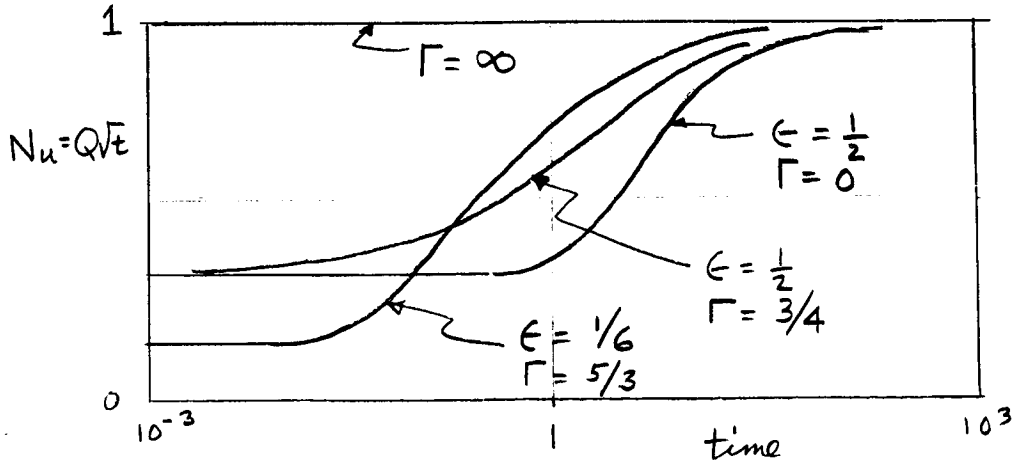

Fig. 34[30]

Fig. 34 shows how Nu is affected by catalycity, as well as by ϵ which compares change in temperature with change in (equilibrium) concentration

$$\frac{\epsilon}{1+\epsilon} \equiv \left(\frac{c_p \Delta T}{c_p \Delta T + h^{(0)} \Delta C} \right)_{eq.}$$

at constant pressure. ϵ can be quite small for air; in effect, because $h^{(0)}$ is large. Especially at low density is this true. The mathematical assumption of small ϵ greatly simplifies the analysis of this problem[30], providing a model which might usefully be extended to other problems.

Fig. 34 is remarkably close, qualitatively, to the more exact results for stagnation-point flow due to Fay and Riddell[31], and thus, this "Rayleigh Problem" provides a useful model for certain hypersonic boundary layers. Such a model for the flat plate boundary layer is provided by assuming that the plate temperature is low, but it is suddenly moved at high speed. Consequent dissipation produces heat flux. In this case, the early and late situations are the same -- no chemistry. At intermediate times, however, atoms are produced in the gas, but may not have had time to recombine at the surface. Thus, at the surface, one has the concentration-history shown in Fig. 35. A corresponding dip in an otherwise constant Nu may be expected at these intermediate times. Here again, small ϵ simplifies the analysis.

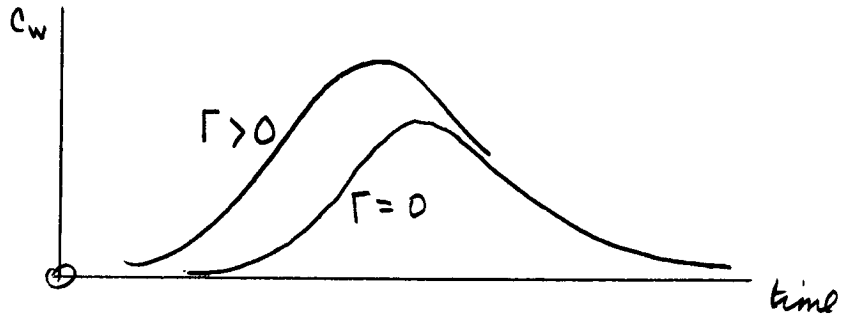

Fig. 35

The Leading Edge Problem

The corresponding problem of the hypersonic boundary layer with chemistry at the leading edge of a flat plate has been studied by Rae[33]. In this case, one is concerned only with dissociation, since recombination is of no consequence in the region near the leading edge, i.e., $t << \tau_{rec}$. As a result, binary scaling is applicable. Rae finds that the temperature exhibits a sharp maximum within the boundary layer, owing to the effect of dissipation. He was able to achieve a simple solution by an approximation of a thin reaction zone at this maximum temperature layer, on either side of which concentration was assumed to change only by diffusion.

The Stagnation Point

As we have mentioned, the stagnation point is the only case for which the nonlinear viscous flow with nonequilibrium chemistry has been solved. In effect, one finds the leading term of a Taylor series in distance away from the stagnation point. The heat transfer results[31] are illustrated

quite well by Fig. 34, except that, instead of real time t, one uses the characteristic time L/U_∞ in forming the abscissa. Thus, a small nose radius would favor "frozen heat blockage", for a noncatalytic surface, for example.

Stagnation Point Heat Transfer at Altitude

Chung[32] has analyzed this problem. For stagnation flows, as altitude increases, τ increases, and this has the same effect as a decrease in L. Thus the flow tends to freeze, even though the boundary layer thickens. At high altitudes, the shock layer, δ is nearly all viscous (refer to Fig. 17); that is, the boundary layer thickness approaches δ. The heat transfer rate calculated by Chung varies with altitude as shown in Fig. 36, for a noncatalytic wall.

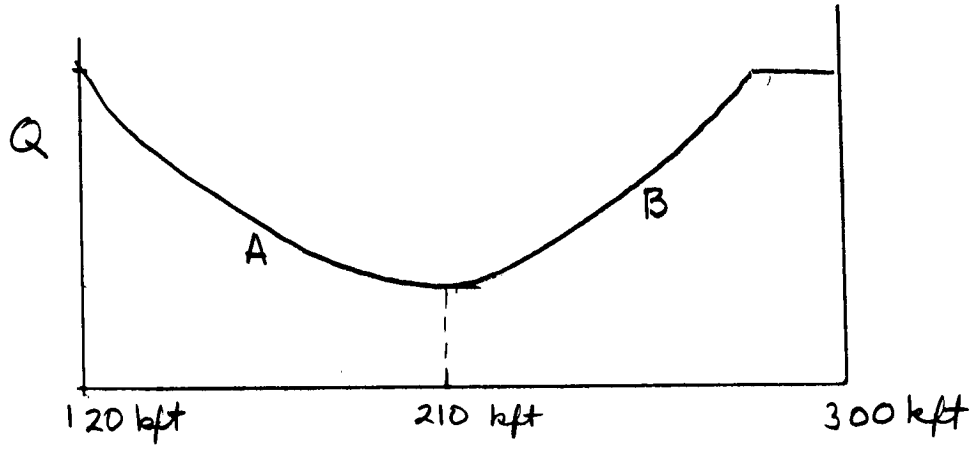

Fig. 36[32]

In region A, heat transfer decreases with increasing altitude due to slow recombination in the frozen boundary layer. The energy is essentially trapped in the form of dissociation energy, and the boundary layer, being almost completely frozen, has reduced heat transfer to the wall. However, as altitude increases still further, the degree of dissociation behind the shock decreases, and less and less energy is taken up in dissociation. Thus, at about 210 kilo feet these two effects are nearly equal and heat transfer reaches a minimum. Further increase in altitude, i.e., region B on Fig. 37, results in failure to reach dissociation equilibrium behind the shock, and finally, at about 300 kilo feet, there is little or no energy going into dissociation at all. Here we approach the condition of an ideal gas, with no chemistry involved in the heat transfer process.

REVIEW OF MODELS DISCUSSED

In these notes, a wide variety of assumptions and physical and mathematical models, useful in the analysis of hypersonic flows of a real dissociating gas, are discussed. In conclusion, these may be listed as follows:

1. Lumped constituents (p. 8): grouping together of nonreacting constituents.
2. Lighthill Ideal Gas (p. 10): vibration 50% excited and a constant; useful as a standard real gas.
3. Nearly-Equal Speeds of Sound : small dispersion of sound waves in either chemical (p. 16) or radiative (19) cases. Leads to Telegraph Equation.

4. Quasi-Equilibrium Radiation (p. 20): even if quite transparent, absorptivity and emissivity at black-body values.

5. Gray Gas (p. 22): Emissivity independent of wave length.

6. Constant pressure, enthalpy behind normal shock (p. 31): For very strong plane shock, and γ nearly 1.

7. Newtonian Flow (p. 39): Enthalpy and velocity nearly constant, for strong (curved) shocks and γ nearly 1.

8. Binary Scaling (p. 31, 41): when low-density flow is initially under-dissociated.

9. Coupling of Vibration and Dissociation (p. 38): behind very strong shocks.

10. Sudden Freezing (p. 50): during expansion of initially fully-dissociated gas.

11. Constant "Entropy" (p. 55): for channel flows with sudden freezing -- Moliere diagram.

12. Channel Flow in Stream Tubes (p. 58): for analysis of nonequilibrium afterbody flows.

13. Viscosity Evaluated in Hottest Part of Flow (p. 63): generally a good rule. Viscosity weakly dependent on c.

14. Constant Pr, Le, $\rho\mu$ (p. 61, 63); Usually done but not fully justified.

15. $Q \propto \Delta H$ (p. 62): Ideal gas result applies to this extent, if $Le = 1$.

16. Couette Flow (p. 65): a model for hypersonic boundary layers.

17. Viscous Waves (Rayleigh Flow) (p. 70): a model for hypersonic boundary layers, especially stagnation point flow.

18. Thin Reaction Layer (p. 73): for leading-edge problem.

19. Equilibrium Change of Internal Energy Much Smaller Than Chemical (p. 72): Small ϵ; Simplifies Rayleigh problem.

REFERENCES

1. Myerott, R.E., Radiation Heat Transfer to Hypersonic Vehicles. Lockheed Aircraft Corp. LMSD 2264-R1 (September 1958)

2. Hayes, W.D. and Probstein, R.F., Hypersonic Flow Theory. Academic Press, New York (1959)

3. Matthews, D.L., Interferometric Measurements in a Shock Tube of the Dissociation Rate of Oxygen. Phys. of Fluids 2, p.170 (1959)

4. Byron, S.R., Interferometric Measurement of the Rate of Dissociation of Oxygen Heated by Strong Shock Waves. Cornell Univ. Thesis (1958)

5. Lighthill, M.J., Dynamics of a Dissociating Gas: Pt. I Equilibrium Flows. Jour. Fluid. Mech. 2, p.1 (1958)

6. Moore, F.K., Propagation of Weak Waves in a Dissociated Gas. Jour. Aero. Sci. 25, p.279 (1958)

7. Moore, F.K. and Gibson, W.E., Propagation of Weak Disturbances in a Gas Subject to Relaxation Effects. J. Aero. Sci., Vol. 27, No. 2, p. 117 (Feb. 1960)

8. Chandrasekhar, S., Radiative Transfer. Dover (1960)

9. Lighthill, M.J., Dynamics of a Dissociating Gas: Part 2 Quasi-Equilibrium Transfer Theory. Jour. Fluid Mech. 8, p. 161 (1960)

10. Goulard, R., Fundamental Equations of Radiation Gas Dynamics. AGARD Fluid Dynamics Panel Meeting. High-Temperature Aspects of Hypersonic Flow (April 1962)

11. Vincenti, W.G. and Baldwin, B.S., Jr., Effect of Thermal Radiation on the Propagation of Plane Acoustic Waves. Jour. Fluid Mech. 12, p.449 (1962)

12. Clarke, J.F., Radiation Resisted Shock Waves. Phys. of Fluids, 5, p.1347 (1962)

13. Baldwin, B.S., The Propagation of Plane Acoustic Waves in a Radiating Gas. NASA TR R-138 (1962)

14. Morrison, J.A., Wave Propagation in Voigt Materials and Visco-Elastic Materials with Three Parameter Models. Quart. Appl. Math. Vol. 14, p. 153 (1956-57)

15. Gibson, W. E., Dissociation Scaling for Nonequilibrium Blunt Nose Flows. ARS Jour. 32, 285 (1962)

16. Duff, R. E. and Davidson, N., Calculation of Reaction Profiles Behind Steady State Shock Waves: II The Dissociation of Air. Jour. Chem. Phys. 31, p. 1018 (1959)

17. Hall, J. G., Eschenroeder, A. Q., and Marrone, P. V., Blunt-nosed Inviscid Air Flows with Coupled Nonequilibrium Processes. Jour. Aero. Sci. 29, p. 1038 (1962)

18. Hammerling, P., Teare, J.D., and Kivel, B., Theory of Radiation from Luminous Shock Waves in Nitrogen. Phys. Fluids 2, p. 422 (1959)

19. Treanor, C. E. and Marrone, P. V., Chemical Relaxation with Preferential Dissociation from Excited Vibrational Levels. Cornell Aeronautical Laboratory Report QM-1626-A-10 (February 1963)

20. Freeman, N. C., Nonequilibrium Flow of an Ideal Dissociating Gas. Jour. Fluid Mech. 4, p. 407 (1958)

21. Gibson, W. E. and Marrone, P. V., Nonequilibrium Blunt Body Flows: A Correspondence Between Normal Shock and Blunt-Body Flows. Phys. of Fluids 5, p. 1649 (1962); Also, A Similitude for Nonequilibrium Phenomena in Hypersonic Flight. AGARD Meeting on High-Temperature Aspects of Hypersonic Fluid Dynamics (March 1962) (To be published by Pergamon Press)

22. Lick, W., Inviscid Flow Around a Blunt Body of a Reacting Mixture of Gases. Rensselaer Poly. Inst. TR AE 5810, May 1958, and TR AE 5814 (December 1958)

23. Bray, K. N. C., Atomic Recombination in a Hypersonic Wind Tunnel Nozzle. Jour. Fluid Mech. 6, p. 1 (1959)

24. Hall, J. G. and Russo, A. L., Studies of Chemical Equilibrium in Hypersonic Nozzle Flows. Proc. First Conf. on Kinetics, Equilibria, and Performance of High-Temperature Systems. Butterworth Sci. Pub. 219 (1960)

25. Bray, K. N. C., Simplified Sudden Freezing Analysis for Nonequilibrium Nozzle Flows. ARS Jour. 31, p. 831 (1961)

26. Eschenroeder, A. Q., Entropy Changes in Nonequilibrium Flows. Cornell Aeronautical Laboratory Report AD-1689-A-2 (September 1962)

27. Lees, L., Convective Heat Transfer with Mass Addition and Chemical Reactions. Combustion and Propulsion Third AGARD Colloquium. Pergammon Press

28. Moore, F. K., Editor, Theory of Laminar Flows. Vol. IV High-Speed Aerodynamics and Jet Propulsion. Princeton University Press (to be published)

29. Goulard, R. and Goulard M., Energy Transfer in the Couette Flow of a Radiant and Chemically Reacting Gas. Heat Trans. and Fluid Mech. Inst. Preprints of paper (Univ. of Calif.) (1959)

30. Moore, F. K. and Rae, W. J., The Rayleigh Problem for a Dissociated Gas. Cornell Aeronautical Laboratory Report AF-1285-A-8 (June 1961); Also, Hypersonic Flow Research, Vol. 7 of Progress in Astronautics and Rocketry, edited by F.R. Riddell, pp. 107-140, Academic Press, New York (1962)

31. Fay, J. A. and Riddell, F. R., Theory of Stagnation Point Heat Transfer in Dissociated Air. Jour. of Aero. Sci. 25, p. 72 (1958)

32. Chung, P. M., Hypersonic Viscous Shock Layer of a Nonequilibrium Dissociating Gas. NASA TR T-109 (1961)

33. Rae, W. J., An Approximate Solution for the Nonequilibrium Boundary Layer near the Leading Edge of a Flat Plate. Inst. Aero. Sci. Paper 62-178 (June 1962)

34. Eschenroeder, A. Q., Boyer, D. W., and Hall, J. G., Nonequilibrium Expansions of Air with Coupled Chemical Reactions. Phys. Fluids, Vol. 5, No. 5, p. 615 (May 1962)

35. Clarke, J. F., Energy Transfer Through a Dissociated Diatomic Gas in Couette Flow. J. Fluid Mech. 4, Pt 5, 441-465 (1958)

36. Chung, P. M. Electrical Characteristics of Couette and Stagnation Boundary Layer Flows of Weakly Ionized Gases. Aerospace Corp. Report No. TDR-169(3230-12) TN-2 (1962)

37. Bade, W. L., Mason, E. A., and Yun, K. S., Transport Properties of Dissociated Air. ARS Journal, Vol. 31, No. 4 (August 1961) p. 1151-1153

38. Moore, F. K., On the Viscosity of Dissociated Air. ARS Journal, V. 32, No. 9 (September 1962)

25106

THE STABILITY BEHAVIOR OF THE SOLUTIONS OF HAMILTONIAN SYSTEMS

by J Moser
New York University
New York City

These notes were written up by Dr. Deutsch after the meeting. For a careful revision and editing I am grateful to Dr. Fred Gustavson who also supplied valuable remarks. I also wish to thank O. Benediktsson for his help in Section V.

I. Introduction.

a. The study of conservative systems has a long history, its aim being mainly the description of planetary orbits. In fact, for a long time this subject was one of the primary fields for applications of the calculus and to a tremendous extent stimulated the development of analysis Following the work of Poincaré and Birkhoff the subject of conservative systems reached an apparent climax which seemed to have brought the development to a stop. Many of the important questions were solved or were shown to be absurd or inappropriate questions. As an illustration of the latter point, recall that for many years mathematicians sought explicit solutions of the equations of motion; first by explicit formulae; then by quadratures, which means that the solution is represented in the form of explicit integrals When it was recognized that this question is closely related to the construction of integrals, one then tried to establish integrals of the motion -- say for the three body problem. It soon became suspected that there may not exist any integrals for the three body motion other than the known energy and momentum integrals. Bruns, by means of a very ingenious argument, showed the nonexistence of algebraic integrals for the planar 3 - body problem, except those which are algebraic functions of the known ones. Later, Poincaré presented an argument which showed that in general a Hamilton system need not have more integrals than the Hamiltonian and functions of it. Even though his argument has been criticized as being incomplete, it does clearly contain the germ of the proof. Further details on this subject are discussed later.

Thus questions related to the search for integrals of the system and the solution by quadratures seemed to have ended with Bruns and Poincaré. This is both a true and a false description of current work. To show that the quest has not really ended, we have to ask what is the principal aim in the study of conservative systems. First of all, it is the description of the solution for long time intervals. The differential equation relates the function and its derivative at a point. One should deduce from this knowledge the behavior of the solutions for long times. For example, can one exhibit solutions of the 3 - body problem which never lead to collisions? The question of collisions is intimately related to the stability problem in the 3 - body problem. The stability problem has also been at the root of the attempts to discover explicit solutions, since these solutions can be

described for all times. In general, the task of describing the behavior of all solutions of a conservative system for all time is a very difficult one because the motion can be ergodic and, therefore, would be much too complicated for an analytical description.

I shall not attempt to give a historical background of the related developments in celestial mechanics. For this purpose, I refer to the very interesting paper of Hagihari *. Hagihari also discusses the point that the problem of describing the motion for all time is an outstanding open problem.

Recently the theory of Hamiltonian systems has received a strong impetus from the investigation of artificial satellite orbits, but an even stronger impetus from the study of charged particles in a magnetic field, e.g. in accelerators, where the particles go around more than 300,000 times in a vacuum chamber and have to be retained in a remarkably narrow chamber by appropriate magnetic fields. These time intervals are relatively much longer than those that one is accustomed to dealing with in astronomy, where one revolution has to be taken as a year for the earth, or a month for the moon. The motion in particle accelerators thus poses the challenging problem of developing a theory for predicting the orbits for such long time intervals.

For the description of satellite orbits the main questions are those of numerical methods; however, the nature of the orbits is still of interest.

b. Within the last ten years, this outstanding old problem has received an immense advance. At the International Congress in Amsterdam (1954), A. N. Kolmogorov announced an outstanding result concerning the existence of almost periodic solutions of Hamiltonian systems. The statement of Kolmogorov's results, its application to celestial mechanics and an indication of its proof will be the topics discussed in these lectures.

Since the announcement of Kolmogorov, one of his students, V. Arnold, has worked on the ideas presented by Kolmogorov and has applied these concepts to the n-body problem. Arnold discussed some of his results at the last International Congress (1962). He also presented the details for some theorems related to

* Y. Hagihari, Notes of the Summer Institute in Dynamical Astronomy, Yale University (July 1960).

that of Kolmogorov and he recently, in a private communication, disclosed that he has written a long paper concerning Kolmogorov's theorem. The publication of this paper will appear in a commemorative volume honoring Kolmogorov.

During the years 1958-1961, I also made an effort to give a full proof of the statements of Kolmogorov. These results were published in the Gött. Nachrichten (1962).

c. To put these results into perspective and to prepare the path properly, the lectures will be organized into the following parts:

I. Introduction

II. Discussion of existence and nonexistence of integrals

III. Statement and discussion of Kolmogorov's theorem and the annulus theorem

IV. Application to the motion of a satellite about an oblate earth -- results of Kyner and Conley

V. Proof of a theorem by C. L. Siegel

II. Existence and Nonexistence of Integrals.

1. Conservative System, transformation theory --

Consider the system of equations of the Hamilton canonical form:

$$\dot{p} = -H_q\ (p, q, t)\ ;\ \dot{q} = +H_p\ (p, q, t)$$

$$p = (p_1, \ldots, p_n) \tag{1}$$

$$q = (q_1, \ldots, q_n),$$

and t is the independent variable. It is known that the canonical system of equations is related to the variational problem

$$\delta \int L(q, \dot{q}, t)\, dt = 0, \quad L = \sum_{\nu=1}^{n} p\ \dot{q} - H(p, q, t)$$

An alternative representation of Hamiltonian systems was given by Cartan (see Leçon sur les Invariants Integraux, A. Hermann et Fils, Paris 1922). Any system

$$\dot{p}_\nu = f_\nu(p, q)$$

$$\dot{q}_\nu = q_\nu(p, q)$$

is Hamiltonian if there exists a function H such that the differential form

$$\sum_{\nu=1}^{n} dp_\nu dq_\nu - dH\,dt$$

is preserved, i.e., if

$$\frac{d}{dt}\left(\sum_{\nu=1}^{n} dp_\nu dq_\nu - dH\,dt\right) = 0 .$$

Consider the following general transformation of the generalized coordinates:

$$p_\nu = \phi_\nu(u, v)$$
$$q_\nu = \psi_\nu(u, v) .$$

In general, such a transformation does not preserve the Hamilton canonical form. A canonical transformation (i.e., one which preserves the Hamilton canonical form (1)) of the variables is required to preserve the differential form

$$\sum_{\nu=1}^{n} dp_\nu dq_\nu = \sum_{\nu=1}^{n} du_\nu dv_\nu .$$

This condition is equivalent to

$$\sum_{k,\ell} \frac{\partial(\phi_\nu, \psi_\nu)}{\partial(u_k, v_\ell)} du_k dv_\ell + \sum_{k,\ell} \frac{\partial(\phi_\nu, \psi_\nu)}{\partial(u_k, u_\ell)} du_k du_\ell$$
$$+ \sum_{k,\ell} \frac{\partial(\phi, \psi)}{\partial(v_k, v_\ell)} dv_k dv_\ell = \sum_{k} du_k dv_k .$$

If the transformation is canonical, the new Hamiltonian is obtained by substituting the new variables into the original Hamilton function. That is,

$$H = H[\phi(u, v), \psi(u, v)] = K(u, v) .$$

A system is said to possess an integral, $G(p, q)$, in some domain D, if

(i) the gradient $(G_{p_\nu}, G_{q_\nu}) \neq 0$ in D,

(ii) $G(p, q)$ is a constant along each orbit in the domain D (in phase space); i.e.,

$$\frac{d}{dt} G(p, q) = \sum_{\nu=1}^{n} (G_{p_\nu} H_{q_\nu} - G_{q_\nu} H_{p_\nu}) \equiv 0 .$$

It is clear that if H is independent of q_1, then $G = p_1$ is an integral. Such a situation arises frequently if the system is independent of some variables. The existence of these ignorable variables can be used to reduce the order of the system.

More generally, it can be shown that if H has an integral G_λ, locally then in appropriate coordinates u, v the Hamilton $H = H(u, v)$ is independent of u_1 and $G = v_1$ is an integral. This statement is proved by showing that

$$v_1 = G(p, q)$$

can be extended to a canonical transformation. The preceding is a special case of a more general theorem. Let $G_1, G_2, \ldots, G_n$ be n functions such that

$$\sum_{\nu=1}^{n} (G_{\mu p_\nu} G_{\mu' q_\nu} - G_{\mu q_\nu} G_{\mu' p_\nu}) = 0 ; \quad \mu, \mu' = 1, \ldots, n$$

and $\left(\frac{\partial G_\mu}{\partial p_\nu}, \frac{\partial G_\mu}{\partial q_\nu}\right)$ is of rank n ;

then there exists a canonical transformation such that

$$v_\mu = G_\mu(p, q), \quad u_\mu = F_\mu(p, q).$$

The preceding is a local statement.

In this case, one would have

$$H = H(v_1, v_2, \ldots, v_n)$$

and $\dot{u}_\nu = H_{v_\nu}, \quad \dot{v}_\nu = 0.$

The solution to the system, therefore, is given by

$$u_\nu = H_{v_\nu}[v(0)]\, t + u_\nu(0)$$
$$v_\nu = v_\nu(0).$$

In the following, systems of the preceding type will be called integrable.

2. We shall illustrate by an example the manner in which rotational symmetry leads to the existence of integrals. This example will again be discussed later on. The example is that of Störmer's problem which deals with the motion of a charged particle in a dipole field which is an idealized model of the earth's magnetic field.

The motion of a charged particle in a magnetic field B is governed by the equation

$$m\dot{v} = e[B \times v],$$

where m, e, v are respectively the mass, charge, and velocity of the charged particle. The dipole field is given by

$$B = c \frac{\partial}{\partial z} \operatorname{grad} \frac{1}{r},$$
$$r^2 = x^2 + y^2 + z^2.$$

By an appropriate stretching of the variables we can effect the normalization

$$\frac{e}{m} c = 1.$$

Therefore, the system equations can be written as

$$\dot{v} = [B \times v]$$
$$B = \frac{\partial}{\partial z} \operatorname{grad} \frac{1}{r}.$$

In order to write these equations in the Hamilton canonical form, we introduce the vector potential A having the components

$$A \cdot \left(\frac{y}{r^3}, \frac{-x}{r^3}, 0 \right)$$

so that

$$\operatorname{curl} A = B.$$

We introduce the Hamiltonian

$$H = \frac{1}{2} [(p_1 - A_1)^2 + (p_2 - A_2)^2 + (p_3 - A_3)^2]$$

where $q = (x, y, z)$.

Then, if one eliminates p_1, p_2, p_3 from the set of equations

$$\dot{q}_\nu = H_{p_\nu} = p_\nu - A_\nu$$
$$\dot{p}_\nu = -H_{q_\nu} = \sum_\mu (p_\mu - A_\mu) A_{\mu q_\nu} = \sum \dot{q}_\mu A_{\mu q_\nu},$$

one finds

$$\ddot{q}_\nu = \sum \dot{q}_\mu (A_{\mu q_\nu} - A_{\nu q_\mu})$$

or

$$\ddot{q} = [\operatorname{curl} A \times \dot{q}] = [B \times \dot{q}].$$

By inspection, it is apparent that these differential equations are invariant with respect to rotations about the z axis. Therefore, it is appropriate to introduce the cylindrical coordinates θ, w, z by the relations

$$x = w \cos \theta$$
$$y = w \sin \theta$$
$$z = z.$$

Extend this introduction of new coordinates to a canonical transformation by introducing the new momenta

$$p_\theta = -p_1 y + p_2 x$$
$$p_w = (p_1 x + p_2 y)\frac{1}{w}$$
$$p_z = p_3 .$$

Using the new variables yields the new Hamiltonian:

$$H = \frac{1}{2}\left[p_w^2 + p_z^2 + \left(\frac{p_\theta}{w} + \frac{w}{r^3}\right)^2\right].$$

This relation demonstrates that θ is an ignorable variable, a result that has already been anticipated. Hence, we have the integral of the motion:

$$G = p_\theta = w^2\dot{\theta} - \frac{w^2}{r^3} .$$

Notice that G is not the angular momentum, which is $w^2\dot{\theta}$.

This result is well known and serves to illustrate the usual construction of an integral by taking advantage of symmetry. The integral, G, serves to reduce the system to two degrees of freedom. Since p_θ = constant, and θ does not appear in the Hamiltonian, one has a system for w, z which takes the form

$$\ddot{w} = -V_w \qquad \dot{w} = p_w$$
(2)
$$\ddot{z} = -V_z \qquad \dot{p}_w = -H_w ,$$

where

$$V = \frac{1}{2}\left(\frac{p_\theta}{w} + \frac{w}{r^3}\right)^2 ; \quad r^2 = w^2 + z^2 .$$

Thus, in the meridian plane, the motion appears like that produced under the influence of a potential force given by (V_w, V_z).

The integration, or study, of these equations is called "Störmer's" problem because Störmer made extensive numerical studies of the solutions which were later continued by Lemaitre, de Vogelaire, and others. It is generally understood that the system (2) is not integrable, although this fact has not been proven.

3. To demonstrate the difficulty lying in the concept of integrability, we want to show that this system, (2), indeed possesses 3 independent analytical integrals in some part of phase space; although in the remainder of the phase space, these integrals need not exist. Yet, analytic

continuation of the integrals cannot be used to construct the integrals over the total phase space.

To show this, we consider the differential equations (2) in the z, w plane which have the integral

$$H = \frac{1}{2}(\dot{z}^2 + \dot{w}^2) + V .$$

This represents 1/2 of the sum of the squares of the velocities; i.e., $\frac{1}{2}(\dot{q})^2$. For each trajectory, except the rest states, we can replace the time variable by ct so as to obtain the normalization

$$H = \frac{1}{2} , \quad \text{or} \quad |\dot{q}| = 1 .$$

Hence, we can study the orbits satisfying the relation

$$\dot{z}^2 + \dot{w}^2 + 2V = 1 ,$$

or

$$\left| \frac{G}{w} + \frac{w}{r^3} \right| \leq 1 .$$

The inequality restricts the w, z plane to a certain admitted region which has different shapes for different values of

$$G(z, w) = g .$$

Typical regions are sketched in the figure.

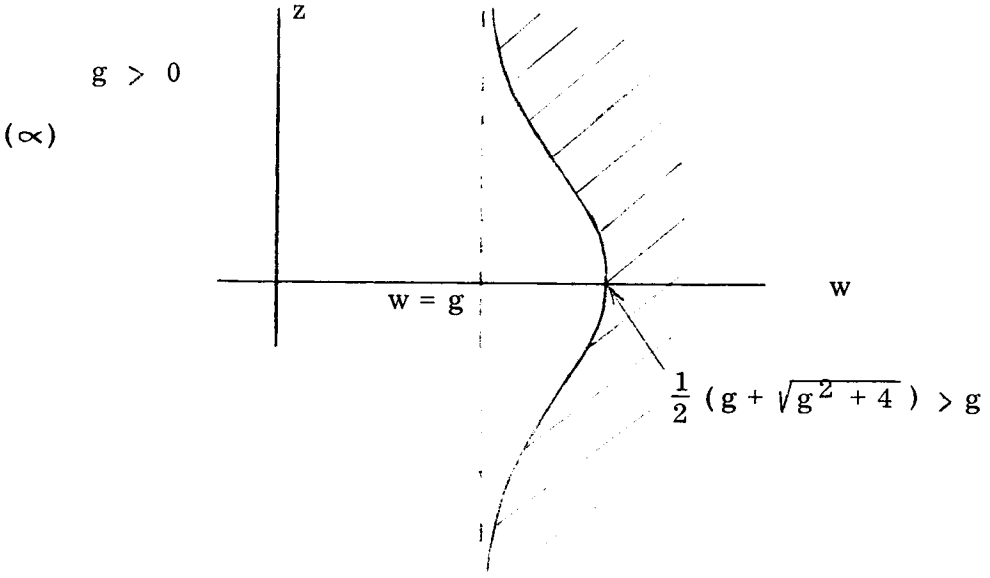

$-2 < g < 0$

(β)

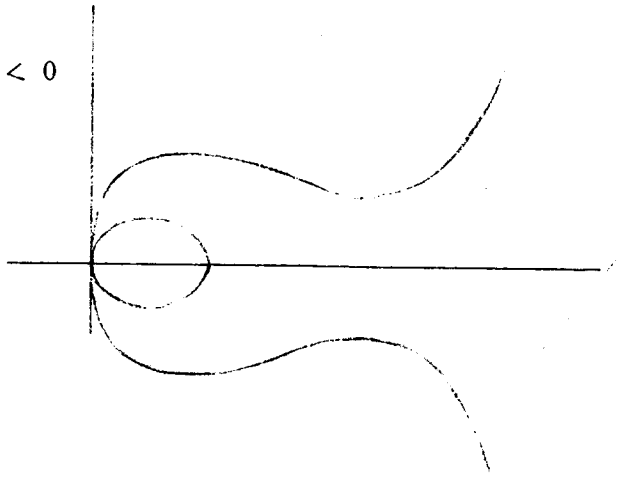

$g = -2$

(γ)

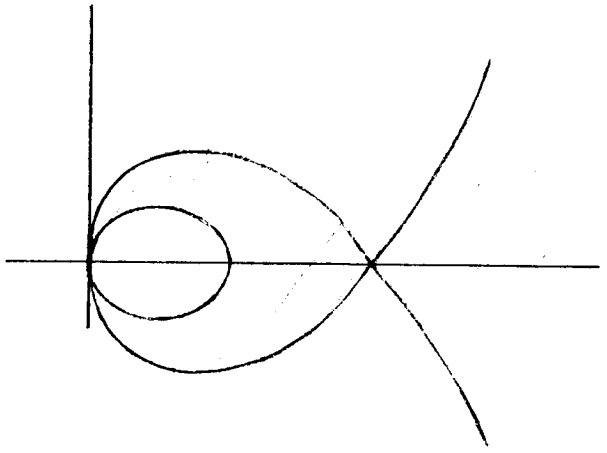

$g < -2$

(δ)

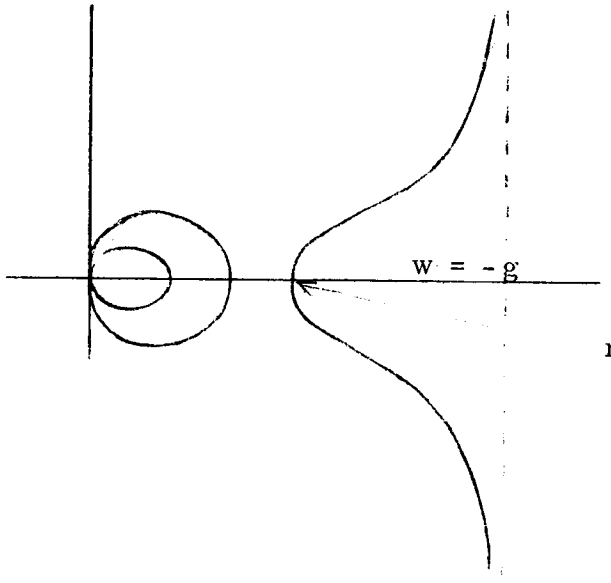

in outside region

$$\min w = \frac{1}{2}\left(|g| + \sqrt{g^2 + 4}\right)$$

4. Now it is easy to see that if $g > 0$ then for all solutions one has

$$r \to \infty \quad \text{as} \quad t \to \infty .$$

The same situation holds if $g < -2$ and one is in the outside region. This follows from a simple estimate for $R = |q|^2$. From the differential equation one finds that

$$\frac{1}{2}\frac{d^2R}{dt^2} = |\dot{q}|^2 + (q, \ddot{q}) = 1 + (q, [B \times \dot{q}]) .$$

But, since

$$B = \frac{3z}{r^5} q - \frac{k}{r^3} ,$$

we have

$$\frac{1}{2}\frac{d^2R}{dt^2} = 1 - \frac{1}{r^3}(q, [k \times \dot{q}])$$

$$= 1 + \frac{1}{r^3}\omega^2 \dot{\theta}$$

$$= 1 + \frac{1}{r^3}\left(g + \frac{\omega^2}{r^3}\right) .$$

For $g > 0$ one observes that $\frac{1}{2}\frac{d^2R}{dt^2} \geq 1$ thus $R(t)$ is a convex function and $R \to \infty$ as $t \to \infty$.

A similar estimate holds in the outside region of case δ since there

$$\min w = \frac{1}{2}\left[|g| + (g^2 - 4)^{1/2}\right] > \delta + 1 , \text{ with } \delta_0 > 0 .$$

Therefore

$$\frac{1}{2}\frac{d^2R}{dt^2} = 1 + \frac{w}{r^3}\left(\frac{g}{w} + \frac{w}{r^3}\right) \geq 1 - \frac{w}{r^3}$$

$$= 1 - \frac{w}{(w^2 + z^2)^{3/2}} \geq 1 - \frac{1}{w^2} > 1 - \frac{1}{(1+\delta)^2} = \delta' > 0 .$$

We are then led to the same conclusion:

$$R \to \infty \quad \text{as} \quad t \to \pm\infty .$$

Therefore, we have shown that $|q| \geq \delta'' t$ for large t. From the differential equation, one concludes that

$$\ddot{q} \to 0\left(\frac{1}{t^3}\right) \quad \text{as} \quad t \to +\infty , \text{ and, moreover,}$$

$$\dot{q} \to a + 0\left(\frac{1}{t^2}\right) ,$$

where a is a vector satisfying $|a| = 1$, since $|\dot{q}| = 1$. Finally, one observes that

$$q(t) - at - b \to 0 ,$$

with a constant vector b.

Conversely, one can find a solution for every given a, b in the form

$$q(t) = at + b + ct^{-1} + \ldots ,$$

as a convergent power series expansion, if t is large enough. The proof of these statements is quite straightforward.

Thus, an orbit $q(t)$ can be specified by the vectors a, b. In order to take into account the fact that $q(t)$ and $q(t+\tau)$ correspond to the same orbit, i.e., a, b and $(a, b+\tau a)$ should be identical; we normalize a, b by the orthogonality relation

$$(a, b) = 0 .$$

Moreover, normalization of the Hamiltonian to $H = 1/2$ yielded

$$|a| = 1 ,$$

and finally, $G = g$ corresponded to

$$(a, b, k) = g .$$

The components of the vectors a, b satisfying the above conditions represent integrals in the part of phase space specified by $g > 0$, $H = 1/2$, or, the outside region in case δ, and $H = 1/2$. That is, for every point P in this portion of the phase space, follow the orbit through P as $t \to +\infty$ to ∞ and associate $a(P), b(P)$ with it. The six components are analytic functions and well defined in this region. The preceding three restrictions altogether provide 3 integrals independent of G and H. Thus, we have the 5 independent integrals which we wanted to show.

5. Nonexistence of integrals

In connection with the nonexistence on integrals, we have to discuss the negative results which state that in general Hamiltonian systems do not possess any integrals independent of H. The best known result in this connection in due to Poincaré. Poincaré's theorem has been criticized because it is not rigorous. A different and rigorous statement has been given by Siegel which states that near an equilibrium integrable systems are rare in the sense of Baire category. We also refer to the papers of Fermi and Moser. We shall not go into details on this subject since

Dr. Contopoulos will discuss the subject at length.

However, for our purposes we wish to emphasize that the concept of integrability (or separability of the Hamilton-Jacobi equation) is not a "physical concept". This is meant in the following sense. If the Hamiltonian is changed arbitrarily little, the integrability of the system can be destroyed; i.e., one cannot distinguish between integrable and nonintegrable systems if the Hamiltonian is known with only a certain degree of accuracy. However, in the following section we shall show that the existence of a set of invariant surfaces can be guaranteed even after small perturbations of the Hamiltonian.

III. Theorem of Kolmogorov

a. Normal Systems:

Kolmogorov considered systems near an integrable system. Specifically he studied "normal systems" which are defined as systems with a Hamiltonian of the form

$$H(p, q, \mu) = H^0(p) + \mu H^{(1)}(p, q) + \mu^2 H^{(2)}(p, q) + \ldots , \tag{1}$$

where H is analytic in all $2n + 1$ arguments, the q_ν, ($\nu = 1, \ldots, n$) are angular variables and μ is a small parameter. For $\mu = 0$, these systems are integrable, and obviously $p_\nu = \text{constant}$, ($\nu = 1, \ldots, n$) constitute n independent integrals of the unperturbed normal system. One then hopes to find n independent integrals for small μ. However, this hope cannot be realized for arbitrary perturbations. The fact that the integrals may not exist follows from Poincaré's statement (Meth. Nouv. I, chapt. 5) on the nonexistence of integrals. Actually one would like to know the behavior of solutions to (1) in the large for arbitrary perturbations. Kolmogorov's theorem does just this, at least for the majority of the solutions.

Before stating the theorem, we will discuss and interpret the solution for the unperturbed system. For $\mu = 0$, we have

$$\dot{q}_\nu = H^0_{p_\nu}(p) \; ; \; \dot{p}_\nu = -H^0_{q_\nu}(p) = 0 . \tag{2}$$

From (2), we immediately have the explicit solution

$$q_\nu = H^0_{p_\nu}(p)t + q_\nu(0) \; ; \; p_\nu = p_\nu(0) . \tag{3}$$

Since the q_ν were defined to be angular variables, we see that $p_\nu = \text{constant}$

represent n-dimensional tori in the 2n-dimensional phase space. The solutions (3) remain on these tori in phase space for all time; we express this fact by saying that these tori are invariant under the flow. Writing

$$\omega_\nu = H^0_{p_\nu}(p),$$

One sees from (3) that these ω_ν represent frequencies of n oscillators.

As an illustration, consider the case $\nu = 2$ and refer to figure 1. Since $q_\nu \pmod{2\pi}$, we may identify points on opposite sides of the square with each

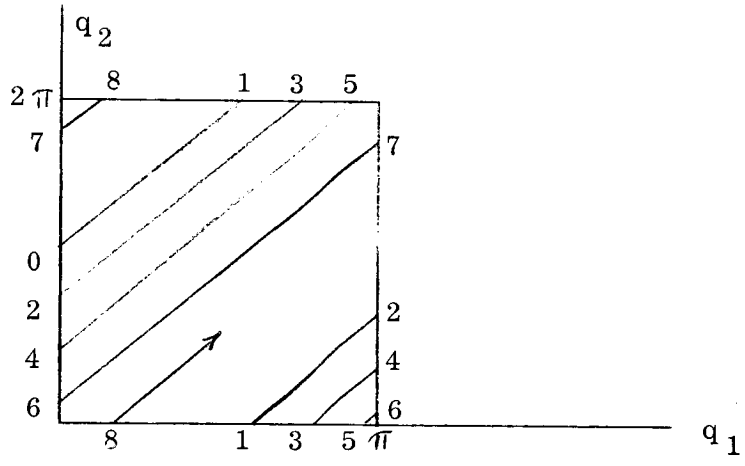

Figure 1.

other. This identification, i.e., $(0, q)$ with $(2\pi, q)$ and $(q, 0)$ with $(q, 2\pi)$ for $0 \leq q \leq 2\pi$ gives rise to a two-dimensional torus. The solutions on the torus, or the flow, are straight lines with slope ω_2/ω_1. One can see that for rational values of ω_2/ω_1, the solutions are almost periodic. Furthermore, if ω_2/ω_1 is irrational, one solution completely covers the torus and we have the ergodic case.

It will be the basic assumption of the following that the frequencies actually depend upon the "amplitude" p_ν which can be expressed by

$$(4) \qquad \det\left(\frac{\partial \omega_\nu}{\partial p_\mu}\right) = \det\left(\frac{\partial^2 H^0(p)}{\partial p_\nu \partial p_\mu}\right) \neq 0.$$

We shall call such systems "non-degenerate". The contents of Kolmogorov's theorem is that under small perturbations most of the n-dimensional tori can be continued to nearby invariant tori. More precisely, we have:

b. Theorem (Kolmogorov): Let (1) represent an analytic non-degenerate normal Hamiltonian system. Then for sufficiently small μ, there exist invariant

tori

$$p_\nu = f_\nu(\phi_1, \ldots, \phi_n) ; q_\nu = \phi_\nu + g_\nu(\phi_1, \ldots, \phi_n),$$

and the solutions on each torus are given by

$$\dot{\phi}_\nu = \omega_\nu$$

or $$\phi_\nu = \omega_\nu t + \phi_\nu(0) .$$

Furthermore, for every set of rationally independent $\omega_1, \ldots, \omega_n$ satisfying the inequalities

$$\left| \sum_{\nu=1}^{n} m_\nu \omega_\nu \right| \geq \frac{c}{\left(\sum_{\nu=1}^{n} |m_\nu|\right)^k}$$

for any set of integers $(m_1, \ldots, m_n) \neq 0$ and $k > 0$, we have the existence of such an invariant torus

Thus, tori on which the flow is ergodic can be "continued" under arbitrary perturbations. On the other hand, tori for which the ω_ν are rationally dependent will in general disintegrate.

c. Two degrees of freedom; reduction to a mapping

We will now discuss a more geometrical formulation of Kolmogorov's theorem. In fact, the following formulation is stronger in the sense that only finitely many derivatives of the variable are required, whereas Kolmogorov's theorem requires infinitely many; i.e., analyticity. In doing this, we shall restrict ourselves to 2 dimensions so that the results can be easily described geometrically. The generalization to higher dimensions does not introduce any new difficulties. Set

$$H(p_1, p_2, q_1, q_2) = H^0(p_1, p_2) + \mu P(p_1, p_2, q_1, q_2, \mu) .$$

Since H does not explicitly depend upon time, we know that the Hamiltonian is an integral and we write $H = h$. Assuming that

$$\frac{\partial H^0}{\partial p_2} \neq 0 ,$$

we may solve $H = h$ for p_2 as a function of p_1, q_1, q_2. Hamilton's equation of motion after the elimination of t yields (with $p_1 = r$, $q_1 = \theta$)

$$\frac{dr}{dq_2} = \frac{\dot{r}}{\dot{q}_2} = -\frac{Hq_1}{Hp_2}$$

(5)

$$\frac{d\theta}{dq_2} = \frac{\dot{\theta}}{\dot{q}_2} = \frac{Hp_1}{Hp_2} .$$

We have the following picture in the 3-dimensional phase space with coordinates (r, θ, q_2). Figure 2.

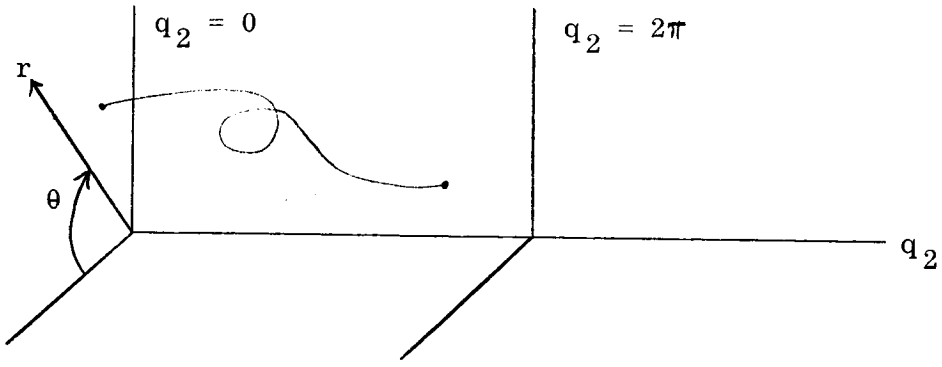

Figure 2.

The study of solutions to (5) may be reduced to the study of mapping M of the plane $q_2 = 0$ onto the plane $q_2 = 2\pi$, the mapping being generated by (5). In fact, choose θ_0, r_0 arbitrarily in the plane $q_2 = 0$; solve (5) for these initial values to obtain

$$\theta = \theta(q_2; \theta_0, r_0)$$
$$r = r(q_2; \theta_0, r_0). \tag{6}$$

The mapping M is given by

$$\theta_1 = \theta(2\pi; \theta_0, r_0) \quad \text{and} \quad r_1 = r(\pi; \theta_0, r_0).$$

For $\mu = 0$, we can write this mapping, which we call M_0, explicitly. Solving (5) in this case we obtain

$$\theta(q_2; \theta_0, r_0) = \theta_0 + \frac{\omega_1}{\omega_2} q_2$$

$$r(q_2; \theta_0, r_0) = r_0,$$

where $\omega_i = H^0_{p_i}[P_1 P_2(p_1, q_1, q_2)] = K_i(p_i) = K_i(r)$, $i = 1, 2$.

Therefore, $\dfrac{\omega_1}{\omega_2} = \dfrac{K_1(r)}{K_2(r)}$,

and we define $\dfrac{\omega_1}{\omega_2} = \dfrac{\alpha(r)}{2\pi}$.

Calculating θ_1 and r_1, we find

$$M_0 : \begin{cases} \theta_1 = \theta + \alpha(r) \\ r_1 = r, \end{cases}$$

where we have dropped the "0" subscripts from θ and r. We shall refer to M_0 as the "twist" mapping. Thus we may write the mapping M in the form

$$M: \begin{cases} \theta_1 = \theta + \alpha(r) + F(r, \theta) ; \ 0 < a \leq r \leq b \\ r_1 = r + G(r, \theta) , \end{cases}$$

where we do not explicitly exhibit the μ dependence of F and G.

As a consequence of the Hamiltonian, we find that M is area preserving. This follows from the well known fact that the differential form

$$\sum_{\nu=1}^{2} dp_\nu dq_\nu - dH\,dt = dr\,d\theta + dp_2\,dq_2 - dH\,dt$$

is preserved for the Hamiltonian systems. Since $H = h$ and $dq_2 = 0$, we find that the "area" element $dr\,d\theta$ is preserved for the mapping M; this means that M is area preserving.

Let us now examine what happens to integrals and periodic solutions under the mapping M. Any integral is of the form:

$$G(p_1, p_2, q_1, q_2) = \Gamma(\theta, r) = \text{constant} ,$$

and under the mapping goes into itself. Therefore,

$$\Gamma(\theta, r) = \text{constant} = \Gamma(\theta_1, r_1)$$

and thus the curve $\Gamma(\theta, r) = \text{constant}$ is invariant under M.

A periodic solution with period $2\pi q$ satisfies (see (6))

$$\theta_0 = \theta(2\pi q ; \theta_0, r_0) = \theta_q$$

$$r_0 = r(2\pi q ; \theta_0, r_0) = r_q .$$

Hence, $M^q F = F$, where F is the point (θ_0, r_0) and F is a fixed point of the mapping M^q.

The question we now pose is whether of not the mapping M has closed invariant curves near the circles $r = r_0$ which are invariant curves of the twist mapping. The following theorem states the conditions for which the mapping M possesses such closed invariant curves. For the formulation of the theorem we introduce the following notation.

If $h(r, \theta)$ is a function with continuous derivatives up to order s, we

denote the s^{th} derivative norm by

$$|h|_s = \sup \left| \left(\frac{\partial}{\partial r}\right)^{\sigma_1} \left(\frac{\partial}{\partial \theta}\right)^{\sigma_2} h(r,\theta) \right| \; ; \quad \sigma_1 + \sigma_2 \leq s ,$$

where r, θ ranges over the domain in which h is defined.

d. Theorem (Moser): For a given $\epsilon > 0$ and a given $s \geq 1$ the mapping M has a closed invariant curve

$$\begin{aligned} \theta &= \theta' + p(\theta') \\ r &= r_0 + q(\theta') , \end{aligned} \tag{7}$$

where the functions p, q are functions of period 2π with s continuous derivatives satisfying $|p|_s + |q|_s < \epsilon$ under the following hypothesis:

Assume for the mapping M that every closed curve $r = f(\theta) = f(\theta + 2\pi)$ near a circle and its image curve intersect. Assume further that $b - a \geq 1$ and

$$C_0^{-1} \leq \frac{d(r)}{dr} \leq C_0 , \tag{8}$$

for some constant $C_0 > 1$. Finally, we will construct a positive number $\delta_0 = \delta_0(\epsilon, s, C_0)$ and an integer $\ell = \ell(s)$ with which we require that F and G have continuous derivatives up to order ℓ and satisfy the inequalities

$$|F|_0 + |G|_0 < \delta_0 \tag{9}$$

$$|\alpha|_\ell + |F|_\ell + |G|_\ell < C_0 . \tag{9'}$$

Moreover, we assert that the mapping induced on the curve (7) is given by

$$\theta'_1 = \theta' + \alpha(r_0) . \tag{10}$$

We remark that there exist many invariant curves which can be labelled by their rotation number $\alpha(r_0) = \omega$ in (10). In fact, given any ω in

$$\alpha(a) + \epsilon < \omega < \alpha(b) - \epsilon \tag{11}$$

for which $\omega/2\pi$ cannot be closely approximated by rationals:

$$|n\omega - m2\pi| \geq \epsilon n^{-3/2} \tag{12}$$

for all integers n, m with $n > 0$, there exists a curve (7) with this rotation number, $\omega = \alpha(r_0)$.

A difficulty in the proof of this theorem has its analytical manifestation in the so-called small divisors. If we now draw our attention to a circle for which

$\alpha(r) = 2\pi p/q$, we observe that the entire circle consists of fixed points M_0^q. The quest for a continuation of such a circle would suggest the search for a curve of fixed points of M^q. However, it is well known that in general only a finite number of fixed points of M^q will exist (in general, 2q). This phenomenon corresponds to the phenomenon of phase-locking in ordinary differential equations. One can say that in general the curves with rational $\omega/2\pi$ cannot be continued; they break up into finitely many points.

e. An extension to the Theorem (Moser):

In part IV of these lecture notes we shall wish to apply the mapping theorem to the oblate earth problem. It will be found that for this problem, the twist $\alpha(r)$ is small, i.e., depends linearly on the parameter μ and so we shall need a result that takes into account small twists. We describe such a result now.

For this purpose we introduce a parameter μ in $0 < \mu \leq 1$ and write the mapping M in the form

$$\begin{aligned} \theta_1 &= \theta + \mu(\alpha(r) + F(r,\theta)) + \beta \\ r_1 &= r + \mu G(r,\theta) \end{aligned} \tag{13}$$

where r ranges over $a \leq r \leq b$, $b - a \geq 1$ and β = constant.

Theorem (Small Twist): Under the assumptions (8), (9), (9') the statements of Theorem (Moser) remain valid if one replaces (10) by

$$\theta_1' = \theta_1 + \mu\alpha(r).$$

The number $\delta_0 = \delta_0(s, \epsilon, C_0)$ can be chosen independently of μ. Note that in this form the unperturbed mapping of (13) is

$$\begin{aligned} \theta_1 &= \theta + \mu\alpha(r) + \beta \\ r_1 &= r \end{aligned}$$

where the variable angle of rotation $\mu\alpha(r)$ ranges over an interval $(\mu\alpha(a), \mu\alpha(b))$ which will be small for small values of μ. In this case it is not clear whether there is a number ω satisfying (12) in such a small interval. Therefore we modify (11) and (12) to

$$\alpha(a) + \epsilon < \frac{\omega - \beta}{\mu} < \alpha(b) - \epsilon \tag{14}$$

$$|n\omega - 2\pi m| \geq \mu\epsilon n^{-3/2} \tag{15}$$

Then the density of admitted ω in (14) will be close to 1.

f. The condition: $\alpha' \neq 0$

The assumption $\alpha' \neq 0$, if interpreted for the original Hamiltonian system, doesn't quite agree with the assumption of non-degeneracy in Kolmogorov's theorem. While it expresses the fact that all frequencies $\omega_1, \ldots, \omega_n$ actually vary independently of the variables $p_1, \ldots, p_n$, we require only that the ratios ω_ν/ω_1, $\nu = 2, \ldots, n$ vary on the $(n-1)$-dimensional surface, $H^0(p_1, \ldots, p_n) = \text{constant}$. For case of $n = 2$, this implies that

$$(16) \qquad \begin{vmatrix} H^0_{p_1p_2} & H^0_{p_1p_2} & H^0_{p_1} \\ H^0_{p_2p_1} & H^0_{p_2p_2} & H^0_{p_2} \\ H^0_{p_1} & H^0_{p_2} & 0 \end{vmatrix} \neq 0 .$$

We shall demonstrate (16). Recall that

$$(r) = 2\pi \frac{H^0_r(r, p_2(r))}{H^0_{p_2}(r, p_2(r))} ,$$

where $p_2(r)$ satisfies $H^0(r, p_2) = h$ and $p_1 = r$. $\alpha'(p_1) = 0$ implies that

$$(17) \qquad H^0_{p_2}(H^0_{p_1p_1} + H^0_{p_1p_2}p'_2) - H^0_{p_1}(H^0_{p_2p_1} + H^0_{p_2p_2}p'_2) = 0 .$$

But from $H^0(p_1, p_2) = h$, it follows that

$$H^0_{p_1} + H^0_{p_2}p'_2 = 0 .$$

Thus (17) becomes

$$(18) \qquad H^0_{p_1}(H^0_{p_2p_1}H^0_{p_2} - H^0_{p_2p_2}H^0_{p_1}) - H^0_{p_2}(H^0_{p_1p_1}H^0_{p_2} - H^0_{p_1p_2}H^0_{p_1}) = 0 .$$

The left hand side of (18) is merely the determinant in the inequality (16). Thus $\alpha'(r) \neq 0$ implies (16).

IV. Oblate Earth Problem.

a. Introductory discussion:

The observation that the oblate earth problem can be approximated by an integrable system was observed by several authors; see Sterne, Garfinkel and Vinti.

As Professor Brouwer pointed out, this problem can be approximated by the two center problem which is known to be integrable.

Therefore, Kolmogorov's theorem is applicable to this problem. In fact, we shall show that in appropriate coordinates we can find a Hamiltonian H for the oblate earth problem dependent upon a small parameter μ such that

(1) $$H(p, q, \mu) = H^*(p, q, \mu) + O(\mu^2)$$

where H^* is integrable. Kolmogorov's statement as amplified by Arnold will then be applied to the system (1) and conditions determined which insure that solutions to (1) can be continued for arbitrary perturbations. The work discussed here is part of the current research of T. Kyner and C. C. Conley and will appear in print elsewhere.

For the oblate earth problem we assume that the gravitational bulge of the earth is rotationally symmetric about the z-axis and symmetric under the reflection $z \rightarrow -z$. The potential $U(x, y, z)$ is harmonic outside the earth and dies out at ∞. The potential can be expanded in the following form as a series of Legendre polynomials.

$$U = \sum_{n=0}^{\infty} \frac{c_n}{r^{2n}} P_{2n}(\cos \theta)$$

$$\cos \theta = z/r .$$

As a first approximation to the earth's potential one finds

$$u = -\frac{\gamma M}{r} \left[1 - J_2 \left(\frac{r_0}{r} \right)^2 P_2(\cos \theta) + \cdots \right]$$

where

$$P_2 = \frac{3 \cos^2 \theta - 1}{2}$$

r_0 = radius of the earth

M = mass of the earth

and measurements of the dimensionless quantity J_2 yield the approximate value

$$J_2 \approx 1.082 \times 10^{-3} ,$$

i.e., J_2 is rather small.

The problem is to discuss the solutions of the equation of motion

$$\ddot{r} = \text{grad } U .$$

Normalize the units of mass, length and time so that $M = 1$, $r_0 = 1$, $\gamma = 1$. J_2, which is of the order of 10^{-3} is considered as a small parameter. In normalized form the potential is

(2) $$U = -\frac{1}{r} + \frac{J_2}{r^3} P_2 \left(\frac{z}{r} \right) .$$

Although we have neglected the effects of the higher spherical harmonics, the above potential represents a better first order approximation for an oblate earth that the simple central force potential.

b. Integrable approximation.

If one admits a change of the potential U in (2) of the order $O(J_2^2)$, we can replace the potential by

$$(3) \qquad \tilde{U} = -\mathrm{Re}\,[x^2 + y^2 + (z + i\sqrt{J_2})^2]^{-1/2} .$$

The simplified oblate earth problem can be reduced to the problem of a masspoint moving under the mutual attraction of two fixed mass points. If a masspoint of mass m is placed at $(0, 0, c)$, the potential at point P is

$$(4) \qquad \frac{m}{R} = \frac{m}{[x^2 + y^2 + (z - c)^2]^{1/2}}$$

$$= \frac{m}{R} \sum_n \left(\frac{c}{r}\right) P_n\left(\frac{z}{r}\right) .$$

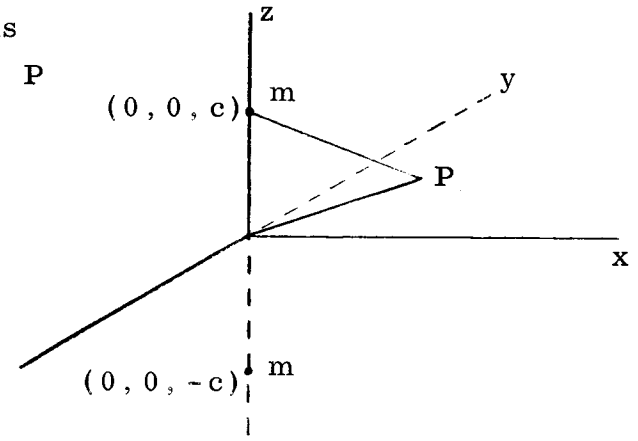

In fact, this is the manner in which Legendre (1785) determined the polynomials $P_n\left(\frac{z}{r}\right)$.

However, the preceding configuration approximates the attraction to an "ovary" ellipsoid instead of the desired oblate ellipsoid. This difficulty can be circumvented by choosing c to be purely imaginary and superimposing two such complex conjugate potentials as one finds in (3) and (4) with $c = iJ_2^{1/2}$. The result is

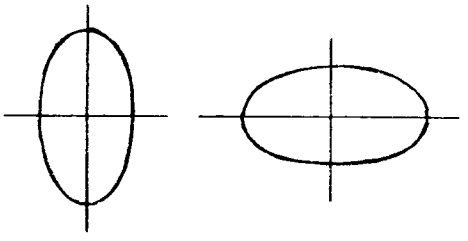

$$\tilde{U} = \mathrm{Re}\,[x^2 + y^2 + (z + i\sqrt{J_2})^2]^{1/2}$$

$$= \frac{1}{r} \sum_{n=0}^{\infty} (-1)^n \frac{1}{r^{2n}} J_{2n} P_n\left(\frac{z}{r}\right) .$$

Since r is restricted to the exterior of the earth, $r \geq 1$, we have ($|P_n| \leq 1$),

$$|U - \tilde{U}| \leq \frac{1}{r} \frac{\left(\frac{J_2}{r}\right)^2}{1 - \frac{J_2}{r}} \leq \frac{J_2^2}{1 - J_2} .$$

c. Integrability in elliptic coordinates.

We use the following fact (see Wintner, Celestial Mechanics):

If $$H(p,q) = [\tfrac{1}{2}\sum p_\nu^2 c_\nu(q_\nu) + \sum b_\nu(q_\nu)][\sum a_\nu(q_\nu)]^{-1},$$

where a_ν, b_ν and c_ν are functions of the variable q_ν alone, then the system is integrable. That is, for $H = h$, the motion is given by quadratures. To prove this statement, transform t by

$$dt = c(p,q)\,d\tau$$

on $H = h$.

Then, $$p' = cH_q$$
$$q' = -cH_p.$$

Since on $H = h$, we have

$$[c(H-h)]q = cH_q,$$

we can use $c(H-h)$ as the new Hamiltonian, wherever this vanishes. With $c = \sum a_\nu$, or

$$dt = (\sum a_\nu)\,d\tau,$$

we find the new Hamiltonian:

$$\tfrac{1}{2}\sum c_\nu p_\nu^2 + \sum b_\nu(q_\nu) - h\sum a_\nu(q_\nu) = \sum H_\nu,$$

where each H_ν depends on p_ν, q_ν only. The solution is obtained from solving n sets of simultaneous differential equations of order two,

$$p_\nu' = H_{\nu q}, \qquad q_\nu' = H_{\nu p}, \qquad \nu = 1, 2, \ldots, n$$

separately, under the side condition $H_\nu = 0$.

Consider the system, which has the Hamiltonian

(5) $$H = \tfrac{1}{2}|p|^2 + U(q),$$

where $$U(q) = -\mathrm{Re}[x^2 + y^2 + (z + i\sqrt{J_2})^2]^{-1/2}.$$

We have that the potential is only a function of $x^2 + y^2$ and z. This implies that $x\dot{y} - \dot{x}y$ is an integral. Introducing the cylindrical coordinates $w = (x^2 + y^2)^{1/2}$, z and θ, we find that the new variables are defined through the relations:

$$p\,dq = p_x\,dx + p_y\,dy + p_z\,dz$$
$$= p_w\,dw + p_\theta\,d\theta + p_z\,dz$$

$$x = w \cos\theta$$
$$y = w \sin\theta$$
$$z = z \ .$$

Thus
$$p_x dx + p_y dy + p_z dz = (p_x c + p_y s)\, dw + w(-p_x s + p_y c)\, d\theta + p_z dz$$
$$c = \cos\theta$$
$$s = \sin\theta \ ;$$

or
$$p_z = p_z \ ; \quad p_w = p_x \cos\theta \ ; \quad p_\theta = w(-p_x s + p_y c)$$
$$|p|^2 = p_x^2 + p_y^2 + p_z^2 = p_w^2 + \frac{p_\theta^2}{w^2} + p_z^2 \ .$$

Hence,
$$H = \frac{1}{2}(p_w^2 + p_z^2) + V$$
$$V = \frac{p_\theta^2}{2w^2} + U(z, w) \ ,$$

and the differential equations of the system are

$$\ddot{w} = -V_w$$
$$\ddot{z} = -V_z \ .$$

In the above,
$$p_\theta = w(-p_x \sin\theta + p_y \cos\theta) = p_x y - p_y x = \dot{x}y - \dot{y}x \ ,$$
is the angular momentum.

We have, therefore, reduced the system to <u>two</u> degrees of freedom, using p_θ = constant and ignoring the equation $\dot{\theta} = f(z, r, p_\theta)$.

To fit this problem into the integrable form mentioned above, we use elliptic coordinates; this was also done by Jacobi for the problem of two centers (see Charlier I, p. 53).

The potential had the form:

$$V = \frac{a}{w^2} + \mathrm{Re}\,[\,w^2 + (z + i\sqrt{J_2})^2\,]^{-1/2} \ .$$

After an appropriate stretching, one can reduce this to $J_2 = 1$ by replacing w with $w\sqrt{J_2}$, z with $z\sqrt{J_2}$. Then $J_2 \to 0$ corresponds to studying the motion with large distances $|w|^2 + |z|^2$.

d. <u>Elliptic Coordinates</u> (see Magnus and Oberhettinger, p. 198)

Put
$$w^2 + (z + i)^2 = (\xi + i\eta) \quad \text{for} \quad 0 \le \xi < \infty$$
$$-1 \le \eta = 1 \ ,$$

or
$$w^2 + z^2 - 1 = \xi^2 - \eta^2$$
$$z = \xi\eta$$
$$(1+\xi^2)(1-\eta^2) = 1 + \xi^2 - \eta^2 - (\xi\eta)^2 = w^2 + z^2 - z^2 = w^2 .$$

Thus,
$$z = \xi\eta$$
$$w = [(1+\xi^2)(1-\eta^2)]^{1/2} ,$$

which are defined for $0 \le \xi < \infty$; $-1 \le \eta \le +1$.
These are well-defined except for $\xi = \eta = 0$, which corresponds to the circle $w = 1$, $z = 0$.

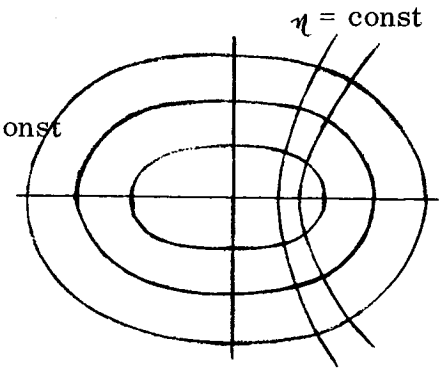

The surface of the earth can be thought of as an ellipsoid of rather large ξ_0 , $\xi = \xi_0$.

Note that for our case, U takes the simple form
$$U = -\mathrm{Re}\,(\xi + i\eta)^{-1} = \frac{-\xi}{\xi^2+\eta^2}$$
and
$$\frac{1}{w^2} = \frac{1}{(1+\xi^2)(1-\eta^2)} = \left(-\frac{1}{1+\xi^2} + \frac{1}{1-\eta^2}\right)\frac{1}{\xi^2+\eta^2} .$$

Extending the transformation to a canonical one using
$$p_\xi d\xi + p_\eta d\eta = p_w dw + p_z dz ,$$
we find from
$$(ds)^2 = \frac{\xi^2+\eta^2}{1+\xi^2}(d\xi)^2 + \frac{\xi^2+\eta^2}{1-\eta^2}(d\eta)^2 ,$$
that
$$T = \frac{1}{2}(p_w^2 + p_z^2) = \frac{1}{2(\xi^2+\eta^2)}[(1+\xi^2)p_\xi^2 + (1-\eta^2)p_\eta^2]$$
and
$$H = \frac{1}{2}\frac{1}{(\xi^2+\eta^2)}[(1+\xi^2)p_\xi^2 + (1-\eta^2)p_\eta^2] + V ,$$
where
$$V = \frac{p_\theta^2}{2(1+\xi^2)(1-\eta^2)} - \frac{\xi}{\xi^2+\eta^2}$$
$$= \frac{1}{\xi^2+\eta^2}\left[\frac{p_\theta^2}{2}\left(-\frac{1}{1+\xi^2} - \xi + \frac{1}{1-\eta^2}\right)\right] .$$

We can now write

$$H = \frac{1}{\xi^2+\eta^2}\left[\frac{1}{2}(1+\xi^2)p_\xi^2 - \frac{p_\theta^2}{2}\left(\frac{1}{1+\xi^2}\right) - \xi\right]$$
$$+ \frac{1}{\xi^2+\eta^2}\left[\frac{1}{2}(1-\eta^2)p_\eta^2 + \frac{p_\theta^2}{2}\left(\frac{1}{1-\eta^2}\right)\right],$$

which makes the integrability evident (see IV c), with

$$c_1 = 1+\xi^2 \qquad c_2 = 1-\eta^2$$
$$a_1 = \xi^2 \qquad a_2 = \eta^2$$
$$b_1 = \frac{p_\theta^2}{2}\left(\frac{1}{1+\xi^2}\right) - \xi \qquad b_2 = \frac{p_\theta^2}{2}\left(\frac{1}{1-\eta^2}\right).$$

In particular, we have the integrals

$$H_1 = \frac{1}{2}(1+\xi^2)p_\xi^2 + b_1(\xi) - h(\xi^2) = h_1 \qquad \text{and}$$

$$H_2 = \frac{1}{2}(1-\eta^2)p_\eta^2 + b_2(\eta) - h(\eta^2) = h_2 = h - h_1 .$$

In principle, the whole solution is contained in these formulae; however, the formulae are unwieldy and rather useless for numerical calculation.

More important than the explicit formulae is the fact that the problem at hand can be approximated to terms of order μ^2 by an integrable one:

$$H(p, q, \mu) = H^*(p, q, \mu) + O(\mu^2).$$

Since H^* takes the linear terms of order μ into account, one can hope that the motion described by H^* is not any more degenerate. This one could check by computing the periods (elliptic integrals) from the explicit formulae. This procedure is still very involved.

Let us denote the two frequencies of H by ω_1, ω_2. Then for $\mu = 0$, $\omega_1/\omega_2 = 0$, or is integral. Note that ω_1, ω_2 can be transformed into $n_1\omega_1 + n_2\omega_2$, $n_1'\omega_1 + n_2'\omega_2$ so that

$$\frac{\omega_1}{\omega_2} \rightarrow \frac{a + b\frac{\omega_1}{\omega_2}}{c + d\frac{\omega_1}{\omega_2}}$$

is unimodular. Thus, ω_1/ω_2 could be rational and constant if it vanishes in some coordinates.

Kyner computed, that in appropriate coordinates

$$(6) \qquad \frac{\omega_1}{\omega_2} = \mu\frac{\pi}{p^2}\cos^2 i_0\,(1 - 5\cos^2 i_0)$$

$$\mu = \frac{2}{3}J_2 \quad \text{and} \quad p = \dot{x}y - x\dot{y} .$$

The expression (6) contains the information necessary to determine whether or not solutions to (1) can be continued for arbitrary perturbations. In order to see this we shall now pass to a discussion of (1) in phase space and set up an approximate mapping.

e. Discussion of Phase Space.

We consider the solutions corresponding to negative values of h. These are described by setting (5) equal to h:

$$\frac{1}{2}|\dot{q}|^2 + U(r, z) = h < 0, \tag{7}$$

where $q = (x, y, z)$. The momentum integral is

$$p = \dot{x}y - x\dot{y} = (\dot{q} \times q, k)$$

where $k = (0, 0, 1)$. Clearly

$$|p| \leq |\dot{q}||q| = |\dot{q}| \cdot r, \tag{8}$$

and equality holds only if $q, \dot{q}, k$ are mutually orthogonal. This means that equality holds only if one is in an equatorial orbit which is also a circle, or at perihelion, or at aphelion.

Eliminate $|\dot{q}|$ from (7) and (8) to obtain the inequality

$$\frac{1}{2}\frac{p^2}{r^2} + U \leq h < 0$$

or

$$\frac{1}{2}\frac{p^2}{r^2} - \frac{1}{r} + O(\mu) \leq h < 0. \tag{9}$$

We shall assume that

$$0 < -h < \frac{p^2}{2}. \tag{10}$$

For $\mu = 0$, the locus can be found to be the space between two spheres, as one can read from the following figure.

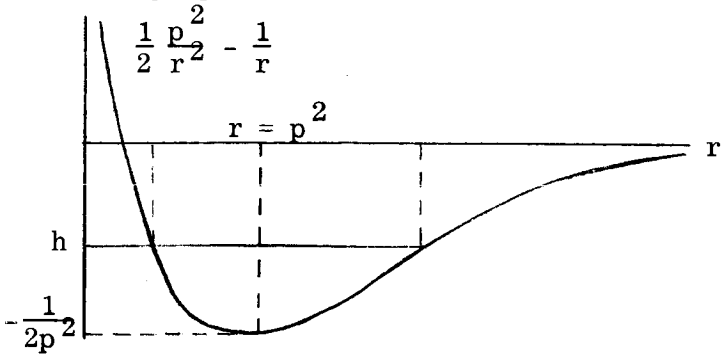

For small values of μ, the inequality (9) also describes a similar shell region. This leads to the observation that under the restriction (10), the solutions of the differential equation never approach $r = 0$ or $r = \infty$, which are the only singularities. Therefore, all solutions satisfying (9) initially can be continued for all values of t, and remain in that region.

In the meridian plane there is an apparent singularity at $x^2 + y^2 = 0$, since $V = U + p_\theta^2 / 2(x^2 + y^2)$. However, this singularity disappears in the 3-dimensional description.

f. Surface of Section -- Conley

Just using the fact that U depends on r and z alone, as well as the symmetry, allows us to deduce some qualitative features. It follows from (5) that

$$U(r, z) = U(r, -z) .$$

We already know that for $z = 0$

$$\frac{p^2}{2r^2} + U = h$$

has two roots: $r = r_1, r_2$ and that

$$\frac{p^2}{2r^2} + U < h \qquad \text{in } r_1 < r < r_2 .$$

We wish to describe every orbit by its intersection with $z = 0$, the equatorial plane. One variable would be θ, which we can ignore. Therefore, we can set $\theta = 0$, or $y = 0$:

$$p = \dot{x}y - x\dot{y} = -x\dot{y}, \quad r = x > 0; \quad 0 < r_1 < x < r_2 .$$

Hence,

$$H = \frac{1}{2}(\dot{x}^2 + \dot{y}^2 + \dot{z}^2) + U = h .$$

Using $\dot{y} = -p/x$, we have

$$\frac{1}{2}(\dot{x}^2 + \dot{z}^2) = h - U(x, 0) - \frac{p^2}{x^2} . \tag{11}$$

Thus, for every x in

$$r_1 < x < r_2 ,$$

one has an associated equation which describes a circle, since the right hand side of (11) is positive in $r_1 < x < r_2$ and zero for $r = r_1, r_2$. This can be visualized as the surface of a topological sphere symmetric with respect to $z \to -z$ and having coordinates x: $\dot{x}^2 + \dot{z}^2 = R(x)$.

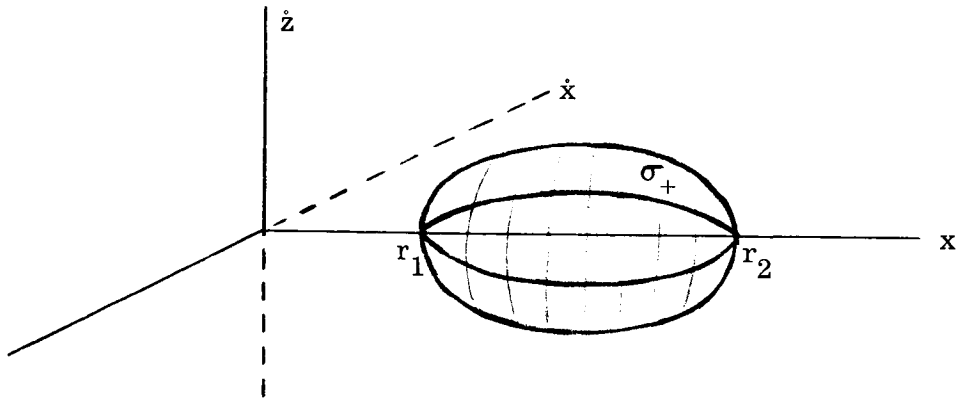

We now consider the flow

$$\ddot{x} = -V_x$$
$$\ddot{z} = -V_z$$

in the 3-dimensional part of the phase space $(x, \dot{x}, z, \dot{z})$ where $H = h$. In this 3-dimensional space we consider the two-dimensional surface σ of initial values. Points with $\dot{z} = 0$ correspond to equatorial orbits. In fact, the equator $\dot{z} = 0$ is invariant under the flow. We shall concentrate our attention on the upper half for which $\dot{z} > 0$. This part of the surface, σ_+, is a surface of section in the sense of Birkhoff. That is, every interior point is intersected by a solution (since here $\dot{z} > 0$). The boundary of σ_+ represents orbits in the equatorial plane.

Every point in σ_+ corresponds to an orbit with given h, p. Conversely, every orbit with given h, p intersects σ_+; in fact, infinitely often -- except for the boundary. This follows from the fact that

$$\frac{\partial U(w, z)}{\partial (z^2)} > 0, \tag{12}$$

holds in the shell $r_1 \leq r \leq r_2$ which is verified in our case for <u>small</u> μ, since

$$\frac{\partial U}{\partial z^2} = -\frac{\partial}{\partial z^2}(x^2 + y^2 + z^2)^{-1/2} = \frac{1}{2} r^{-3/2} > 0, \text{ for } \mu = 0.$$

Hence, $\frac{\partial u}{\partial z^2} \geq \delta > 0$ and

$$\ddot{z} = -V_z = -U_z(w, z) = -2\frac{\partial U}{\partial (z^2)} \cdot z$$
$$> 2\delta z > 0.$$

Since $2\frac{\partial U}{\partial (z^2)} < 2\delta$, it follows from the oscillation theorem that z has at least 2 zeroes in every interval of length greater than $\pi(2\delta)^{-1/2}$, and one of them has $\dot{z} > 0$.

Therefore, one can properly describe any orbit with given $H = h$ and $p = \sqrt{-2h}$, by points on σ_+ with coordinates $x, \dot{x}$.

g. Mapping.

The flow of the differential equation can be properly described by following point p on σ_+ along an orbit to the next point of intersection.

We now follow the work of Conley, who suggested that one identity σ_+ and σ_- (the lower half of σ) by $(\dot{z}, \dot{w}) \rightarrow (-z, +\dot{w})$.

According to our preceding arguments, every solution intersects σ_+ and σ_- infinitely often -- alternately. Following the solution for increasing t, we find a sequence of image points

$$p_0 \rightarrow p_1 \rightarrow p_2 \rightarrow \cdots ,$$

and $p_0 \rightarrow p_1$ defines a mapping M of the disc σ_+ onto itself, the boundaries being invariant.

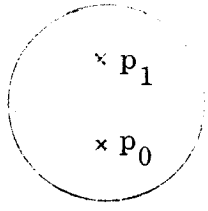

This fact immediately demonstrates the existence of a fixed point F of the mapping M; i.e.,

$$MF = F ,$$

by Brouwer's fixed point theorem. For small μ, this fixed point can be shown to be in the interior of σ_+. The solution through F is periodic and symmetric with respect to $z \rightarrow -z$. For $\mu = 0$, we have the circular solution.

The preceding arguments show the existence of periodic solutions, without a definite restriction. For the case $\mu = 0$, this mapping can be verified as a rotation about the angle π, the domain being a disc. On this disc the 2-differential form

$$d\dot{x} \wedge dx + d\dot{z} \wedge dz - dH \wedge dt$$

is preserved under the mapping M. On $z = 0$, $H = h$, the differential form reduces to $d\dot{x} \wedge dx$, which is the element of area on the surface σ_+. Therefore, M preserves the area element, which is certainly the case for a rotation.

Kyner investigated this mapping and showed that in appropriate coordinates, the mapping is a rotation about the angle

$$\alpha = \pi + \frac{2\pi}{3} J_2 p^{-2} \cos^2 i_0 (1 - 5 \cos^2 i_0) ,$$

where i_0 is the inclination angle.

h. Conclusion.

We have seen that in appropriate coordinates, the mapping M has the form

$$\theta_1 = \theta + \pi + \mu\alpha(r) + O(\mu^2)$$
$$r_1 = r + O(\mu^2) ,$$

in a disc where

$$\frac{\alpha(r)}{2\pi} = \frac{\cos^2 i}{2p_\theta^2}(1 - 5\cos^2 i)$$

and

$$\mu = \frac{2}{3} J_2 .$$

Here the inclination i is related to r, the energy h, and the momentum p.

One sees that α is not a constant and so our theorem concerning annulus mapping (with small twist) is applicable if μ is sufficiently small. We find a set of invariant curves, which for small μ cover all points of the disc with the exception of a set of small measure.

This implies, for the solution of the differential equations

$$\ddot{q}_\nu = -U_{q_\nu}$$
$$U = -\frac{1}{r}\left[1 - \frac{\mu}{r^2} P_2\left(\frac{z}{r}\right) + \mu^2 F(z, r, \mu)\right]$$
$$F(z, r, \mu) = F(-z, r, \mu) ,$$

the existence of a set of almost periodic solutions. For any value $h < 0$

$$H = h$$

and

$$x\dot{y} - \dot{x}y = p > \sqrt{-2h} ,$$

these form the majority of the solutions.

To make this statement somewhat more precise, we recall that the system was reduced to two degrees of freedom:

$$\ddot{w} = -\frac{\partial V}{\partial w}$$
$$\ddot{z} = -\frac{\partial V}{\partial z}$$
$$w = (x^2 + y^2)^{1/2} ,$$

and the invariant curves correspond to almost periodic solutions

$$w = g_1[\phi_1(t), \phi_2(t)]$$
$$z = g_2[\phi_1(t), \phi_2(t)] ,$$

where $g_\nu(\phi_1, \phi_2)$ have period 2π in ϕ_1, ϕ_2, and

$$\dot{\phi}_\nu = \omega_\nu , \quad \nu = 1, 2 .$$

Finally, the variable θ can be recovered from

$$\dot{\theta} = \frac{p}{w^2} ,$$

yielding $$\theta = \theta(0) + \omega_0 t + g_0(\phi_1, \phi_2) .$$

Combining this, we find that in the original coordinates

$$g_\nu(t) = f_\nu(\phi_0, \phi_1, \phi_2) ; \quad \nu = 1, 2, 3 ,$$

where f_ν have the period 2π in ϕ_λ, $(\lambda = 0, 1, 2)$ and

$$\dot{\phi}_\lambda = \omega_\lambda .$$

The application of Birkhoff's fixed point theorem shows, moreover, the existence of infinitely many periodic solutions of our system.

V. Proof of a Theorem by C. L. Siegel.

a. In a paper by C. L. Siegel, the problem of small divisors was overcome for the first time for the following problem. Let

$$(1) \qquad \begin{aligned} z_1 &= F(z) = \lambda z + f(z) \\ f(z) &= \sum_{k \geq 2} a_k z^k , \end{aligned}$$

be a conformal mapping near the fixed point $z = 0$. According to a known result, there is a substitution of variables

$$(2) \qquad z = \zeta + u(\zeta)$$

such that in the new variables the mapping is linear and of the form

$$(3) \qquad \zeta_1 = \lambda \zeta ,$$

provided that $|\lambda| \neq 1, 0$. However, Siegel's result refers to the case for which $|\lambda| = 1$. This situation can be considered as a model case of the small divisor difficulty.

It was shown by Cremer that for unit roots $\lambda^q = 1$, and even for numbers λ on $|\lambda| = 1$, which can be well approximated by unit roots, such a substitution cannot exist. In other words, it was shown that the formal expansion (2) must diverge for a particular choice of f and $|\lambda| = 1$, when λ is closely approximated by unit roots.

The contents of Siegel's theorem, however, is that for λ on $|\lambda| = 1$, which is badly approximated by unit roots; e.g.,

$$|\lambda^{\nu} - 1| = c_0^{-1} \nu^{-2}, \text{ for } \nu = 1, 2, \ldots, \quad c_0 > 1, \tag{4}$$

there exists a substitution $z = \zeta + u(\zeta)$ given by a convergent power series expansion. In particular, this implies the stability of the mapping. The iterates

$$z_n = F(z_{n-1})$$

are given by

$$z_n = \zeta_n + u(\zeta_n),$$

where

$$\zeta_n = \lambda^n \zeta.$$

We wish to give a proof of this theorem using the ideas of Kolmogorov. Siegel's proof is intricate and makes use of the fact that $|\lambda^{\nu} - 1|$ is only rarely small, while our proof will just use the estimate (4). Even though this proof may not be in the literature, it is a direct application of the concepts used by Kolmogorov and Arnold; the latter mentioned to the author, by informal communication, that he found a proof of this type. We use this proof as an illustration of the principle.

b. One could proceed directly to construct the power series expansion of u by comparison of coefficients which are obtained in a unique way and then proceed to prove the convergence of the series thus obtained. However, the last step is just the true difficulty, and we shall, instead, obtain u by a succession of substitutions (coordinate transformations) each approximating the desired transformation to a higher degree. In fact, the convergence will be faster than the usual convergence and, therefore, the effect of the small denominators does no harm.

c. To turn the proof, we construct a coordinate transformation

$$z = V(\zeta) = \zeta + v(\zeta), \tag{5}$$

which transforms the mapping into

$$\zeta_1 = \lambda\zeta + \phi(\zeta), \tag{6}$$

which is approximately linear. A simple calculation shows that

$$v(\zeta_1) - \lambda v(\zeta) = f[\zeta + v(\zeta)] - \phi(\zeta).$$

To make ϕ small, solve the "linearized" equation (linearized with respect to v.f. ϕ). We set

(7) $$v(\lambda\zeta) - \lambda v(\zeta) = f(\zeta) .$$

The solution to (5) is readily given. If

$$f(z) = \sum_{k\geq 2} f_k z^k ,$$

then, by comparing coefficients, one obtains

(8) $$v(\zeta) = \sum_{k\geq 2} \frac{f_k}{\lambda^k - \lambda} \zeta^k .$$

This formula exhibits the small divisors, $|\lambda^k - \lambda|$.

We shall now show that this choice of v leads to a ϕ which is smaller than f; thus we will have achieved a closer approximation to the linear mapping. This is shown in the following lemma.

d. We shall assume that f is analytic in $|z| < r$, where $r \leq 1$. Moreover, let

$$|f| < \epsilon \quad \text{in} \quad |z| < r$$

and let ρ be chosen so that

$$0 < \rho < r = 1 .$$

We set $\rho = r - 4h > 0$ and prove:

Lemma -- If v is chosen according to (8), and if the transformed mapping is given by (6), then there is a constant c depending on c_0 only such that

$$|v'| < c\frac{\epsilon}{(r-\rho)^4} \quad \text{in} \quad |\zeta| < r - h$$

$$|\phi| < 2c\frac{\epsilon^2}{(r-\rho)^5} \quad \text{in} \quad |\zeta| < \rho = r - 4h ,$$

provided that

(9) $$\frac{c\epsilon}{(r-\rho)^5} < \frac{1}{2} .$$

Proof: First we find an estimate for v' and v. Using Cauchy's estimates for the f_k, we have

$$|f_k| < \frac{\epsilon}{r^k} .$$

Thus,

$$|v'| \leq \frac{c_0\epsilon}{r} \sum_{k\geq 2} k(k-1)^2 \left(\frac{|\zeta|}{r}\right)^{k-1}$$

$$\leq \frac{c_0\epsilon}{r} \sum_{k=0}^{\infty} (k+1)k^2 \left(\frac{|\zeta|}{r}\right)^k \leq 6\frac{c_0\epsilon}{r} \sum \frac{(k+3)(k+2)(k+1)}{6} \left(\frac{|\zeta|}{r}\right)^k$$

$$\leq \frac{1}{r} \frac{6c_0\epsilon}{\left(1 - \frac{|\zeta|}{r}\right)^4} \leq \frac{6c_0\epsilon r^3}{h^4} \leq \frac{c\epsilon}{(r-\rho)^4} \quad ; \quad c = 6\cdot 4^4 c_0 .$$

Similarly,

$$|v| \leq \sum_{k\geq 2} \frac{|f_k|}{|\lambda^k - \lambda|} |\zeta|^k \leq 2c_0\epsilon \sum_{k\geq 2} \frac{(k+1)(k+2)}{2} \left(\frac{|\zeta|}{r}\right)^k$$

$$\leq \frac{2c_0\epsilon}{\left(1 - \frac{|\zeta|}{r}\right)^3} = \frac{c\epsilon r^3}{12(r-\rho)^3} < \frac{c\epsilon r}{4(r-\rho)^4}$$

It follows from (9) that

$$(10) \qquad \frac{c\epsilon}{(r-\rho)^4} < \frac{r-\rho}{2r} = \frac{2h}{r}$$

Then using (10) we have

$$(11) \qquad |v'| < \frac{2h}{r} \leq \frac{1}{2} \quad \text{for} \quad |\zeta| < r - h$$

Furthermore, since $c_0 > 1$, then (9) implies that

$$(12) \qquad \epsilon < h^5 < h$$

The inequality (11) implies the following:

α. The circle $|\zeta| < \rho = r - 4h$ is mapped into

$$|z| \leq \rho + |v| < \rho + \frac{c\epsilon r}{4(r-\rho)^4}$$

$$< \rho + \frac{1}{2}h < r - 3h .$$

β. The image of $|\zeta| < r - h$ covers at least

$$|z| < r - 2h ;$$

i.e., in $|z| < r - 2h$, the inverse mapping is defined and gives ζ with $|\zeta| < r - h$.

Statement (β) is a simple consequence of the implicit function theorem[1].

---

1. If $z = \zeta + v(\zeta)$ in $|\zeta| < r - h$, and $|v'| < 2h/r \leq 1/2$ in $|\zeta| < r - h$, then for $|z| < r - 2h$ there is a ζ such that $|\zeta| < r - h$.

Proof: We construct the inverse mapping $\zeta = z + w(z)$ by iteration in the following manner:

Set $w_0 = 0$

and $w_{n+1} = -v(z + w_n)$, for $|z| < r - 2h$

as long as $|w_n| < h$.

For those indices we have

$$|w_{n+1} - w_n| = \max_{|z| < r-h} |v'| \cdot |w_n - w_{n-1}|$$

$$= \theta |w_n - w_{n-1}|,$$

With the preceding assumption we see that $\zeta_1 = \zeta + \phi$ is defined in $|\zeta| < \rho$. Namely, if $|\zeta| < \rho = r - 4h$, then by (α) we have $|z| < r - 3h$ and by assumption

$$|z_1| = |\lambda z + f(z)| < |z| + |f| < r - 3h + \epsilon < r - 2h \text{ by } (12).$$

Since in $|z_1| < r - 2h$, the inverse map of $z_1 = \zeta_1 + v(\zeta_1)$ is defined, we have from (β) that ζ_1 is defined and is $|\zeta_1| < r - h$. Thus ϕ is defined in $|\zeta| < \rho$.

It remains to estimate ϕ in $|\zeta| < \rho$. Subtracting (7) from the equation preceding it, we see that

$$\phi(\zeta) = -v[\lambda\zeta + \phi(\zeta)] + v(\lambda\zeta) + f[\zeta + v(\zeta)] - f(\zeta),$$

or, since $|\zeta_1| = |\lambda\zeta + \phi| \leq r - h$,

$$\max_{|\zeta| < \rho} |\phi| = \max_{|z| < r-h} |v'| \cdot \max_{|\zeta| < \rho} |\phi| + \max_{|\zeta| < r-h} |f'| \cdot \max_{r-h} |v| .$$

From (11) $\max |v'| \leq 1/2$,

so that

$$\frac{1}{2} \max_{\rho} |\phi| \leq \max_{r-h} |f'| \cdot \max_{r-h} |v| .$$

In $|\zeta| < r - h$ $|f'| < \epsilon/h$ so that

$$\max_{\rho} |\phi| \leq 2 \frac{c\epsilon^2}{(r - \rho)^5}$$

which thereby proves the lemma.

e. Iteration.

We start with a mapping

$$z_1 = F(z) = \lambda z + f(z) \text{ in } |z| < 1 = r_0,$$

and in this region assume that $|f| < \epsilon_0$. Applying the preceding lemma, we construct a transformation

$$z = U_1(z^{(1)})$$

such that

$$z_1^{(1)} = z^{(1)} + f_1(z^{(1)}),$$

where $z^{(1)} < r_1$ and $f_1 = \phi$. We now use a new notation because we shall repeat the procedure again and again, constructing a transformation

---

where $\theta = \frac{2h}{r} \leq \frac{1}{2}$.

Iterating, we obtain

$$|w_{n+1} - w_n| = \theta^n |w_1 - w_0| = \theta^n |v| = \theta^{n+1} \cdot \frac{r}{4}$$

or

$$|w_{n+1}| = \left| \sum_{\nu=0}^{n} (w_{\nu+1} - w_\nu) \right| \leq (\theta + \theta^2 + \cdots + \theta^{n+1}) \frac{r}{4}$$

$$< \frac{\theta}{1 - \theta} r = 2\theta \frac{r}{4} = h .$$

Thus $|w_n| < h$ for all n. Now the convergence is obvious, so we have

$$|w| \leq h$$

or

$$|\zeta| = |z| + h \leq r - 2h + h = r - h .$$

$$z^{(n-1)} = U_n(z^{(n)}) = z^{(n)} + u_n(z^{(n)})$$

which takes the mapping F_{n-1} into

$$z_1^{(n)} = F_n(z^{(n)}) .$$

At each step, we have to diminish the radius of validity. Therefore, we set

$$|z^{(n)}| < r_n$$

and $$\max_{r_n} |f_n| = \epsilon_n .$$

Our lemma now guarantees that

$$\epsilon_{n+1} \leq 2c \frac{\epsilon_n^2}{(r_n - r_{n+1})^5} ,$$

provided that

$$\frac{c\epsilon_n}{(r_n - r_{n+1})^5} < \frac{1}{2} . \tag{13}$$

We have to choose the decreasing sequence r_n so that it does not tend to zero, which makes $r_n - r_{n+1}$ very small, and thereby endanger the convergence of ϵ_n. But since ϵ_n enters quadratically, we obtain a convergent sequence as we shall now show.

Let $$r_n = \frac{1}{2} + \frac{1}{2^{n+1}} ,$$

then $$r_0 = 1$$
$$r_n \geq 1/2 ,$$

and $$r_n - r_{n+1} = \frac{1}{2^{n+2}}$$

Hence, $$\epsilon_{n+1} \leq 2c \cdot 2^{5(n+2)} \epsilon_n^2 \leq c_1^{n+1} \epsilon_n^2 ,$$

with $c_1 = 2^{11}c$. It is easy to deduce that

$$\epsilon_n \leq (c_1^2 \epsilon_0)^{(2^n)}$$

and thus $\epsilon_n \to 0$ provided

$$(c_1^2 \epsilon_0) < 1 .$$

To verify the condition (13), we show that we can satisfy the inequality

$$c(c_1^2 \epsilon_0)^{(2n)} < 2^{-5n-11} .$$

This is obviously possible if ϵ_0 is sufficiently small, i.e., if $\epsilon < 1/c_2$ where c_2 depends only on c_0. For instance, $c_2 = c_1^4$ will do.

Thus we have established that the sequence of mappings F_n converges, and, in fact, converges quadratically.

It remains to relate the new variables to the old variables. This is accomplished with the transformation

$$z^{(n-1)} = U_n(z^{(n)})$$

or

$$z = z^{(0)} = U_1 \circ U_2 \circ \cdots \circ U_n(z^{(n)}) = V_n(z^{(n)}).$$

This transformation is defined in $|z^{(n)}| < r_n$ and satisfies $|V_n| < r_0 = 1$ and

$$V_n'(z^{(n)}) = U_1' \cdot U_2' \cdots U_n' = \prod_{\nu=1}^{n} U_\nu' = \prod_{\nu=1}^{n} (1 + u_\nu'),$$

and the convergence of $V_n(\zeta)$ follows easily from

$$|u_\nu'| = (c_2\epsilon)^{2^\nu} \to 0 \; ; \; c_2 = c_1^4 .$$

Therefore, if ϵ_0 is sufficiently small, the convergence of the iteration procedure is established. That means, the mapping

$$z_1 = \lambda z + f_0(z) \quad \text{in} \quad |z| < 1$$

with $|f_0| < \epsilon_0$ can be transformed into the linear mapping (3).

Finally, we show that we always can choose ϵ_0 arbitrarily small. Suppose the given mapping is

$$z_1 = \lambda z + f(z) \quad \text{in} \quad |z| < r .$$

Then with $z = rz^*$, we have in $|z^*| < 1$,

$$z_1^* = z^* + \frac{1}{r} f(rz^*) = \lambda z^* + f^*(z^*),$$

where

$$|f^*(z)| = \left|\frac{1}{r} f(rz^*)\right| \leq r \max_{|z| < r} |f''|$$

which can be made arbitrarily small. This concludes the proof.

Conclusion: The proof of the theorem on the annulus mapping uses very similar ideas, but the estimates are much more complicated. The details can be found in a paper, "On Invariant Curves of Annulus Mapping," Göttinger Nach. (1962). Another difference, in the case of differentiable mappings, is that the approximate transformations have to be smoothened -- i.e., approximated by infinitely differentiable transformations.

Although these technoques look quite different from the usual methods of celestial mechanics, there is a strong resemblance in this approach to von Zeipel's method. If

$$F = F_0(x) + \mu F_1(x, y, \mu) \quad *$$

is a Hamiltonian, which for $\mu = 0$ is integrable, then Kolmogorov's approach consists of the construction of a canonical transformation

$$x = \xi + \mu u(\xi, \eta)$$
$$y = \eta + \mu v(\xi, \eta)$$

which transforms F into the Hamiltonian

$$F = \Phi(\xi, \eta) = \Phi_0(\xi) + O(\mu^2) ,$$

which deviates from an integrable Hamiltonian only by terms which are quadratic in μ^2. Repeated application of this procedure leads to quadratic convergence.

This shows that the technique for removing the angular variables remains as it has been previously. The new feature is that the expansion method has been replaced by an iteration procedure in which the domain of applicability is carefully controlled. Since these methods are so rapidly convergent, it can be hoped that they can also be made useful for numerical computation.

---

* $x = (x_1, \ldots, x_n)$, $y = (y_1, \ldots, y_n)$ and y_ν are angular variables.

LIST OF REFERENCES

Sections I and II.

1. Poincaré, Les Méthodes Nouvelles de la Mecanique Céleste, vol. 1, 2, 3, Paris 1892.
2. Fermi, E., "Beweis, dass ein mechanisches Normalsystem im allgemeinen quasiergodisch ist," Phys. Z. 24, 261-264 (1923).
3. C. L. Siegel, "Über die Existenz einer Normalform analytischer Hamiltonscher Differentialgleichungen in der Nähe einer Gleichgewichtlösung," Math. Ann. 128, 144-170 (1954).
4. J. Moser, "On Nonexistence of Integrals," Comm. on Pure and Applied Math., 1955.
5. J. Moser, "On Invariant Curves of Area-Preserving Mappings of an Annulus," Nachrichten des Akademie des Wissenschaften in Göttingen, No. 1, 1962.

Section III.

1. A. N. Kolmogorov, Doklady Akad. Nauk 98, 527-530 (1954).
2. A. N. Kolmogorov, "General Theory of Dynamical Systems and Classical Mechanics," Proceedings of the International Congress of Math. 1954, vol. 1, pp. 315-333, Amsterdam 1957.
3. V. I. Arnold, Doklady Akad. Nauk 137, 255-257 (1961).
4. V. I. Arnold, Doklady Akad. Nauk 138, 13-15 (1961).
5. V. I. Arnold, Doklady Akad. Nauk 145, 487-490 (1962).

Section IV.

1. The work of W. T. Kyner and C. C. Conley is going to appear in the Communication on Pure and Applied Math.
2. W. T. Kyner, "A Mathematical Theory of the orbits about an oblate planet," Technical Report, University of Southern California, February 1963.
3. V. I. Arnold, Doklady Akad. Nauk 138, 13-15 (1961).
4. Legendre, "Recherches sur l'attration des sphéroïdes homogènes," Akad. des Sciences, Paris, Memoires des Math. et de Phys. présentés . . . par divers savants, t. 10, 1785.
5. C. L. Charlier, Die Mechanik des Himmels, vol. 1, Leipzig 1902.
6. T. E. Sterne, An Introduction to Celestial Mechanics, Interscience Tracts on Physics and Astr. 9, 1960.
7. B. Garfinkel, Astr. Journal 63, 88- (1958).

8. J. P. Vinti, "New method of solution for unretarded satellite orbits," Journal of Research of National Bureau of Standards 63B, 105 (1959).

9. W. Magnus and F. Oberhettinger, Formeln und Sätze für die speziellen Funktionen der mathematischen Physik, Springer - Verlag, 1948, in particular, p. 198.

Section V.

1. C. L. Siegel, Vorlesung über Himmelsmechanik, Sections 23 and 24, Springer - Verlag, 1956

2. C. L. Siegel, "Iteration of Analytic Functions," Ann. of Math. 43, 607 - 612 (1942).

3. F. Schröder, "Über iterierte Funktionen," Math. Ann. 3, 296 - 392 (1871).

4. H. Cremer, "Über die Häufigkeit der Nichtzentren," Math. Ann. 115, 573 - 580.

25107

Lunar and Solar Perturbations on Artificial Satellites

Peter Musen
Goddard Space Flight Center
Greenbelt, Maryland

Lecture notes prepared by Ralph Deutsch.

The long-range (secular) effects caused by the moon and the sun are of primary importance for establishing the stability of highly eccentric orbits of satellites. At present no complete analytical theory exists that can treat such orbits. Thus we have to resort to numerical integration to obtain information about the stability of the orbit over a long interval of time or about the lifetime of the satellite.

Methods based on the use of an unaveraged disturbing function, such as those of Cowell or Ercke, contain both short- and long-period terms. For artificial satellites these methods require that the interval of integration be much less than the period of the satellite, thus causing a large accumulation of round-off errors. The main long-range effects in the elements are produced by the long-range terms in the disturbing function and by their "cross actions". The short-period terms can also produce long-range effects through their mutual cross actions in higher approximations, but such effects are very small, and over a very long interval of time, they can be neglected. For these reasons, as well as to diminish the accumulation of round-off errors, it is necessary at the very beginning to remove the short-period terms from the disturbing function or from the components of the disturbing force.

Musen [1] suggested the use of Halphen's [2] form of the Gaussian theory [3] as a practical method for determining the long-range effects through a step-by-step integration. Previously Halphen's method was not in use, probably because of several numerical errors in the original publication. All of them were corrected by Goriachev [4], whose name should be associated with the method as well; the method in its present form could justly be called the Halphen-Goriachev method. Some parts of Halphen's original exposition can be easily recognized from the modern standpoint as an application of the calculus of dyadics (matrices) in a hidden form. The problems connected with the determination of directions are sometimes sources of errors in Halphen's original presentation.

In Goriachev's work all the formulas given in the final collection are correct, but there are some misprints in the theoretical exposition, which are corrected in reference [5]. Musen [1] suggested the use of Goursat [6] transformation and the E summability to speed up the convergence of hypergeometric series that appear in the Halphen-Goriachev method and to facilitate numerical computation.

Disturbed body

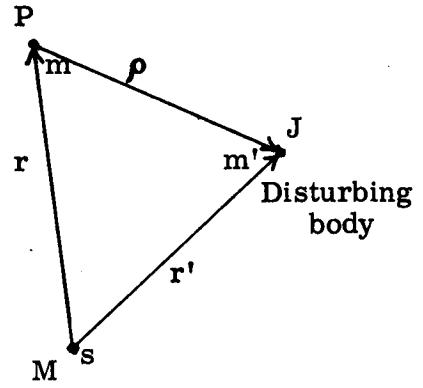

Let:

m' = mass of disturbing body

m = mass of disturbed body

The disturbing force is

$$(1) \qquad F = k^2 m' \left(\frac{\rho}{\rho^3} - \frac{r'}{r'^3} \right) ,$$

$$(2) \qquad \rho = r' - r .$$

If the disturbing force is developed into a double Fourier series with arguments ℓ and ℓ', the secular disturbing force $[F]$ is equal to the constant term of the expansion. Thus

$$(3) \qquad [F] = \frac{k^2 m'}{4\pi^2} \int_0^{2\pi} \int_0^{2\pi} \left(\frac{\rho}{\rho^3} - \frac{r'}{r'^3} \right) d\ell \, d\ell' .$$

Thus $[F]$ is deduced from (1) by applying a double process of averaging over the orbit of the disturbing body and over the orbit of the disturbed body.

The "area integral" for the disturbing body can be written in the form

$$(4) \qquad d\ell' = (r'^2 dv') / a'b' .$$

Hence

$$(5) \qquad \frac{1}{2\pi} \int_0^{2\pi} \frac{r'}{r'^3} d\ell' = \frac{1}{2\pi a'b'} \int_0^{2\pi} r'^0 dv' = 0 .$$

Thus the indirect part $-r'/r'^3$ of the disturbing force does not produce any secular effects, and (3) becomes

$$(6) \qquad [F] = \frac{k^2 m'}{2\pi} \int_0^{2\pi} \int_0^{2\pi} \frac{\rho}{\rho^3} d\ell' \, d\ell .$$

Let F_0 be the average of $[F]$ over the orbit of the disturbing body. Then

$$F_0 = \frac{k^2 m'}{2\pi} \int_0^{2\pi} \frac{\rho}{\rho^3} d\ell' .$$

In the process of determining F_0, the position of the disturbing body is imagined to describe the complete osculating ellipse. However, we are interested neither in short-period terms nor in knowing at what moment of time the disturbing body will occupy a particular position in its ellipse. This process of averaging is evidently a purely geometrical one.

The geometrical locus of vectors ρ is an elliptical cone with its apex in the disturbed body. Taking (4) into account, we can also write

$$(7) \qquad F_0 = \frac{k^2 m'}{2\, a' b'} \int_0^{2\pi} \frac{\rho}{\rho^3}\, r'^2\, dv' \,.$$

If we consider two neighboring position vectors ρ and $\rho + d\rho$ with respect to the disturbed body m, then $\frac{1}{2} r'^2\, dv'$ represents the area of an elementary sector with the center in the central body.

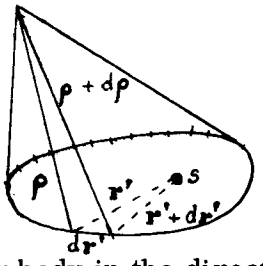

Using (7) and defining

$$(8) \qquad d\mu = \frac{m' r'^2\, dv'}{2\, a' b'} \,,$$

we deduce

$$(9) \qquad F_0 = k^2 \oint \frac{\rho}{\rho^3}\, d\mu \,.$$

The integral is taken along the ellipse of the disturbing body in the direction of the motion. Equation (9) represents the Gaussian result: F_0 is equal to the attraction of an elliptic ring over which the mass is distributed proportionally to the area of the sector described by the radius vector r'.

Based upon the preceding theory, a collection of formulas has been obtained and programmed for the actual computation of long-range effects in the motion of artificial satellites, minor planets, and comets, using step-by-step integration, [5]. For an artificial satellite, Halphen's method might give the information of the long-range effects and the stability of orbits over intervals of approximately 15-20 years. For minor planets, it can supply long-range (secular) effects in the elements of motion over the interval of hundreds of thousands of years. The integration step can be taken to be 100-500 years.

References

1. Musen, P., "On the long-period lunisolar effect in the motion of the artificial satellite," J. Geophys. Res., 66, 1659-1665, 1961.

2. Halphen, G.H., Traité des fonction élliptiques, vol. 2, Paris, 1888.

3. Gauss, K.F., Determinatio attractionis quam in punctum quodvis positionis data exerceret planeta, si ejus massa, etc., Collected Works, vol. 3, p. 331, 1818.

4. Goriachev, N.H., "On the method of Halphen of the computation of secular perturbations" (in Russian), pp. 1-115, University of Tomsk, 1937.

5. Musen, P., "A Discussion of Halphen's Method of Secular Perturbations and Its Application to the Determination of Long-Range Effects in the Motion of Celestial Bodies," Rev. of Geophysics, Vol. 1, no. 1, February 1961, pp. 85-122.

6. Goursat, E., Ann. Sci. École Norm. Suppl. 2, 10, 3-142, 1881.

25108

Heat Transfer with Receding Boundaries and Other Complications

by Simon Ostrach

I. Introduction.

There are many important heat transfer problems in which a material changes phase or in which one material is transformed into another. The melting or solidification of a substance, such as the formation of ice or solidification of castings, is an example of the former; the progress of a temperature-dependent chemical reaction through a solid is representative of the latter. The first published discussion of such problems seems to be that of Stefan (1891) in connection with a study of the thickness of polar ice; therefore, the "freezing" problem is often referred to as the Stefan problem.

The essential new characteristic of this type of problem is the existence of a moving surface of separation between the two phases. Heat can be liberated or absorbed at this interface, and the dynamic and thermal properties on either side of this surface can also be different, so that the problem is of considerable difficulty. The motion of the interface has to be determined to obtain a solution so that the problem is nonlinear. For special cases, exact solutions have, nevertheless, been obtained. See Carslaw and Jaeger (1959) for further discussion and details of such problems where conduction is considered to be the only heat transfer mechanism.

Considerable new interest in problems of the general type mentioned above began to be shown in the early 1950's in connection with the cooling of vehicles which reenter the Earth's atmosphere. At the hypersonic speeds of reentry, the hot gas in the layer between the bow shock wave

(Fig. 1) and the body is partly or fully dissociated.

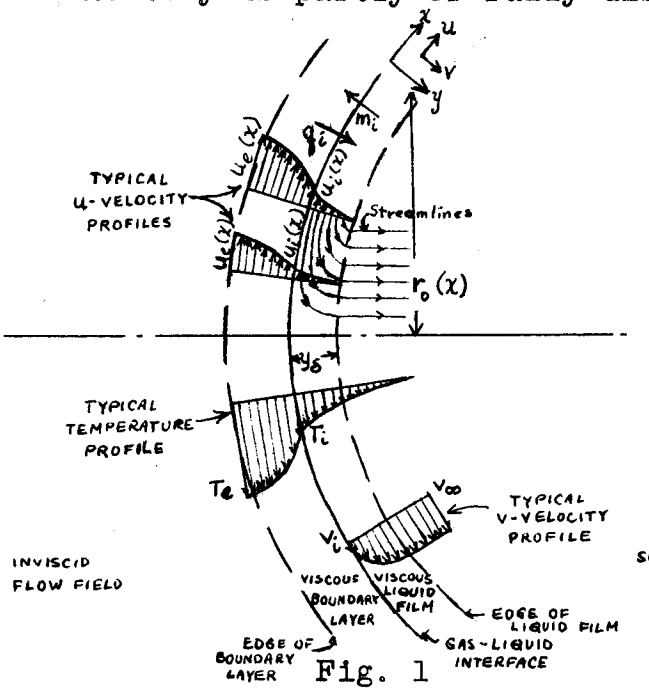

Coordinate system for melting surface at a stagnation point.

Fig. 1

Strong concentration gradients are produced when this mixture of atoms and molecules enters the boundary layer around the body and heat energy is transferred toward the surface, partly by diffusion and partly by heat conduction. Recombination reactions occur in the boundary layer, and some of the gas components may react with the vaporizing surface material. In addition, the high-velocity, high-temperature air flowing around the body leads to aerodynamic heating and heat convection. The details of these phenomena are extremely complicated, but it has been shown by Lees (1956, 1958, 1959a) and Fay and Riddell (1958) that the heat transfer rate from the gas depends primarily on the total enthalpy difference across the boundary layer, and not on these details, provided that the ratio of mass diffusivity to thermal diffusivity of the gas is nearly

unity, i.e. that the Lewis - Seminov number, Le = Pr/Sc = $\rho D_{12} \bar{c}_p / K = 1$, where Pr = $\bar{c}_p \mu / k$ is the Prandtl number, Sc = $\mu / \rho D_{12}$ is the Schmidt number, ρ is the gas density, D_{12} is the mass diffusion coefficient between species 1 and 2, $\bar{c}_p$ is the average specific heat at constant pressure, k is the thermal conductivity, and μ is the absolute viscosity coefficient. The additional effects occurring when the Lewis - Seminov number is not equal to unity are discussed by Lees (1958).

At hypersonic speeds heat is also transported to a body by radiation from the hot gas in the shock layer. However, from the work of Kivel and Bailey (1957) it can be deduced that for most entry trajectories, the radiative heat transfer rate from the gas is much smaller than that by convection except for direct entry into a planetary atmosphere at near-normal incidence, in which case, gas radiation can be dominant. However, infra-red radiation away from the body is important at high temperatures. See Lees (1959b) for additional comments on radiation. The net effect of all this is that the peak reentry heat transfer rates for ballistic missiles with a low drag to weight ratio are of the order of 2500 - 3000 Btu/ft^2/sec, which results in a power input of 15 kilowatts over an area about the size of a small postage stamp.

The use of a solid heat sink i.e., a good thermal conductor, to keep body surface temperatures at reasonable values was shown by Soloman (1959) to be inadequate at the large heat transfer rates associated with ballistic

reentry. Therefore, other means of thermal protection are necessary. Consequently, forced mass transfer systems, i.e., transpiration (fluid injection) cooling devices and self-regulating mass transfer systems, i.e., ablative processes were considered. Of the two, the latter showed the greater promise.

The term ablation refers, in general, to processes in which surface material is removed together with an associated amount of heat. However, this process can occur by any one or combinations of the following phenomena:

(1) melting, possibly in conjunction with vaporization of the molten layer. Such a process occurs when the heat absorbed by the ablating material causes two phase changes. Materials which lead to this type of behavior are usually said to be glassy. Typical of this class are refractory oxides such as quartz, fused silica, and Pyrex glass. These materials are characterized by high viscosity at elevated temperatures and the viscosity decreases rapidly with small increases in temperature. In addition, these materials have quite low thermal conductivities, good thermal shock properties, and high heats of vaporization. All these properties are desirable for ablation materials. Since the melting and vaporization temperatures for glassy materials are relatively high, surface temperatures as high as 3000 - 4000^{o}K can be attained during reentry or similar conditions and re-radiation from the hot surface can be appreciable.

(2) sublimation, which occurs when the static pressure in the shock layer is below that of the triple point of the material. Under such conditions the liquid phase of the material cannot exist. Thus, the material goes directly from the solid to the vapor state as the temperature increases. Sublimation thus basically refers to a physical change of state. Similar results, from a thermal protection point of view, can be also obtained by any one of the following forms of chemical decomposition of an ablating material; The distinction is, however, that a chemical change occurs with the latter:

(a) depolymerization, when a complex hydrocarbon polymer breaks down into a number of monomers due to chemical reactions at high temperatures. The monomer may then react with any oxygen in the surrounding gas by a combustion process thus increasing the heat transfer to the ablating substance. Many plastics such as polytretra fluoroethylene, commonly known as Teflon fall into this category. Although there are exceptions these materials also have very low thermal conductivities and low heats of vaporization. Some of these materials, like Teflon, decompose (sublime) at low temperatures (and low heat transfer rates) and the surface temperature remains at or below the sublimation temperature. This fact together with the low thermal conductivity minimizes the heat conduction problem for such materials, but also precludes any beneficial effects of re-radiation.

(b) pyrolysis of the solid phase, due to thermal decomposition of molecules at high temperatures. For organic compounds this usually results in the formation of such gases as methane, acetylene, or hydrogen and a solid char-like residue. This process is not one of combustion so that it need not occur in the presence of oxygen. Complication may occur since combustive reactions usually occur between the gaseous hydrocarbons produced and the oxygen in the surrounding air. This type of process is usually associated with reinforced plastics such as phenolics and polyesters with glass, nylon, and asbestos reinforcing fibers. In contrast to the low temperature sublimers, such materials as phenolics sublime at high temperatures and, therefore, can have surface temperatures of several thousand degrees kelvin. The re-radiation is, however, complicated by the erosion of the char.

(c) surface combustion which depends on the oxidation process of the material. Graphite and carbonaceous materials are typical for this type of ablation.

In each of these processes there is essentially a moving interface, whose motion must be found. Since, as was indicated above, the relatively simple problem of pure heat conduction with a moving interface was difficult to solve it would appear that the additional complexities associated with aerodynamic ablation viz., aerodynamic and pressure forces resulting from the surrounding high-temperature high-velocity gas stream, mass transfer, chemical reaction, etc., make the description of the ablation process nearly impossible. Nevertheless, considerable work on this type of problem has been done.

Since it is the purpose of this series of lectures to show how so complex a physical phenomenon can be analyzed theoretically attention will be given only to materials which melt before they vaporize. Although materials of this type do not offer the best thermal protection for ballistic-type reentry (as will be discussed below) they are of considerable interest in other regards. Also the rather extensive work dealing with melting ablation affords numerous examples for the present purposes. The work of Lees (1958) and Roberts (1959) are representative of treatments of subliming materials and that of Scala (1959) reviews the studies of decomposing materials.

The principal thesis of this lecture series is that deductive rather than inductive methods are essential for the description of new and complex phenomena, that is, specializations from the most general situation should be made in studying such problems rather than making generalizations from simplified cases. In this way, not only is a deeper understanding of the problem obtained and the primary physical aspects retained, but also the justifications and limitations of the simplifications are explicitly indicated.

2. General Considerations.

In order to control the ablation process it is essential to have as clear a detailed description of the associated phenomena as possible. The heating mechanism has been described above; the physical mechanisms of melting

ablation will now be discussed. It should, however, first be noted that some materials that melt before they vaporize have a distinct melting temperature whereas others, like glassy materials, do not. Attention will be given herein only to the latter type; the differences in the formulation between the two is shown, for example, by Chen and Allen (1962).

As the material is heated, energy is absorbed in the solid phase by the material's heat capacity. The surface temperature rises and the viscosity decreases (i.e. the substance melts) and more heat is absorbed by the latent heat of fusion. When the viscosity becomes sufficiently low the material starts to flow under the influence of the aerodynamic shear and pressure forces and body forces, if they are of sufficient relative magnitude. This represents the onset of ablation and heat is then also convected by the motion of the liquid layer. It is also possible that the liquid layer will reduce the radiation transfer from the hot gas to the surface. Since viscosity of such materials increases essentially exponentionally with decreasing temperature the flow of material is confined mostly to a thin layer very near the surface. As the ablated material flows it is further heated by aerodynamic heat transfer and some of it can vaporize as the surface temperature of the liquid layer increases. Good ablation materials absorb a large amount of heat through vaporization and/or decomposition. However, more important than this absorption are the phenomena that occur in the gas boundary layer as a result of the addition of foreign material vapor. These phenomena result in lower heat transfer from the hot gas and are usually referred to as "blocking" effects. This reduction in the heat transfer

from the hot gas by adding mass to the gas boundary layer results from the absorption of heat by the vapor due to its heat capacity as it diffuses through the gas boundary layer and by changing the gas boundary layer velocity and temperature distributions (and, in some cases, the gas transport properties). The latter have been extensively studied (see Lees (1958), for example). As the material flows downstream along the body, it may reach a region of lower heating and freeze there; if not it will continue to behave as described above.

Thus, the entire complex nature of the physical problem is now apparent. On the gas-side of the moving gas-liquid interface not only are there the aerodynamic and radiation heat transfer phenomena to be considered, but also the influence of foreign mass addition on these must be accounted for; on the liquid side the coupled dynamic and thermal phenomena must be treated. Finally the mutual influence of one side on the other results in a problem to be solved that is orders of magnitude more difficult than the Stefan problem, which is the classical problem of heat transfer with a moving interface.

The question now arises how to proceed to analyze a problem of this sort. Due to the urgency for practical answers in the nation's embryonic space program emphasis was first placed on the rapid acquisition of gross design criteria from simple analyses in conjunction with some experimentation. A survey of these design techniques is given by Adams (1959). This work was limited to aerodynamic forebodies (in particular to their stagnation region); also only gross characteristics such as heat transfer and total material loss were of primary interst. On the basis of such work, interest in the dynamics and heat transfer of melting layers waned when it was found

that the vaporization effects were dominant for thermal protection, particularly for ballistic-type reentry.

In addition to the design studies there were attempts made to describe the melting ablation process in detail. It is this work which will be discussed in some detail herein. Recently manned-vehicle reentry with its relatively low-intensity long-duration heating during which melting can occur before vaporization has restimulated work on melting ablation. Perhaps the greatest impetus for continued studies of this kind is provided by Chapman and his co-workers (1960), (1962a), (1962b). They applied entry flight dynamics and melting ablation theory to the question of the origin of tektites. Briefly, tektites are natural silica glass objects of similar composition that have been found in seemingly disparate regions around the world; furthermore they bear little resemblence to the local terrain in which they are found. (See Baker (1959) for an extensive account of tektites.) On the basis of existing ablation theory Chapman has implied that some of the tektites are of lunar origin. Clearly more detailed information on melting ablation is necessary to determine the validity of this assertion. In particular, most tektites are distinctively characterized by concentric ring waves on their surfaces and the relation of these waves to the dynamics and the heat transfer of the body must be established.

3. Inductive Analyses.

Most all the approaches to determine the detailed characteristics of melting ablation are based on inductive reasoning, i.e., special models are analyzed in the hope that they will indicate the significant general behavior of melting layers. One of the earliest analyses of this type appears to be that of Landau (1950). He treats the problem of the melting of a solid under the assumption that the liquid is immediately removed on formation. This prime assumption is presumably made on the basis that the large aerodynamic forces would lead to such behavior. Clearly, then this model denies any important role of the liquid layer, but other than intuitively, this assumption is not as yet justified. The distinction between Landau's problem and the Stefan problem is that in the latter the liquid is taken to remain on the solid and, thereby, influence its heat transfer; in the former the liquid plays no important role. Landau suggests that his analysis could also apply to the case of sublimation, and it seems as if his "model" does, in fact, more closely simulate that case.

To obtain some general results and an idea of the structure of the problem, it is first formulated somewhat generally. Specialization is then made to obtain more detailed results. Consideration is, accordingly, given to the one dimensional heat conduction in a solid which initially extends from $X = 0$ to $X = a$. Heat is considered to flow into the solid through the surface $X = 0$ at a rate $H(\bar{t})$ per unit area. The other surface, $X = a$, is

taken to be insulated. If heating continues long enough, the face at $X = 0$ reaches the melting temperature T_m and melting starts. Note that this analysis does not pertain directly to glassy materials which have no distinct melting temperature. The liquid is assumed to be blown away immediately on formation so that the surface of the solid at $X = 0$ moves inward and at time $\bar{t}$ is at the position $X = S(\bar{t})$. If the heating rate $H(\bar{t})$, decreases enough, the surface temperature can become lower than the melting rate so that $S(\bar{t})$ remains constant; melting can resume if $H(\bar{t})$ increases sufficiently. The temperature of the solid $T(X,\bar{t})$ and the thickness melted $S(\bar{t})$ are the quantities to be determined; their existence and uniqueness are assumed on physical bases (see Boley (1963) for a uniqueness proof).

The process is governed by the dimensional equation expression conservation of energy for unsteady, one-dimensional heat conduction, viz.:

$$\rho c \frac{\partial T}{\partial \bar{t}} = \frac{\partial}{\partial X}\left(k \frac{\partial T}{\partial X}\right) \quad \text{for } S(\bar{t}) < X < a \quad \bar{t} > 0 \tag{3.1}$$

and the boundary and initial conditions:

$$T(X,0) = T_o(X) \leq T_m \qquad 0 \leq X \leq a \quad \bar{t}=0 \tag{3.2}$$

$$\frac{\partial T}{\partial X} = 0 \qquad X = a \qquad \bar{t} > 0 \tag{3.3}$$

$$H(\bar{t}) = -k \frac{\partial T}{\partial X} + \rho_L \frac{dS}{d\bar{t}} \qquad X = S(\bar{t}) \quad \bar{t} > 0 \tag{3.4}$$

where ρ denotes the density of the solid, c its specific

heat, k its thermal conductivity, T the temperature, $\bar{t}$ the time, X the distance from the initial position of the heated surface, T_o (X) the initial temperature distribution, and L the latent heat of fusion. The physical interpretation of the initial and boundary conditions expressed by Equations (3.2) and (3.3) has already been given. The last equation expresses the fact that the heat input $H(\bar{t})$ equals the rate of heat flow into the solid plus the rate of heat absorption by melting. Equation (3.4) will be valid both during melting and non-melting if it is specified that at the heated surface $X = S(\bar{t})$.

$$\frac{dS}{d\bar{t}} \geq 0 \qquad \text{for } T(S(\bar{t}), \bar{t}) = T_m \tag{3.5}$$

$$\frac{dS}{d\bar{t}} = 0 \qquad \text{for } T(S(\bar{t}), \bar{t}) < T_m \tag{3.6}$$

To eliminate the moving boundary from the boundary conditions let

$$\xi = (a-X)/\left[a-S(\bar{t})\right] \quad .$$

The boundaries are then fixed at $\xi = 0$ and $\xi = 1$ and Equations (3.1) to (3.6) become

$$\rho c \left[\frac{\partial T}{\partial \bar{t}} + \frac{\xi}{a-S} \frac{dS}{d\bar{t}} \frac{\partial T}{\partial \xi}\right] = \frac{1}{(a-S)^2} \frac{\partial}{\partial \xi} \left(k \frac{\partial T}{\partial \xi}\right)$$

$$0 < \xi < 1, \ \bar{t} > 0 \tag{3.1a}$$

$$T(X,0) = T_o(\xi) < T_m \qquad 0 \leq \xi \leq 1, \ \bar{t} = 0 \qquad (3.2a)$$

$$\frac{\partial T}{\partial \xi} = 0 \qquad \xi = 0, \quad t > 0 \qquad (3.3a)$$

$$\left.\begin{aligned} H(\bar{t}) &= \frac{k}{a-S} \frac{\partial T}{\partial \xi} + \rho_L \frac{dS}{d\bar{t}} \\ \frac{dS}{d\bar{t}} &\geq 0 \qquad \text{for } T(1,\bar{t}) = T_m \\ \frac{dS}{d\bar{t}} &= 0 \qquad \text{for } T(1,\bar{t}) < T_m \end{aligned}\right\} \quad \xi = 1, \ \bar{t} > 0 \qquad (3.4a)$$

In this form the nonlinearity of the problem is readily apparent from the fact that S and its derivative, which occur in the coefficients of the differential equation, depend on the temperature gradient (see Equation (3.4a)). This nonlinearity constitutes the essential difficulty in determining the unknown moving boundary $S(\bar{t})$. Landau obtains some qualitative results on the melting rate and time and expressions for the temperature distribution in terms of the moving surface from the above boundary value problem and he suggests that numerical methods be used to obtain explicit solutions.

To obtain a more tractable mathematical problem, Landau (1950) considers an even more special problem than the above. On the basis that in practice the melting will proceed only a relatively small distance into the solid he assumed that the body can be taken to be semi-infinite, i.e., $a \rightarrow \infty$. Also it is now assumed that the specific heat, c, the thermal conductivity, k, the initial temperature T_o and the heat input rate are all

constants with $H > 0$. Even though the variation of these quantities can be important in some cases, the greater detail obtained from the solution found by taking them to be constant is considered to justify this assumption.

The boundary condition given by Equation (3.3) now becomes

$$\frac{\partial T}{\partial X} \to 0 \qquad \text{as } X \to \infty \qquad \bar{t} > 0 \tag{3.7}$$

which is equivalent to

$$T \longrightarrow T_o \qquad X \to \infty \ , \ \bar{t} > 0$$

The temperature distribution $T(X,\bar{t})$ during any period where there is no melting is not difficult to find, when c and k are constant. Various well-known methods such as the use of Luplace transforms (Churchill (1944)) or the method of sources and sinks (see Chapter X of Carslaw and Jaeger (1959)) can be used to find that it is

$$T(X,t) = T_o + 2H\left(\frac{\bar{t}}{\rho c k}\right)^{\frac{1}{2}} \left\{ \pi^{\frac{1}{2}} \exp\left(-\frac{X^2}{4\alpha \bar{t}}\right) - \frac{X}{2(\alpha \bar{t})^{\frac{1}{2}}} \operatorname{erfc}\left[\frac{X}{2(\alpha \bar{t})^{\frac{1}{2}}}\right] \right\} \tag{3.8}$$

$$= T_o + 2H \left(\frac{\bar{t}}{\rho c k}\right)^{\frac{1}{2}} \operatorname{ierfc}\left[\frac{X}{2(\alpha \bar{t})^{\frac{1}{2}}}\right]$$

where $\alpha = k/\rho c$ is the thermal diffusivity and ierfc denotes the integral of the complementary error function in the notation introduced by Hartree (1935-1936).

The time when melting starts, $\bar{t}_m$, (at X = 0) can be found from Equation (3.8) to be

$$\bar{t}_m = \frac{\pi}{4} \frac{\rho c k}{H^2} (T_m - T_o)^2 = \alpha \left(\rho \frac{L}{H} m\right)^2 \tag{3.9}$$

where

$$m = \frac{\pi^{\frac{1}{2}} c(T_m - T_o)}{2 L}$$

represents the ratio of the heat content change from T_o to T_m to the heat of fusion with a convenient multiplicative constant. Transformations will be made below such that the entire problem is expressed in terms of only the one parameter, m.

For the semi-infinite case being treated now the moving boundary can be eliminated from the boundary conditions by introducing a new coordinate, $X - S(\bar{t})$ which is the distance measured from the moving interface of the solid. Since only the melting process is of interest, time will be measured from t_m. To make the equations dimensionless, the following new variables are introduced

$$\theta = \theta(Z, t) = \frac{T - T_o}{\pi^{\frac{1}{2}} (T_m - T_o)} \tag{3.10}$$

$$Z = \frac{X - S(\bar{t})}{(\alpha t_m)^{\frac{1}{2}}} \tag{3.11}$$

$$t = \frac{\bar{t}}{\bar{t}_m} - 1 \tag{3.12}$$

$$\sigma = \frac{\rho_L}{H} \frac{S}{t_m} \tag{3.13}$$

$$\zeta = \frac{d\sigma}{dt} = \frac{\rho_L}{H} \frac{dS}{d\bar{t}} \tag{3.14}$$

Thus the heat conduction equation and the initial and boundary conditions become:

$$\frac{\partial \theta}{\partial t} = \frac{\partial^2 \theta}{\partial Z^2} + m\ \zeta(t) \frac{\partial \theta}{\partial Z} \qquad Z > 0 \quad t > 0 \tag{3.15}$$

$$\theta = \text{ierfc}\left(\frac{Z}{2}\right) \qquad Z \geq 0\ , \quad t = 0 \tag{3.16}$$

$$\theta \rightarrow 0 \qquad Z \rightarrow \infty \qquad t \geq 0 \tag{3.17}$$

$$1 = -2 \frac{\partial \theta}{\partial Z} + \zeta(t) \qquad Z = 0\ , \quad t > 0 \tag{3.18}$$

$$\theta = \pi^{-\frac{1}{2}} \qquad Z = 0\ , \quad t \geq 0 \tag{3.19}$$

This formulation is particularly convenient for both numerical and approximate solutions because only the single parameter, m appears in the differential equation and no parameters occur in the initial and boundary conditions.

Equation (3.18) should be regarded as the defining relation for the unknown reduced melting rate $\zeta(t)$. This quantity can be eliminated from the equations by substituting it from Equation (3.18) into Equation (3.15). Thus, it follows that

$$\frac{\partial \theta}{\partial t} = \frac{\partial^2 \theta}{\partial Z^2} + m\left[1 + 2\frac{\partial \theta(0,t)}{\partial Z}\right]\frac{\partial \theta}{\partial Z} \qquad (3.15a)$$

which is clearly nonlinear.

A number of special cases of the above defined boundary-value problem are amenable to further analysis and can give worthwhile information. Firstly, a steady-state (time-independent) solution will be sought for, i.e., one in which the temperature of the melting, semi-infinite solid approaches a state characterized by the inward movement at a constant velocity of a fixed temperature distribution. For continued heating it is clear that the temperature must increase or remain constant with time, i.e.,

$$\partial\theta/\partial t \geq 0.$$

Since, from Equation (3.19),

$$\theta \leq \pi^{-\frac{1}{2}}$$

it follows that $\partial\theta/\partial t \rightarrow 0$ as $t \rightarrow \infty$ and that θ tends to a steady state. If $\partial\theta/\partial t = 0$ then ζ is

constant, say $\zeta = \zeta_c$, the constant steady-state value of the reduced melting rate. From Equations (3.15) and (3.17) through (3.19) this steady state is found to be

$$\theta \rightarrow \theta(Z) = \pi^{-\frac{1}{2}} \exp(-m\,\zeta_c Z) \tag{3.20}$$

with

$$\zeta_c = (1+2m\pi^{-\frac{1}{2}})^{-1}$$

For the steady state rate of melting in terms of dimensional variables, there follows directly from Equations (3.14) (3.18) and (3.20)

$$\frac{dS}{d\bar{t}} \rightarrow V = \frac{H}{\rho[L+C(T_m - T_o)]} \tag{3.21}$$

which is perhaps physically obvious. To obtain the thickness melted Equation (3.21) would have to be integrated. However, the heating rate is in reality not constant as given by Equation (3.21) for the steady state. Therefore, integration of Equation (3.21) gives an approximation (for constant melting rate) for the thickness melted which is

$$S(\bar{t}) \cong V(\bar{t} - \bar{t}_m) \tag{3.22}$$

and the corresponding approximate temperature distribution is obtained from Equations (3.9) through (3.11) and (3.20) to (3.22) as

$$T \cong T_o + (T_m - T_o) \exp\left\{\frac{V}{\alpha}\left[X - V(\bar{t} - \bar{t}_m)\right]\right\} \tag{3.23}$$

Actually, the melting rate is initially less than its steady-state value, so that Equations (3.22) and (3.23) give values that are too large.

To obtain the proper asymptotic (for large time) expression for the thickness melted, one starts with the complete unsteady heat-conduction equation, Equation (3.1). Upon integration of this equation over a region in the X, $\bar{t}$ - plane, application of Gauss's theorem and the boundary conditions there is obtained (See Landau (1950) for details) an equation expressing the equality between the total heat inflow to a given time and the sum of the change in heat content in the remaining solid and the liquid. This last equation can be solved explicitly for the thickness melted to give (in dimensionless form)

$$\sigma(t) = \zeta_c\left(t + 1 - 2\int_0^\infty \theta(Z,t)\, dZ\right) \qquad (3.24)$$

The asymptotic or steady-state value of σ is obtained by use of Equation (3.20) in (3.24) and is

$$\sigma(t) \rightarrow \sigma_c(t) = \zeta_c(t + 1) - {}^2/\pi^{\frac{1}{2}}m \qquad (3.25)$$

or, in dimensional form

$$S(\bar{t}) = V\bar{t} - ({}^k/H)\,(T_m - T_o) \qquad (3.26)$$

The corresponding exact steady-state temperature distribution is

$$T = T_o + (T_m - T_o) \exp\left\{ - \frac{V}{\alpha} \left[X - V\bar{t} + k (T_m - T_o)/ H \right] \right\} \qquad (3.27)$$

Since $\theta (Z,t)$ increases with t, in general, it can be seen from Equation (3.24) that the steady state value gives a lower bound for the thickness melted. Also since from Equation (3.8)

$$\int_o^\infty \theta (Z,0) \, dZ = \int_o^\infty \text{ierfc} \left(Z/2 \right) dZ = \tfrac{1}{2}$$

an upper bound is obtained from Equation (22), that is,

$$V(\bar{t} - \bar{t}_m) \geq S(\bar{t}) > V\bar{t} - (k/H) (T_m - T_o) \qquad (3.28)$$

The difference between these two bounds is

$$\frac{k(T_m - T_o)}{H} \left[1 - \frac{\pi}{4} \left(1 + \frac{L}{c(T_m - T_o)} \right)^{-1} \right]$$

In practice, this last quantity is often small so that the steady-state value is a good approximation of $S(\bar{t})$ for all $t > t_m$.

By taking derivatives of Equation (3.24) it is found that the melting rate is always less than its steady state value, i.e.,

$$\frac{dS}{d\bar{t}} < V.$$

Physically, this result is also obvious since the heat content of the solid is increasing during the melting.

The next approximate solution of the boundary-value problem defined by Equations (3.15) to (3.19) is the unsteady one for m = 0. The parameter m in Equation (3.15) can take on any positive value. The value m = 0 does not correspond to a physically realizable situation but it can be considered to be a limit when the latent heat, L, becomes large. In this case the boundary-value problem can be solved in terms of tabulated functions. This solution is of value since it is one limit of the set of solutions for $0 < m < \infty$; also it will represent an approximation for any finite m when the dimensionless time, t, is small, because then $\zeta(0) = 0$ and the last term of Equation (3.15) vanishes for that reason.

For m = 0 the equations are linear. The solution of Equation (3.15) does not involve Equation (3.18); the latter serves merely to find the melting rate $\zeta(t)$ from the solution. For this case then the solution can be written as

$$\theta_o(Z,t) = \pi^{-\frac{1}{2}} \operatorname{erfc}(Z/2t) + (4\pi t)^{-\frac{1}{2}} \int_0^{\infty} \operatorname{ierfc}\left(\frac{Z}{2}\right) \cdot \left\{ \exp\left[- \frac{(Z-\zeta)^2}{4t} \right] - \exp\left[- \frac{(Z+\zeta)^2}{4t} \right] \right\} d\zeta \qquad (3.29)$$

The indicated integrations are quite tedious, therefore, only the final result is given as

$$\theta(Z,t) = \pi^{-\frac{1}{2}} \operatorname{erfc}(Z/2t) - (Z/\pi) \arctan\left(t^{-\frac{1}{2}}\right) + \left[(t+1)/\pi\right]^{\frac{1}{2}} \exp\left[-Z^2/4(t+1)\right] \operatorname{erf}\left\{ Z/2 \left[t(t+1)\right]^{\frac{1}{2}} \right\} + 2ZW\left(Z/\left[2(t+1)\right]^{\frac{1}{2}}, t^{-\frac{1}{2}} \right) \qquad (3.30)$$

where

$$W(\beta,\gamma) = (2\pi)^{-1}\int_0^{\beta}\int_0^{\gamma x} \exp\left[-(x^2 + y^2)/2\right] dy\, dx$$

is a function tabulated by Nicholson (1943).

The dimensionless melting rate corresponding to this solution is

$$\zeta_o(t) = (2/\pi) \text{ arc tan } (t^{\frac{1}{2}}) \qquad (3.31)$$

and the melt thickness is

$$\sigma_o(t) = (2/\pi)\left[(t+1) \text{ arc tan } (t^{\frac{1}{2}}) - t^{\frac{1}{2}}\right] \qquad (3.32)$$

Note again that these can be considered as approximations for small dimensionless times.

The other limiting case, $m = \infty$, can be interpreted as that for no latent heat ($L = 0$). For steel with T_o as the room temperature, the value of the parameter m is 27, which is "practically infinite" in the sense that the temperature and melting rates will be close to those for m infinite.

For L = 0 the definitions of σ and ζ by Equations (3.13) and (3.14) must be modified. Therefore, quantities independent of L are defined as

$$\omega = m\sigma = \frac{2}{\pi^{\frac{1}{2}}} \frac{HS}{k(T_m - T_o)} \qquad (3.33)$$

$$\lambda = m\,\zeta = \frac{d\omega}{dt} = \frac{\pi^{\frac{1}{2}}}{2} \frac{\rho c}{H} (T_m - T_o) \frac{dS}{d\bar{t}} \qquad (3.34)$$

Equation (3.15) is now

$$\frac{\partial \theta}{\partial t} = \frac{\partial^2 \theta}{\partial z^2} + \lambda(t) \frac{\partial \theta}{\partial z} \qquad z > 0 \qquad t > 0 \tag{3.35}$$

and the interface condition, Equation (3.18), is

$$1 = -2 \frac{\partial \theta}{\partial z} \qquad z = 0, \quad t > 0 \tag{3.36}$$

There is thus no equation defining λ that is similar to Equation (3.18) for ζ. However, from Equation (3.19), $\partial\theta/\partial t = 0$ at $z = 0$ so that if the derivatives are continuous at $z = 0$, $t > 0$ Equation (3.35) gives

$$\frac{\partial^2 \theta}{\partial z^2} + \lambda \frac{\partial \theta}{\partial z} = 0 \qquad z = 0, \; t > 0$$

and by use of Equation (36)

$$\lambda(t) = 2 \frac{\partial^2 \theta}{\partial z^2} \qquad z = 0, \; t > 0 \tag{3.37}$$

which takes the place of Equation (3.18). The modified boundary-value problem for the case $m = \infty$ is then defined by Equations (3.35), (3.16), (3.17), (3.37) and (3.19).

It is to be noted that no important mathematical simplification resulted by considering the limiting case $m = \infty$ as it did for $m = 0$. Landau, therefore, obtained solutions for the case $m = \infty$ by numerical methods after first rewriting the problem in terms of the dependent variable $\partial\theta/\partial z$ so that λ would be determined with greater accuracy than is possible by numerically obtained second derivatives (Equation (3.37)). The results of

his solution for m = 0 and calculations for m > 0 are shown on Figures 2 and 3. In Fig. 2 it can be seen that for all m, the values of ζ approximate those for m = 0 for small values of t. Furthermore ζ approaches its steady state more rapidly the larger the value of m. The curves in Fig. 3 approach unity as an asymptote. (The ordinate on this figure for m = ∞ is ζ/ζ_c rather than ζ/ζ_c.) It can be seen on this figure that as m becomes large the slope of the curves near t = 0 becomes very large. The thickness melted is also presented by Landau.

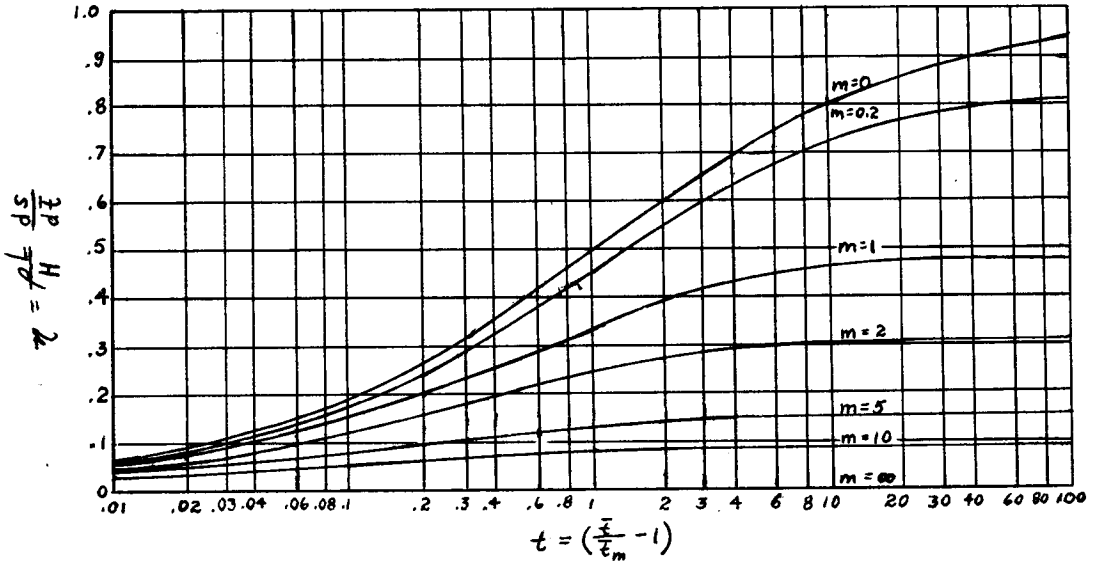

Fig. 2. Rate of melting of the semi-infinite solid for various values of m: $m = \pi^{1/2} c (T_m - T_0)/2L$, ds/dt = rate of melting, ρ = density, L = latent heat, H = heat input rate per unit area, t = time, t_m = time when melting begins

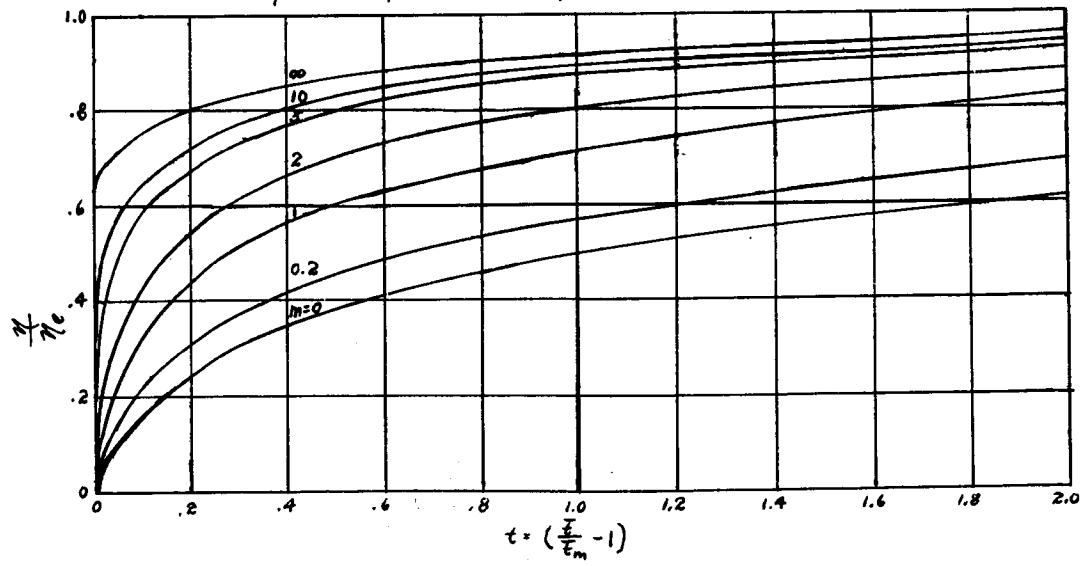

Fig. 3 Rate of melting as fraction of the steady melt rate: $V = H/\rho [L + c(T_m - T_0)]$, steady state rate of melting.

For large valves of m it would seem that the last term in Equation (3.15) would be dominant and that the other two terms could, therefore, by a perturbation analysis be shown to be negligible. However, such an approach leads to a singular perturbation problem, i.e., one in which the highest-order derivatives (here both the ones in the variables t and Z) would be eliminated. The order of the differential equation would be reduced in this way and, as a consequence, all the boundary and initial conditions could not be satisfied. Therefore, the highest derivative terms cannot be neglected near the boundaries although they may be negligible away from them. On this basis it can be concluded that in problems of this type the derivatives of the dependent variable near the boundaries should be very large. Such problems form the basis for the so-called boundary-layer theory of viscous fluids. See Lagerstrom et al (1949) and Friedrichs and Wasow. (1946) for further discussion of such problems). For the present problem then it is to be expected that in cases of m large, the time and space derivatives of the dimensionless temperature, θ, should be very large for small time ($t \approx 0$) and near the surface ($z \approx 0$). This qualitative behavior can, of course, be determined before any calculations are made and should be made then. In this way, one can make certain that small enough mesh size is taken in regions where large derivatives are expected. Relatively simple observations, such as were made above, which give qualitative trends are most helpful to avoid errors in the numerical calculations and to shorten the computation time. Note on Fig. 3 that the type of behavior

predicted by the above analysis is, of course, obtained. Landau (1950) gives no such discussion in his paper but does mention in the course of his formulation of the numerical procedure that rapid changes are to be expected at the start and, therefore, small mesh sizes are to be used there.

In accord with the above discussion note, on Fig. 3, the difference between the curve for $m = \infty$ $(L=0)$ and those for all other values of m $(L > 0)$, the former does not satisfy the initial condition, i.e., that the melting rate be zero at the start of melting. This behavior also was predicted in the discussion above and explained on the basis that the highest derivative is eliminated at the limiting value of m. This situation is analagous to the neglect of viscosity in fluid mechanics in which case nonzero tangential surface velocities are obtained rather than zero values. Landau merely points out that this discontinuity in time does not influence the continuity of the spatial temperature gradient $(\partial T/\partial X)$, but says nothing more about it. However, this says nothing about the continuity of T with respect both to time and space and no temperature distributions are presented in the paper.

The result of Landau's analysis of a model which neglects any influence of the liquid on the heat transfer process is that melting rates and temperature distributions for unsteady one-dimensional conduction are obtained. Obviously, nothing can be said about the heat transfer around a given body from this analysis. The melting rates then are of value to give indications of local ablations, and the temperature distributions also lead to estimates of local heat transfer.

Because the analysis and computations for even so idealized a problem as Landau's are so difficult and tedious approximate methods of solution have received considerable attention. In this regard it is surprising that Landau did not use a perturbation method to obtain approximate solutions for small values of m (see Equation (3.15)). Many of these approximate methods of solution follow directly from methods used in heat-conduction problems without melting, while others introduce new procedures particular to melting and ablation. A comparison of some of these methods for a particular re-entry heating rate is given by Blecher and Sutton (1961). Extensive reference lists can be found in the work of Economus (1961), Sunderland and Grosh (1960), Murray and Landis (1959) and Dewey et al. (1960).

Two of the methods for solving melting and ablation problems that have been in the fore are the heat balance integral method of Goodman and his coworker (1958), (1960a) and (1960b) and the variational method of Biot (1957), (1958), (1959a) and (1959b). Goodman's technique is similar to the Karman-Pohlhausen method for viscous flows and uses the integrated heat-conduction equation with an assumed temperature distribution. Thus the governing differential equation is not satisfied point by point but rather on the average and the boundary conditions are satisfied exactly. The advantage of this method lies in its ease of application, although there are in some cases difficulties in satisfying the imposed boundary conditions. This aspect of the problem is discussed by Goodman (1960b).

Biot's variational method is based on the concepts of irreversible thermodynamics and has not been applied as much as the heat-balance integral method. Citron (1959) and (1960) extended Biot's method to ablation problems but due to his application of an inconsistent constraint obtained poor agreement with the more exact numerical solutions. This defect was corrected by Biot and Daughaday (1962) and better results were obtained.

It should be kept in mind that both of these methods are approximate ones. Therefore, some lack of agreement with exact solutions is to be expected. For the ablation problem treated by Landau (1950) good agreement is obtained between Landau's results and those from the two approximate methods for times that correspond to steady-state conditions. In the transient range after melting starts, the agreement is not as good. Under all conditions, however, Goodman's treatment of the problem (1958) gave better results than Biot's. The shortcomings of the two methods are described by Lardner (1962) and the explicit comparisons are made therein with Landau's calculations.

Some Liquid-Layer Effects Included.

Another mathematical model related to melting ablation was studied by Goodman (1958b). The melt is considered to be an incompressible viscous fluid with constant properties that is swept off the solid by aerodynamic forces and the solid is considered to be at its melting temperature.

The latter together with the constant viscosity assumption, of course, precludes any relation to glassy materials; also solids to have a constant temperature, as assumed, would have to have large thermal conductivities and would, therefore, not tend to ablate.

Unfortunately, little motivation for the choices of this model is given in the paper and its relation to situations occuring in practice is not discussed; an inference is only made that the model should approximate conditions immediately after the start of melting. Presumably, this model was chosen to show, in contra-distinction to Landau's problem, some influence of the liquid layer on the heat transfer and to gain some understanding of the dynamics of the liquid layer. However, it should be clear that Goodman's model completely neglects the effects of convection (heat capacity of the liquid) so that the only influence of the liquid layer on the heat transfer is restricted to its effect on the interface motion. No attempt is made to justify this assumption as to the dominant effect of the liquid layer. In a sense, this model essentially describes what happens in an airstream to a layer of water on a solid under isothermal conditions. As a matter of fact, Goodman used just such an experiment to indicate the same qualitative trends which he predicted in his analysis. It may well be that this model simulates closely conditions at the start of melting, but this certainly needs further substantiation.

After the formulation of the general equations that govern this model, specialization is made to the case of a flat plate, because analytical soltuions are possible then. Basically these are obtained by integrating across the liquid layer to eliminate the coordinate normal to the body and then to apply a similarity transformation which reduces the partial differential equation to an ordinary one. A similarity transformation is one in which the independent variables are grouped together like $\zeta = tx^m$ and explicit dependence on either variable is removed from the differential equation and boundary conditions. The solutions so obtained implicitly are such that the dependent variables at a fixed value of one of the independent variables have similar distributions in terms of the second independent variable. Clearly, such solutions are meaningful for restricted physical situations. This point will be discussed in greater detail subsequently. Goodman obtained the melt thickness as a function of time for several different thermal boundary conditions, but unfortunately made no comparison of his results with Landau's (1950). Such a comparison, if possible, should be of some importance.

One particularly interesting result of Goodman's analysis is the prediction that as part of the starting phenomena the liquid moves downstream in a wave. His simple experiment, described above, gave qualitative support to this prediction.

Liquid-Layer Effects at Stagnation Point.

The last of the inductive approaches to be discussed in detail is that of Sutton (1958). This work, too, has as its primary objective to consider the influence of the liquid film on the heat transfer and ablation of bodies. It is, furthermore, explicitly formulated for glassy materials. Specific consideration is given to the stagnation point of aerodynamic forebodies on the basis that the heating is greatest there. Sutton further assumes that the viscosity is a function of temperature and that the process is quasi-steady, i.e., that the behavior at each instant can be determined by the time-independent solutions at conditions appropriate to that time. The conditions under which quasi-steady behavior is to be expected are not delineated.

Sutton starts from the basic equations for incompressible laminar boundary-layer flow, i.e. the equations which are associated with large Reynolds numbers. The coordinate system used for his analysis is shown in Fig. 1; it is fixed to the interface between the gaseous boundary-layer and the molten material. It is assumed that the rate of change of the body shape due to melting is small. For either two-dimensional or axisymmetric bodies the equations governing the liquid flow and heat transfer which express, respectively, the conservation of mass, momentum, and energy are

$$\frac{\partial}{\partial X}\left(UR_o^{\epsilon}\right) + \frac{\partial}{\partial Y}\left(VR_o^{\epsilon}\right) = 0 \qquad (3.38)$$

$$\rho\left(U\frac{\partial U}{\partial X} + V\frac{\partial U}{\partial Y}\right) = -\frac{\partial P}{\partial X} + \frac{\partial}{\partial Y}\left(\mu\frac{\partial U}{\partial Y}\right) \qquad (3.39)$$

$$\frac{\partial P}{\partial Y} = 0 \qquad (3.40)$$

$$\rho c_p\left(U\frac{\partial T}{\partial X} + V\frac{\partial T}{\partial Y}\right) = U\frac{\partial P}{\partial X} + \frac{\partial}{\partial Y}\left(k\frac{\partial T}{\partial Y}\right) + \mu\left(\frac{\partial U}{\partial Y}\right)^2 \qquad (3.41)$$

where $\epsilon = 0$ for two-dimensional bodies and $\epsilon = 1$ for axisymmetric ones. The other quantities either have been previously defined or are given on Fig. 1; c_p denotes the specific heat at constant pressure. Sutton states that if the Reynolds number were of unit order of magnitude the inertia terms (left side of Equation (3.39)) could be omitted, but that the convective terms (left side of Equation (3.41)) would, nevertheless have to be retained if the Prandtl number of the melted layer is large. However, he makes no mention of what justification there would be to neglect the terms for unit order Reynolds number that were omitted from the equations on the assumption of large Reynolds number. No further mention is made of what the values of the Prandtl or Reynolds numbers are for glassy films and, therefore, none of the simplifications indicated are made. It is then stated that for glassy materials the variations in density, specific heat, and thermal conductivity are small compared to the variation of viscosity with temperature. Therefore, they are taken to be constants.

The action of the aerodynamic forces and heat transfer on the molten surface material is described by the boundary conditions. At the interface, Y = 0, the shear of the liquid layer must equal that of the gas layer

$$\frac{\partial U}{\partial Y}(0) = -\tau_i/\mu_i \qquad (3.42a)$$

where τ is the shear stress and the subscript i denotes gas-liquid interface conditions. The temperature of the gas and liquid are equal.

$$T(0) = T_i \qquad (3.42b)$$

In addition, there may be mass transfer into the gaseous layer due to evaporation or pyrolysis of the liquid film. In the former case the mass transfer is controlled by the vapor pressure of the material and by diffusion in the boundary layer; in the latter case the chemistry of the material is the determining factor. The mass transfer condition is

$$V(0) = -m_I/\rho \qquad (3.42c)$$

where m is the mass transfer. Two additional boundary conditions in the interior of the surface material must be given. For glassy materials these are that at large enough distances from the interface the temperature is low and, therefore, there is no flow, i.e.,

$$\lim_{Y\to\infty} T(Y) = T_o \qquad \lim_{Y\to\infty} U(Y) = 0 \tag{3.43}$$

It is implicit in these boundary conditions that the material is semi-infinite.

To convert Equations (3.39) and (3.41) into ordinary differential equations, the mangler transformation (see Lees(1956)) and a similarity transformation are made:

$$S = \rho\mu^* \int_o^X U_c(X)\, R_o^{2\epsilon}(X)\, dX \tag{3.44}$$

$$\zeta = \left[\rho/(2S)^{\frac{1}{2}}\right] U_c(x)\, R_o^{\epsilon}(X)Y \tag{3.45}$$

A stream function

$$\Psi = (2S)^{\frac{1}{2}} F(\zeta) \tag{3.46}$$

is defined, where

$$\rho U R_o^{\epsilon} = \frac{\partial\Psi}{\partial Y} \quad , \quad \rho V R_o^{\epsilon} = -\frac{\partial\Psi}{\partial X} \tag{3.47}$$

Also, let

$$\theta = \frac{T - T_o}{T^*} \tag{3.48}$$

where the asterisk denotes a reference condition, the subscript c denotes conditions at the outer-edge of the gas boundary layer and the subscript o denotes the interior of the solid. Equations (3.39) and (3.41) then become, respectively,

$$\left[(\mu/\mu_*)F_{\zeta\zeta}\right]_\zeta + F_{\zeta\zeta} + \beta\left[(\rho_c/\rho) - F_\zeta^2\right] = 0 \qquad (3.49)$$

$$F\theta_\zeta + (k/c_p\mu^*)\,\theta_{\zeta\zeta} + (U_c^2/c_pT^*)\left[(\mu/\mu^*)F_{\zeta\zeta}^2 - \beta(\rho_c/\rho)F_\zeta\right] = 0 \qquad (3.50)$$

where

$$\beta \equiv 2s(\partial U_c/\partial s)_{\bar{s}}/U_c$$

$\bar{s}$ denotes conditions at the stagnation point, and subscripts denote differentiation. At an axially symmetric stagnation point $\beta = \frac{1}{2}$ and $\beta = 0$ for flows with zero pressure gradient. For stagnation point calculations the last term in Equation (3.50) can be neglected because

$$U_c^2 \prec\prec c_pT^*.$$

Sutton restricts further consideration to the stagnation point not only because the mathematics is much simpler, but also because the greatest heating occurs there and the gas boundary layer is most likely to be laminar there.

The relations between the physical variables and the dimensionless ones at a stagnation point are listed below for convenience

$$F = -\left[(\epsilon + 1)\mu^*(\partial U_c/\partial x)_{\bar{s}}\,\rho^{-1}\right]^{-\frac{1}{2}} V \qquad (3.51)$$

$$F_\zeta = U/U_c \qquad (3.52)$$

$$F_{\zeta\zeta} = -(\mu^*/\mu)\left[(\epsilon+1)\mu^*\rho\left(\partial U_c/\partial x\right)_s^3\right]^{-\frac{1}{2}}(\partial\tau/\partial x) \quad (3.53)$$

$$\theta = (T - T_o)/T^* \quad (3.54)$$

$$\theta_\zeta = -(1/kT^*)\left[(\epsilon+1)\rho\left(\partial U_c/\partial x\right)_s\mu^{*-1}\right]^{-\frac{1}{2}} q \quad (3.55)$$

$$\zeta = \left[(\epsilon+1)\rho\left(\partial U_c/\partial x\right)_s\mu^{*-1}\right]^{-\frac{1}{2}} Y \quad (3.56)$$

where q is the heat-transfer rate. The dimensionless boundary conditions for Equations (3.49) and (3.50) can be obtained by substitution of Equations (3.42) and (3.43) into Equations (3.51) to (3.56). The melting rate is given by $\lim_{Y\to\infty} V(Y)$.

It can be seen from Equations (3.49) and (3.50) that stagnation-point ablation depends on two parameters, the viscosity ratio which describes how the viscosity varies with temperature and the Prandtl number at some reference temperature, $c_p\mu^*/k$. Since for most liquids the viscosity-temperature variation is essentially the same, the Prandtl number is the primary parameter. The Prandtl number can be seen to be the coefficient of the convection terms in Equation (3.50). Therefore, the maximum effect of the molten film will be obtained with high Prandtl number liquids. One could now infer that Landau's and Goodman's work relates to liquids with low Prandtl number. For this reason Sutton chose to make his calculations for Pyrex since also its high-temperature properties are available. The thermal conductivity was taken as 1.71×10^{-3} Btu/ft°F, the density

131 lb./ft^3, specific heat 0.29 Btu/lb. and the viscosity-temperature variation is approximated closely by

$$\mu = 0.0672 \exp (8720/T)^{1.612} \quad 16/\text{ft-sec.} \qquad (3.57)$$

The density ratio ρ_c/ρ was taken to be 1.37×10^{-4} which corresponds to a Mach number of 18 at 90,000 ft. altitude. At this altitude, the density ratio does not vary appreciably with Mach number. The interior temperature of the glass, T_o, is assumed to be zero. The reference temperature was arbitrarily chosen as 4000°F. The calculations were made on a REAC differential analyzer for several values of the interface temperature, shear stress and mass transfer. Sutton reports that preliminary calculations indicated that F_{ζ^2} and $F_{\zeta\zeta}$ were negligible so that these terms were omitted from the momentum equation (3.49). As mentioned above, however, these are the inertia terms and could have been eliminated at the start on the basis that a modified Reynolds number is small (as it is for the problem studied). In order to apply the results to an actual case, m_i, U_i, T_i, q_i, and τ_i must be matched with gas flow boundary-layer solutions (see Scala and Sutton (1958) for the details of the matching procedure). However, the calculations were made using estimates of the aerodynamic heat-transfer rate.

A typical set of profiles is shown in Fig. 4.

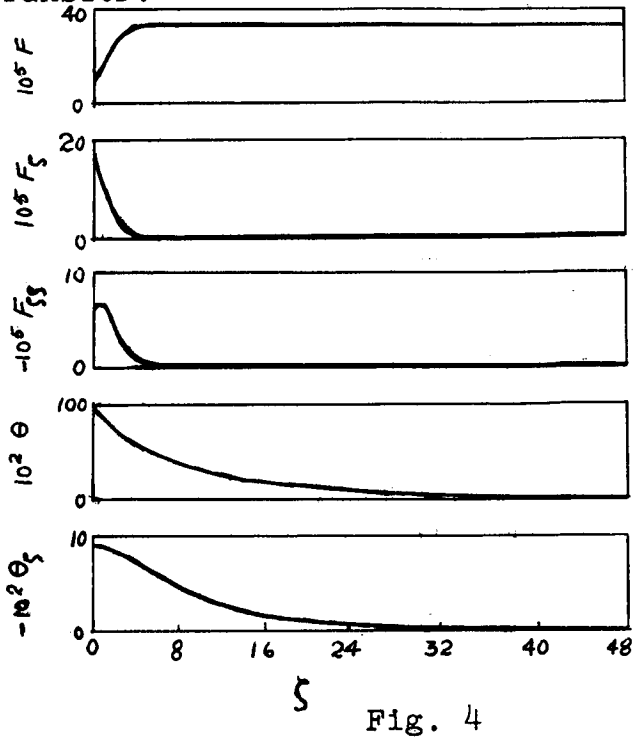

Typical set of profiles for $T_i = 4{,}000\,^\circ F$

Fig. 4

All curves, except $F_{\zeta\zeta}$, resemble exponential functions which might be expected from the form of the equations. Note also that the thickness of the flowing region is much less than that of the heated region. Also at the point of no flow, $F_\zeta = 0$, the value of the heat transfer rate Θ_ζ is about 70 per cent of its value at the interface. This means that only 70 per cent of the energy originally transferred to the interface is conducted into the non-flowing solid interior. In other words, about a third of the energy is convected away by the liquid film. Thus the presence of the film cannot be ignored.

For the conditions investigated it was found, as expected, that the interface temperature increased monotonically with interface energy transfer, but varied only slightly with the interface shear stress and mass transfer. A representative set of curves showing this behavior is presented in Fig. 5.

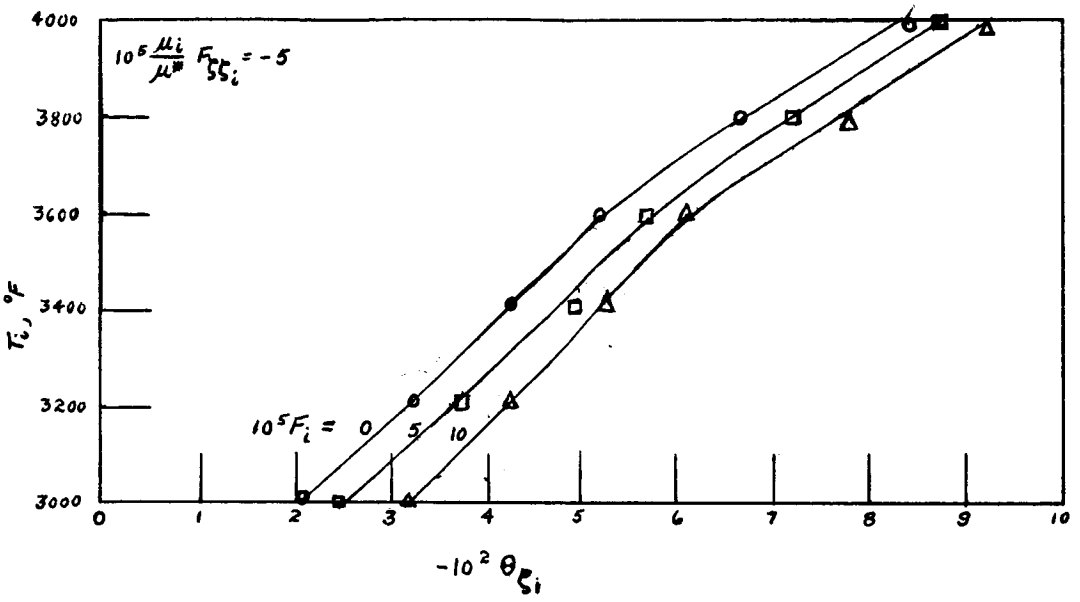

Fig. 5. Typical variation of surface temperature with non-dimensional heat-transfer rate.

A high interface temperature markedly decreases the viscosity of glass so that the liquid flows more readily under the action of a given pressure gradient and shear stress. The decrease in viscosity thus causes the surface to recede at a faster rate as shown in Fig. 6.

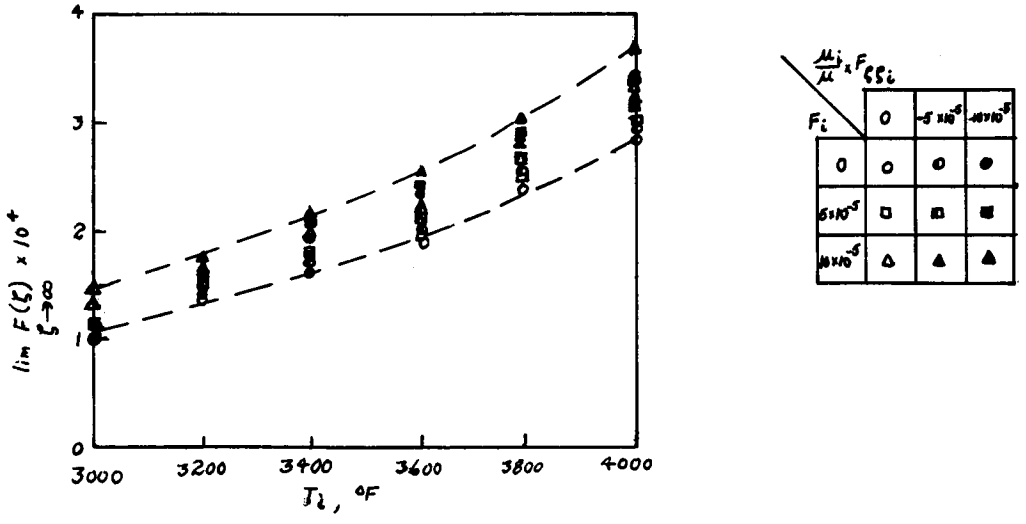

Fig. 6. Variation of nondimensional melting rate with surface temperature.

Hence as the heat transfer to the surface is increased the rate at which the surface recedes is increased as can be seen in Fig. 7; there the relation between heat-transfer and melting rates can be seen to be nearly linear.

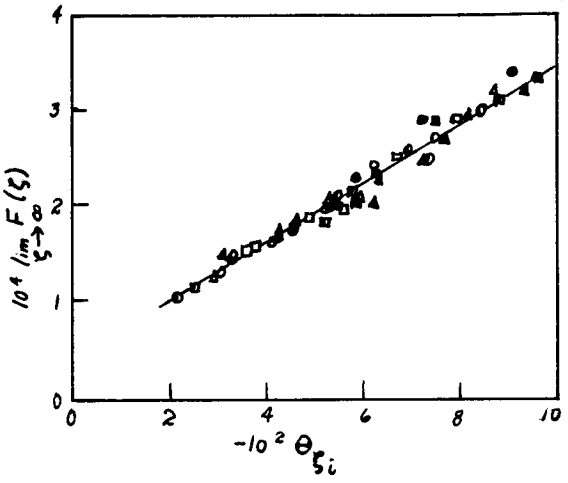

Variation of melting rate with heat-transfer rate

Fig. 7.

The surface shear or interphase mass transfer have negligible effect on the melting rate over the range of conditions studied by Sutton. The results of Fig. 7 were almost exactly reproduced for calculations at other hypersonic flight speeds and altitudes.

The calculations were repeated for common lime glass whose high-temperature viscosity is much less than Pyrex. For this glass the melting rates, $\lim_{Y \to \infty} V(Y)$, were five times greater than for Pyrex with the same energy flux to the interface. Thus, viscosity plays an extremely important role in determing melting rate.

It is of interest now to compare Sutton's results with those of Landau wherein the liquid layer was ignored completely. For glassy materials Landau's expression for the melting rate can be modified so that, written in terms of Sutton's notation, it is

$$\lim_{Y\to\infty} V(Y) = -\left[{}^{q_i}/_{\rho c_p (T_i - T_o)} \right] \qquad (3.58)$$

or, nondimensionally,

$$\lim_{\zeta\to\infty} F(\zeta) - (T^* \theta_{\zeta_i} / Pr^* T_i) \qquad (3.59)$$

Equation (3.59) predicts a value of the melting rate which is too small by 23 per cent for $T_i = 3000^{\circ}F$ and 28 per cent too small for $T_i = 4000^{\circ}F$. This is to be expected since most of the material that flows is at a lower temperature than T_i. Use of the liquid-solid interface temperature rather than T_i in Equation (3.59) results in larger melting rates being predicted from the simpler analysis. Thus Sutton has shown the essential role of the liquid film both with regard to the heat transfer and the melting rate. However, Sutton's analysis neglected transient effects, which he acknowledged are of greatest technical interest, and it is limited to the stagnation-point of a body.

A great deal of work has been done on the problem formulated by Sutton, see, for example, Bethe and Adams (1959) and Roberts (1959). This work attempts to simplify the computational work of Sutton by using integral

methods (that yield only approximate solutions) and also treats the matching of the conditions at the gas-liquid interface in a more convenient way so that the vaporization effects and influence of gas turbulence can be studied more readily.

By using an inductive philosophy, i.e., choosing specific relatively simple special problems, some of the essential behavior of melting films has been determined. Whereas some of the limitations and conditions of applicability can, in retrospect, be determined by careful study of all these solutions, not all of them are as yet apparent. Little or no comparisons among the various special problems were made by the authors themselves. It is also not certain at this point whether some other important physical aspects have been omitted that may be equally as important as those studied. The main results thus far are that the liquid layer cannot be neglected in melting ablation studies for materials with large Prandtl numbers. This type of material is best for melting ablation because the large viscous forces (associated with large viscosities) will prevent the molten layer from leaving the surface before its energy of vaporization has been utilized to reduce the heat energy to the body and the low conductivity retards the heat flow into the body and thereby yields a more efficient ablation process.

4. Deductive Analyses.

Consideration will now be given to the deductive analyses of the problem as represented essentially by

the analyses of Ostrach and his coworkers (1960), (1962). The approach in this work is to start from the most general governing equations and then to analyse them in detail to determine the governing dimensionless parameters and the essential physical aspects of the problem. Specific problems then are solved to show the influence of the physically significant quantities on the ablation process. In particular, the objectives of this work were to describe the dynamic and thermal behavior of melting layers all around a body and to find the influence, if any, of deceleration forces on the liquid layer. The latter was considered because although reentering bodies can be subject to a strong body force due to the strong decelerations, the effect of this type of force on the flow and heat transfer of melting layers had not been investigated in general. In determining conditions away from the stagnation region, it would seem particularly important to include body force effects, because for decelerating bodies the body force could oppose the downstream flow of liquid.

The specific problem analyzed by Ostrach and his coworkers is the thermal and dynamic behavior of melting materials on the exterior of a body of revolution or symmetric two-dimensional body that enters the atmosphere at high speed and experiences a large deceleration and surface heating. The viscosity of the liquid layer increases from some value at the gas-liquid interface to very large values near the body because of the

temperature change. Density, specific heat, and thermal conductivity are assumed constant. For suitable materials and expected physical conditions the thickness of the region where the viscosity is low enough for the ablating material to be considered as fluid is very small compared with the body scale.

Some additional assumptions are made in the case to be analyzed in detail in order to show the physical phenomena most clearly and simply. In particular the body is assumed to be subjected to a constant deceleration, although in an actual case the trajectory will determine the deceleration rate. Furthermore the temperature at the gas-liquid interface is assumed constant, and the vaporization rate will be neglected; indications as to how these restrictions might be relaxed for a more realistic calculation can be found in Ostrach et al (1962).

Because the liquid-layer thickness is small compared with the radius of curvature of the body, a system of coordinates parallel to and normal to the gas-liquid interface can be considered as a Cartesian coordinate system (see Fig. 1). The interface is taken to be the surface $Y = 0$, and Y increases into the liquid. The acceleration terms resulting from the unsteady motion of the interface relative to the body are neglected but this is considered as a steady velocity at any instant.

The resulting equations of motion for the liquid layer are:

Continuity:

$$\frac{\partial}{\partial X}\left(R^{\epsilon} U\right) + \frac{\partial}{\partial Y}\left(R^{\epsilon} V\right) = 0 \qquad (4.1)$$

where $\epsilon = 0$ for two-dimensional bodies and $\epsilon = 1$ for axisymmetric bodies.

Momentum:

$$\rho\left[\frac{\partial U}{\partial t} + U\frac{\partial U}{\partial X} + V\frac{\partial U}{\partial Y} - \sqrt{1 - \left(\frac{dR}{dX}\right)^2}\, A\right] = -\frac{\partial P}{\partial X} + \frac{\partial}{\partial Y}\left[\bar{\mu}\left(\frac{\partial V}{\partial X} + \frac{\partial U}{\partial Y}\right)\right] + 2\frac{\partial}{\partial X}\left(\bar{\mu}\frac{\partial U}{\partial X}\right) \qquad (4.2)$$

$$\rho\left(\frac{\partial V}{\partial t} + U\frac{\partial V}{\partial X} + V\frac{\partial V}{\partial Y} - \frac{dR}{dX}A\right) = -\frac{\partial P}{\partial Y} + 2\frac{\partial}{\partial Y}\left(\bar{\mu}\frac{\partial V}{\partial Y}\right) + \frac{\partial}{\partial X}\left[\bar{\mu}\left(\frac{\partial U}{\partial Y} + \frac{\partial V}{\partial X}\right)\right] \qquad (4.3)$$

Energy, neglecting thermal expansion of the liquid:

$$\rho c_p\left(\frac{\partial \bar{T}}{\partial t} + U\frac{\partial \bar{T}}{\partial X} + V\frac{\partial \bar{T}}{\partial Y}\right) = k\left(\frac{\partial^2 \bar{T}}{\partial X^2} + \frac{\partial^2 \bar{T}}{\partial Y^2}\right) + \phi \qquad (4.4)$$

Dissipation:

$$\phi \equiv \bar{\mu}\left[2\left(\frac{\partial U}{\partial X}\right)^2 + 2\left(\frac{\partial V}{\partial Y}\right)^2 + 2\frac{\partial U}{\partial Y}\frac{\partial V}{\partial X} + \left(\frac{\partial U}{\partial Y}\right)^2 + \left(\frac{\partial V}{\partial X}\right)^2\right] \qquad (4.4a)$$

The transformation from stationary coordinates to accelerating coordinates fixed in the body gives rise to an equivalent body force $\rho \vec{A}$ per unit volume with the components of equations (4.2) and (4.3), where A is the acceleration rate of the body.

Scaling and Reduction of Equation.

In order to compare the various terms and to determine their relative magnitudes, all variables will be transformed to dimensionless variables in such a way that they are of order one; the magnitudes of the terms will then be indicated by the fixed coefficients. This is, in general, not a trivial or automatic procedure. A clear understanding of the physics of the problem is essential to do this properly.

For X and R the clear choice of scale is the body scale size L, so that

$$X = xL, \qquad R = rL \quad .$$

The pressure, temperature, and viscosity are scaled by their values at the stagnation point (X = 0) interface (Y = 0), giving

$$\bar{T} = T_o T \quad , \quad P = P_o p \qquad \bar{\mu} = \mu_o \mu$$

The Y coordinate is nondimensionalized with respect to the liquid layer thickness, δ , which is so defined that it makes the ablation velocity (or rate), v_∞ , of unit order of magnitude. An explicit derivation of this

scaling factor is presented by Ostrach (1962). Thus $Y = L\,\delta\,Y$.

Since there exists no explicit characteristic velocity of the liquid layer, one is obtained by equating the magnitudes of the viscous and pressure forces. This implicitly assumes that liquid inertia forces may be less important. Therefore the characteristic velocity W is found to be $W = (P_o L/\bar{\mu}_o)\,\delta^2$ so that

$$U = Wu \text{ and } V = W\,\delta v$$

The choice of a proper time scale poses another important problem. One time scale, viz., L/W could be obtained from the first term of the inertia terms. However, because it is anticipated that the viscous liquid velocities could be small, this time scale is considered inadequate; also the physical meaning of L/W does not appear to be crucial to the problem. The energy equation provides the only other means for the selection of a time scale. As a matter of fact, this is the most important unsteady effect, since the heating of the liquid will determine the rate of softening and, hence, the rate of velocity increase. Because of the anticipated slow motion, the rate of temperature increase should be balanced by the conduction term. In this way the time scale σ is found to be $\sigma = (\rho c_\rho L^2/k)\,\delta^2$ which is a measure of the time required for a change to be transmitted through a layer of thickness $L\,\delta$. Thus $\bar{t} = \sigma t$ and the dimensionless time, t, is like the Fourier number which appears in classical heat conduction theory (see the footnote on page 25 of Carslaw and Jaeger (1959)).

In terms of the new variable the equations are

$$\frac{\partial(r^{\epsilon}u)}{\partial x} + \frac{\partial(r^{\epsilon}v)}{\partial y} = 0 \qquad (4.5)$$

$$\frac{1}{Pr}\left[\frac{\partial u}{\partial t} + Re\ Pr\,\delta^2\left(u\frac{\partial u}{\partial x} + v\frac{\partial u}{\partial y}\right)\right] - g\sqrt{1 - \left(\frac{dr}{dx}\right)^2} =$$

$$-\frac{\partial p}{\partial x} + 2\delta^2\frac{\partial}{\partial x}\left(\mu\frac{\partial u}{\partial x}\right) + \frac{\partial}{\partial y}\left[\mu\left(\frac{\partial u}{\partial y} + \delta^2\frac{\partial v}{\partial x}\right)\right] \qquad (4.6)$$

$$\frac{\delta^2}{Pr}\left[\frac{\partial v}{\partial t} + Re\ Pr\,\delta^2\left(u\frac{\partial v}{\partial x} + v\frac{\partial v}{\partial y}\right)\right] - \delta\frac{dr}{dx}g =$$

$$-\frac{\partial p}{\partial y} + 2\delta^2\frac{\partial}{\partial y}\left(\mu\frac{\partial v}{\partial y}\right) + \delta^2\frac{\partial}{\partial x}\left[\mu\left(\frac{\partial u}{\partial y} + \delta^2\frac{\partial v}{\partial x}\right)\right] \qquad (4.7)$$

$$\frac{\partial T}{\partial t} + Re\ Pr\,\delta^2\left(u\frac{\partial T}{\partial x} + v\frac{\partial T}{\partial y} - \delta^2\frac{\partial^2 T}{\partial x^2}\right) = \frac{\partial^2 T}{\partial y^2} +$$

$$\frac{Pr\ W^2}{c_p T_o}\left\{\left(\frac{\partial u}{\partial y}\right)^2 + 2\delta^2\left[\left(\frac{\partial u}{\partial x}\right)^2 + \frac{\partial u}{\partial y}\frac{\partial v}{\partial x} + \right.\right.$$

$$\left.\left.\frac{1}{2}\left(\frac{\partial v}{\partial y}\right)^2\right] + \delta^4\left(\frac{\partial v}{\partial x}\right)^2\right\} \qquad (4.8)$$

where $r = R/L$ and the dimensionless acceleration g is $A\rho L/P_o$.

The small terms are deleted from these equations on the assumptions that $\delta << 1$, $Re\ \delta^2 << 1$, $Pr >> 1$, and

$$Pr\ \frac{W^2}{c_p T_o} << 1$$

for glassy materials at the conditions of interest.

The analysis will be applied to the case of sudden heating of the interface, where $\frac{\partial T}{\partial t}$ is initially indefinitely large at $y = 0$. However, because of the small extent of the region of softened material, $\frac{\partial u}{\partial t}$ and $\frac{\partial v}{\partial t}$ are not indefinitely large. Thus the assumptions yield

$$\frac{\partial}{\partial y}\left(\mu \frac{\partial u}{\partial y}\right) = \frac{\partial p}{\partial x} - g\sqrt{1 - \left(\frac{dr}{dx}\right)^2} \equiv f(x) \qquad (4.9)$$

$$\frac{\partial p}{\partial y} = \delta g \frac{dr}{dx} \sim 0 \qquad (4.10)$$

$$\frac{\partial T}{\partial t} + \beta\left(u\frac{\partial T}{\partial x} + v\frac{\partial T}{\partial y}\right) = \frac{\partial^2 T}{\partial y^2} \qquad (4.11)$$

as well as the unaltered continuity equation (4.5). Note that Equations (4.9) and (4.11) are coupled by means of a viscosity-temperature relation so that, in general, the problem is nonlinear and $\beta = \text{Pr Re}\,\delta^2$.

The fact that the main unsteady effect in the ablation process is due to the unsteady term in the energy equation was also mentioned after a qualitative discussion in the stagnation-point analysis by Georgiev(1959). Because of equation (4.10), p is constant through the liquid layer at any fixed station X on the body and is equal to its value at the interface ($p = p(X) = p_i(X) = p(X,0)$). The Newtonian pressure distribution is used for p(X). The importance of deceleration is seen to depend on the magnitude of the parameter $g(\equiv \rho LA/P_o)$ which represents the ratio of the deceleration body force to the pressure force and is, in a sense, a reciprocal Froude number.

From Newtonian fluid mechanics, the decelerating force on the body is of order $P_o S$, where S is the projected cross-sectional area of the body. If LS is the body volume, and $\rho_B LS$ the mass (ρ_B is average mass density), then the deceleration is

$$A = P_o / L \rho_B \quad \text{or} \quad g = \rho / \rho_B \quad . \qquad (4.12)$$

Thus for a reentering ballistic vehicle, g can be very large, whereas for a meteorite g is of order unity. The second parameter β which appears in equation (4.11) indicates the importance of heat convection relative to heat conduction and depends upon shear stress (through δ) as well as properties of the liquid layer.

The initial conditions of the body for the sudden application of boundary-layer heating are determined by the assumption of a cold glassy layer. The initial temperature is assumed to be zero, so that

$$t = 0, \quad T = u = v = 0 \qquad (4.13)$$

At the interior of the body ($y \to \infty$), the temperature remains low, but the melting away of the liquid layer results in a relative velocity v_∞ between the interface and the body. Therefore

$$y \to \infty, \quad T = u = 0, \quad v = v_\infty \qquad (4.14)$$

If $v_\infty < 0$, the glassy liquid is being carried away; if $v_\infty > 0$ the liquid is accumulating. Because of symmetry at the stagnation point,

$$x = 0, \quad \frac{\partial T}{\partial x} = \frac{\partial u}{\partial x} = \frac{\partial v}{\partial x} = 0 \tag{4.15}$$

At the interface, the temperature and shear stress of the liquid are equal to those in the gas;

$$y = 0, \quad \bar{T}_g = \bar{T}_i, \quad \bar{\tau}_g = \bar{\tau}_i = -\bar{\mu}_i \left(\frac{\partial U}{\partial Y}\right)_i = \frac{\bar{\mu}_i W}{L\delta\mu_i} \tau_i = P_o \delta\tau_i \tag{4.16}$$

And finally the heat balance condition is

$$k_g \left(\frac{\partial \bar{T}_g}{\partial Y}\right)_i = k \left(\frac{\partial \bar{T}}{\partial Y}\right)_i + \rho v_i H \tag{4.17}$$

as a restatement of equation (4.18) given by Lees (1958). The convection of enthalpy by diffusion has been neglected, since a noncatalytic wall is assumed. Also, the radiation terms in the energy equation which are included by Hidalgo (1959) have been neglected.

Equation (4.9) can be integrated for u, to yield

$$\mu \frac{\partial u}{\partial y} = -\tau_i + fy \tag{4.18}$$

$$u = f \int_\infty^y \frac{y}{\mu}\, dy - \tau_i \int_\infty^y \frac{dy}{\mu} \tag{4.19}$$

If some dependence of μ on y (and x) is assumed, equation (4.19) will yield a solution for u, which when inserted

into the continuity equation (4.5) results in a first-order non-linear differential equation in x of the boundary conditions with explicit dependence on y. Thus the variation with x originates in conditions in the gaseous boundary layer. The integral of equation (4.5) is

$$v - v_\infty = - \frac{1}{r^\epsilon} \frac{\partial}{\partial x} \left(r^\epsilon \int_\infty^y u \, dy \right) \tag{4.20}$$

$$v_i - v_\infty = - \frac{1}{r^\epsilon} \frac{\partial}{\partial x} \left(r^\epsilon \int_\infty^o u \, dy \right) \tag{4.21}$$

However, the viscosity depends on the temperature, which is to be found as a solution of a partial differential equation with x, y, and t as independent variables. Because of the complicated form for the convection terms, the general solution of the energy equation is difficult.

A number of possibilities are available to resolve this problem. Hidalgo (1959) who also wanted to find the ablation characteristics around a body used a Kármán-Pohlhausen type integral method to obtain approximate solutions, but he treats only the steady problem and gives no velocity or temperature profiles. Furthermore, although Hidalgo's basic equations contain a deceleration term, no discussion or calculations of its significance is given therein. Because one of the primary objectives of Ostrach's work was to obtain some details of the structure of the liquid layer, it was considered desirable to simplify the energy equation somewhat and to solve the approximate equation in detail. The approach used by Ostrach and his coworkers (1962) is to replace the convection terms by a simpler expression that, however, represents the dominant convection effects. The details

follow below. Another approach, to be described subsequently, is followed by one of Ostrach's students, Mr. D. McConnell, in his doctoral thesis. This is a perturbation method in the parameter β, since for quartz, $\beta = .09$ and for Pyrex $\beta = 0.2$.

The convection term, $u\ \partial T/\partial X$, is eliminated by Bethe and Adams, because their analysis is limited to the stagnation point where $u = \partial T/\partial X = 0$; also for their steady-state problem they further simplify the equation by replacing v by v_∞, the ablation velocity. Carrier (1958) describes a formal method by which the latter simplification can be made with good accuracy. Ostrach et al. (1962) made the same simplifications (as Bethe and Adams) for their more general problem with the following justification. In the first approximation it is assumed that the interface temperature $T_i(X,t)$ varies only slowly with X. Only in the thin region where $T \sim T_i$ are there appreciable flows, so that the effect of convection in this region of nearly uniform temperature is small. The only important effect of convection is then the transport of the high-temperature interface toward the body as the viscous liquid layer is swept away or evaporated, i.e., the convection along the body is neglected relative to that normal to it. The energy equation with these assumptions reduces to

$$\frac{\partial T}{\partial t} + \beta\, v_\infty \frac{\partial T}{\partial y} = \frac{\partial^2 T}{\partial y^2} \qquad (4.22)$$

A discussion of the errors arising from this approximation is given in an appendix by Ostrach and his coworkers (1962).

The inadequacy of the steady-state approach for application over the whole body (suggested by Bethe and Adams (1959) and used by Hidalgo (1959)) can be seen by integration of equation (4.22). For steady state there is obtained

$$\frac{dT}{dy} = \left(\frac{dT}{dy}\right)_i e^{\beta v_\infty y}$$

This equation shows that dT/dy is unbounded as $y \to \infty$, in regions of X where $v_\infty > 0$, i.e., where there is an accumulation of liquid. Such regions can exist and should not be precluded by the method of analysis.

At the stagnation region, $v_\infty < 0$, so that no difficulty arises there. Although the energy equation (4.22) from which this result is derived is of questionable accuracy near the interface, it closely describes conditions for large values of y. The essential unsteadiness determined from the analysis can be explained physically as follows: Since the gas shear and pressure forces decrease around a body, at some position they can be insufficient to move the molten material. With continued heating the liquid viscosity decreases, i.e., the layer becomes thicker and the pressure force is larger so that the liquid can move again at a later time. This situation is accentuated if a deceleration force is present, because it can dominate the gas shear and pressure forces at some

location along the body. The deceleration force acts like gravity on a liquid layer clinging to a wall. The liquid will, therefore, slump forward. Because of the equivalence of conditions at all locations far back on the body the liquid motion will approximate that of uniform layers of fluid sliding over each other. The continued application of heat will cause a growth in thickness of the thermal layer on this section of the body so that steady-state conditions are never attained, i.e., the liquid behaves like a heated semi-infinite slab that is characterized by unsteady effects. Secondly, the forward slumping flow from the back region and the backward-swept flow from the front region will meet at some intermediate station where the fluid will continue to accumulate. (This result will be modified when the accumulation of material is sufficient to alter the pressure distribution.) This region will also not approach a steady-state condition. Near the forward stagnation point, a steady-state solution is nearly attained.

No details except results of the computations made by Hidalgo (1959) are contained therein, but because of the reasons cited above, those numerical results could not have included deceleration effects. The fact that no discussion of these effects is given therein seems to substantiate this supposition.

Method of Solution.

The boundary conditions for calculation of the liquid layer are not all known a priori. At the interface there

must be a match of temperature, shear stress, heat flow, and mass evaporation rate. If a temperature distribution $T_i(x,t)$ is assumed, all other quantities may be calculated from solutions of gaseous boundary layer. Various methods of making this match can be used (see Scala and Sutton (1958), for example); in addition to the description of some of these methods contained in the previously mentioned references, a comprehensive discussion of this problem is presented by Lees(1958). In the present analysis the gas boundary-layer characteristics of Cohen and Reshotko (1956) were used for the assumed Newtonian pressure distribution, and hence the calculations (but not the analysis) are restricted to the class of bodies for which those similarity solutions apply. A representative two-dimensional body of this class is shown by Ostrach et al. (1960); for axisymmetric bodies (see Figure 8 for the one studied by Ostrach and his coworkers (1962)) the Mangler transformation is applied to permit use of the results of Cohen and Reshotko. Since this procedure of using exact similar gas solutions is rather lengthy and involved and is not as convenient as direct use of the tables of Cohen and Reshotko, which can be used for any body shape, the details will be omitted herein.

Onemay expect on solving the liquid-layer flow and heat-transfer equations that a discrepancy will exist in the heat balance for each assumed interface temperature distribution. From several assumptions of the interface temperature distribution $T_i(X,t)$ it should be possible to find a distribution by interpolation for which the heat balance conditions are satisfied. This procedure could be applied at each instant of time starting with the value at X=0 and working downstream by integration of the continuity equation. For the problem considered in this paper, of sudden application of the hot gas, a selection of $\bar{T}(S,0,\bar{t}) = 4000^{\circ}F$(and $T_i=1.0$) was chosen in order to permit a solution which will indicate the main kinematic features of the liquid glass layer as a whole and to show time and x variation of the heat flux parameter $\left(\frac{\partial T}{\partial y}\right)_i$. It was also assumed that

there is no evaporation, that is,

$$v_i = v(x,o,t) = 0$$

The energy equation is integrated directly to give

$$T = \frac{T_i}{2}\left[e^{\beta v_\infty y}\ \text{erfc}\ \tfrac{1}{2}\left(y/\sqrt{t} + \beta v_\infty \sqrt{t}\right) + \text{erfc}\ \tfrac{1}{2}\left(y/\sqrt{t} - \beta v_\infty \sqrt{t}\right)\right] \qquad (4.23)$$

for the assumption that both T_i and v_∞ are independent of time but v_∞ is a function of x. These assumptions are more realistic for t large rather than initially (t small).

To complete the solution, there is now required an explicit form for the dependence of μ on y. For this purpose, we assume

$$\mu = \mu_i \exp(ay + by^2)$$

The functions "a" and "b" are determined from the assumed dependence of viscosity on the temperature;

$$\mu = \mu_i (T/T_i)^{-n}$$

If we differentiate,

$$\frac{1}{\mu_i}\left(\frac{d\mu}{dy}\right)_i = a = -n\left(\frac{dT}{dy}\right)_i / T_i \equiv -nT'$$

From equation (4.23) the required gradient T' is found for identifying a:

$$\frac{1}{T_i}\left(\frac{\partial T}{\partial y}\right)_i \equiv T' = \frac{1}{2}\left[\beta v_\infty \operatorname{erfc}\left(\frac{\beta v_\infty \sqrt{t}}{2}\right) - \frac{2}{\sqrt{\pi t}} e^{-\beta^2 v_\infty^2 t/4}\right] \tag{4.24}$$

The quadratic term is determined by the temperature at large values of y, where equation (4.23) is approximated by

$$\frac{T}{T_i} \sim \frac{2}{\sqrt{\pi}} \quad \frac{\exp\left(-y^2/4t + \beta v_\infty y/2 - \beta^2 v_\infty^2 t/4\right)}{y/\sqrt{t} - \beta^2 v_\infty^2 t^{3/2}/y}$$

The dominating factor in determining the rate of decrease of the temperature at large y is

$$\exp\left(-y^2/4t\right)$$

Hence we choose b = n/4t, from which

$$\mu = \mu_i \exp\left[-n(T'y - y^2/4t)\right] \tag{4.25}$$

with this viscosity relation, equation (4.19) may be explicity integrated to

$$u = -\frac{\exp n\left(yT' - \frac{y^2}{4t}\right)}{n(T' - y/2t)}\left\{\frac{f}{\mu_i}\left[\frac{\theta}{nT'\left(1 - y/2tT'\right)^2} - y\right] + \frac{\tau_i}{\mu_i}\left[1 - \frac{\theta}{2n(y/2\sqrt{t} - T'\sqrt{t})^2}\right]\right\} \tag{4.26}$$

where the abbreviations are

$$\theta \equiv 2Z^2 \left(1 - \sqrt{\pi}\, Z e^{Z^2} \operatorname{erfc} Z\right)$$

$$Z \equiv \sqrt{n}\left(y/2\sqrt{t} - T'\sqrt{t}\right)$$

Also, by integration of the continuity equation,

$$v - v_\infty = \frac{e^{-ny^2/4t}}{n^2 r^\epsilon} \frac{\partial}{\partial x}\left(\frac{r^\epsilon e^{nyT'}}{(T' - y/2t)^2}\left\{-\frac{f}{\mu_i}\left[y + \frac{\theta}{n(T' - y/2t)} + 2tT'(\theta - 1)\right] + \frac{\tau_i \theta}{\mu_i}\right\}\right) \tag{4.27}$$

At the interface $v = v_i$, $Z = -\sqrt{nt}\, T' \equiv Z_i$, $\theta = \theta_i$, and

$$v_i - v_\infty = \frac{1}{n^2 r^\epsilon} \frac{\partial}{\partial x}\left(\frac{r^\epsilon \theta_i}{\mu_i T'^2}\left\{-f\left[\frac{1}{nT'} + 2tT'\left(\frac{\theta_i - 1}{\theta_i}\right)\right] + \tau_i\right\}\right) \tag{4.28}$$

At the stagnation point $r = x$, $f = x\left(\frac{df}{dx}\right)_o$, $\tau_i = x\left(\frac{d\tau_i}{dx}\right)_o$, $\mu_i = 1$, $T' = T'_o$, θ_i = constant, so that

$$u_i(x = 0) = -\frac{x}{nT'}\left[\frac{\theta_i}{nT'_o}\left(\frac{df}{dx}\right)_o + \left(\frac{d\tau_i}{dx}\right)_o \cdot\left(1 + \frac{\theta_o}{2ntT'^2}\right)\right] \tag{4.26a}$$

$$v_i(0) - v_\infty(0) = \frac{1 + \epsilon}{n^2 T'^2_o}\theta_o\left\{-\left(\frac{df}{dx}\right)_o\left[\frac{1}{nT'_o} + 2tT'_o\frac{(\theta_o - 1)}{\theta_o}\right] + \left(\frac{d\tau_i}{dx}\right)_o\right\} \tag{4.28a}$$

The limiting steady-state case is obtained when t is large, $Z_i = -\sqrt{nt}\,T'$ is large, and

$$\theta \sim 1 - \frac{1.5}{Z^2} \rightarrow 1 - \frac{1.5}{nt(T' - y/2t)^2} \rightarrow 1 - \frac{1.5}{ntT'^2}$$

At this point the problem is completely solved for dependence of u, v, and T on x, y, and t, provided the dependence of the boundary parameters, v_∞, T', T_i, v_i, and τ_i on the variables X and t is found. For our approximate solution, $v_i = 0$, but in general the temperature balance ($\bar{T}_i = \bar{T}_g$) will determine the vapor pressure of the components of the liquid glass and the diffusion rate through the boundary layer (see Bethe and Adams (1959) and Baron (1956)) will depend on the external conditions and the wall temperature. Similarly the shear stress and heat transfer will depend on T_i and external conditions. This leaves T_i and v_∞ to be found from equations (4.24) and (4.28).

Numerical Procedure.

To solve for the parameters v_∞ and T' which are required before u, v, and T can be calculated, equations (4.24) and (4.28) must be solved simultaneously. To facilitate the discussion, the differential equation (4.28) is written in the form

$$v_\infty - v_i = \frac{1}{r^\epsilon} \frac{\partial}{\partial x} r^\epsilon (Bf + C\tau_i) \qquad (4.29)$$

where B and C are functions of T' and t. On differentiation,

$$v_\infty - v_i = B\left(\frac{df}{dx} + \epsilon \frac{f}{r}\frac{dr}{dx}\right) + C\left(\frac{d\tau_i}{dx} + \frac{\epsilon\tau_i}{r}\frac{dr}{dx}\right) + \left[\left(f\frac{\partial B}{\partial T'} + \tau_i \frac{\partial C}{\partial T'}\right)\frac{\partial T'}{\partial v_\infty}\right]\frac{dv_\infty}{dx} \qquad (4.30)$$

from which, together with Equation (4.24), the nonlinearity is apparent. In the particular problem solved (the first approximation where $\bar{T}_i = \bar{T}_o$,

$$\frac{d\bar{T}_o}{dt} = 0\ )$$

it was found that the coefficient of $\frac{dv_\infty}{dx}$ was a small quantity; at $x = 0$, the conditions $f = \tau_i = 0$ cause the coefficient to vanish there. Once again, then the problem is of the singular-perturbation type with, however, the additional complication that the coefficient of the highest derivative term is variable. Therefore, it can be immediately concluded that dv_∞/dx must be very large near the stagnation point ($x = 0$). The usual integration procedure was therefore found to be unsuitable in that successive approximations to the solution at a point frequently failed to converge. Equation (4.30) was therefore solved for the term v_∞ by writing the equation with numerical evaluation of the derivative from the argument itself:

$$v_\infty^i = D + E\frac{dv_\infty}{dx} = D + \frac{E}{\Delta x}\left(S^{i-2}v_\infty^{i-2} + S^{i-1}v_\infty^{i-1} + S^i v_\infty^i\right) \qquad (4.31)$$

where the definitions of D and E are obtained by comparing Equations (4.30) and (4.31) and S^i denote weighting factors.

This method of solution encountered difficulty in an intermediate region for certain cases of large time and deceleration; the possible cause of this failure will be discussed subsequently. In those cases it was possible to begin the solution at $x \rightarrow \infty$, leaving an intermediate region with the solution undetermined. For large x, it was assumed

$$V_\infty = \frac{dv_\infty}{dx} = 0.$$

Results.

In the example calculated the ablating material was taken to be Pyrex and the conditions assumed were (similar to Sutton's (1959)): Flight Mach number, 18.0; altitude, 90,000 feet; $L = R_o = 1$ foot; $\rho = 131$ lb/ft^3; $k = 1.71 \times 10^{-3}$ Btu/(ft)($^\circ$F)(sec); $c_p = 0.29$ Btu/(lb)($^\circ$F); μ_o (at 4000°F) = 0.07 slug/(ft)(sec). Body shape is shown in Figure 8. From these it is found that Pr = 383; Re = 79.6; $\delta = 2.510 \times 10^{-3}$; $\beta = 0.1929$; W = 1.370 ft/sec; F = 3.446×10^{-3} ft/sec. For Pyrex under the conditions of the problem a value of n = 8 was assumed. The gasious boundary layer adjoining the liquid layer was assumed to be laminar throughout its entire extent.

(See Figure 8 on following page)

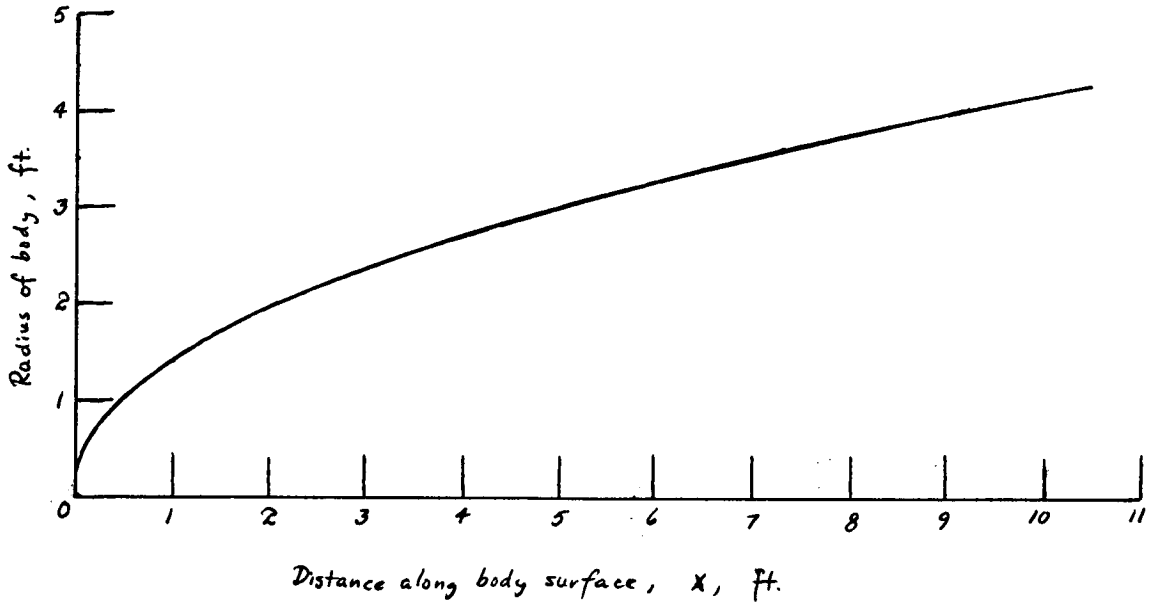

Shape of Ablating Body
Fig. 8.

Development of the normal interface (ablation) velocity, v_{∞}, along the body for no deceleration force is shown in Figure 9.

Fig. 9.

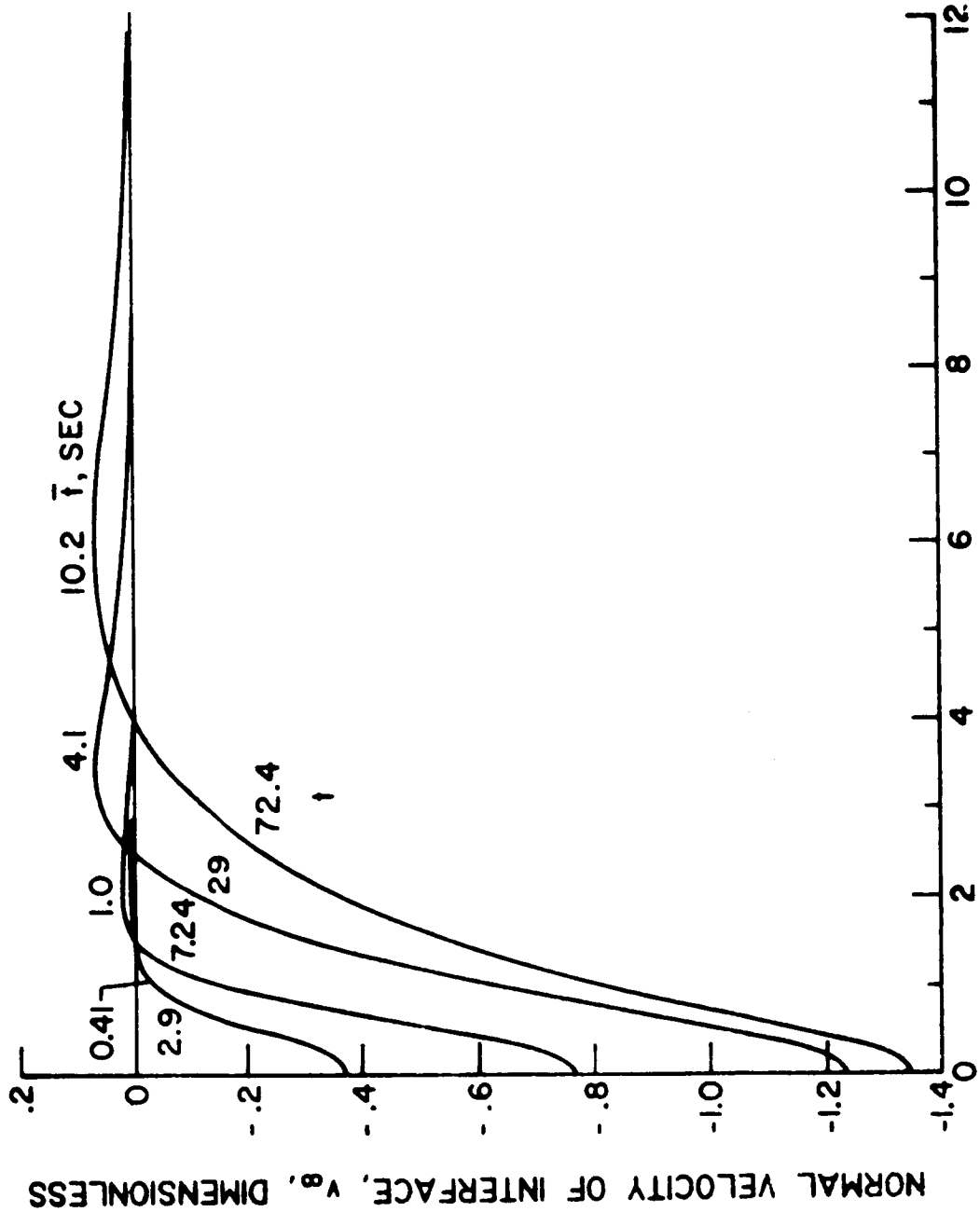

Fig. 9. - Interface normal velocity distribution. No deceleration.

Recall $v_\infty < 0$ indicates thinning of the molten layer. Thus, fluid leaves the stagnation region and tends to accumulate downstream, because the shear and pressure forces decrease away from the stagnation point. At some later time, as mentioned previously, the thicker layer results in a greater pressure force and liquid moves rearward in a wave pattern. Therefore, away from the stagnation point there exists an accumulation of molten material into a slight bump that is followed by ablation as the bump moves down stream as a kind of single wave. Note that no wave motion is predicted during the initial ablation period. The corresponding interface normal temperature gradient (heat flux) is shown in Figure 10. With increasing time the temperature gradient decreases

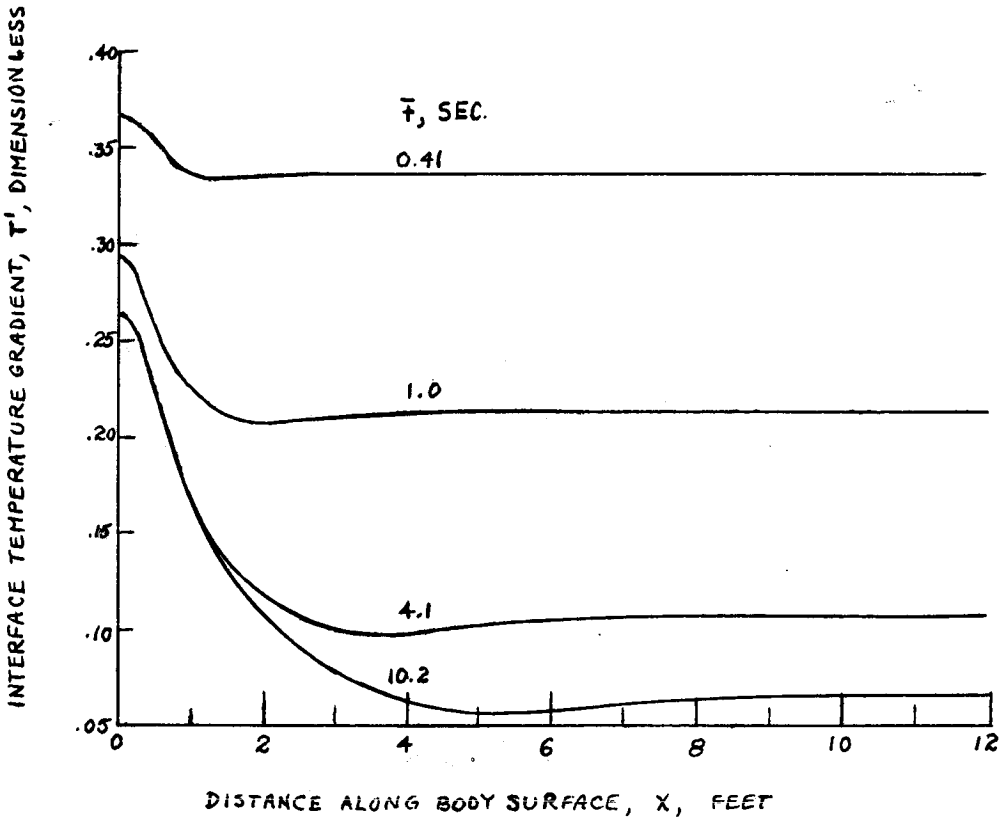

Fig. 10. Interface temperature gradient distribution. No deceleration.

from a relatively high uniform value, as might be expected from the initial sudden application of T = 1 and relatively small convection, to a lower steady-state value near the stagnation region. The temperature gradients for very short times cannot be accurate, because the gas boundary layer, as a result of thickening, will provide gradients which decrease as X increases, whereas the figure shows constant values. Steady-state conditions in the stagnation region are approximately attained at t = 29 (corresponding to 4.1 sec) at which time ablation is proceeding at the rate of $v_{\infty} \sim -1.25$ (corresponding to removal of material at the rate of 0.052 in./sec). At all times the most severe thermal load is imposed at the forward stagnation point. This is easily understood to occur because (1) the thickness of the gaseous boundary layer is a minimum near the stagnation point and (2) there is a large negative normal velocity, which results from the flowing away of material and which reduces the thickness of the thermal layer.

Details of the structure of the viscous layer for no deceleration are shown in Figure 11.

All temperature profiles are about the same for short time, but with increasing time the stagnation-point profile approaches a steady-state curve, whereas the others are all nearly the same as for unsteady heating of a slab. (After X = 0, the next profile is selected for such a value of X that $v_\infty = 0$; therefore u_i is nearly a maximum there.)

Deceleration of the body gives rise to changes in the behavior of the liquid layer as shown by comparison of figures 12 to 14 with previously mentioned results. The normal interface velocity at the stagnation point is reduced 6 percent for maximum deceleration. Farther back the calculations break down in a region where the normal interface velocity v_∞ exhibits large gradients. The inadequacy of the equations used herein to describe the condition in this region probably arises from the failure of the boundary-layer assumption (i.e. that $h/L \ll 1$) because of the accumulation of fluid and thickening of the liquid layer. The results of the present calculations show this region of large positive normal velocity v_∞, which results from the fluid arriving from the forward section by boundary-layer drag and from slumping forward of material from the back end because of deceleration; at this location the forces balance. The accumulation of liquid into a bump may be directly inferred from the normal interface velocity (v_∞) curves of Figures 12(a) and 12(b). Definite values of v_∞ and the growth of the bump size cannot be given because of the failure of the backwards and forwards solutions to coalesce, but order of magnitude

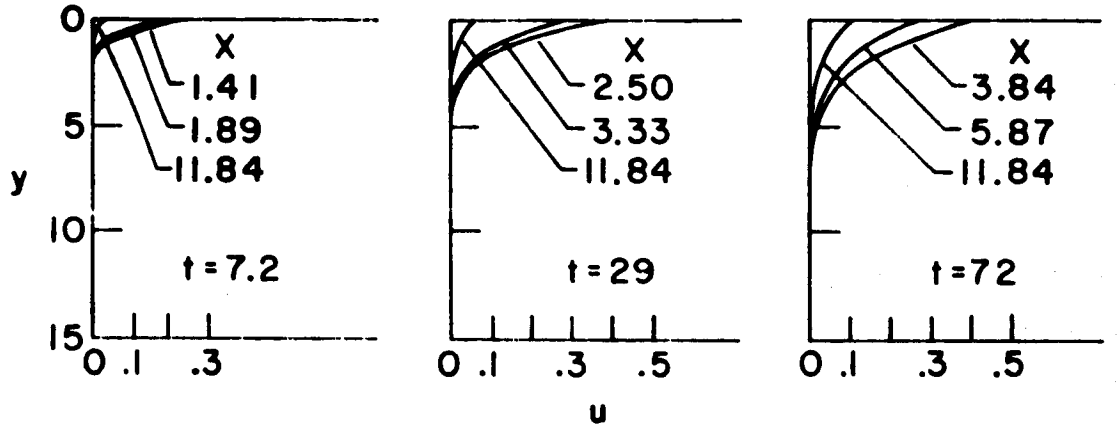

Fig. 11. - Flow velocity profiles. g = 0.

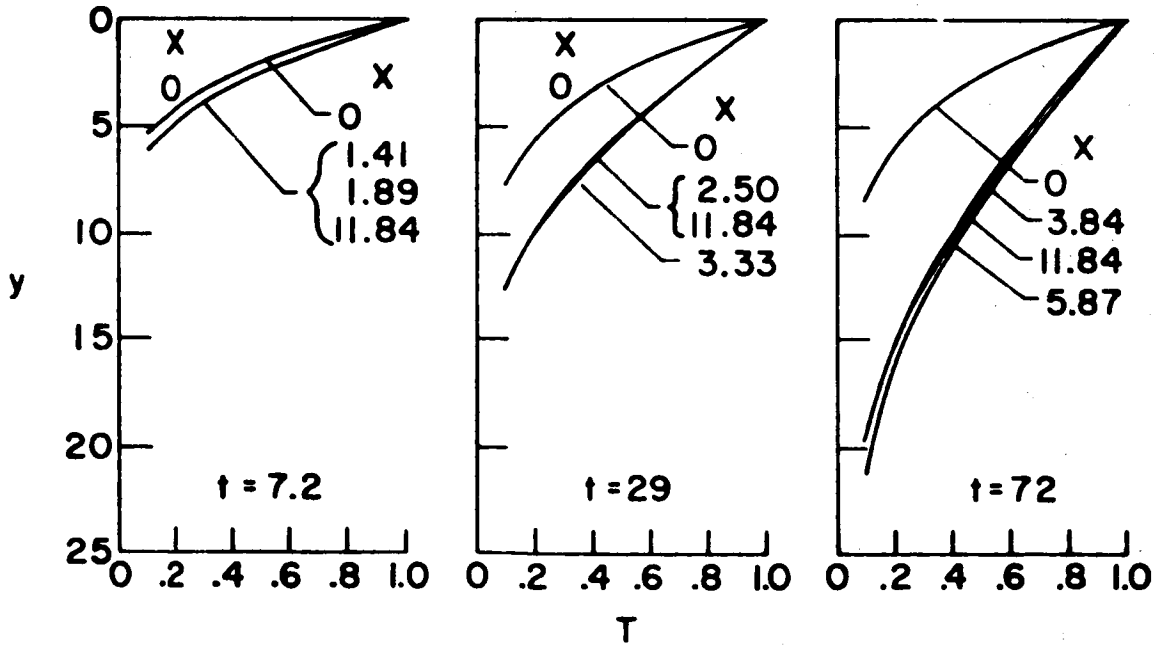

Fig. 11. - Temperature profiles. g = 0.

interpretation of the curves indicates the growth rate to be comparable with ablation rate at the stagnation region. Calculations could be made downstream of the critical region because of the small influence of the derivative and the resulting local character of the solution.

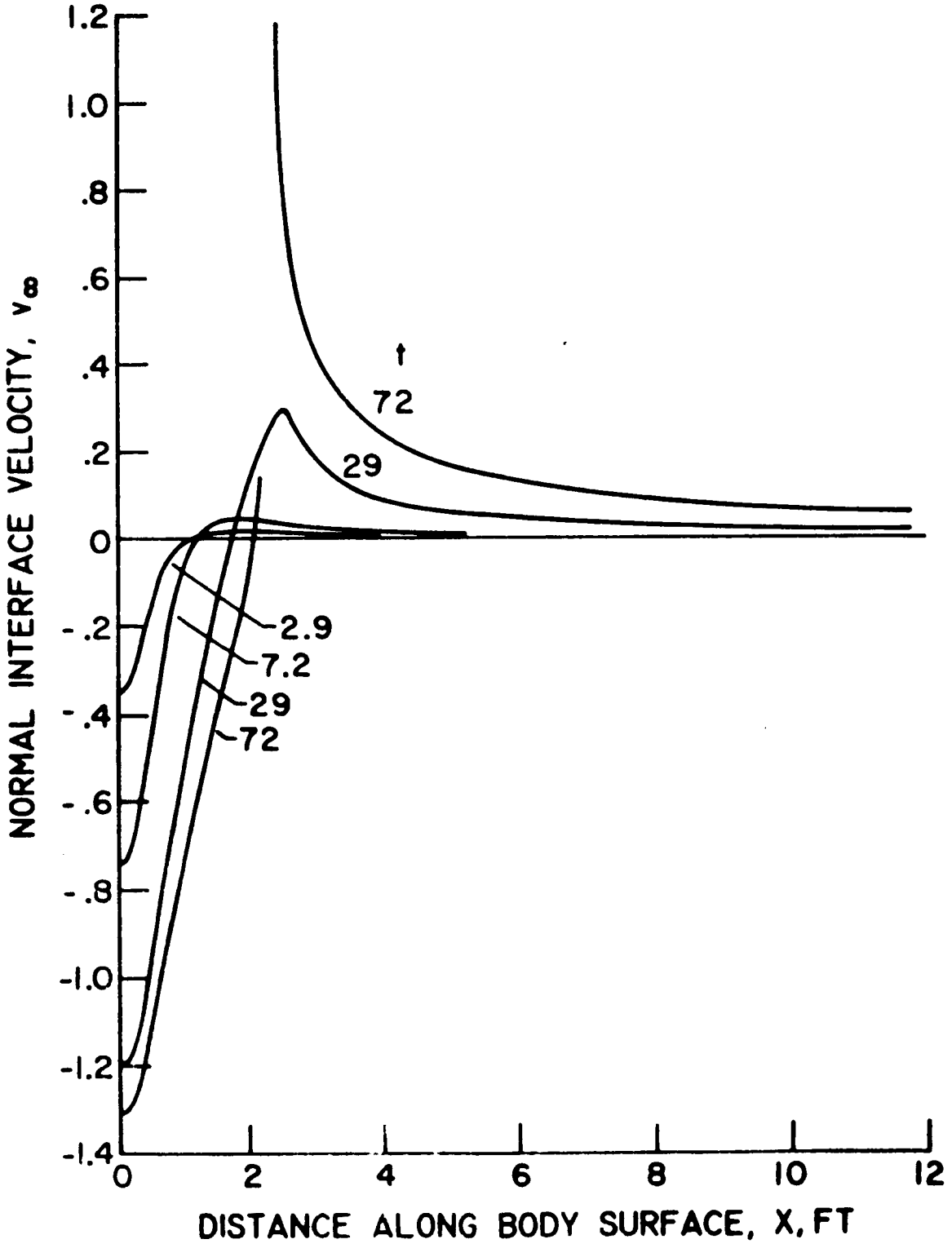

Fig. 12(a). - Interface normal velocity distribution. $\varepsilon = -0.2$.

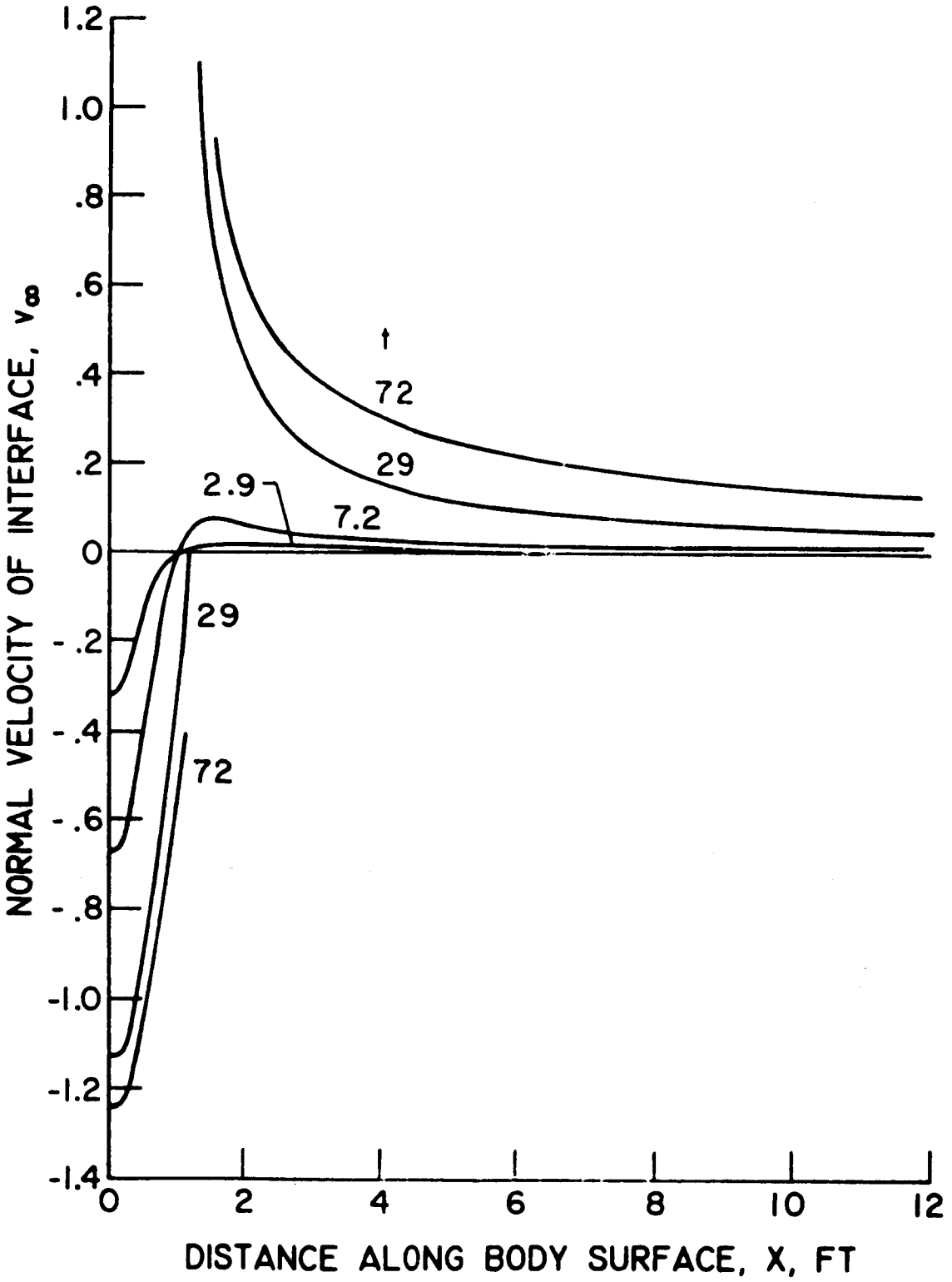

Fig 12(b). - Interface normal velocity distribution. g = -0.6.

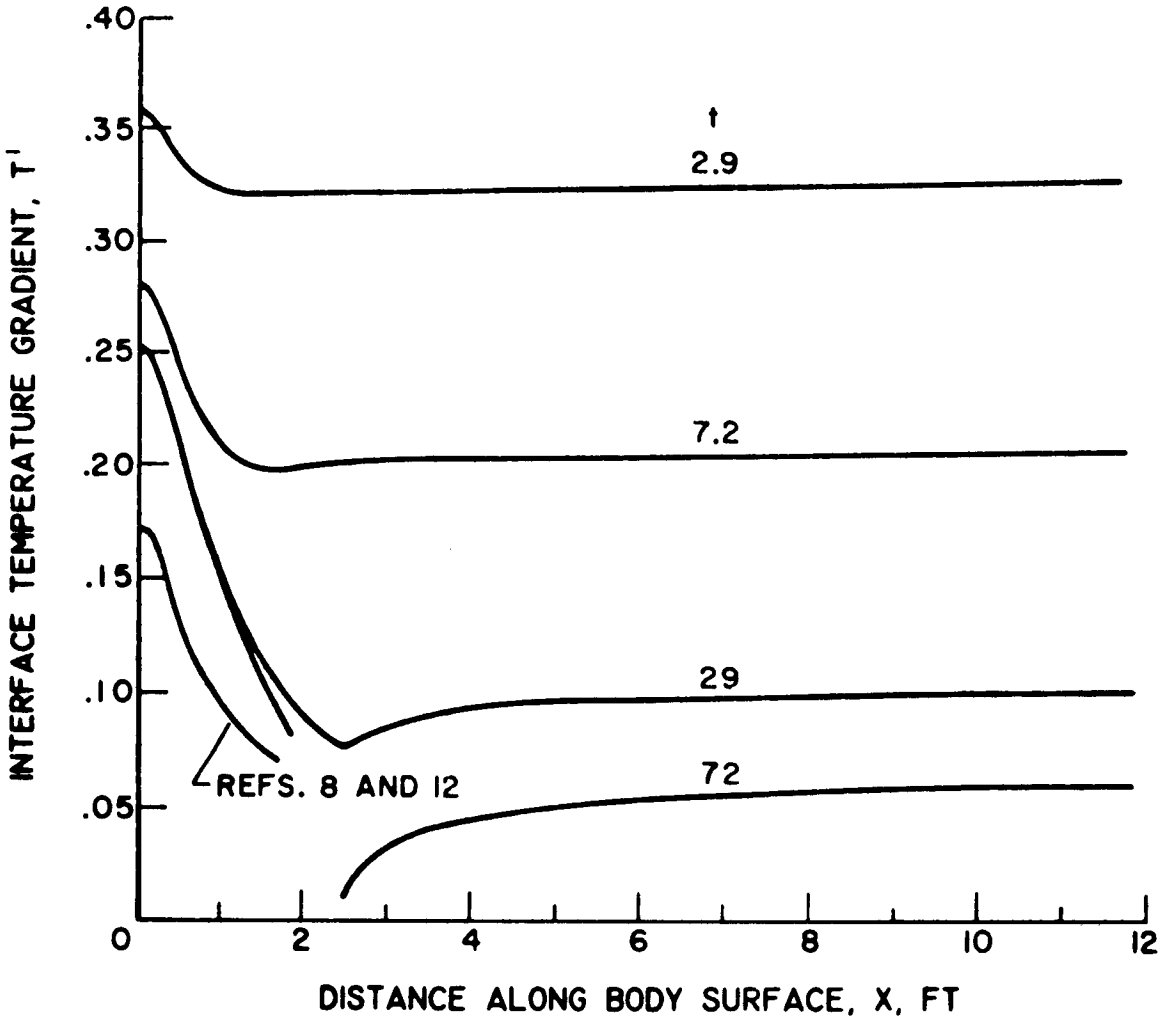

Fig. 13(a). - Interface temperature gradient distribution. g = -0.2.

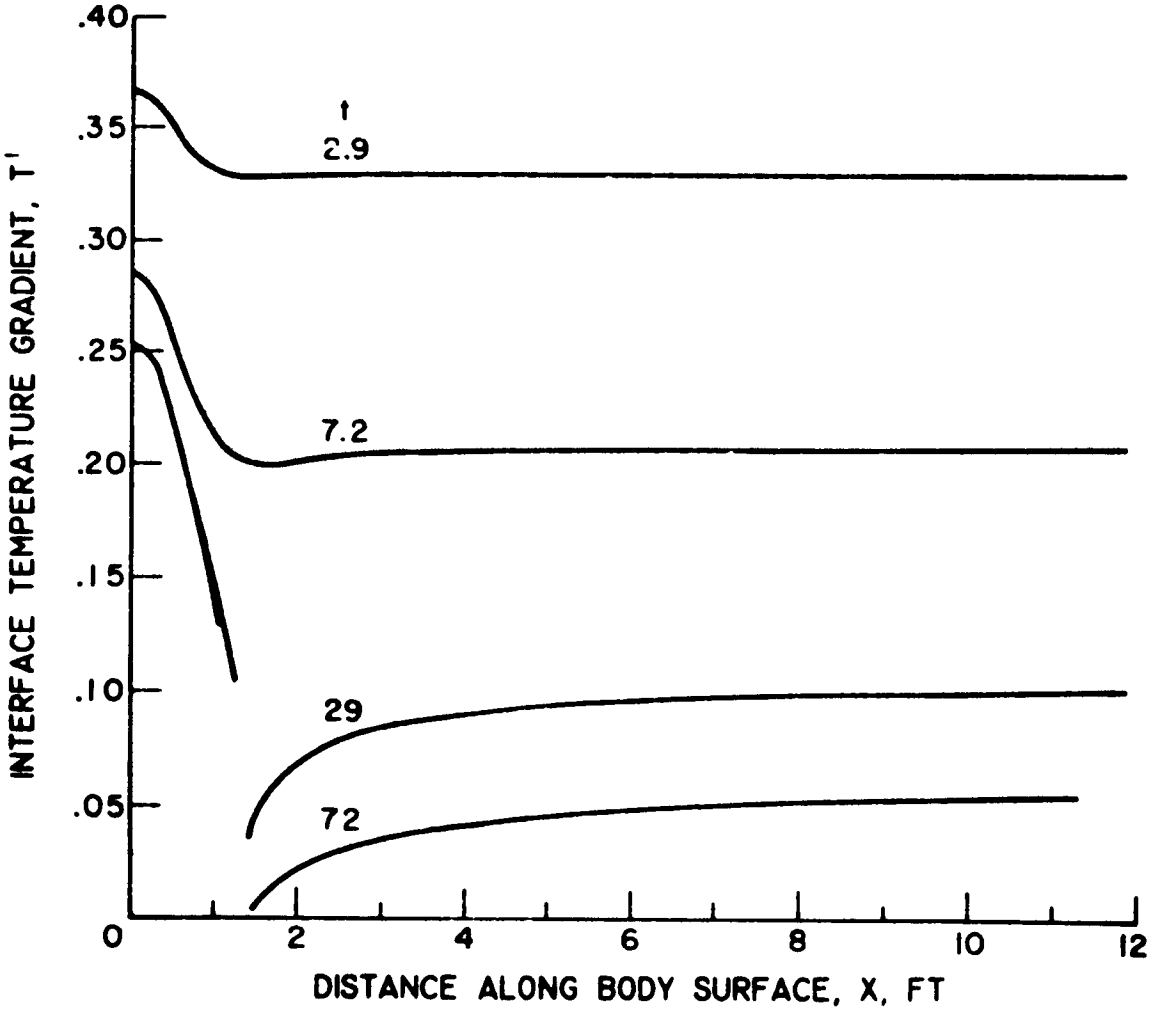

Fig. 13(b). - Interface temperature gradient distribution. $\gamma = -0.6$.

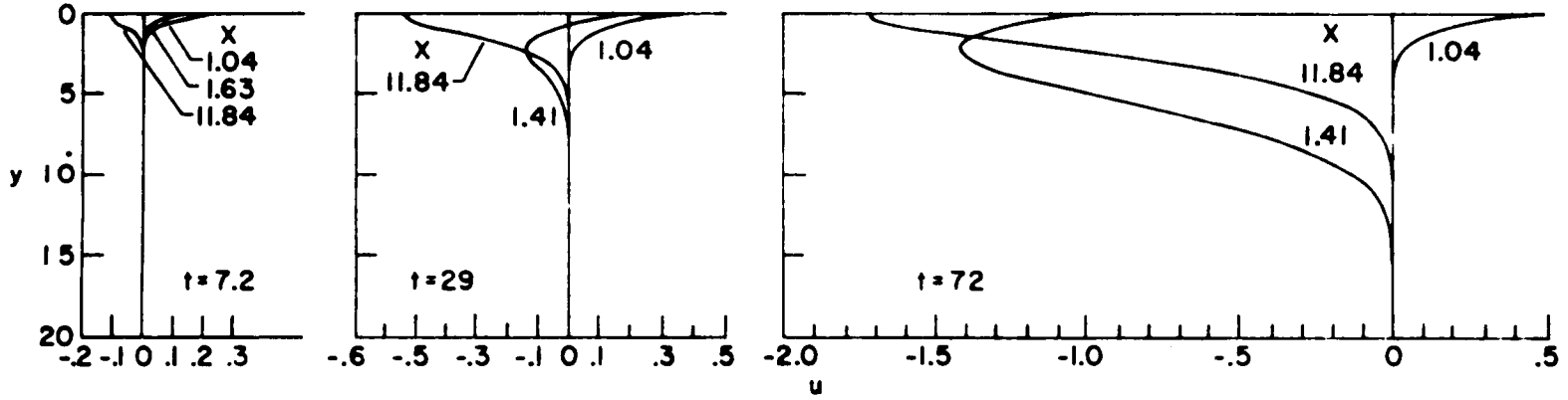

Fig. 14 . - Flow velocity profiles. g = -0.6.

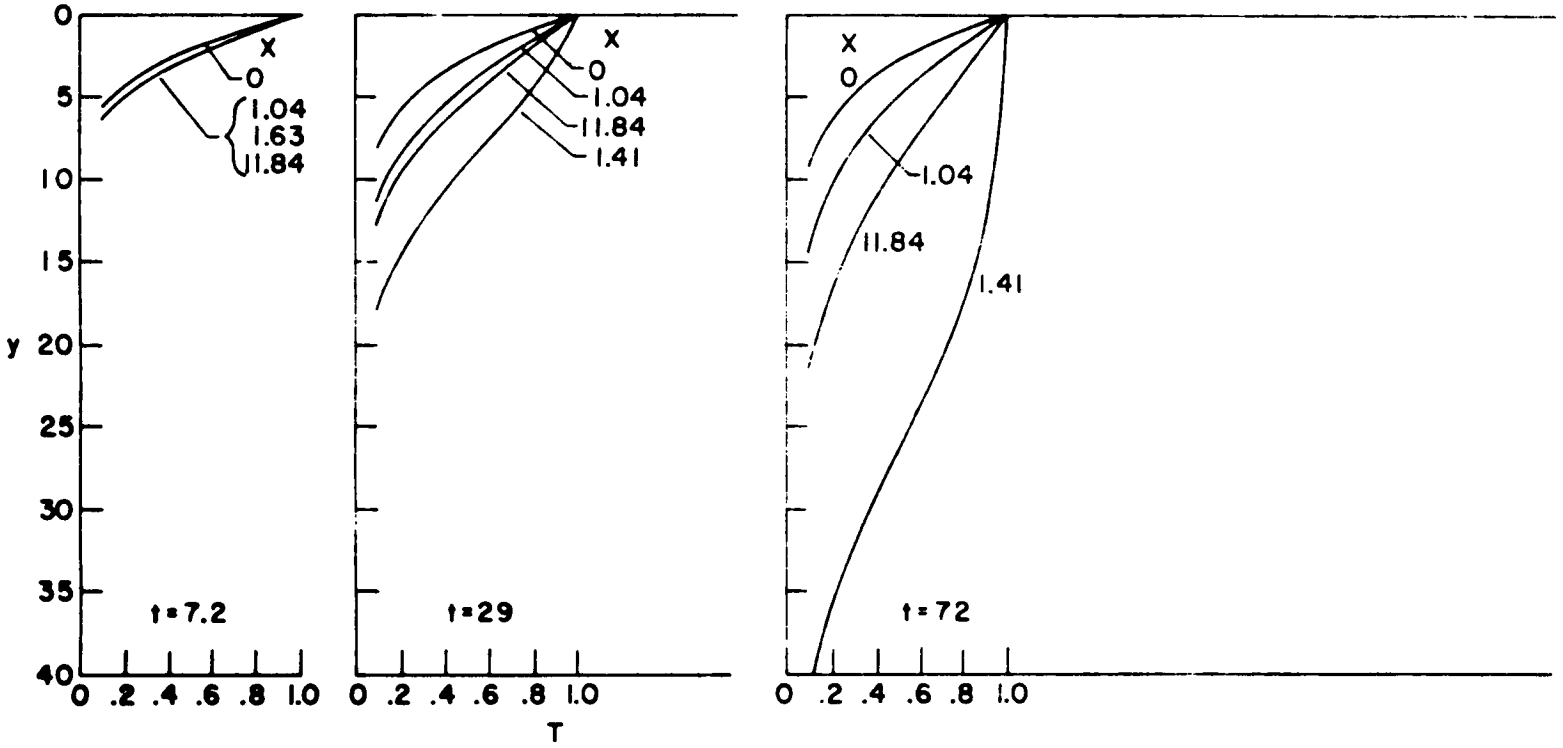

Fig. 14 . - Temperature profiles. g = -0.6.

The failure of the solutions obtained by forward and rearward integration to match in the region of liquid accumulation is not surprising. In general, two asymptotic solutions (here for small and large distances from the stagnation point) cannot be joined without careful analysis. Sometimes the matching is further complicated because of the occurence of a singularity in the intermediate region due to the omission of terms in the asymptotic equations which are significant there. To match the asymptotic solutions properly in such a region the analytic form of the solution there must be found. For the present problem there appears to be a distinct possibility of finding the solution of the Navier-Stokes equations in this accumulation region because the inertia terms should be negligible there. Further consideration is being given to this point.

The interface temperature gradient approaches very small values at the bump because of the accumulation of the hottest liquid there. The temperature gradient at the stagnation point is reduced only 3.5 percent for maximum deceleration under the conditions of the calculations.

Both the velocity and temperature profiles for high deceleration rates show clearly a dissimilarity of shape at various locations; there is even a case of flow reversal which results from the opposing effects of surface shear and body force. Such deceleration effects are qualitatively described by Cheng (1958).

A large accumulation of material in a bump will probably not be realized in a real situation because it would be torn off by the airstream if it grows sufficiently large.

The heat flow from the gas to the liquid was calculated at the stagnation point to be 53,200 Btu/(ft^2)(sec) by the method of Fay and Riddell (1958) and the results of Lees(1958) for q_i/q_o for a hemisphere were used to estimate the value elsewhere. If vaporization is neglected, the temperature gradient in the liquid at the interface is then 311,000° F/ft. On a dimensionless basis, the stagnation-point temperature gradient approaches the limit

$$T' = 311{,}000\,\delta_L/\bar{T}_i = 0.1755$$

This value and those at several other locations are shown in Figure 13. Thus, the heat load estimated from the liquid layer herein is too high. This error follows from having taken too high a value for the interface temperature.

The temperature gradient of the liquid at the interface will depend on the ablation rate v_∞, which, through the viscosity, will depend strongly on the temperature. Thus an assumption of a lower temperature will greatly reduce the interface temperature gradient and heat flow; closer agreement with other results (Bethe and Adams(1950))can then be expected.

For a very short time, the correction required is much greater; the corrected temperature will, therefore, rise from a low initial value to the final equilibrium value.

The general deductive-type analysis of Ostrach and his coworkers (1960) (1962) has thus led to the following results:

1. Flow, temperature, and heat transfer in the liquid layer depend on the deceleration parameter $g = A\rho_L/P_o$, the heat convection parameter $\beta = Pr\ Re\ \delta^2$, and the body shape in addition to those quantities already found for the steady-state condition at the stagnation point.

2. A steady-state solution is possible only in the forward part of the body where $v_\infty < 0$. On the aft part an unsteady solution is required.

3. Similarity solutions are not possible; the velocity and temperature profiles vary radically in shape from one portion of the body to another and at different instants of time.

4. The heaviest heat load and ablation rate occur at the stagnation point; deceleration affects these values slightly.

5. An accumulation of fluid occurs in the region where body, shear, and pressure forces are approximately balanced. This might cause a substantial change in the body shape for small bodies where the fluid will be blown off a shoulder rather than flow off the back end.

Thus limitations of the various studies are made clear and new physical phenomena are described by the general-type of analysis.

Numerous specific problems, in accordance with the inductive-viewpoint, were studied concurrently with the development of the general analysis described above. In particular, Fanucci and Lew (1959), Hidalgo (1959) and Tellep (1959) all were concerned with conditions away from the stagnation point. Fanucci and Lew used an integral approach and assumed steady flows. The form of their assumed velocity profiles precluded the occurrence of flow accumulation and back flow. Hidalgo also used an integral approach for steady flows and although he originally included a deceleration term in his equations gave it no further attention. Tellep also treated the problem as a steady one and chose a very special configuration so that similarity solutions could be obtained. Clearly none of the unusual features of the problem can be described by similar solutions. Recall how dissimilar the velocity and temperature profiles are from Ostrach's solutions. Thus, the significance of all this work, if any, is questionalbe in view of the assumption of steady flow and the special types of solutions that do not permit accumulation and backflow. Certainly, the relation of these special problems is unknown.

In a similar way Georgiev (1959) and Chen and Allen (1962) attempted to find the unsteady characteristics of ablation. Georgiev restricted his consideration to the stagnation region and concluded, in agreement with Ostrach and his coworkers, that the unsteady effects

there are not too important. Cheng and Allen introduced only the unsteadiness due to time-dependent gas flow velocities, but neglected unsteady thermal effects in their stagnation point analysis. This work is essentially a generalization of Sutton's analysis, but no justification is given for neglecting the unsteady thermal effects. Cheng and Allen find that acceleration and deceleration effects are very important.

The work of Ostrach and his coworkers has recently been extended by one of his students, D. McConnell, in a doctoral thesis. Since some of the simplifications of the former work are related to conditions at larger times, the initial period of melting is studied in more detail by applying the previously-mentioned perturbation method in the small parameter β that indicates relative convection and conduction effects. In order to match interface conditions more easily McConnell specifies the interface heat flux in terms of a gas heat-transfer coefficient rather than an interface temperature. Finally, McConnell considers a spherical body rather than an aerodynamic one as was the case in all previous work. Interest in the tektite problem motivated the study of this shape.

The governing equations and boundary-conditions for McConnell's analysis are the same as Ostrach's, i.e., Equations (4.5), (4.9), to (4.11), and (4.13) to (4.16). Equation (4.17), however, is now written as, neglecting vaporization,

$$k\left(\frac{\partial \bar{T}}{\partial Y}\right)_i = h(X)\ (T_{aw} - T_i) \qquad (4.17a)$$

where $h(X)$ is the heat-transfer coefficient (assumed known from the gas flow) and T_{aw} is the adiabatic wall temperature. The body is again assumed to semi-infinite, but the shear stress $\tau(X)$ and $h(X)$ appropriate for spheres are now used.

The fact that β is of the order of 0.1 for materials of interest suggests a perturbation expansion in powers of β for the solution of the problem. Since the limiting case of β equal to zero corresponds to pure heat conduction which is relatively easy to describe and which is the dominant state of affairs at the onset of the ablation process, such a solution should give the desired type of information for short times to supplement the essentially quasi-steady solutions of Ostrach and his coworkers. Accordingly the expansions

$$T = \Sigma \beta^n T_n,\quad u = \Sigma \beta^n u_n,\quad v = \beta^n v_n \text{ and } \mu = \Sigma \beta^n \mu_n$$

are substituted into the governing equations and the power-law viscosity-temperature relation to give

$$\beta_n \left[\frac{\partial}{\partial x}(r\, u_n) + \frac{\partial}{\partial y}(r\, v_n)\right] = 0$$

$$\left[\frac{\partial}{\partial y}\left(\mu_o \frac{\partial u_o}{\partial y}\right) - f(x)\right] + \beta\left[\frac{\partial}{\partial y}\left(\mu_1 \frac{\partial u_o}{\partial y} + \mu_o \frac{\partial u_1}{\partial y}\right)\right] +$$

$$\beta^2\left[\frac{\partial}{\partial y}\left(\mu_o \frac{\partial u_2}{\partial y} + \mu_1 \frac{\partial u_1}{\partial y} + \mu_2 \frac{\partial u_o}{\partial y}\right)\right] + \ldots = 0$$

$$\left(\frac{\partial T_o}{\partial t} - \frac{\partial^2 T_o}{\partial y^2}\right) + \beta\left(\frac{\partial T_1}{\partial t} + u_o \frac{\partial T_o}{\partial x} + v_o \frac{\partial T_o}{\partial y} - \frac{\partial^2 T_1}{\partial y^2}\right) +$$

$$\beta^2\left(\frac{\partial^2 T_2}{\partial t} + u_1 \frac{\partial T_o}{\partial x} + u_o \frac{\partial T_1}{\partial x} + v_o \frac{\partial T_1}{\partial y} + v_1 \frac{\partial T_o}{\partial y} - \frac{\partial^2 T_2}{\partial y^2}\right) + \ldots = 0$$

$$\left(\mu_o - T_o^{-n} + \beta\left[\mu_1 + nT_o^{-(n+1)}T_1\right] + \beta^2\left[\mu_2 + nT_2T_o^{-(n+1)} - \frac{n(n+1)}{2!} T_1^2 T_o^{-(n+2)}\right] + \ldots = 0\right.$$

The boundary-conditions are satisfied by the zeroth-order solutions and homogeneous conditions are imposed on the higher-order ones.

Thus the zeroth-order (in B) problem is

$$\frac{\partial (ru_o)}{\partial x} + \frac{\partial (rv_o)}{\partial y} = 0$$

$$\frac{\partial}{\partial y}\left(\mu \frac{\partial u}{\partial y}\right) = f(x)$$

$$\frac{\partial T_o}{\partial t} = \frac{\partial^2 T_o}{\partial y^2}$$

$$\mu_o = T_o^{-n}$$

with

$$v = 0, \mu \frac{\partial u}{\partial y} = \tau_i(x), \frac{\partial T}{\partial y} = h\left[1 - T_i\right] \quad T_g = T_i \quad \text{at } y = 0$$

$$T = u = 0 \qquad \text{at } y \to \infty$$

$$u = v = T = 0 \qquad \text{at } t = 0$$

The zeroth-order temperature is immediately written as

$$T_o = \operatorname{erfc}\,(y/2\sqrt{t}) - \exp(hy + h^2t)\,\operatorname{erfc}\,(y/2\sqrt{t} + h^2t)$$

From this, the viscosity relation, and the conditions on u_o, the equation for u_o can be solved to give

$$u_o = f(x)\int_{\infty}^{y} m\left[\operatorname{erfc}(m/2\sqrt{t}) - \exp(hm+h^2t)\,\operatorname{erfc}(m/2\sqrt{t} + h\sqrt{t})\right]^{h}_{dm} +$$

$$\tau_i(x)\int_{\infty}^{y}\left[\operatorname{erfc}(m/2\sqrt{t}) - \exp(hm+h^2t)\,\operatorname{erfc}(m/2\sqrt{t}+h\sqrt{t})\right]^{h}_{dm}$$

For convenience let $\zeta \equiv m/2\sqrt{t}$ and $\theta \equiv h\sqrt{t}$ then

$$u_o = 4ft\int_{\infty}^{y/2\sqrt{t}} \zeta\, F^n\, d\zeta + 2\tau_i\sqrt{t}\int_{\infty}^{y/2\sqrt{t}} F^n\, d\zeta$$

where

$$F(\zeta,\theta) = \operatorname{erfc}\zeta - \exp(2\zeta\theta + \theta^2)\,\operatorname{erfc}\,(\zeta+\theta)$$

From the continuity equation there is then obtained

$$v_o = -8\frac{(rt)'}{r}\,t^{3/2}\int_{o}^{y/2\sqrt{t}}\int_{\infty}^{\xi}\zeta F^n\, d\zeta\, d\xi - \frac{4(r\tau_i)'}{r}\,t\int_{o}^{\frac{1}{2}\sqrt{t}}\int_{\infty}^{\xi} F^n\, d\zeta\, d\xi - 8ft^{3/2}$$

$$\int_{o}^{\frac{1}{2}\sqrt{t}}\int_{\infty}^{\xi}\zeta\left(\frac{\partial F^n}{\partial x}\right) d\zeta\, d\xi - 4\tau_i t\int_{o}^{\frac{1}{2}\sqrt{t}}\int_{\infty}^{\xi}\frac{\partial F^n}{\partial x}\, d\zeta\, d\xi$$

But

$$\frac{\partial F}{\partial x} = \frac{\partial F}{\partial\theta}\frac{\partial\theta}{\partial x} = -\left[2(\zeta+\theta)\exp(2\zeta\theta+\theta^2)\,\operatorname{erfc}(\zeta+\theta) - (2/\sqrt{\pi})\right.$$

$$\left.\cdot\exp(-\zeta^2)\right]\frac{\partial\theta}{\partial x} \approx -(2/\sqrt{\pi})\exp(-\zeta^2)\left\{2(\zeta+\theta)\right.$$

$$\left.\cdot\left[\frac{1}{2(\zeta+\theta)} - \frac{1}{4(\zeta+\theta)^3} + \ldots\right] - 1\right\}\frac{\partial\theta}{\partial x}$$

so that

$$\frac{\partial F}{\partial x} \approx \frac{\exp(-\zeta^2)}{\sqrt{\pi}(\zeta+\theta)^2}\left(\frac{\partial \theta}{\partial x}\right)$$

Also

$$\frac{\partial F}{\partial \zeta} = -2\theta \exp(2\zeta\theta + \theta^2)\operatorname{erfc}(\zeta+\theta) \approx \frac{4\theta}{\sqrt{\pi}} e^{-\zeta^2}\left[\frac{1}{2(\zeta+\theta)} - \frac{1}{4(\zeta+\theta)^3} + \cdots\right]$$

so that

$$\frac{\partial F}{\partial \zeta} \approx -\frac{2}{\sqrt{\pi}}\left(\frac{\theta}{\theta+\zeta}\right)\exp(-\zeta^2) \approx -\frac{2}{\sqrt{\pi}}\exp(-\zeta^2)$$

on the basis that $\zeta \ll \theta$ or $y/2h \ll t$. For a particular y this places a lower bound on t for which the expansions are valid. Combination of the two derivatives of F yields

$$\frac{\partial F}{\partial x} = -\frac{1}{2\theta^2}\frac{\partial F}{\partial \zeta}\frac{\partial \theta}{\partial x} = -\frac{1}{2}\frac{h^1}{h^2\sqrt{t}}\frac{\partial F}{\partial h}$$

so that v_o can be written as

$$v_o = -8\frac{(rf)^1}{r}t^{3/2}\int_0^{y/2\sqrt{t}}\int_\infty^\xi \zeta F^n \, d\zeta \, d\xi - \frac{4(r\tau_1)^1}{r}t \int_0^{y/2\sqrt{t}}\int_\infty^\xi F^n \, d\zeta \, d\xi + \frac{4fh't}{h^2}\int_0^{\frac{1}{2}\sqrt{t}}\int_\infty^\xi \zeta\left(\frac{\partial F^n}{\partial h}\right) d\zeta \, d\xi + \frac{2\tau_1 h'\sqrt{t}}{h^2}\int_0^{\frac{1}{2}\sqrt{t}} \frac{\partial F^n}{\partial \zeta} \, d\zeta \, d\xi$$

Now

$$\int_0^{\eta}\int_{\infty}^{\xi}\zeta\left(\frac{\partial F^n}{\partial\eta}\right)d\zeta\ d\xi=\int_0^{\eta}\left[\xi F^n(\xi,\theta)-\int_{\infty}^{\xi}F^n(\zeta,\theta)\,d\zeta\right]d\xi=$$
$$\int_{\infty}^{\eta}\xi F^n(\xi,\theta)d\xi-\int_{\infty}^{0}\xi F^n(\xi,\theta)\,d\xi-\int_0^{\eta}\int_{\infty}^{\xi}F^n(\zeta,\theta)\,d\zeta\,d\xi$$

and

$$\int_0^{\eta}\int_{\infty}^{\xi}\left(\frac{\partial F^n}{\partial\xi}\right)d\zeta\,d\xi=\int_0^{\eta}F^n(\xi)\,d\xi=\int_{\infty}^{\eta}F^n(\xi,\theta)\,d\xi-\int_{\infty}^{0}$$
$$\cdot F^n(\xi,\theta)\,d\xi$$

All the integrals have either of two forms, so define

$$k_1(\xi,\theta)=\int_{\infty}^{\xi}F^n(\zeta,\theta)\,d\zeta \qquad k_2(\xi,\theta)=\int_{\infty}^{\xi}\zeta F^n(\zeta,\theta)\,dd\zeta$$
$$k_3(\xi,\theta)=\int_0^{\xi}k_1(\zeta,\theta)\,d\zeta \qquad k_4(\xi,\theta)=\int_0^{\xi}k_2(\zeta,\theta)\,d\zeta$$

and the zeroth-order solutions can be summarized as

$$T_o=\operatorname{erfc}(y/2\sqrt{t})-\exp(\eta y+\eta^2 t)\operatorname{erfc}(y/2\sqrt{t}+\eta\sqrt{t})$$

$$u_o=4ft\,k_2(y/2\sqrt{t},\eta\sqrt{t})+2\tau_1\sqrt{t}\,k_1(y/2\sqrt{t},\eta\sqrt{t})$$

$$v_o=-8\frac{(rf)'}{r}t^{3/2}k_4(y/2\sqrt{t},\eta\sqrt{t}-4\frac{(r\tau_1)'}{r}t\,k_3(y/2\sqrt{t},\eta\sqrt{t})$$
$$+\frac{4f\eta' t}{\eta^2}\left[k_2(y/2\sqrt{t},\eta\sqrt{t})-k_2(0,\eta\sqrt{t})-k_3(y/2\sqrt{t},\eta\sqrt{t})\right]$$
$$+\frac{2\tau_1\eta'\sqrt{t}}{\eta^2}\left[k_1(y/2\sqrt{t},\eta\sqrt{t})-k_1(0,\eta\sqrt{t})\right]$$

where primes denote differentiation with respect to x.

The first-order correction functions are found from

$$\frac{\partial (ru_1)}{\partial x} + \frac{\partial (rv_1)}{\partial y} = 0$$

$$\mu_1 \frac{\partial u_o}{\partial y} + \mu_o \frac{\partial u_1}{\partial y} = 0$$

$$\frac{\partial T_1}{\partial t} = \frac{\partial^2 T_1}{\partial y^2} - \left(u_o \frac{\partial T_o}{\partial x} + v_o \frac{\partial T_o}{\partial y}\right)$$

$$\mu_1 + n\, T_1 T_o^{-(n+1)} = 0$$

with the initial and boundary conditions

$v_1 = o$, $\partial T_1/\partial y = 0$ at $y = 0$; $T_1 = 0$, $u_1 = 0$ at $y = \infty$;

$T_1 = u_1 = v_1 = 0$ at $t = 0$.

The nonhomogeneous term in the energy equation is a product of the $\exp(-y^2/4t)$ and terms involving the integrals. The exponential behavior in y dominates the integral variations so the latter are replaced by their limiting values. Then the Fourier Cosine transform can be used to solve for T_1. The other functions follow from the remaining equations so that

$$T_1 = -(1/\sqrt{\pi}) \left[G(x,t) \right] \exp(-y^2/4t)$$

$$u_1 = G\left\{ 2ft \left[(y/2\sqrt{t})\, F^n(\zeta, \theta) - k_1(\zeta,\theta) \right] + \tau_i \sqrt{t}\, F^n(\zeta,\theta) \right\}$$

$$v_1 = -\left\{ \frac{4(rfG)' t^{3/2}}{r} \left[k_2(\zeta,\theta) - k_2(0,\theta) - k_3(\zeta,\theta) \right] + \frac{2(r\tau_i G)' t}{r} \left[k_1(\zeta,\theta) - k_1(0,\theta) \right] - \frac{2fGh' t}{h^2} \right.$$

$$\cdot \left[\zeta F^n - 2(k_1(\zeta,\theta) - k_1(0,\theta)) \right] - \frac{\tau_i G \eta' \sqrt{t}}{\eta^2} \left[F^n(\zeta,\theta) - F^n(0,\theta) \right] \Bigg\}$$

where

$$G(x,t) \equiv \frac{2}{5} \left[8 \frac{(rf)'}{r} k_4(\infty,\theta) \right] t^2 + 2 \left[\frac{(r\tau_i)'}{r} k_3(\infty,\theta) + \frac{f\eta'}{\eta^2} (k_2/0,\theta) + k_3(\infty,\theta) \right] t^{3/2} + \frac{4}{3} \left[\frac{\tau_i \eta' k_1(0,\theta)}{\eta^2} \right] t$$

The second-order correction for the stagnation region was also found but the details will be omitted here.

The perturbation analysis, just presented, describes conditions from the initial state onward. The analysis of Ostrach et al. essentially moves backward in time from an anticipated steady-state condition. It is, therefore, desirable to compare the results of the two schemes. Thus a quasi-steady analysis similar to Ostrach's will now be made with the exception that the interface heat flux will be specified. In this way a relation between the heat flux and interface temperature is immediately obtained (Equation (4.17a)) and the interface matching is simplified thereby and, furthermore, the interface temperature can be variable which is more realistic. The argument for simplifying the convection terms has to be modified from that given by Ostrach and his coworkers, but it can still be justified. Thus the problem is defined by

$$\frac{\partial T}{\partial t} + \beta v_\infty \frac{\partial T}{\partial y} = \frac{\partial^2 T}{\partial y^2}$$

$$v_\infty = -\frac{1}{r} \frac{\partial}{\partial x} \int_0^\infty \int_\infty^\omega \frac{(f_m + \tau_i)}{\mu(m,t)} \, dm \, d\omega$$

$$\mu(m,t) = \left[T(m,t) \right]^{-n}$$

with

$$\frac{\partial T}{\partial y} + h(T_{aw} - T_i) = 0 \qquad \text{for } y = 0 \qquad t > 0$$

$$T(y,0) = 0$$

A closed-form solution can be obtained by Laplace transforms with $2\alpha(x) = \beta v_\infty$, viz.,

$$T = \frac{1}{2} \left\{ \operatorname{erfc} \frac{y - 2\alpha t}{2\sqrt{t}} + \frac{h}{h + 2\alpha} \exp(2\alpha y) \operatorname{erfc} \frac{y + 2\alpha t}{2\sqrt{t}} \right.$$
$$\left. - \frac{2(h - \alpha)}{(h - 2\alpha)} \exp\left[h(y - 2\alpha t) + h^2 t \right] \operatorname{erfc} \left(\frac{y - 2\alpha t}{2\sqrt{t}} + h\sqrt{t} \right) \right\}$$

This solution is valid for all times for both positive and negative values of α (i.e., v_∞). Furthermore if $\alpha = 0$ the conduction solution is obtained. If $\alpha < 0$ the asymptotic temperature has the form

$$T_{asym} \approx \frac{h}{h - 2\alpha} \exp(2\alpha y)$$

This corresponds to the exponential temperature variation often assumed and it indicates an interface temperature. If this interface expression is substituted into the equation for v_∞ there results

$$(2\alpha)_{asym} = \beta\left(\frac{h}{h+2}\right)^n \left[\frac{(rf)'}{r}\frac{2}{(2\alpha n)^3} + \frac{(r\tau_1)'}{r}\frac{1}{(2\alpha n)^2}\right]$$

This then is the time-independent value of v_∞ that could go together with the boundary functions $h(x)$, $f(x)$, and $\tau_1(x)$ to form a steady system.

McConnell carried out calculations for the same specific case treated by Ostrach and his coworkers so that the results of the two studies can be compared. On Figure 15 is shown the stagnation-point interface temperature computed by both McConnell's perturbation and quasi-steady solutions; the interface temperature assumed by Ostrach and his coworkers is also shown therein.

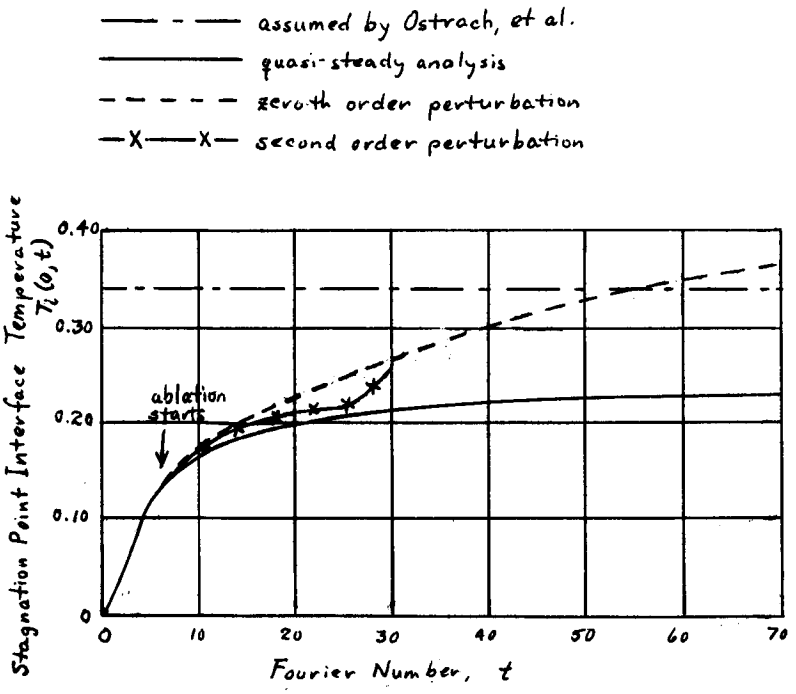

Fig. 15.

Comparison of Stagnation Point Gas-Liquid Interface Temperature

The latter is higher than either of McConnell's results but this is because Ostrach did not match the heat flux at the interface to obtain the lower value. Note also that the quasi-steady solution predicts a lower interface temperature than the perturbation solution. The reason for this can be more clearly seen after consideration of Figure 16 which presents a comparison of the stagnation-point ablation velocities predicted by all the analyses.

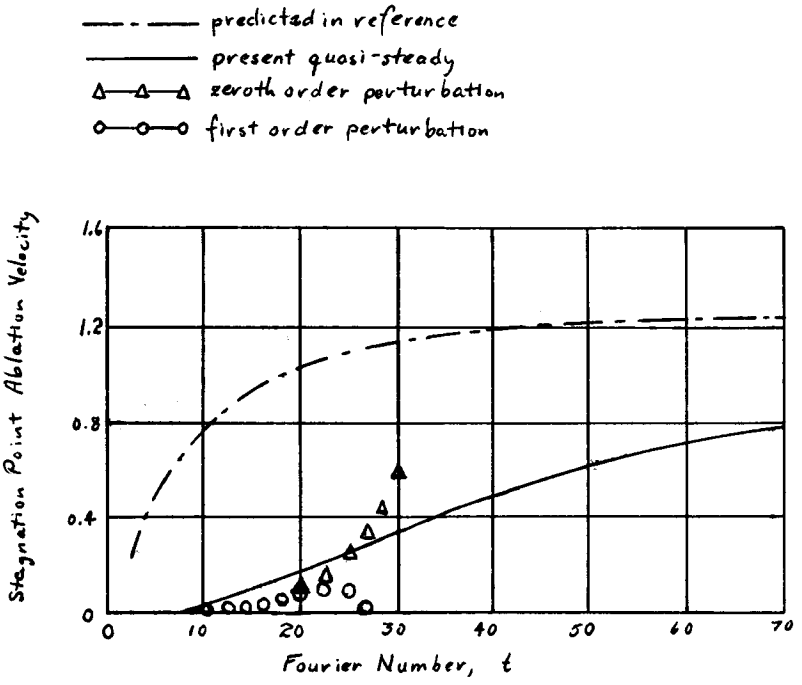

Comparison of Stagnation Point Ablation Velocity

Fig. 16.

As expected, the values predicted by Ostrach et al. (1962) are larger than any of McConnell's values. Ostrach's values follow, of course, from his higher interface temperature. The quasi-steady analysis predicts a larger

value than the perturbation analysis. This can be explained by consideration of the asymptotic interface temperature relation $T_i = h/(h-2\alpha)$, where recall $2\alpha < 0$. If the asymptotic value of the interface temperature is specified then both T_i and h will be overestimated for small times; this leads to an overestimate for $|2\alpha|$ for small times. The same applies to Ostrach's results. In the present analysis h is specified and an overestimate of $|2\alpha|$ leads to an underestimate of T_i. The quasi-steady analysis overestimates $|2\alpha|$ because it overestimates the small time effect of $|2\alpha|$ on the temperature distribution. The perturbation solution shows that for small time the temperature is essentially that due to conduction; whereas the quasi-steady solution immediately takes account of any motion that exists. Figure 16 shows, in addition, that the zeroth and first order velocities tend to diverge at about $t = 22.0$ so that the perturbation analysis can be considered to be valid until that time. Figure 15 shows that at $t = 22$ the interface temperature appears to be leveling off at about the asymptotic value predicted by the quasi-steady analysis. Thus it can be concluded that the quasi-steady analysis reasonably describes the long-time behavior of the ablation process.

The ablation velocities around a spherical body are shown on Figure 17. These calculations were stopped at the point of separation of the gas boundary layer as predicted by Meksyn (1948). For these particular calculations, the gas boundary-layer shear and pressure gradient were calculated from Meksyn. It is seen that even for early times, the rate of change with respect

to tangential distance, $\partial v_\infty / \partial x$, is of unit order of magnitude. This is in accord with Ostrach's results (Figs. 3, 5 and 6 (1962)) and contradicts those of Adams (1961) who stated that $\partial v_\infty / \partial x \approx 0$. It can further be seen that a 250 percent change in g(g = -0.51 to g = -1.30) results in only a 20 percent change in stagnation point ablation velocity.

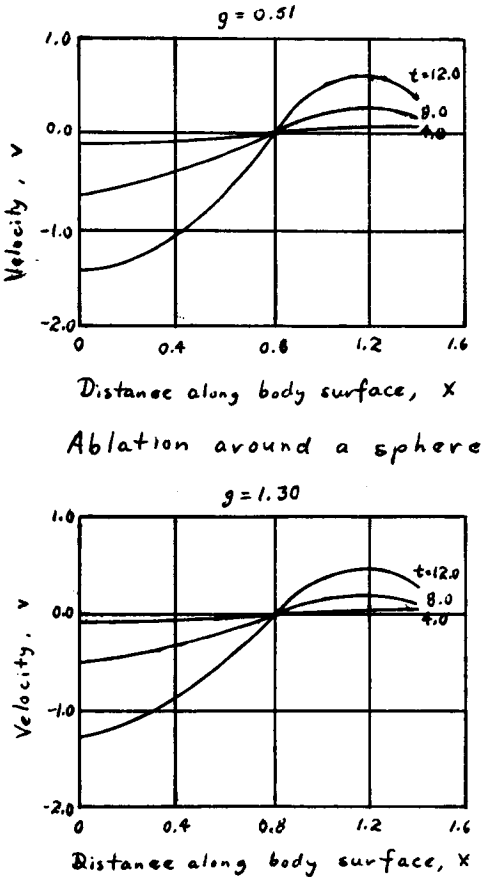

Fig. 17.

Ostrach also showed that stagnation conditions are not strongly affected by deceleration effects. Note also that no wave motion is indicated by the early time solutions

and this too is in accord with Ostrach's results. Finally, the initial increase in stagnation-point radius of curvature is indicated here as predicted by Chapman.

A concurrent experimental study was made by McConnell in a vertical wind-tunnel with heated gas flow upward and spherical tar-balls used as the test models. In this way the gravitational force simulated deceleration forces and by varying the gas flow rate the parameter g can be made to take on a range of values. Photographs of the melting process were taken and the temperature at the bottom of the tar layer (which covered a wooden sphere) was measured. Recession of the stagnation point was measured from the photographs.

The photographs show the significance of the parameter g; for larger g the melt accumulation is closer to the stagnation region and the surface waves can be seen.

The ablation velocity was determined from the measurements and the results were compared on Figures 18 and 19 with the theory. Figure 18 shows results for $\frac{1}{4}$" layer of tar; good agreement with perturbation solutions to $t \approx 7$. For a long time it was not close enough to quasi-steady because the layer was all melted. There, the tests were repeated with $\frac{1}{2}$" layer of tar. Now we can see that for $t > 28$ agreement with the quasi-steady solution is good. Similar temperature comparisons were made.

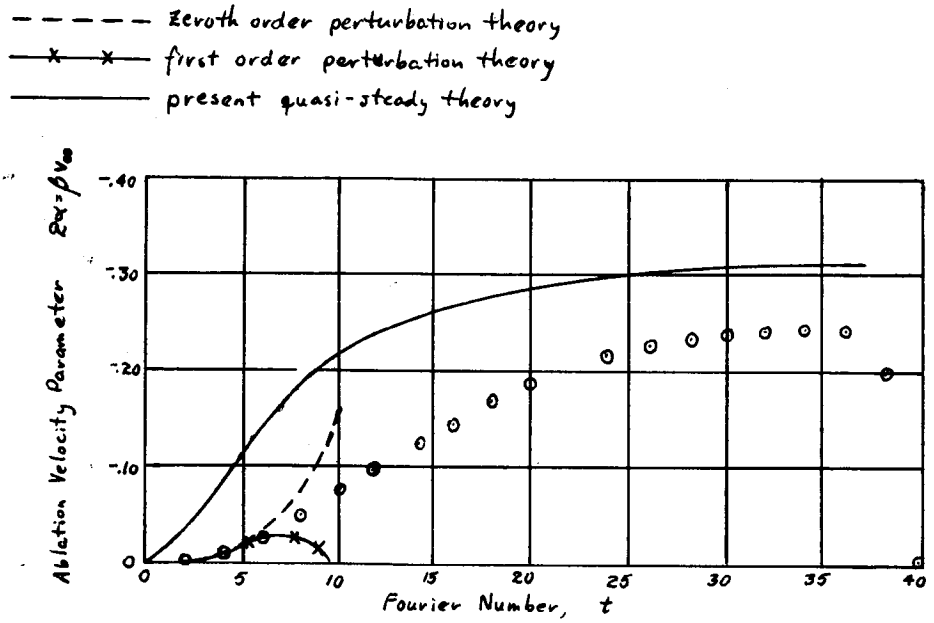

T_{in} = 46°F β = 0.157 = 9.5 sec. g = -0.51 $F = 4.87 \times 10^{-5}$ fps

Fig. 18.

Measured and Predicted Ablation Velocity Parameter

$2\alpha = \beta V_\infty$

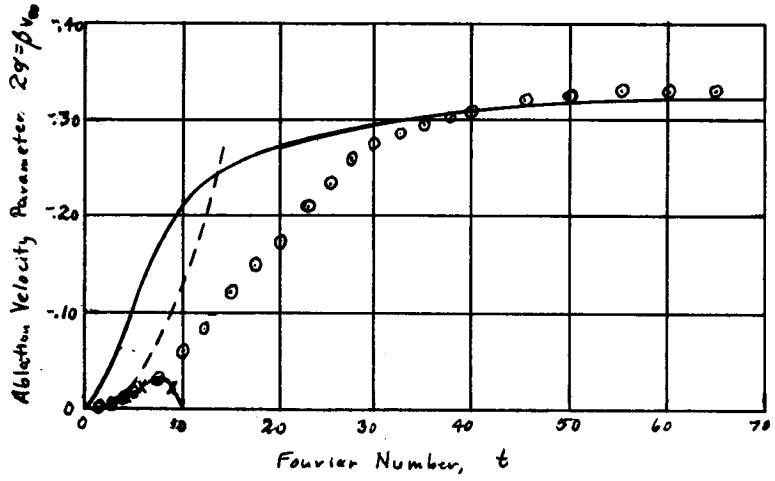

T_{in} = 62°F β = 0.216 = 6.1 sec. $F = 8.39 \times 10^{-5}$ fps h = 0.754

Fig. 19.

Adams, E.W.: Proc. 1961 H.T. and F.M. Inst.

Adams, M.C. (1959): Recent Advances in Ablation, ARS Jour., vol. 29, No. 9, 625-632.

Baker, G. (1959): Tektites, Memoirs of the Natl'l Museum of Victoria, Melbourne, Australia.

Baron, J.R. (1956): The Binary-Mixture Boundary Layer Associated with Mass Transfer Cooling at High Speeds, MIT Naval Supersonic Lab., Tech. Rept. 160, May.

Bethe, H.A. and Adams (1959): A Theory for the Ablation of Glassy Materials, Jour. Aero. Sci., vol. 26, No. 6.

Biot, M.A. (1957): New Methods in Heat Flow Analysis with Application to Flight Structures, J. Aero. Sci., Vol. 24, 857-873.

Biot, M.A. (1958): Linear Thermodynamics and the Mechanics of Solids, Proc. Third U.S. Congress of Appl. Mechs., ASME.

Biot, M.A. (1959a): Thermodynamics and Heat Flow Analysis by Lagrangian Methods, IAS Paper 59 - 137.

Biot, M.A. (1959b): Further Developments of New Methods in Heat Flow Analysis, Jour. Aero. Sci., Vol. 26, 367-381.

Biot, M.A. and Daughaday, H. (1962): Variational Analysis of Ablation, Jour. Aero. Sci., Vol. 24, 227-229.

Blecher, S. and Sutton, G.W. (1961): Comparison of Some Approximate Methods of Calculating Re-Entry Ablation of Subliming Material, ARS Jour., Vol. 31, 433-435.

Boley, B.A. (1963): Upper and Lower Bounds for the Solution of a Melting Problem, Quart. Appl. Math., Vol. XXI,No. 1.

Carrier, G.F. (1958): Aerodynamic Heat Transfer to a Melting Body, Space Tech. Labs., GM-TM-0165-00268.

Carslaw, H.S. and Jaeger, J.C. (1959): Conduction of Heat in Solids, Oxford Press, 282-296.

Chapman, D.R. (1960): Recent Re-entry Research and the Cosmic Origin of Tektites, Nature, vol. 188, No. 4748.

Chapman, D.R., Larson, H.K., and Anderson, L.A. (1962a): Aerodynamic Evidence Pertaining to the Entry of Tektites into the Earth's Atmosphere, NASA TR R-134.

Chapman, D.R. and Larson, H.K. (1962b): The Lunar Origin of Tektites, 13th Intern'tl. Aero. Congr., Varna, Bulgaria.

Cheng, S.I. (1958): On the Mechanisms of Atmospheric Ablation, presented at the 9th International Astronautical Congress, Amsterdam, August.

Chen, S.Y. and Allen, S.J. (1962): Similarity Analysis for Transient Melting and Vaporizing Ablation, ARS Jour., Vol. 32, No. 10, 1536 - 1543.

Churchill, R.V. (1944): Modern Operational Mathematics in Engineering, McGraw-Hill, New York, 107.

Citron, S.J. (1959): Heat Conduction in a Melting Slab, Part II--Columbia University, Inst. of Flight Structures, CU-15-59-ONR-266(20)-CE.

Citron, S.J.: A Note on the Relation of Biot's Method in Heat Conduction to a Least Square Procedure, Jour. Aero. Sc., vol. 27, 1960.

Citron, S.J. (1960): A Note on the Relation of Biot's Method in Heat Conduction to a Least Square Procedure, Jour. Aero. Sci., Vol. 27, 317-318.

Cohen, C.B., and Reshotko, E. (1956): Similar Solutions for the Laminar Compressible Boundary Layer with Heat Transfer and Pressure Gradient, NACA Rept. 1293 (supercedes NACA TN-3325).

Dewey, C.F. Jr., Schlesinger, S.I., and Sashkin, L. (1960): Temperature Profiles in a Finite Solid with Moving Boundary, Jour. Aero. Sci., Vol. 27, 59-64.

Economos, C. (1961): Results of Ablation Tests on Several Plastic Models in a Hypersonic Wind Tunnel, Polytech. Inst. of Brooklyn, PIBAL Rept. No. 606.

Fanucci, J.B., and Lew, H.G. (1959): Effect of Mass Transfer and Body Forces on Two Phase Boundary Layers, General Electric Co., Tech. Inf. Series, Research Memo no. 35, April.

Fay, J.A., and Riddell, F.R. (1958): Theory of Stagnation Point Heat Transfer in Dissociated Air, Jour. Aero. Sci., vol. 25, no. 2, Feb., pp. 73-86.

Friedrichs, K.O. and Wasow, W.R. (1946): Singular Perturbations of Non-Linear Oscillations, Duke Math. Jour., Vol. 13, 367-381.

Goodman, T.R. (1958a): The Heat Balance Integral and Its Application to Problems Involving a Change of Phase, Trans. ASME, Vol. 80, 335-342.

Goodman, T.R. (1958b): Aerodynamic Ablation of Melting Bodies, Proc. Third U.S. National Congress Appl. Mech., Brown University.

Goodman, T.R. and Shea, J.J. (1960a): The Melting of Finite Slabs, J. Appl. Mech ., Vol. 27, 16-24.

Goodman, T.R. (1960b): The Heat Balance Integral--Further Considerations and Refinements, ASME Paper 60-SA-9.

Georgiev, S. (1959): Unsteady Ablation, AVCO Everett Research Lab., Research Rept. 94.

Hartree, D.R. (1935-1936): Properties and Applications of the Repeated Integrals of the Error Function, Mem. and Proc. Manchester Lit. and Phil. Soc., Vol. 80, 85-102.

Hidalgo, H. (1959): A Theory of Ablation of Glassy Materials for Laminar and Turbulent Heating, AVCO Research Rept. 62, AFBMD-TN-59-13.

Kivel, B. and Bailey, K. (1957): Tables of Radiation from High Temperature Air, AVCO Res. Rept. No. 21.

Lagerstrom, P., Cole, J.D., and Trilling, L. (1949): Problems in Theory of Viscous Compressible Fluids, Guggenheim Aero. Lab., Calif. Tech. 38-40.

Landau, H.G. (1950): Heat Conduction in a Melting Solid, Quart. of Appl. Math., Vol. 8, 81-94.

Lardner, T.J. (1962): Approximate Solutions for Melting and Ablation Problems, Polytech. Inst. of Brooklyn, PIBAL Rept. No. 654.

Lees, L. (1956): Laminar Heat Transfer over Blunt-Nosed Bodies at Hypersonic Flight Speeds, Jet Propulsion, Vol. 26, No. 4, 259-269.

Lees, L. (1958): Convective Heat Transfer with Mass Addition and Chemical Reactions, Third Combustion and Propulsion Colloquium, Advisory Group for Aeronautical Research and Development, NATO, Palermo, Italy, Pergamon Press.

Lees, L. (1959a): Recovery Dynamics--Heat Transfer at Hypersonic Speeds in a Planetary Atmosphere, Chapt. 12, Space Technology, John Wiley and Sons, N.Y., 1-20.

Lees, L. (1959b): Ablation in Hypersonic Flows, presented at the Seventh Anglo-American Conference, Royal Aero. Soc. and Inst. of Aero. Sci., N.Y.

Meksyn, D. (1948): Proc. Roy. Soc. (London), vol. 194A.

Murray, W.D. and Landis, F. (1959): Numerical and Machine Solutions of Transient Heat-Conduction Problems Involving Melting and Freezing, Part I--Method of Analysis and Sample Solutions, J. Heat Transfer, 106-112.

Nicholson, C. (1943): The Probability Integral for Two Variables, Biometrika, Vol. 33, 59-72.

Ostrach, S., Goldstein, A.W. and Hamman, J. (1960): The Effect of a Deceleration Force on a Melting Boundary Layer, Jour. Aero. Sci., Vol. 27, No. 8.

Ostrach, S., Goldstein, A.W. and Hamman, J. (1962): Analysis of Melting Boundary Layers on Decelerating Bodies, NASA TN D-1312.

Roberts, L. (1959): A Theoretical Study of Stagnation Point Ablation, NASA TR R-9.

Roberts, L. (1959): NASA TR R-10.

Scala, S.M. (1959): A Study of Hypersonic Ablation, Xth Int. Astronautical Congr. London.

Scala, S.M. and Sutton, G.W. (1958): The Two-Phase Laminar Boundary Layer--A Study of Surface Melting, Proc. Heat Transfer and Fluid Mechs. Inst., Stanford University Press, 231-240.

Solomon, G. (1959): The Nature of Re-Entry, Astronautics, Vol. 4, No. 3, 20-21, 98, 100.

Stefan, J. (1891): Über die Theorie der Eisbildung Insbesondere Über die Eisbildung in Polarmeere, Ann. Phys. u. Chem. (Weidemann), N.F. 42, 269-286.

Sunderland, J.E. and Grosh, R.J. (1960): Transient Temperature in a Melting Solid, ASME Paper 60-WA-277.

Sutton, G.W. (1958): The Hydrodynamics and Heat Conduction of a Melting Surface, Jour. Aero. Sci., Vol. 25, No. 1.

Tellep, D.M. (1959): The Effect of Vehicle Deceleration on a Melting Surface, Lockheed Missiles and Space Division, Tech. Rept. LMSD-48381, January.